Western Washington University
Western CEDAR

WWU Graduate School Collection
WWU Graduate and Undergraduate Scholarship

Spring 2023

Stereoselective Synthesis of (+)- and (-)-Cananodine

Haley Holliday
Western Washington University, hollidh@wwu.edu

Follow this and additional works at: https://cedar.wwu.edu/wwuet

Part of the Chemistry Commons

Recommended Citation

Holliday, Haley, "Stereoselective Synthesis of (+)- and (-)-Cananodine" (2023). *WWU Graduate School Collection*. 1184.
https://cedar.wwu.edu/wwuet/1184

This Masters Thesis is brought to you for free and open access by the WWU Graduate and Undergraduate Scholarship at Western CEDAR. It has been accepted for inclusion in WWU Graduate School Collection by an authorized administrator of Western CEDAR. For more information, please contact westerncedar@wwu.edu.

Stereoselective Synthesis of (+)- and (-)-Cananodine

By

Haley M. Holliday

Submitted in Partial Completion
of the Requirements for the Degree
Master of Science

ADVISORY COMMITTEE

Dr. James R. Vyvyan, Chair

Dr. Amanda Murphy

Dr. Steven Emory

GRADUATE SCHOOL

Dr. David L. Patrick, Dean

Master’s Thesis

In presenting this thesis in partial fulfillment of the requirements for a master’s degree at Western Washington University, I grant to Western Washington University the non-exclusive royalty-free right to archive, reproduce, distribute, and display the thesis in any and all forms, including electronic format, via any digital library mechanisms maintained by WWU.

I represent and warrant this is my original work, and does not infringe or violate any rights of others. I warrant that I have obtained written permissions from the owner of any third party copyrighted material included in these files.

I acknowledge that I retain ownership rights to the copyright of this work, including but not limited to the right to use all or part of this work in future works, such as articles or books.

Library users are granted permission for individual, research and non-commercial reproduction of this work for educational purposes only. Any further digital posting of this document requires specific permission from the author.

Any copying or publication of this thesis for commercial purposes, or for financial gain, is not allowed without my written permission.

Haley M. Holliday

May 19th, 2023

Stereoselective Synthesis of (+)- and (-)-Cananodine

A Thesis
Presented to
The Faculty of
Western Washington University

In Partial Fulfillment
Of the Requirements for the Degree
Master of Science

by
Haley Holliday
June 2023

Abstract

Natural products are an important class of molecules utilized in traditional medicine and inspire drug design in medicinal chemistry. *Cananga odorata*, a tree commonly known as ylang-ylang, contains natural products known to positively benefit health, and specifically promote liver health. One alkaloid isolated from *Cananga odorata*, cananodine, possesses cytotoxic properties, specifically against hepatocellular carcinoma (HCC). HCC is the most common type of liver cancer, with one million diagnoses projected by 2025 globally. Cananodine is a member of the guaipyridine alkaloid family, a class of compounds that feature a substituted pyridine bonded to a seven-membered ring. The first enantiomer of interest, (+)-cananodine, has demonstrated greater activity against HCC compared to the second target, (-)-cananodine. The molecule's activity likely depends on its stereochemistry, so this efficient, enantioselective synthesis is critical since previous attempts yielded little product or lacked selectivity. In this study, the first proposed synthesis utilizes a modern enantioselective Heck reaction. The second unique route features a diastereoselective Evans alkylation that yields both (+)- and (-)-cananodine enantiomers. The selective synthesis of these small but intricate molecules makes progress in the development of new compounds that could improve the treatment of HCC.

Acknowledgments

Research Advisor:	Dr. James R. Vyvyan
Thesis Committee Members:	Dr. Amanda Murphy Dr. Steven Emory
Financial Support:	WWU Research and Sponsored Programs Bob Lyon and Sharsti Sandall at SeaGen Inc. Dr. Clint Spiegel Dr. James Ross WWU Chemistry Department
Instrument Technicians and Collaborators:	Dr. Hla Win Sarina Kiesser

Table of Contents

Abstract……………………………………………………………… iv

Acknowledgements……………………………………………………… v

List of Tables and Figures………………………………………………… vii

1. **Introduction**……………………………………………………………… 1
    - **1.1** Natural Products: Guaipyridine Alkaloids……………………………… 1
    - **1.2** Hepatocellular carcinoma (HCC) and Current Therapies……………… 3
    - **1.3** Cananodine and HCC: Biological activity of sesquiterpene alkaloids………… 5
    - **1.4** Previous synthetic studies on guaipyridine and rupestines A-M……………… 7
    - **1.5** Previous synthetic studies on (+)-, (-)-, (±)-cananodine……………… 13
2. **Synthesis of (+)-cananodine: Redox-relay Heck reaction**……………………… 19
    - **2.1** Background: Mizoroki-Heck Reaction………………………………… 19
    - **2.2** Enantioselective redox-relay Heck reaction……………………………… 22
    - **2.3** Exploratory Studies……………………………………………… 24
3. **Synthesis of (+)-cananodine: Asymmetric Alkylation**………………………… 27
    - **3.1** Diastereoselective Evans Alkylation……………………………… 27
    - **3.2** Exploratory Studies……………………………………………… 29
4. **Synthesis of (-)-cananodine:** Synthetic Route Flexibility……………………… 32
    - **4.1** Capitalizing on Evans Alkylation……………………………………… 32
    - **4.2** Exploratory Studies……………………………………………… 32
5. **Optimization and Characterization** ……………………………………… 35
    - **5.1** Optimization……………………………………………………… 35
    - **5.2** Characterization…………………………………………………… 43
6. **Conclusions**……………………………………………………………… 46
7. **Experimental**……………………………………………………………… 48
8. **References** ……………………………………………………………… 74
9. **Supporting Information**…………………………………………………… 80

List of Figures and Schemes

Figure 1. Sesquiterpene guaipyridine alkaloids…………………………………………………………………… 2

Figure 2. Leads inspiring design of sorafenib and final structure……………………………………………… 4

Figure 3. Compound A34 proven to have promising activity against HCC………………………………… 5

Figure 4. Compound K117 with high activity against *Huh7* cell proliferation…………………………… 5

Figure 5. Hypothesis of (+)-cananodine activity-- 6

Figure 6. Rupestonic acid and YZH-106…………………………………………………………………………… 7

Figure 7. Synthesis of guaipyridine alkaloids by van der Gen et al……………………………………………… 7

Scheme 1. Synthesis of rupestine G and epimers……………………………………………………………… 8

Scheme 2. Synthesis of (±) rupestine B and C………………………………………………………………… 9

Scheme 3. Rupestine D and epimer ……………………………………………………………………………… 10

Scheme 4. Synthesis of (±)-rupestine A and epimers………………………………………………………… 11

Scheme 5. Synthesis of rupestines L and M…………………………………………………………………… 12

Scheme 6. Craig and Henry’s synthesis of (+)-cananodine…………………………………………………… 13

Scheme 7. Synthesis of (±)-cananodine by Shelton et al……………………………………………………… 14

Scheme 8. Second synthesis of (±)-cananodine by Shelton et al…………………………………………… 15

Scheme 9. Synthesis of (-)-cananodine by Zhang et al………………………………………………………… 16

Figure 8. Discoveries by Mizoroki and Heck…………………………………………………………………… 19

Figure 9. Conventional vs. reductive Mizoroki-Heck reactions………………………………………………… 20

Figure 10. Oxidative Mizoroki-Heck reaction…………………………………………………………………… 21

Scheme 10. Enantioselective redox-relay Heck reaction……………………………………………………… 23

Scheme 11. First envisioned synthetic route of current study………………………………………………… 24

Scheme 12. Pyridine / redox-relay proof of concept…………………………………………………………… 25

Table 1. Exploration of pyridine / redox-relay compatibility ………………………………………………… 26

Scheme 13. Retrosynthesis of (+)-cananodine…………………………………………………………………… 27

Scheme 14. Synthesis of (+)-cananodine by Holliday et al……………………………………………………… 30

Table 2. Optical rotation comparison of (+)-cananodine intermediates……………………………………… 30

Table 3. Analysis of (+)-cananodine NMR data versus literature……………………………………………… 31

Scheme 15. Retrosynthesis of (-)-cananodine…………………………………………………………………… 32

Scheme 16. Synthesis of (-)-Cananodine by Holliday et al……………………………………………………… 33

Table 4. Optical rotation comparison of (-)-Cananodine intermediates……………………………………… 33

Table 5. Analysis of (-)-Cananodine NMR data versus literature……………………………………………….. 34
Figure 11. Formation of alkylation side product…..…………………………………………………………………….... 36
Figure 12. Hydroxyamide side product…...…………………………………………………………………………………….. 37
Scheme 17. Optimization of exocyclic methylene reduction…………………………………..…………………… 39
Figure 13. Collaborative methylene reduction effort………………………………………………………….……….. 40
Scheme 18. Route optimization attempt……………………………………………………………………………………….. 42
Figure 16. Protonated (-)-Cananodine ^{1}H comparison………………………………………………………………… 43
Table 6. Comparison of specific rotation $[\alpha]_D$ of both enantiomers………………………………………….. 44
Scheme 19. Envisioned modification of hydrogenation……………………………………………………………… 46

1. Introduction

1.1 Natural Products: Guaipyridine Alkaloids

Natural products (NP's) are an indispensable inspiration in the field of medicinal chemistry and pharmaceutical design. The most obvious but important examples critical to the shaping of modern medicine today are aspirin from willow tree bark, morphine from opium, and several popular antibiotics.[1] Many drugs are either adapted or derivatized from NP's. Since 1981, 185 novel small molecule anti-tumor drugs were approved, of which only 15.7% were classified as 'totally synthetic'.[2]

These standard 'totally synthetic' pharmaceuticals are discovered via high throughput screening (HTS) and/or analysis of structure activity relationship (SAR). An active functional group or specific structural moiety is first identified, and a lead compound is selected. Then, many analogs of the lead are produced to test for increased activity after structural modifications. The compound that is most selective and potent is identified, and further biological testing is conducted. However, dependence on discovery via SAR analysis is not always foolproof. Many NP's deviate from Lipinski's Rule of Five where they often have a larger mass (>500 g/mol), higher numbers of H-bond donors (>5) and acceptors (>10), lower cLogP values (octanol:water partition coefficient significantly less than 5), and higher rigidity compared to traditional synthetic therapeutics.[3] Natural products have already been 'optimized' by evolution, making them critical building blocks as hit or lead compounds.

On the other hand, the number of research groups pursuing the discovery and synthesis of natural products as drug leads declined significantly in recent years.[2] Technical difficulties involving screening, characterization, and optimization present barriers that explain this trend. Additionally, the unique deviation from the Rule of Five plus NP's inherent complexity makes them hard to synthesize, let alone optimize. In modern times, however, opportunities for NP discovery are growing as technology and advanced analytical tools improve.

Alkaloids, nitrogenous NP's that induce physiological effects, serve many of us in our day-to-day lives. From caffeine and nicotine to morphine, alkaloids have been utilized in society for many different purposes.[4] A specific class of these molecules, guaipyridine alkaloids, have a unique structure comprised of a seven-membered ring fused to a 2-methylpyridine core (Figure 1). This class includes guaipyridine (**1**), cananodine (**2**), and a family of molecules called rupestines (A-M, **3**-**14**). While this family shares the same structural skeleton, they feature unique stereochemistry and functional groups.

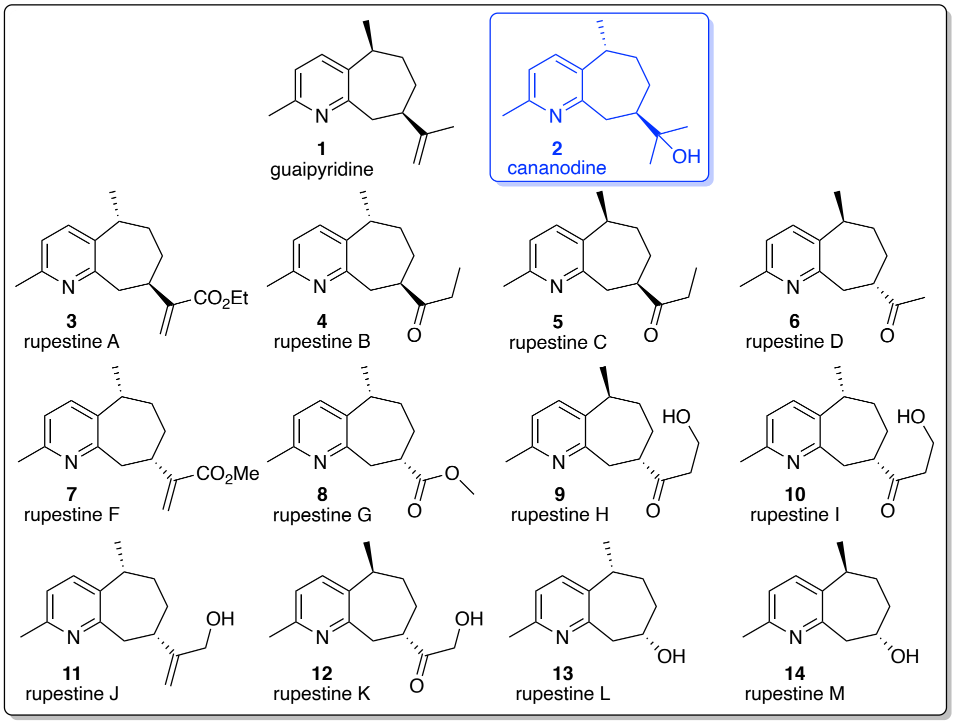
1
guaipyridine
2
cananodine
3
rupestine A
4
rupestine B
5
rupestine C
6
rupestine D
7
rupestine F
8
rupestine G
9
rupestine H
10
rupestine I
11
rupestine J
12
rupestine K
13
rupestine L
14
rupestine M
N
OH
HO
O
CO2Et
CO2Me

Figure 1. Structures of sesquiterpene guaipyridine alkaloids.

Guaipyridine (**1**) was first isolated in 1967 from patchouli oil[5] and later synthesized in 1972.[6] The isolation of cananodine (**2**) in 2001 resulted in its demonstration of activity against HepG2 cancer cell lines: HepG2 IC_{50} = 0.22 μg/mL and Hep 2,2,15 IC_{50} = 3.8 μg/mL[7] Since then, the compound has been successfully synthesized by several groups.[8–11,12] Aisa et al. first reported total characterization of the rupestines (**3**-**14**) by 2012.[13,14] Several of them have been synthesized since then,[10,14-18] but no data on their anti-cancer properties have yet been published.

With the eventual total synthesis of all members of the guaipyridine family, assessment of their biological activity will be interesting due to their structural similarity to cananodine. This is the overall goal of the Vyvyan lab: implement practical and efficient synthetic routes to construct select guaipyridine alkaloids using simple, readily available starting materials.

1.2. Hepatocellular Carcinoma (HCC) and current therapies

The most common form of liver cancer is hepatocellular carcinoma (HCC) and is projected to affect over one million people across the globe annually by 2025.[19] HCC makes up approximately 90% of all patient diagnoses and Hepatitis B and C are the most common risk factors.[20] Recovery rates are low, and if the disease has progressed significantly, the most common treatments such as liver resection and transplantation are not always viable.

To begin explaining the likely origin of HCC, researchers have built on evidence that receptor tyrosine kinases (RTKs) play an integral in tumor growth and metastasis.[21,22] The most notable RTK groups are the RAS and RAF families, composed of proteins that play key roles in control of cell proliferation, apoptosis, and cell differentiation. In general, activating mutations in RAS family genes are the most common cause of human tumors.[23] These mutations can lock RAS proteins into an active state, increasing unabated signaling downstream related to the overexpression of other RTK's such as the epidermal growth factor receptor (EGFR), platelet derived growth factor receptor (PDGRF), and/or the vascular-endothelial growth factor receptor (VEGFR).

The RAF family is made up of serine threonine kinases binding to RAS-GTP which induces movement to the plasma membrane, activating and phosphorylating RAF proteins which increases the chance of tumorigenesis.[24] Hwang et al. summarized that it is likely RAF activation has a critical influence in the development of HCC after observing RAF overexpression in 100% of 30 HCC tissue samples.[25] Whittaker et al. reported that in the majority of advanced-stage HCC, the RAS/RAF/MAPK pathway is activated.[25,26]

This could be due to increased signaling from upstream growth factors and inactivated genes that suppress tumors. Different factors may activate HCC cells which can increase RAS/RAF/MAPK signaling.[27]

Understanding the origin and mechanism of HCC allows for the design of pharmaceuticals that can specifically target these pathways to stop the overexpression of select RTKs. Sorafenib (Nexavar) was introduced to the market in 2007.[20] The lead compound (**15**) preceding sorafenib was isolated in 1995 through HTS of 200,000 compounds investigating RAF-1 kinase inhibitory activity.[28] This selected lead inhibits RAF-1 (IC_{50} = 17 μM). Using rapid parallel synthesis techniques, ~1,000 lead analogs were investigated to improve the potency of this selected lead compound.[29,30] Preservation of the urea moiety while modifying the distal phenyl group led to the structure shown in Figure 3**.** These modifications improved activity by more than ten-fold, bringing RAF-1 inhibition of **16** to 1.1 μM. Further modification of the substituents progressed and the final compound, sorafenib (**17**) was selected. One key element is the addition of the pyridine ring to the pre-existing distal phenyl group, which increased activity to 6 nM against RAF-1.

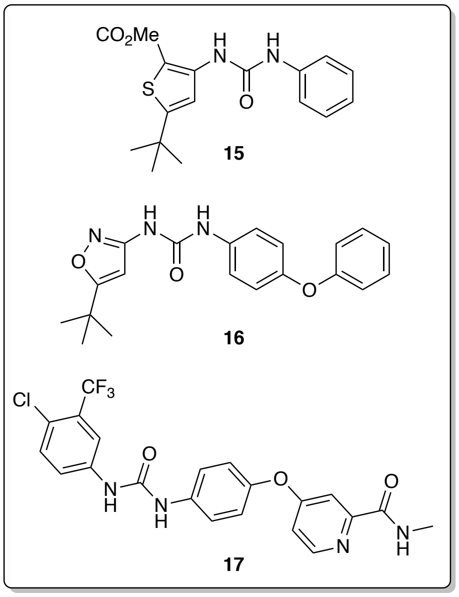

Figure 2. Lead compounds **15** and **16** inspired design of sorafenib (**17**).

Through modern optimization methods investigating structure activity relationships (SAR), researchers used x-ray crystallography to find that the activity of the molecule against cancer cells was highly dependent on several key functional groups: the 4-pyridyl ring, and the trifluoromethyl phenyl and urea groups.[32,33] Specifically, the 4-pyridyl ring occupies the ATP adenine binding pocket of the kinase domain while the trifluoromethyl phenyl group inserts snugly into a hydrophobic pocket. The urea forms two critical H-bonds, one to the backbone aspartate of the aspartic acid-phenylalanine-glycine (DFG) loop and the second to the glutamate side chain. Overall, sorafenib works to stabilize DFG in an inactive conformation. Since its release to the market, this drug has demonstrated inhibition of RAS/RAF pathways and major pro-angiogenic RTKs.[32–34] While still used as a modern first-line treatment for HCC, administration of sorafenib only increases patient survival from 7.9 months to 10.7 months on average.[20] Given the low impact of sorafenib treatment, the alternative design and discovery of drug leads inhibiting RAS/RAF pathways is imperative to improve the outcome for patients suffering from HCC. The targeting of other pathways will be reviewed next.

Recent studies[35,36] have synthesized other products to target fibroblast growth factor receptor 4 (FGFR4) using 1,6-naphthyridin-2(1H)-one derivatives. Their most selective compound (**18**) demonstrated excellent inhibition against FGFR4-dependent HCC cell lines.

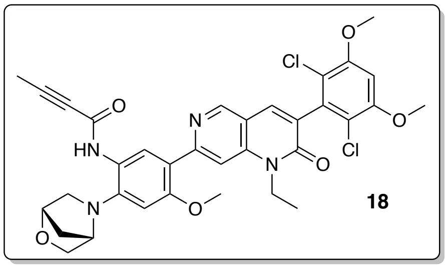

Figure 3. A34 (**18**) is active against HCC.[35]

Another interesting example was reported by Kant et al. in 2021 who synthesized compound K117 (**19**) in a demonstration of activity against Huh7 cell growth.[36] This study capitalized on glycine-N-transferase (GNMT) downregulation which was cited leads to spontaneous development of hepatocellular carcinoma.

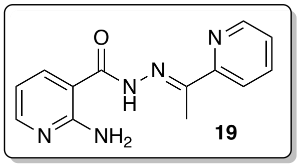

Figure 4. K117 (**19**) has high activity against Huh7 cells.[36]

There is a growing need to fight resistance to sorafenib and improve its efficacy, and extended exploration of new compounds to combat HCC is highly valuable. This study demonstrates an effective method to produce (+)- and (-)-cananodine, constructed to verify if they are viable candidates as hits against cancerous cell lines.

1.3. Cananodine and HCC: Biological activity of sesquiterpene alkaloids

In general, substituted cycloheptane rings are an important scaffold in NP's with regard to their biological activity.[37] Construction of smaller sized rings is favored in the synthetic field due to ring strain, however. In the past decade, natural products featuring cycloheptanes such as cortistatins and englerins have been isolated,[38,39] leading to compounds with nM activity against various cancer cell lines.

Additionally, the pyridine ring moiety is a simple, classic feature common to many pharmaceuticals. As previously discussed, the current therapy sorafenib features a pyridine ring which plays a critical role in its activity as a hydrogen bond acceptor.

The rupestines have not yet been tested for biological activity. Given their eventual total synthesis, they should be evaluated against various cell lines due to their structural similarity to cananodine. If the initial activity values are verified, cananodine could have the potential to become a drug lead, as past studies on the compound have proven that it has noteworthy potential.

Both isolation[7] and synthetic investigations[11] on cananodine found *in vitro* activity against liver, breast, and cervical cancer cell lines. The need to quantify cananodine's activity against HepG2 cell lines is exacerbated by the fact that highly conflicting values were reported by Hsieh et al. in 2001[7] and Yusuf et al. in 2021.[11] The first source gave a value of 1.7 μM while the latter gave a value of 48 ± 2 μM using different cell assays. Hsieh et al. cited a neutral red and methylene blue assay while Yusuf et al. utilized a MTT colorimetric assay. Even though different cell assays were utilized in the two studies, this fifty-fold discrepancy is unacceptable in definitively assessing cananodine's cytotoxic activity.

Another characterization confliction with studies on (+)-cananodine is its true optical rotation value. See Section 1.5 for detailed discussion of the difference the measured value of the natural product by Hsieh in 2001 and Craig and Henry's synthetically derived product in 2006. The uncertainty of these critical characterization parameters increases the need for the selective synthesis of (+)-cananodine to verify both its optical properties and its potency as an anti-cancer compound. These characteristic values are a subject of conflict, but the hypothetical inhibitory mechanism of cytotoxicity against HepG2 cancer cell lines surrounds the hydrogen bonding of a cysteine residue on the backbone of b-Raf, with the pyridine nitrogen as an H-bond acceptor, and the hydroxyl hydrogen as an H-bond donor (Figure 5).

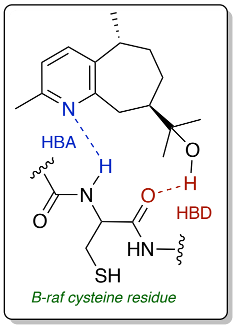

Figure 5. Proposed interaction causing inhibition by **2** on B-Raf

The first reported *in vitro* activity of cananodine against HepG2 cells in 2001 rivals that of the current treatment, sorafenib.[7] The challenge is that only minute amounts of pure, biologically active product can be isolated out of a large mass of the fruit of *Cananga odorata*, which necessitates the optimization of a synthetic route to create the product artificially.

Given that the rupestine family has structural moieties similar to cananodine as well as various modern pharmaceuticals, their biological activity is likely. Although this has not yet been demonstrated, one of their analogs, rupestonic acid (**20a**) has been modified to give a structure (**20b**) with highly potent anti-viral activity.[40] Featured structures synthesized by the group exhibited potent activities against influenza H1N1 with micromolar activities (IC_{50} = 1.71-2.12 μM), giving inspiration for the development of new lead compounds treating the flu.

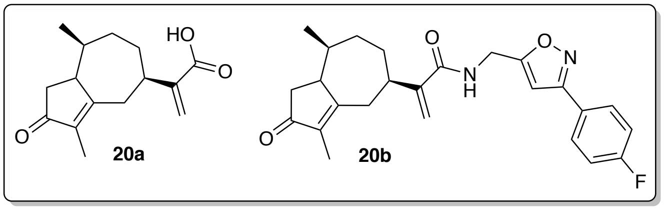

Figure 6. Rupestonic acid (**20a**) and YZH-106 (**20b**).[40]

The successful synthesis of (+)-cananodine will allow for further biological testing to assess its potential as an anti-cancer drug lead. In the past, students in the Vyvyan research group have successfully synthesized and characterized cananodine,[9,10] but with low yields and utilizing routes that lacked enantioselectivity. The featured route in this study is designed to capitalize on synthetic successes from the past while optimizing enantioselectivity and efficiency.

1.4 Previous synthetic studies on guaipyridine and rupestines A-M.

As previously mentioned, the first reported isolation of sesquiterpene guaipyridine alkaloids was by Buchi et al in 1966.[5] Several associated compounds were synthesized by van der Gen et al. in 1972, including guaipyridine (**1**) and epi-guaipyridine (**21**) using guaiol as starting material.[6]

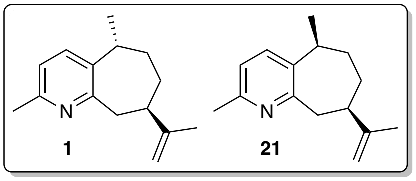

Figure 7. Synthesis of guaipyridine alkaloids by van der Gen.[6]

Aisa et al. reported on the isolation of the rupestine class of guaipyridine alkaloids isolated from *Artemesia Rupestris* L. in 2010.[13] They first characterized rupestine A-D and two years later, the group isolated rupestines F-M.[14] Under the guidance of Aisa, the first synthesis of rupestine G and its epimers was accomplished in 2018[16] via a purposefully non-selective method. This allowed for the characterization of all substrates, furthering the field in identification of structures and likely biological activity. The group isolated all four isomers in 9 steps in 18.9% yield (Scheme 1).

Scheme 1. Synthesis of rupestine G and its epimers.[16]

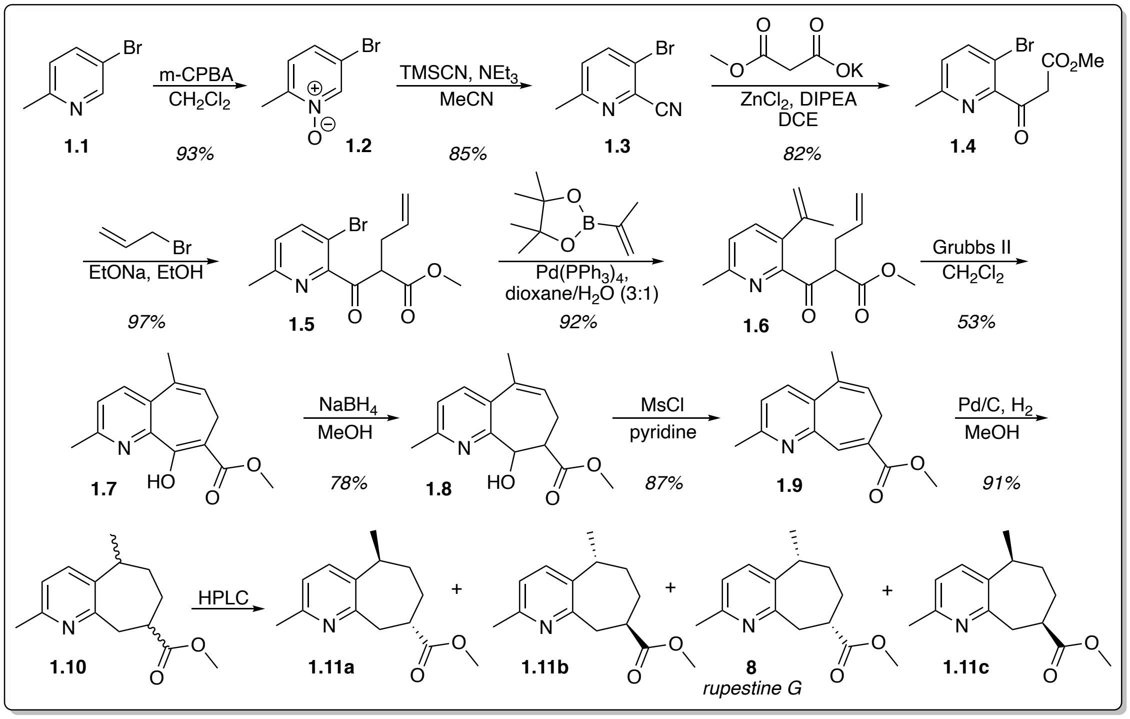
m-CPBA
CH_2Cl_2
93%
TMSCN, NEt_3
MeCN
85%
$ZnCl_2$, DIPEA
DCE
82%
EtONa, EtOH
97%
$Pd(PPh_3)_4$,
dioxane/H_2O (3:1)
92%
Grubbs II
CH_2Cl_2
53%
$NaBH_4$
MeOH
78%
MsCl
pyridine
87%
Pd/C, H_2
MeOH
91%
HPLC
1.1
1.2
1.3
1.4
1.5
1.6
1.7
1.8
1.9
1.10
1.11a
1.11b
8
rupestine G
1.11c

First, 5-bromo-2-methylpyridine (**1.1**) was oxidized using *m*-CPBA followed by treatment with trimethylsilyl cyanide and triethylamine to yield 2-cyanopyridine **1.3** . The following intermediate **1.4** was produced using zinc chloride and potassium methyl malonate via a decarboxylative Blaise reaction. Allyl bromide with sodium ethoxide afforded **1.5** in excellent yield. To obtain **1.6**, a Suzuki cross-coupling reaction was utilized employing isopropenylboronic acid pinacol ester and a Pd catalyst. To assemble the cycloheptene core (**1.7**), Grubbs II catalyst was used. Both the keto and enol isomers were present but by

^1H NMR, the enol tautomer **1.7** was favored over the keto tautomer. This enol was reduced using sodium borohydride to yield **1.8** which was dehydrated using methanesulfonyl chloride. Diene **1.9** was afforded in two steps, which was hydrogenated non-selectively using palladium on carbon and H_2 gas to give rupestine G (**8**) and associated epimers (**1.11a-c**) after separation using preparative chiral HPLC.

Rupestines B and C were synthesized by the Vyvyan group[15] in a simple and sophisticated fashion (Scheme 2). The first alkylation was by allyl 3-oxopentanoate (**2.1**) after treatment with K_2CO_3 with picolyl bromide **2.2**. A second alkylation utilized a different base, LHMDS, after trials with several others. Thus, 4-iodo-1-butene (**2.4**) underwent a substitution reaction to give **2.5**. The next step cleaved the two allyl protecting groups, producing phenol **2.5** which was treated with *N*-phenyltriflamide to yield the triflate product (**2.6**). **2.6** was an ideal substrate for accomplishing the intramolecular ring closing Mizoroki-Heck reaction using a Pd^0 catalyst under basic conditions to form carbocycle **2.7**. Finally, the exocyclic alkene was hydrogenated using palladium on carbon under H_2 atmosphere to yield both targets.

Scheme 2. Synthesis of (±)-rupestine B and C.[15]

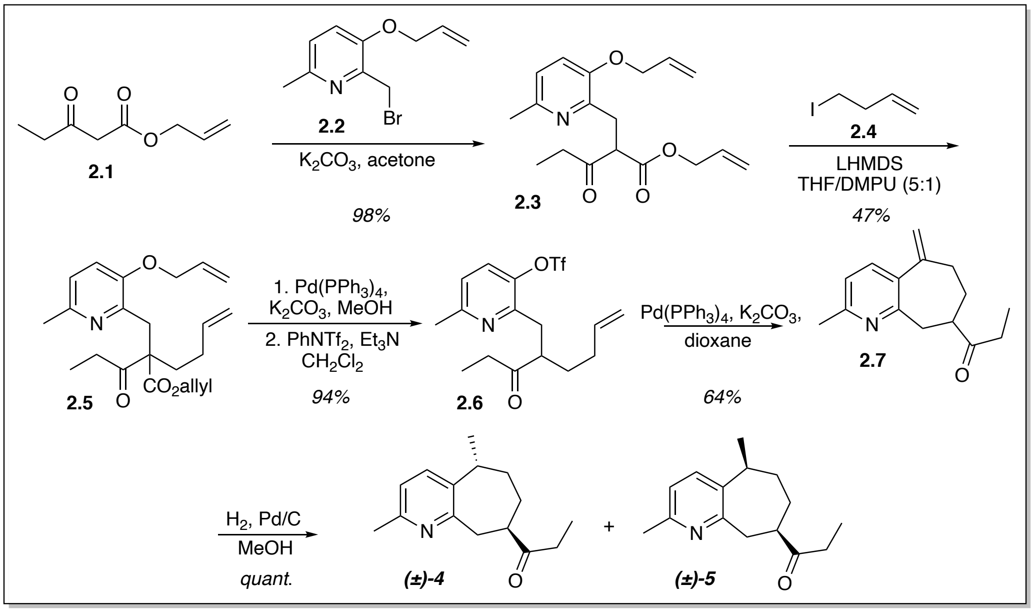
2.1
2.2
Br
K2CO3, acetone
98%
2.3
2.4
LHMDS
THF/DMPU (5:1)
47%
2.5
CO2allyl
1. Pd(PPh3)4, K2CO3, MeOH
2. PhNTf2, Et3N CH2Cl2
94%
OTf
2.6
Pd(PPh3)4, K2CO3, dioxane
64%
2.7
H2, Pd/C
MeOH
quant.
(±)-4
+
(±)-5

Products (±)-rupestine B ((±)-**4**) and C ((±)-**5**) were afforded in a 1:2 ratio, with an overall yield of 9% and 18% after separation of diastereomers using reverse phase MPLC.

Around the same time, (±)-rupestines D and G were also synthesized by the Vyvyan group[10] using the same intramolecular Mizoroki-Heck reaction (Scheme 3). Similar theory and techniques were used as the previously discussed synthesis, the difference being varying starting materials were used to achieve the desired products. For example, when constructing rupestine D, instead of alkylation by allyl 3-oxopentanoate (**2.1**), 5-hexenenitrile (**3.1**) was used. When constructing (+)-cananodine and rupestine G, various 5-hexenoate esters were used to assess compatibility. To summarize, this synthesis followed the same route as the synthesis of (±)-rupestines B and C from simple commercially available starting material, followed by deprotection of the phenol and triflation. The intramolecular ring closing Heck reaction, non-selective hydrogenation, and ester reduction was also used to produce the final targets.

Scheme 3. Rupestine D (**6**) and epimer **3.6**.[10]

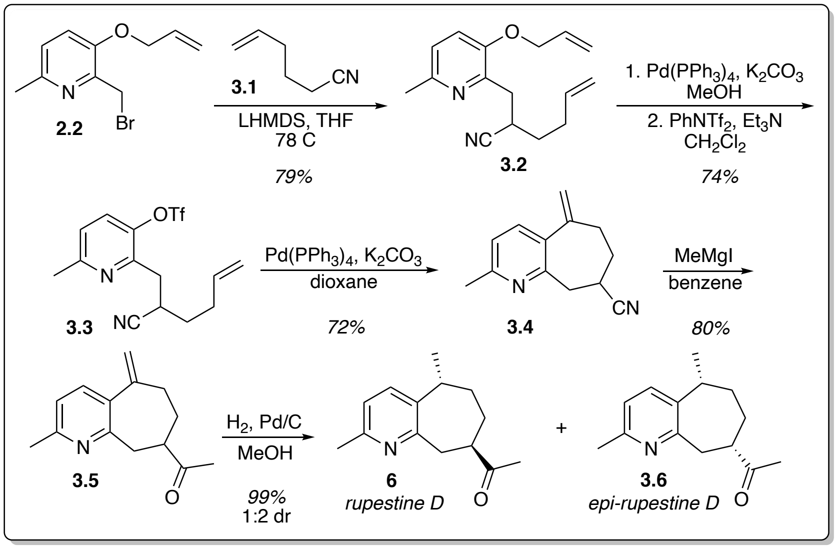

Another study by the Aisa group detailed the synthesis of (±)-rupestine A and (±)-rupestine J in 2021 (Scheme 4).[17] Key transformations include a Suzuki cross-coupling[41], Krapcho decarboxylation,[42] and RCM.[43] Starting material (**4.1**) was formed readily from 5-bromo-2-methylpyridine. A decarboxylative Blaise reaction[44] was used to form **4.2** and alkylation with ethyl bromoacetate (**4.3**) gave **4.4**. Reacting this intermediate with allyl bromide and sodium ethoxide yielded **4.5**. Next, the decarboxylation product (**4.6**) was procured by reaction with LiCl in DMSO. A Suzuki reaction was utilized to couple isopropenylboronic acid pinacol ester **4.7** with Pd^0 catalyst. Ring closing metathesis using Grubbs II catalyst yielded cycloheptene product **4.9**. Reduction by sodium borohydride led to **4.10** whose secondary alcohol at C7 was protected using an acetyl group. This allowed for hydrogenation by palladium over carbon of the exocyclic alkene and removal of the acetyl group to produce two diastereomers in a 4:1 ratio. The next desired product (**4.13**) was formed from methyl formate and LDA. Finally, this was reduced to an alcohol, protected with a *p*-toluenesulfonyl group, then subjected to elimination under basic conditions to give the final products, (±)-rupestine A ((±)-**3**) and epimers (**4.15a, b**).

Scheme 4. Synthesis of (±)-rupestine A and respective epimers.[17]

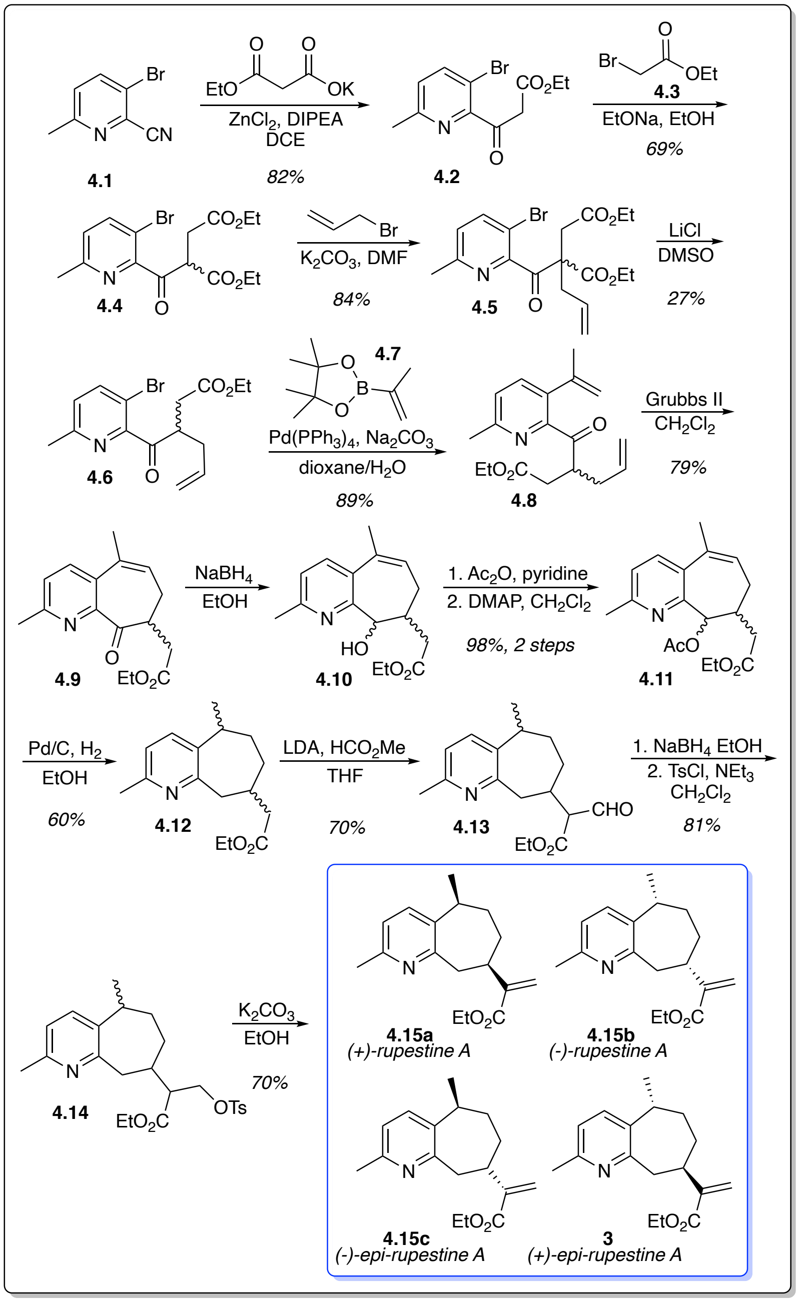
Br
CN
N
4.1
EtO
OK
ZnCl$_2$, DIPEA
DCE
82%
CO$_2$Et
4.2
Br
OEt
4.3
EtONa, EtOH
69%
4.4
Br
K$_2$CO$_3$, DMF
84%
4.5
LiCl
DMSO
27%
4.6
4.7
Pd(PPh$_3$)$_4$, Na$_2$CO$_3$
dioxane/H$_2$O
89%
EtO$_2$C
4.8
Grubbs II
CH$_2$Cl$_2$
79%
4.9
NaBH$_4$
EtOH
HO
4.10
1. Ac$_2$O, pyridine
2. DMAP, CH$_2$Cl$_2$
98%, 2 steps
AcO
4.11
Pd/C, H$_2$
EtOH
60%
4.12
LDA, HCO$_2$Me
THF
70%
CHO
4.13
1. NaBH$_4$ EtOH
2. TsCl, NEt$_3$
CH$_2$Cl$_2$
81%
OTs
4.14
K$_2$CO$_3$
EtOH
70%
4.15a
(+)-rupestine A
4.15b
(-)-rupestine A
4.15c
(-)-epi-rupestine A
3
(+)-epi-rupestine A

The final and most recent synthesis of guaipyridine alkaloid rupestines was by Scheerer[18] in early 2023 (Scheme 5). Rupestine L and M were isolated in relatively few steps, envisioned from a creative route featuring a cycloaddition/reversion Diels Alder reaction and an aza-conjugate addition and lactonization to access the critical pyridine moiety. Also, the study simultaneously developed a new method to access oxazinone substrates using electron-deficient alkynes which had not yet been demonstrated in recent literature.

Preparation of starting material (*S*)-4-methylhex-5-ynal (**5.4**) from (-)-citronellal (**5.1**) proceeded smoothly via the bromination of the aldehyde, subsequent elimination to form alkyne **5.3**, and ozonolysis and reduction. Acetylide addition of **5.5** and oxidation using Dess-Martin periodinane gave acetylenic ketone **5.6**, the requisite substrate for the aza-conjugate addition of 2-amino-1,3,propanediol (**5.7**) and lactonization using acetic anhydride, triethylamine, and DMAP to form the key oxazinone intermediate (**5.8**), the guaipyridine skeleton precursor. Subsequent reflux of **5.8** in chlorobenzene and NEt_3 initiated the featured domino sequence: acetate elimination, alkene isomeration, and cycloaddition/reversion ([4+2]/retro[4+2]), yielding ketone **5.12**. Reduction of **5.12** using DIBAL-H afforded diastereomers **13** and **14**, rupestine L and M, in a 1.5:1 diastereomeric ratio.

Scheme 5. Synthesis of rupestines L and M.[18]

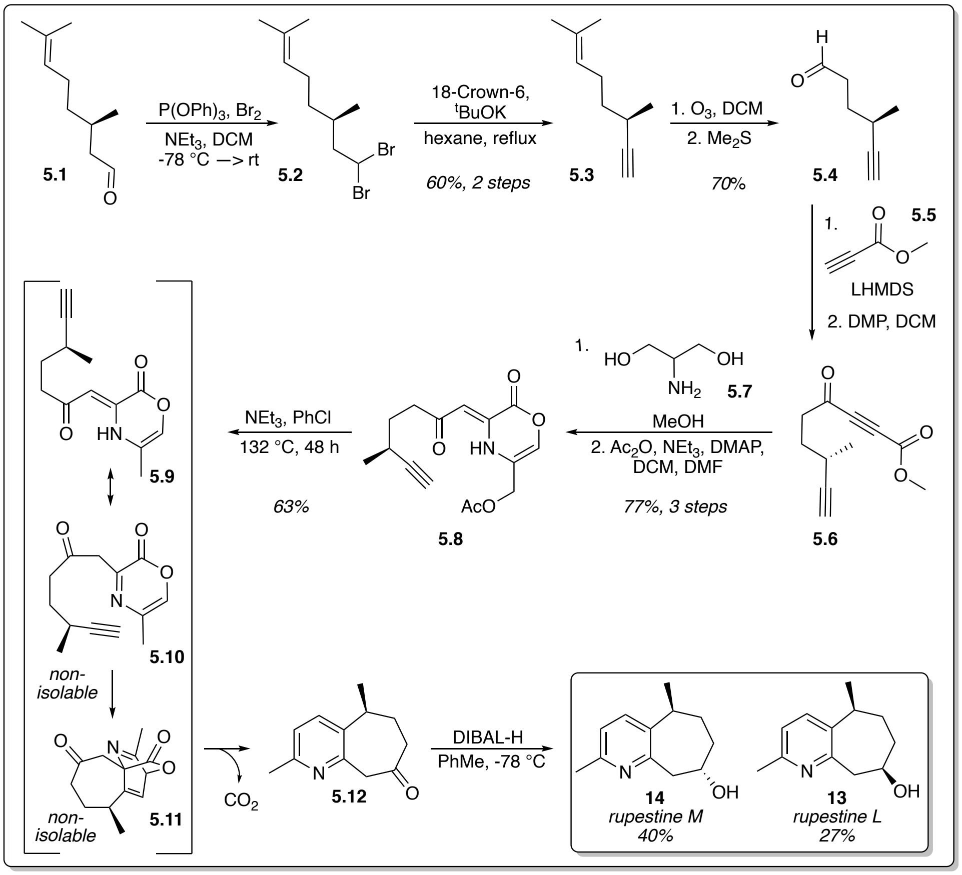

5.1
P(OPh)3, Br2
NEt3, DCM
-78 °C —> rt
5.2
Br
Br
18-Crown-6,
tBuOK
hexane, reflux
60%, 2 steps
5.3
1. O3, DCM
2. Me2S
70%
5.4
H
O
1.
5.5
LHMDS
2. DMP, DCM
5.6
1. HO OH NH2 5.7
MeOH
2. Ac2O, NEt3, DMAP, DCM, DMF
77%, 3 steps
5.8
AcO
HN
NEt3, PhCl
132 °C, 48 h
63%
5.9
5.10
non-isolable
5.11
non-isolable
CO2
5.12
DIBAL-H
PhMe, -78 °C
14
rupestine M
40%
13
rupestine L
27%
OH
N

1.5 Previous synthetic studies on (+)-, (-)-, (±)-cananodine

Five years after cananodine's isolation and characterization, a synthetic route was established to produce (+)-cananodine.[8] Lengthy and relatively inefficient (15 steps, 4% yield), the methods developed left room for progress to be made modifying and optimizing the synthesis of the molecule (Scheme 6). Craig and Henry chose to access the C5 stereocenter through the selection of (*R*)-(-)-citronellene as starting material**.** A chiral auxiliary was used to prepare starting material **6.1**. This underwent a diastereoselective allylation using sodium hexamethyldisalizide as a base with **6.2** to provide **6.3**. Next, desilylation of the protecting group gave **6.4**. The second key reaction closed the carbocycle **6.5** via ring closing metathesis employing the classic Grubbs II catalyst. The chiral auxiliary was removed using sodium methoxide, followed by esterification of the primary alcohol using 4-methyl-2-(-4-tolylsulfonyl)-4-pentenoic acid to provide **6.7**. Microwave-irradiation facilitated the decarboxylative Claisen rearrangement step that yielded **6.8**, one of two diastereomers that were separated by flash column chromatography. To access the critical pyridine ring, the unique Chichibabin synthesis[45] was implemented using ozonolysis plus ethanolic ammonia and triphenylphosphine. This concluded the construction of the guaipyridine skeleton (**1.11b**) whose subsequent reduction using methyl magnesium bromide gave the final product, (+)-cananodine (**2**).

Scheme 6. Craig and Henry's synthesis of (+)-cananodine.[8]

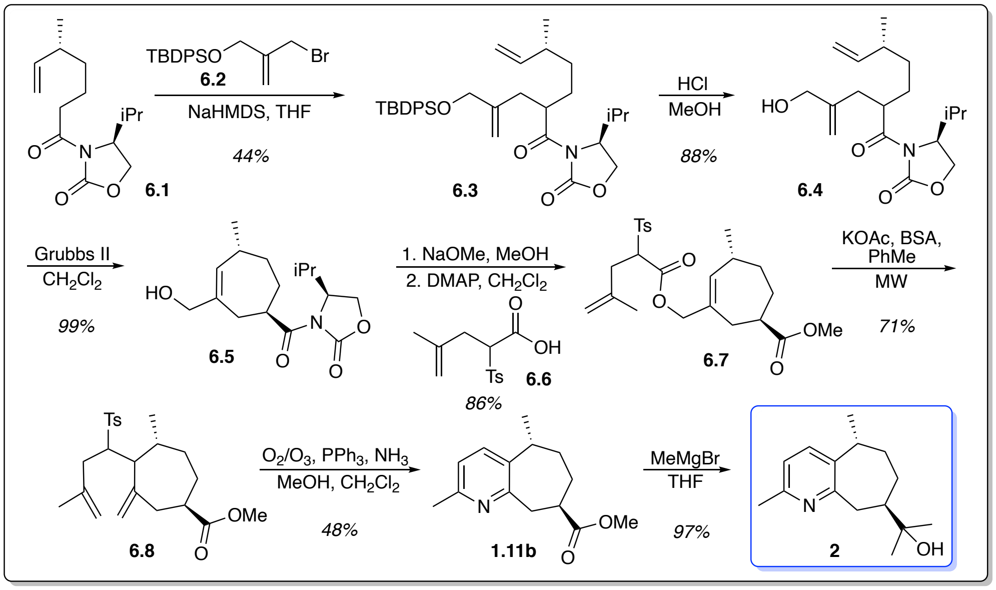

TBDPSO
Br
6.2
NaHMDS, THF
44%
iPr
O
N
6.1
6.3
HCl
MeOH
88%
HO
6.4
Grubbs II
CH2Cl2
99%
6.5
1. NaOMe, MeOH
2. DMAP, CH2Cl2
OH
Ts
6.6
86%
6.7
OMe
KOAc, BSA, PhMe
MW
71%
6.8
O2/O3, PPh3, NH3
MeOH, CH2Cl2
48%
1.11b
MeMgBr
THF
97%
2
OH

Their synthetic success and characterization brought into question the true specific rotation value of (+)-cananodine. Hsieh et al. cited {$[\alpha]^{25}_{D}$ -76.2° (*c* 0.06, $CHCl_3$)} in the first isolation of the compound,[7] while Craig and Henry reported {$[\alpha]^{21}_{D}$ +17.9° (*c* 1.34, $CHCl_3$)}.[8] The latter source believes their rotation value is more accurate as they used a higher concentration and received a value of greater magnitude after normalizing the data.

Approximately ten years later, under the advisement of Dr. James Vyvyan, the second synthesis of (+)-cananodine was attempted (Scheme 7).[9] First, the pyridine backbone was accessed through a strategic choice of starting material, pyridyl iodide **7.1**. This underwent a Suzuki-Miyaura coupling using a palladium catalyst and silver oxide to set the stage for an asymmetric dihydroxylation, giving the diene intermediate **7.2**. Diene **7.2** was modified to diol **7.3** using methanesulfonamide in an enantioselective Sharpless dihydroxylation,[46] which established the desired stereochemistry at C8. After epoxidation of diol using methanesulfonyl chloride, the key reaction in the study was employed, the intramolecular epoxide opening reaction. The picolyl proton was deprotonated using *n*-butyllithium to form the seven-membered carbocycle (**7.5**). The synthetic route was concluded with setting the final C5-stereocenter via hydrogenation of the exocyclic alkene, giving (+)-cananodine (**2**) and epi-cananodine (**7.6**) (1:1). These same methods were utilized to produce (-)-cananodine and its epimer with the same results. AD-mix β was used instead of AD-mix α, setting the opposite stereocenter at C8.

Scheme 7. First attempt of (+)-cananodine by the Vyvyan group.[9]

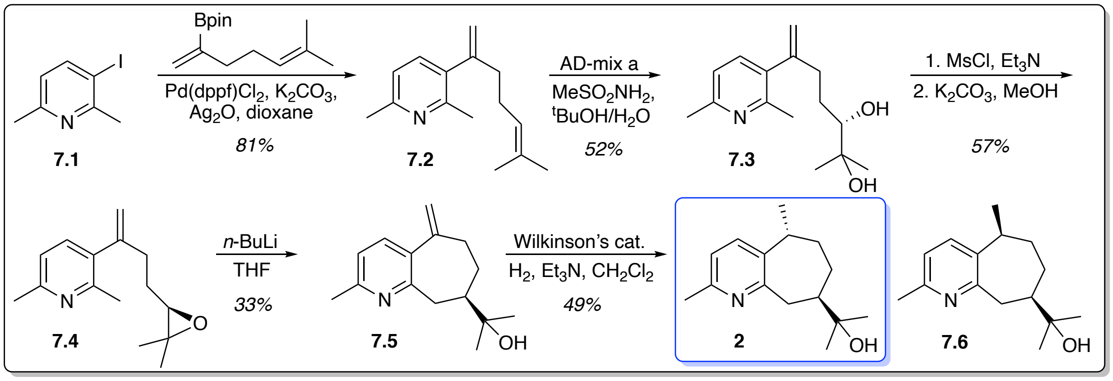

Several issues arose with this route. First, deprotonation of the picolyl proton (**7.4**) was non-selective, explaining the low yield observed in this step (33%). Second, the final step involving the non-diastereoselective hydrogenation produced a 1:1 mix of inseparable diastereomers.

A second attempt by the Vyvyan group in 2020 sought to address the downfalls of the first attempt (Scheme 8).[10] Starting with picolyl bromide **2.2** established the crucial pyridine backbone, similar to the first attempt. The guaipyridine skeleton was established by first alkylating **8.2** using lithium hexamethyldisalizide and methyl-5-hexenoate. Intermediate **8.3** was deprotected using a palladium catalyst, then **8.4** was formed using *N*-phenyltriflamide and triethylamine. Execution of an intramolecular Heck reaction with a palladium catalyst was to follow, forming the seven-membered carbocycle (**8.5**). The final step utilized palladium on carbon to hydrogenate the exocyclic alkene- giving two diastereomers (**8**, **11b**). Using methyl lithium to reduce the methyl ester, (+)-cananodine (**2**) and rupestine D (**6**) was isolated (70%, 9%). The final yield of (±)-cananodine was 8%.

Scheme 8. Second attempt of (±)-cananodine synthesis by the Vyvyan group.[10]

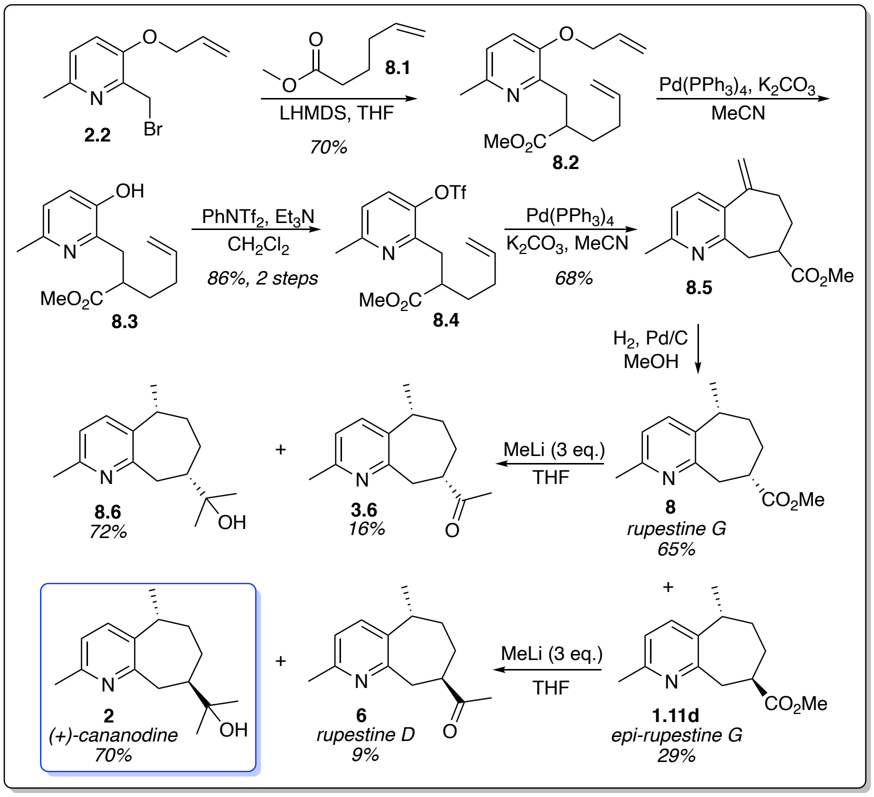

2.2
Br
N
O
8.1
LHMDS, THF
70%
MeO2C
8.2
Pd(PPh3)4, K2CO3
MeCN
OH
8.3
PhNTf2, Et3N
CH2Cl2
86%, 2 steps
OTf
8.4
Pd(PPh3)4
K2CO3, MeCN
68%
8.5
CO2Me
H2, Pd/C
MeOH
8.6
72%
OH
3.6
16%
MeLi (3 eq.)
THF
8
rupestine G
65%
2
(+)-cananodine
70%
6
rupestine D
9%
1.11d
epi-rupestine G
29%

While this route succeeds in its efficiency and simplicity, the final steps to set both stereocenters were non-selective, leading to low yields of the desired cananodine diastereomer and production of less desirable side-products: rupestine G, epi-cananodine, and associated epimers.

The most recent synthesis of cananodine was of the (-)-enantiomer by Zhang et al[12] in 2021 which excelled in enantioselectivity and creativity (Scheme 9). It is highly adaptable to achieve other desirable synthetic targets. Scheme 9 visualizes the full synthetic path to (-)-cananodine, but it must be noted that intermediate **9.8** can be manipulated to additionally achieve the enantioselective synthesis of (-)-rupestine D, (-)-guaipyridine, and (-)-epiguaipyridine.

Scheme 9. Zhang et al. synthesis of (-)-cananodine.[12]

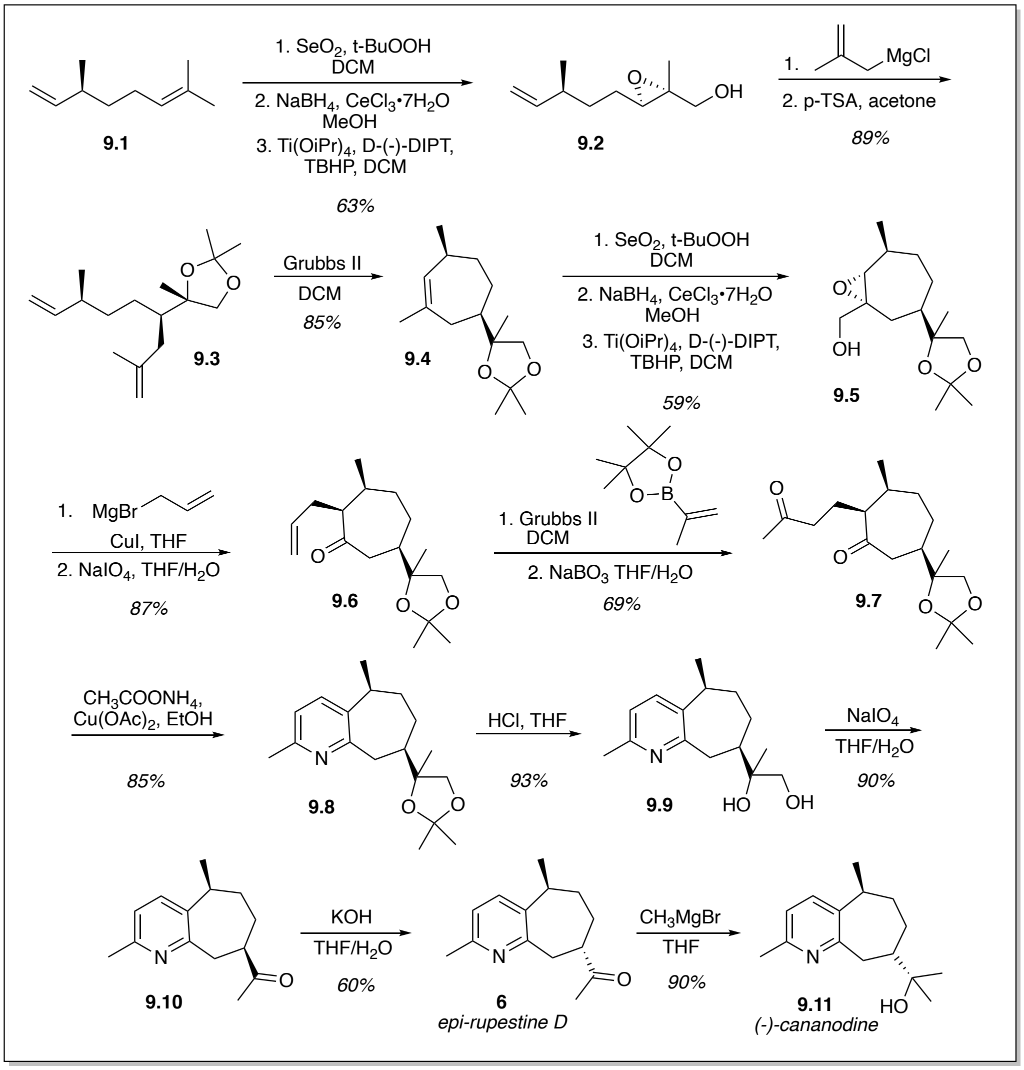
9.1
1. SeO2, t-BuOOH DCM
2. NaBH4, CeCl3•7H2O MeOH
3. Ti(OiPr)4, D-(-)-DIPT, TBHP, DCM
63%
9.2
1. MgCl
2. p-TSA, acetone
89%
9.3
Grubbs II DCM
85%
9.4
1. SeO2, t-BuOOH DCM
2. NaBH4, CeCl3•7H2O MeOH
3. Ti(OiPr)4, D-(-)-DIPT, TBHP, DCM
59%
9.5
1. MgBr
CuI, THF
2. NaIO4, THF/H2O
87%
9.6
1. Grubbs II DCM
2. NaBO3 THF/H2O
69%
9.7
CH3COONH4, Cu(OAc)2, EtOH
85%
9.8
HCl, THF
93%
9.9
NaIO4 THF/H2O
90%
9.10
KOH THF/H2O
60%
6
epi-rupestine D
CH3MgBr THF
90%
9.11
(-)-cananodine

While this route capitalized on important synthetic highlights from 2006[8] and 2017[9], the desired enantiomer (**9.11**) was isolated in only 6% yield in over 15 steps. Two Sharpless epoxidations[47], two ring-closing metatheses[43], and the classic Chichibabin pyridine synthesis[45] was employed to achieve the target product. The C5 stereocenter was accessed using (*S*)-(+)-citronellene (**9.1**). This starting material underwent a Riley oxidation[48] and Sharpless asymmetric epoxidation[47] in three steps to give epoxide **9.2**. Using 2-methylallylmagnesium chloride, an intramolecular epoxide ring opening set the C8-stereocenter. Protection of the 1,2-diol using acetone gave ketal **9.3.** Ring closing metathesis with Grubbs II catalyst provided **9.4**, which closed the seven-membered ring as a cycloheptene product. Verification of the stereocenter orientations was determined using single crystal X-ray analysis. Re-using methods from step 1, another epoxide was formed to undergo a second diastereoselective epoxide ring opening step. A single isomer was produced which was then reacted with allylmagnesium bromide in the presence of copper iodide, followed by oxidation of the primary alcohol to give ketone **9.6**. The second cross-metathesis reaction was conducted using Grubbs II catalyst again and excess boronate ester. The resultant alkenyl boronate was oxidized using sodium perborate, affording diketone **9.7**. In a 'biomimetic' fashion, the pyridine ring was formed using ammonium acetate and copper acetate in ethanol. This critical step formed the last key element of the guaipyridine skeleton. The ketal formed diol (**9.9**) in excess acid. **9.9** underwent oxidative cleavage with sodium iodate to give ketone **9.10**, another epimer of rupestine D. Finally, excess methylmagnesium bromide was used to reduce **9.10** and give (-)-cananodine (**9.11**) at 6.4% yield in 11 steps.

This interesting synthetic route is highly versatile: divergence from intermediate **9.8** readily produces (-)-rupestine D, (-)-guaipyridine, (-)-epiguaipyridine, and (-)-cananodine. It is also scalable: intermediate **9.4** was produced in a yield of six grams. Finally, the route enables access to the opposite enantiomers of all products by using (*R*)-(+)-citronellene as starting material and the opposite stereoisomer of the *D*-(-)-DIPT Sharpless reagent for both epoxidations.[47]

While an interesting and noteworthy method, its lengthiness and reduced yield leaves plenty of room for progress to be made in establishing an optimized route to access (+)- and (-)-cananodine, and fellow rupestine targets. The following chapters detail the most current research toward the synthesis of the target guaipyridine alkaloids, (+)- and (-)-cananodine.

Chapter 2: Synthesis of (+)-cananodine: Redox-relay Heck reaction

2.1 Background: Mizoroki-Heck Reaction

The biological activity of the first target compound, (+)-cananodine, is likely instrinsically tied to its absolute stereochemistry, making selectivity the major challenge of this study. The first envisioned synthetic route focuses on setting the C5 stereocenter first using a novel enantioselective redox-relay Heck reaction. This method was "high-risk" due to minimal study of this reaction with pyridine moieties.

The novel redox-relay reaction was based on work by Mizoroki[49] and Heck[50] who separately but simultaneously discovered the utility of Pd^0 catalysts with aryl halogens/triflates coupling with alkyl pi-systems to form substituted alkenes. (Figure 8). The coupling capability of this classic reaction comes from the reactivity of Pd^0 to form C-X bonds after oxidative addition (Pd^{II}) and migratory insertion. Subsequent reductive elimination forms the desired C-C bond, and regenerates the reactive Pd^0 species.

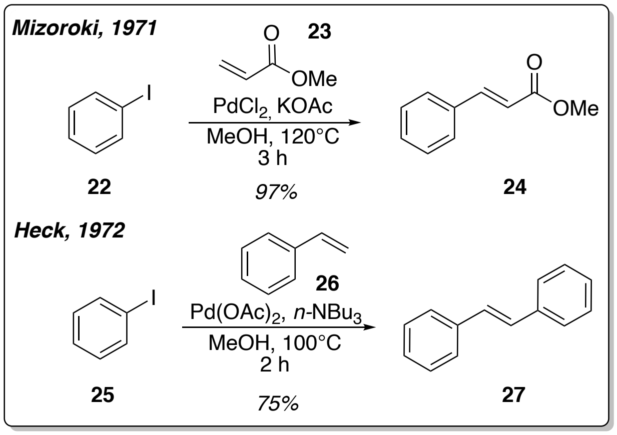

Figure 8. Original coupling reactions by Mizoroki and Heck.

This ground-breaking discovery was the first documented methodology using Pd-catalysis to form C-C bonds. A versatile reaction, the alkene substrate need not be activated[51] enabling accessibility to a diverse number of products. Since its discovery, the Mizoroki-Heck reaction has been used in the optimized synthesis of common commodities: naproxen[52] and octyl methoxy cinnamate[53], a common active ingredient in sunscreen. In recent years, the synthesis of asymmetric natural products has flourished using unique modifications to the Mizoroki-Heck/Heck reaction.[54]

The conventional Mizoroki-Heck coupling proceeds by the initial oxidative addition of Pd^0 into a halide or triflate, followed by migratory insertion of the olefin to access the short-lived intermediate alkylpalladium(II) species[55] (Figure 9). Quickly, beta-hydride elimination follows to give the coupled olefin product. The final step regenerates Pd^0 via reductive elimination of the β-H by the selected base.

Mizoroki-Heck-type reactions can proceed via oxidative or reductive routes. The reductive variant follows a similar mechanism as the classic iteration, but diverges after the formation of the Pd^{II} intermediate to give an unsaturated aliphatic product[55] (Figure 11).

The alternate product is intercepted by a hydride source that forms a new C-H bond after reductive cleavage. This route is restricted by the orientation of the β-H in respect to the palladocycle intermediate. Most commonly, substrates with the ability to form enolate intermediates are best equipped to undergo the reductive Heck reaction.

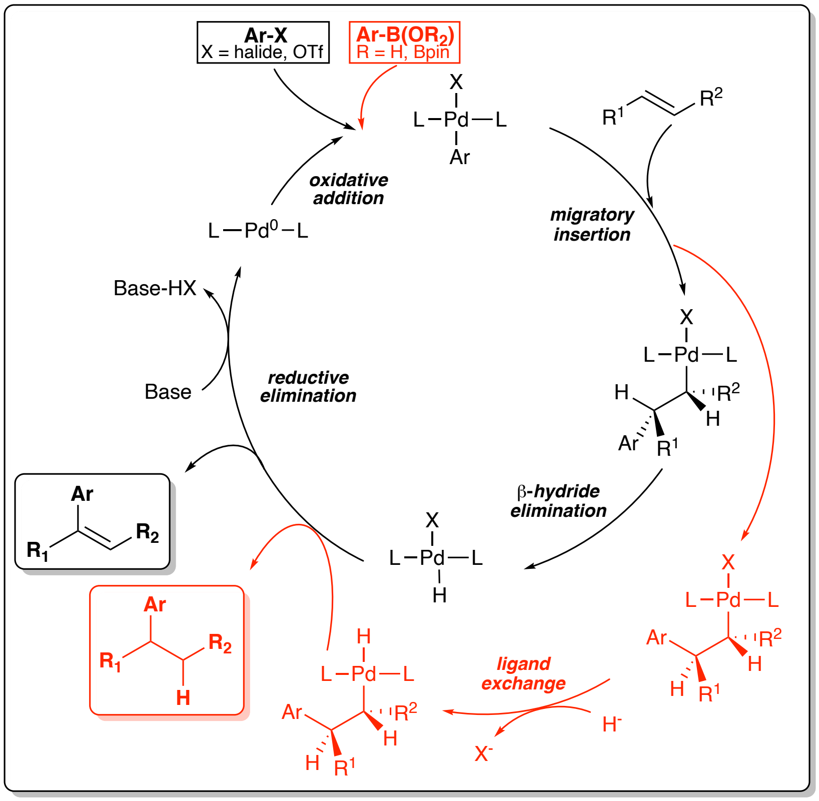
Ar-X
X = halide, OTf
Ar-B(OR2)
R = H, Bpin
oxidative addition
migratory insertion
reductive elimination
β-hydride elimination
ligand exchange
Base-HX
Base
L–Pd0–L
H-
X-

Figure 9. Comparison of conventional and reductive Heck reactions.

The oxidative route utilizes a Pd^{II} catalyst and an organoboronic acid or ester (Figure 10). This variant method is formally the "oxidative boron Heck" reaction, but generallly called the "oxidative Heck" reaction. This route varies mechanistically in the first catalytic cycle step.[54] Instead of oxidative addition of Pd^0 to the reactive leaving group, transmetallation occurs between the organoboron substrate and a Pd^{II} catalyst. The last step requires an oxidant (e.g. O$_2$, air, etc) to regenerate the resultant Pd^{II} species after coupling.

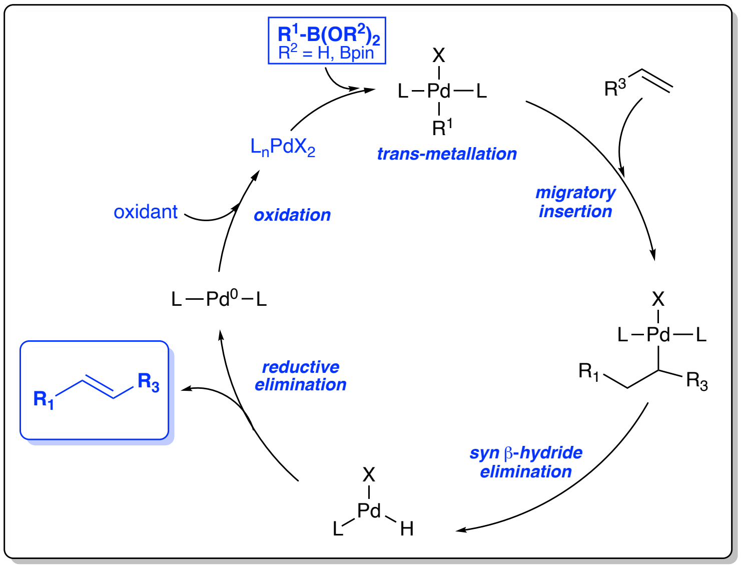

Figure 10. Oxidative Heck catalytic cycle.

In the last decade, both conventional and variant Heck systems have undergone strategic modifications to control regio-, stereo-, and chemo-selectivity using chiral ligands and/or substrates.[56-59] The first demonstrations of an *asymmetric* Heck reaction to set tertiary and quaternary stereocenters were reported by Shibasaki[60] and Overman[61] in 1989. Only modest enantioselectivity was achieved, but in the following decades, great strides were made in improving selectivity.

In 2004, Shibasaki successfully synthesized several chiral natural products using this method in enantiomeric excess (ee%) up to 99%. Following the success of these preliminary enantioselective endeavors, research towards their optimization flourished. The next section details the versatility of the asymmetric Heck to function with many functional groups, catalyst systems, and enol substrates.

Controlling stereoselectivity is critical in the quest towards synthesizing desirable natural products. The progression of increasingly complex Heck methodologies are highly useful in the synthesis of chiral natural products and the synthetic development of chiral pharmaceutical agents. Ensuring proper stereochemistry is a worthy challenge in modern organic synthesis, and this progress towards discovering the full capability of the enantioselective Heck reaction is a worthwhile investment.

2.2 Enantioselective redox-relay Heck reaction

One of the leaders developing new enantioselective Heck methodologies is Sigman at the University of Utah, whose findings have propelled the conceptualization of the enantioselective redox-relay Heck reaction. His research group has successfully demonstrated compatibility of a vast range of starting materials, coupling partners, chiral ligands, and catalyst systems to selectively produce optically pure products.

The redox-relay reaction differs from conventional Heck-type reactions in several intriguing ways. The redox-relay results in the oxidation of the alcohol after the migratory insertion step, at which time the Pd-complex migrates along the alkenol alkyl chain via a series of beta-hydride elimination steps, a process known as "chain walking".[58] Chain-walking is terminated upon alcohol oxidation when subsequent tautamerization of an enol yields the carbonyl product.

The traditional Heck reaction generally requires electron-deficient alkenes, resulting in the unsaturated arene-alkene coupling product following dissociation of the Pd-complex from the alkene.[59] To favor migration of the metal, Sigman hypothesized that an electrophilic catalyst and an electron-poor arene source were required. These assumptions led to the use of diazonium salts and PyrOx ligands- whose diminished Lewis basicity were likely more compatible than phosphine ligands.

In 2012, Sigman and coworkers[59] published the first enantioselective redox-relay Heck reaction via arylation of acyclic alkenyl alcohols. The electron-poor aryldiazonium salts were coupled with simple alkenols to produce β-, γ-, or δ-aryl optically pure carbonyls using the chiral Pyr-Ox ligand (**10.3**) (Scheme 10). Reaction of both (*E*)- and (*Z*)- alkenyl substrates resulted in high ee%, producing the respective enantiomer opposite from the starting material configuration.

Scheme 10. Stereoselectivity of the redox-relay product is contingent on the orientation of the starting alkeneol substrate.[59]

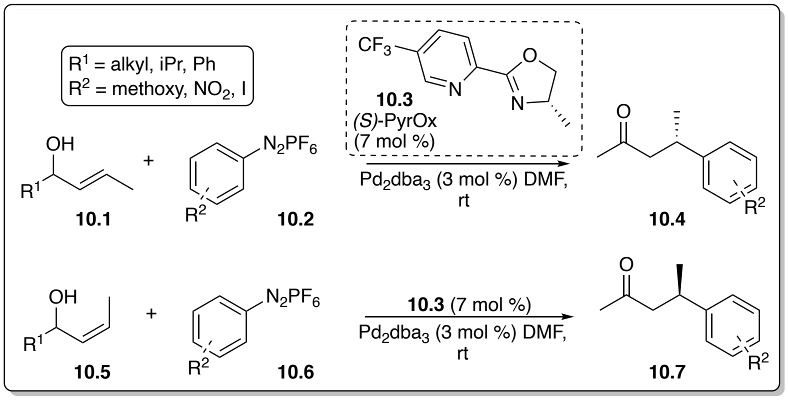

Racemic allylic alcohols, homoallylic primary and secondary alcohols, and bis-homoallylic alcohols all yielded aldehyde or ketone products with >90-95% ee, However, Sigman reported diminished regio-selectivity with increasing distance of the alcohol, and observed a 4:1 ratio of δ- or γ-products. ($\delta : \gamma$).[59] The success of these experiments prompted the continued exploration of redox-relay using varying substrates and the assessment of limitations of the methodology.

Since this 2012 publication, Sigman has continuously proven the utility of the mechanism using a diverse range of starting materials and catalyst systems. Under varying conditions, target carbonyl products were produced using a wide number of uniquely substituted cycloalkanes,[62-65] lactams,[66] allylic alkenols and ethers,[59,65,67-69] among others. Variations of aryl starting materials also selectively yielded desired product: aryl boronic acids,[68] vinyl triflates,[69] and alternative diazonium salts.[59]

Although there is a rich history exploring Pd cross-coupling over the last half century, pyridine substrates have not yet been proven to be universally compatible with popular Pd catalyst systems and/or electron poor enols. The preliminary trials in this study sought to set C5 of the (+)-cananodine skeleton using redox-relay conditions to assess the coupling capability of pyridine substrates with (*Z*)-2-buten-1-ol.

Exploratory studies in this synthetic route (Scheme 11) towards the first target compound, (+)-cananodine, envisioned accessing the first stereocenter using Sigman's enantioselective redox-relay Heck reaction. The outcome of this proof of concept is discussed in the following section.

2.3 Exploratory Studies

This synthetic route begins with a nucleophilic of addition of the picolyl bromide **2.2** with methyl acetate using LHMDS at -75 °C to form pyridyl ester **11.1**. Next, in a two-step process, **11.1** is deprotected using a Pd^0 catalyst under basic conditions to provide the corresponding phenol, followed by reaction with $PhNTf_2$ and NEt_3 to yield the triflate. This reaction provides a prime leaving group to undergo the enantioselective Heck redox-relay coupling. This is the key reaction in the study using a Pd^0 catalyst, chiral ligand (*S*)-PyrOx (**10.3**), and enol **11.3**. The asymmetric Heck reaction using the triflate **11.2** yields the optically active aldehyde **11.4**. The new stereocenter at C5 defines the first of two stereocenters, whose enantiomeric excess is determined using chiral GC.

Subsequent reduction of **11.4** using sodium borohydride in MeOH and bromination using NBS and PPh_3 yields the alkyl halide **11.5** whose formation is critical in forming the final critical feature of the guaipyridine skeleton, the seven-membered carbocycle. Intramolecular ring closure is instigated by deprotonation using LHMDS. Diastereomers **8** and **1.11d** are produced which are readily isolable by column chromatography. The synthesis is concluded with reduction of the ester to the target tertiary alcohol using MeLi at -78 °C.

Scheme 11. The first synthetic route sought to set the C5 stereocenter first.

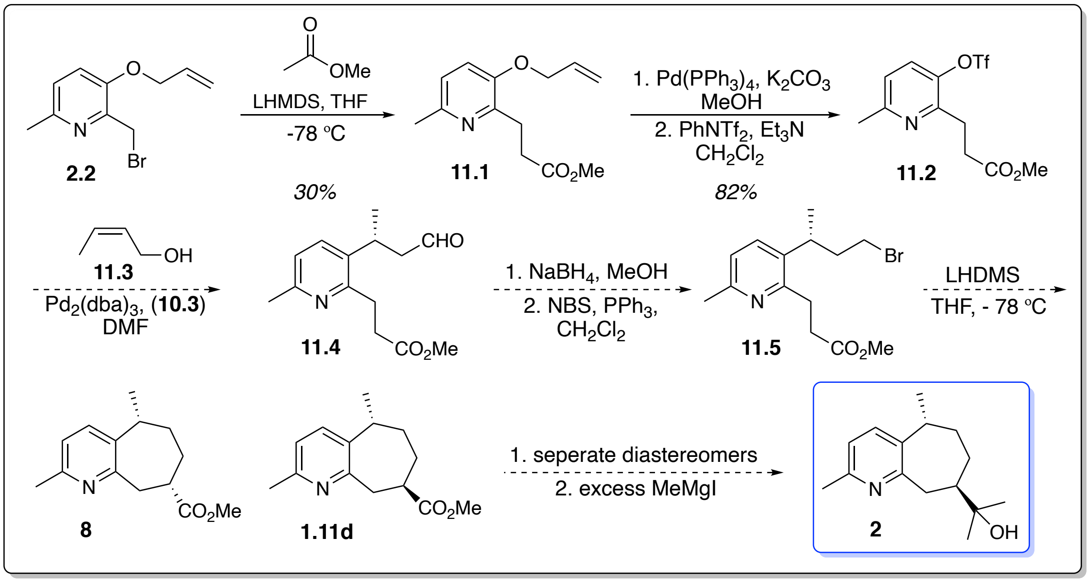

2.2
Br
OMe
LHMDS, THF
-78 °C
30%
11.1
CO₂Me
1. Pd(PPh₃)₄, K₂CO₃
MeOH
2. PhNTf₂, Et₃N
CH₂Cl₂
82%
OTf
11.2
CO₂Me
OH
11.3
Pd₂(dba)₃, (10.3)
DMF
CHO
11.4
CO₂Me
1. NaBH₄, MeOH
2. NBS, PPh₃,
CH₂Cl₂
Br
11.5
CO₂Me
LHDMS
THF, - 78 °C
N
8
CO₂Me
1.11d
CO₂Me
1. seperate diastereomers
2. excess MeMgI
2
OH

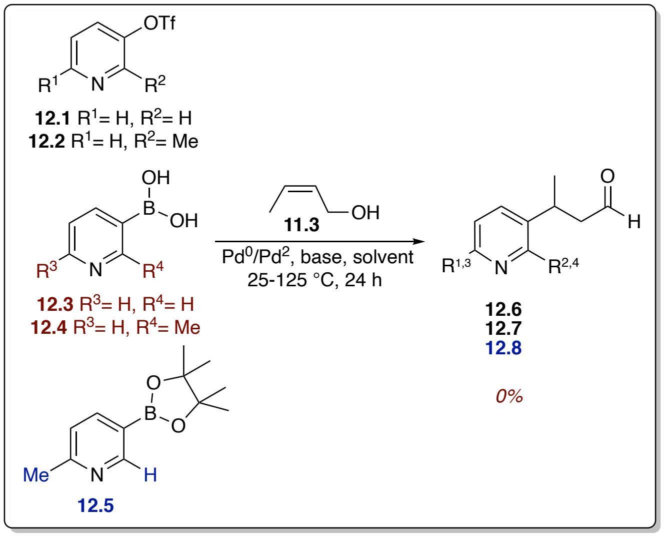

Scheme 12. Proof of concept experiments

The compatibility of the enantioselective redox-relay Heck reaction with the guaipyridine skeleton was first assessed using readily synthesized triflates starting materials in preliminary trials. Pyridyl triflates (**12.1** and **12.2**) were used to determine the eventual success of the redox-relay with the guaipyridine skeleton (**11.2**). Initially leaving out a chiral ligand made the reaction conditions non-selective, but allowed for testing of the reaction's viability. Using inexpensive starting materials enabled low-stakes optimization of chiral GC methods necessary to later separate the resultant minor/major enantiomers. Later trials would attempt to optimize enantiomeric purity of the aldehyde (**11.4**) using other catalyst/ligand systems once feasibility with the guaipyridine moiety was verified. Promising Pd catalysts were paired with different additives/atmospheres in variable conditions for reaction with the test materials. Ultimately, all permutations of conditions did not yield desired product; only triflate starting material was recovered (Scheme 12, Table 1). Next, commercially available boronic acids and esters (**12.3** – **12.5**) were tested for compatibility with the selected pyridine test materials. At best, trace product was observed via ^{1}H NMR along with four side products that were inseparable by column chromatography. An *oxidative* redox-relay Heck reaction[71] was tested to see assess a different system's productivity. A Pd^{II} catalyst instead of Pd^{0} was utilized, along with O$_2$ gas or air as an oxidant. This method failed to yield isolable aldehyde (**12.6-12.8**) using boronic acids/esters and triflates.

Table 1. Proof-of-concept redox-relay reactions using pyridine triflate substrates. Enol (**A**) signifies (*Z*)-4-buten-1-ol. Enol (**B**) denotes (*Z*)-4-hexen-1-ol.

Catalyst	Substrate	Enol	Base	T °C	Solvent	Additives	Yield %
Pd(PPh$_3$)$_4$	12.1	A	-	rt	DMF	-	0
	12.2	A	-	rt	DMF	-	0
Pd(OAc)$_2$	12.1	A	-	rt	DMF	-	0
	12.3	A	-	rt	DMF	O_2	*trace*
	12.3	A	BiPy	80	DMSO	CuCl, air	0
	12.3	A	BiPy	80	DMSO	CuCl, air, 3A MS	0
	12.4	A	-	rt	DMF	O_2	0
	12.5	A	-	rt	DMF	O_2	0
Pd$_2$(dba)$_3$	12.1	A	-	rt	DMF	-	0
	12.1	A	-	rt	DMF	3A MS	0
	12.1	A	K_2CO_3	rt	DMF	-	0
	12.1	B	-	rt	DMF	(*S*)-PyrOx, 3A MS, O_2	0
Pd(MeCN)$_2$-(OTs)$_2$	12.3	B	-	rt	DMF	Cu(OTf)$_2$, (*S*)-PyrOx, 3A MS, O_2	0

No formal conclusion was reached regarding why no single starting material tested was converted to product. It was speculated that due to the increased electronic density of the pyridine ring, the slower migratory insertion step was not feasible. After determining that the redox-relay Heck reaction was not compatible with any commercially available/readily synthesized pyridine substrates, the first proposed synthetic route was abandoned.

Although these pyridines were not reactive using redox-relay, it illuminated a shortcoming of Sigman's novel reaction. This concept has not yet been extensively reported in the literature, making these findings important for future work in coupling pyridine substrates. Further mechanistic interrogation is required to definitively answer why desired aldehyde product was not readily produced using pyridine substrates.

Chapter 3: Synthesis of (+)-cananodine: Asymmetric Alkylation

3.1 Diastereoselective Evans Alkylation

Although the first proposed synthetic route using the redox-relay Heck reaction was not fruitful, the featured back-up plan uses an alternative type of Mizoroki-Heck type reaction with great success. The alternative synthetic route transitions to setting the C8 stereocenter first instead of C5. The retrosynthetic analysis detailed in Scheme 13 was implemented to continue progress toward the target compound, (+)-cananodine.

Scheme 13. Retrosynthesis of (+)-cananodine

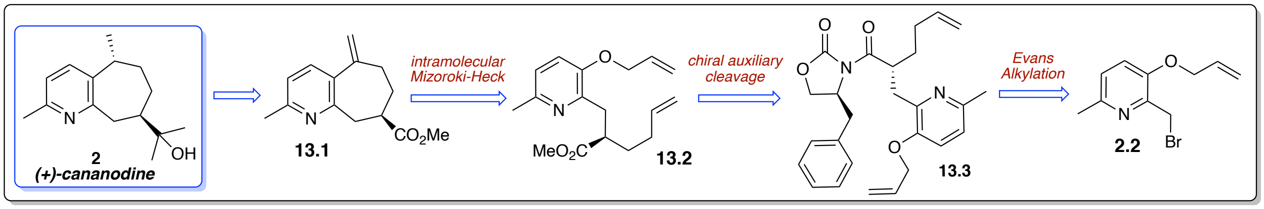

This new proposed route sought to diastereoselectively set C8 first and isolate the isomer with desired stereochemistry at C5 second. Using a non-selective hydrogenation method of the exocyclic methylene group at C5, two diastereomers are produced which require separation by column chromatography to isolate the optically pure penultimate intermediate.

Pictured in Scheme 13, the most critical reaction in this route is the Evans alkylation.[72] This reaction relies on steric hindrance to promote diastereoselectivity during alkylation of a substituted chiral auxiliary. In this study, the oxazolidinone auxiliary **14.1** includes a bulky benzyl group that provides the steric hindrance necessary to set the desired orientation of the stereocenter at C5. Using a strong base, the adjacent methylene is deprotonated, forming an enolate that attacks the picolyl bromide in an S_N2 fashion.

Evans pioneered the use of chiral oxazolidinone auxiliaries in 1982, using sodium or lithium amide bases to form the respective imide enolate to react with various benzylic or allylic electrophiles.[72] The diastereoselectivity of this method is noteworthy: the group reported ratios of greater than or equal to 99:1 of the specified desired diastereomer. Later, Evans expanded the use of the chiral oxazolidinone auxiliaries to explore asymmetric Diels-Alder reactions[73] which he later used in the total synthesis of (+)-himgaline, (+)-galbulmima alkaloid 13,[74] and (+)-lepicidin A.[75]

His work encouraged the subsequent development of a wide range of asymmetric synthetic methods important in the synthesis of chiral natural products and pharmaceutical intermediates, in which it is critical to set stereocenters during early stages of the synthesis.[76] The increasing importance of chirality in modern drug design further increased the stakes to find new ways to promote enantio- and diastereoselectivity.

After ensuring the orientation of C8 using the diastereoselective alkylation, the next most important reaction is the intramolecular Heck ring-closing reaction to achieve the last signature feature of the guaipyridine skeleton: the seven-membered carbocycle. The first attempt of this reaction was conducted by Mori et al[77] in 1977 using Pd^{II} to catalyze the synthesis of indoles and isoquinolines from aryl halides. This discovery was highly important due to the lack of reports on intramolecular Pd-catalyzed couplings since Mizoroki and Heck's discovery earlier that decade. Additionally, the Mori publication was the first to demonstrate the formation of heterocycles using this methodology. Further conceptualization of merging the concepts of asymmetry in an intramolecular fashion took place over the following decades, leading to the development of many modifications to achieve the asymmetric intramolecular Heck reaction.[78-80] The mechanism of this reaction mirrors that of the redox-relay (Scheme 11), except lacks the chain-walking step which yields the carbonyl product. The oxidative addition of the aryl halide/triflate into the Pd complex, followed by alkene coordination to the central Pd atom. Migratory insertion completes the C-C bond formation in which the product is afforded after β-hydride elimination, with subsequent reduction of Pd^{II} to Pd^0, regenerating the catalytic cycle.

The envisioned route of this study utilizes a triflate intermediate under basic conditions to access the desired carbocycle using a Pd^0 catalyst at an elevated temperature. This method was utilized with great success in past campaigns by the Vyvyan lab synthesizing ±- cananodine and ±- rupestines D and G[14] as well as ±-rupestines B and C.[16] This step was assumed to proceed without incident due to the positive results from previous studies.

3.2 Exploratory Studies

The complete reaction scheme is pictured below in Scheme 14 in which 5-hexenoic acid is reacted with thionyl chloride to form starting material 5-hexenoyl chloride **14.2**. In the first alkylation, a cheap, commercially available chiral auxiliary **14.1** is deprotonated using *n*-BuLi to react with acid chloride **14.2**. Using picolyl bromide **2.2**, a second alkylation using Evans chiral oxazolidinone is initiated to ensure the proper orientation of the new stereocenter at C8 (**13.3**). The chiral auxiliary was cleaved using $LiOH•H_2O$ and H_2O_2 using optimized conditions[81] after the Evans cleavage procedure[8] using NaOMe and MeOH failed to yield methyl ester **13.2**. Instead, only a hydroxyamide side product was isolated which proved impossible to cleave from the guaipyridine skeleton. However, peroxide-mediated cleavage using LiOOH converts the product first to the corresponding carboxylic acid, followed by acid-catalyzed esterification. After auxiliary cleavage, the route followed similar methods developed in 2020[10] in which the allyl protecting group is cleaved using $Pd(PPh_3)_4$ under basic conditions and subsequent triflation using $PhNTf_2$ and NEt_3 to produce **14.4**. The intramolecular ring-closing Mizoroki-Heck reaction yields carbovycle **13.1** whose exo-methylene group is reduced using a series of hydrogenation systems, the first employing Wilkinson's catalyst and the second using Pd/C and H_2. Extended discussion of this optimization is detailed in Chapter 5.1. The two diastereomers produced, **1.11b** and **1.11c**, were separated using flash column chromatography to isolate **1.11b,** whose ester was reduced using excess methyllithium. Isolation of the resultant tertiary alcohol completes the synthesis of (+)-cananodine (**2**).

Scheme 14. Stereoselective synthesis of (+)-cananodine in 11% yield in 7 steps.

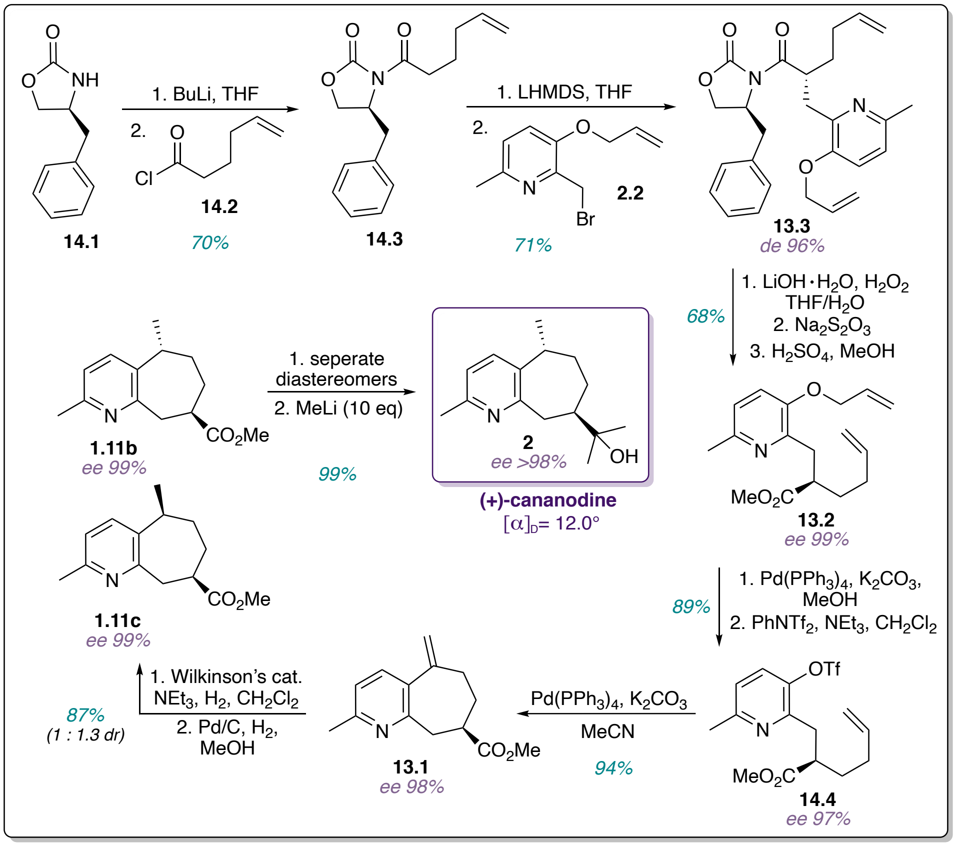
14.1
1. BuLi, THF
2.
Cl
14.2
70%
14.3
1. LHMDS, THF
2.
2.2
Br
71%
13.3
de 96%
68%
1. LiOH·H2O, H2O2
THF/H2O
2. Na2S2O3
3. H2SO4, MeOH
MeO2C
13.2
ee 99%
89%
1. Pd(PPh3)4, K2CO3,
MeOH
2. PhNTf2, NEt3, CH2Cl2
OTf
14.4
ee 97%
Pd(PPh3)4, K2CO3
MeCN
94%
CO2Me
13.1
ee 98%
87%
(1 : 1.3 dr)
1. Wilkinson's cat.
NEt3, H2, CH2Cl2
2. Pd/C, H2,
MeOH
1.11c
ee 99%
1.11b
ee 99%
1. seperate
diastereomers
2. MeLi (10 eq)
99%
2
ee >98%
OH
(+)-cananodine
[α]D= 12.0°

Spectroscopic data[8,10,11] (Table 3) and specific rotation [α]D of previously documented intermediates matched the literature except for **1.11c** (Table 2). This discrepancy is addressed in Chapter 5.2. Analysis by chiral GC verified the route selectivity: ee% of all intermediates is greater than 97%. To conclude, the selective synthesis of (+)-cananodine was achieved with a final yield of 11% after optimization (Chapter 5.1).

Table 2. Literature comparison of documented intermediates

Compound	[α]D	Lit
14.3	+57.0°	+56.7°[82]
1.11b	-47.8°	-44.0°[8]
1.11c	-55.2°	-18°[16], -16°[12,14]
2	+12.0°	+10°[11], +17.3°[8]

Table 3. Comparison of ^{1}H and ^{13}C NMR shifts observed between this study versus the first isolation[8] and first synthesis[7] of (+)-cananodine.[8] Data is reported as [chemical shift, multiplicity, coupling constant (Hz)].

	Natural product[7]		*Holliday*		*Craig and Henry*[8]	
	^{1}H	*^{13}C*	*^{1}H*	*^{13}C*	*^{1}H*	*^{13}C*
2	-	153.8	-	154.3	-	154.2
3	6.97, d (*8.0*)	121.0	6.94, d (*8.0*)	120.6	6.93	120.7
4	7.39, d (*8.0*)	133.0	7.34, d (*8.0*)	132.4	7.34	132.5
5	3.00, m	35.2	2.97, m	35.3	2.97, m	35.2
6α	1.35, m	36.0	1.25, m	36.1	----------	36.2
6β	1.90, m	-	1.89 ddq (*13.7, 6.5, 4.9*)	-	1.90, m	-
7β	1.61, m	32.7	1.60 dddd (*12.1, 12.1, 12.1, 3.6*)	32.6	1.59, qd (*12.0, 3.5*)	32.8
7α	2.07, m	-	2.10, m	-	2.10, m	-
8	1.42, m	47.9	1.42, dddd (*11.8, 10.3, 2.9, 1.5*)	48.0	1.59	48.0
9β	2.88, dd (*13.2, 6.4*)	38.9	2.88, dd (*13.4, 10.4*)	39.8	2.87, dd (*13.5, 10.5*)	39.4
9α	3.32, d (*13.2*)	-	3.21, app d	-	3.23, dt (*13.5, 1.5*)	-
4a	-	138.3	-	137.9	-	138.0
4b	-	160.6	-	160.9	-	160.9
8C	-	73.2	-	73.3	-	73.3
8-Me$_2$	1.24, s	27.8	1.26, s	27.6	1.25, s	27.9
	1.24, s	25.7	1.25, s	26.0	1.24, s	25.6
Me-2	2.51, s	23.3	2.48, s	23.9	2.49	23.7
Me-5	1.32, d (*6.8*)	20.6	1.32, d (*6.8*)	20.7	1.31, d (*7.0*)	20.7

Chapter 4: Synthesis of (-)-cananodine: Synthetic Route Flexibility

4.1 Capitalizing on Evans Alkylation

Versatile and flexible, this route facilitates the total synthesis of both target compounds. Using the same synthetic methods as the synthesis of (+)-cananodine, the opposite optically pure enantiomer, (-)-cananodine, was produced in 7 steps with a yield of 8%. Scheme 15 visualizes the retrosynthetic route towards the second target. By reversing the absolute stereochemistry at C4 of the chiral auxiliary **16.1**, the secondary alkylation establishes the desired stereochemistry at C8 of all intermediates, producing the respective opposite enantiomers isolated during the synthesis of (+)-cananodine. (Scheme 16)

Scheme 15. Retrosynthesis of (-)-cananodine

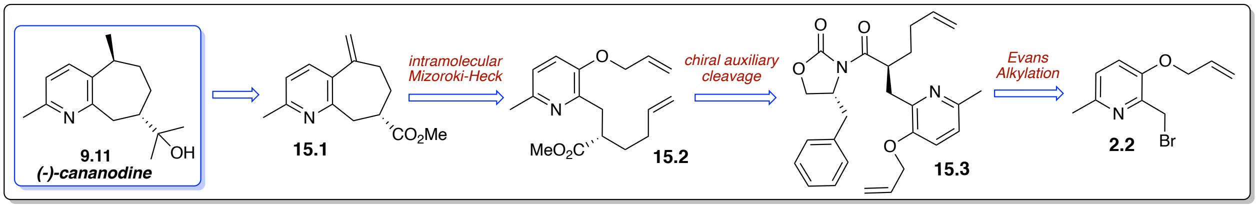

Making this minor modification to the Evans alkylation using the opposite commercially available chiral auxiliary efficiently reversed the orientation of the C8 stereocenter of all guaipyridine intermediates. Optical purity of the compounds was verified via comparison of each intermediate: the specific rotation $[\alpha]_D$ of all intermediates of (-)-cananodine were of equal magnitude and opposite sign of respective (+)-cananodine intermediates. Spectroscopic characterization of all isomers using mass spectrometry, ^{1}H and ^{13}C NMR, and IR mirrored each optically pure pair as no structural difference is detectable between two enantiomers using these methods.

4.2 Exploratory Studies

The use of starting material (*R*)-oxazolidinone **16.1** in the first alkylation with 5-hexenoyl chloride **14.2** is the only divergence from the route Scheme 14 towards (+)-cananodine. Cheap, readily available, and optically pure starting material **16.1** undergoes two alkylations to establish configuration of the C8 stereocenter, followed by cleavage of the chiral auxiliary to give ester **15.2**. Conversion to the triflate and intramolecular cyclization yields the exo-methylene carbocycle **15.1**, and subsequent hydrogenation affords two *epi*-rupestine G diastereomers. Separation of the penultimate compound from undesired isomer **8** is followed by ester reduction, giving the target tertiary alcohol which concludes the synthesis of (-)-cananodine.

Scheme 16. The second target molecule, (-)-cananodine, is produced in 8% in 7 steps.

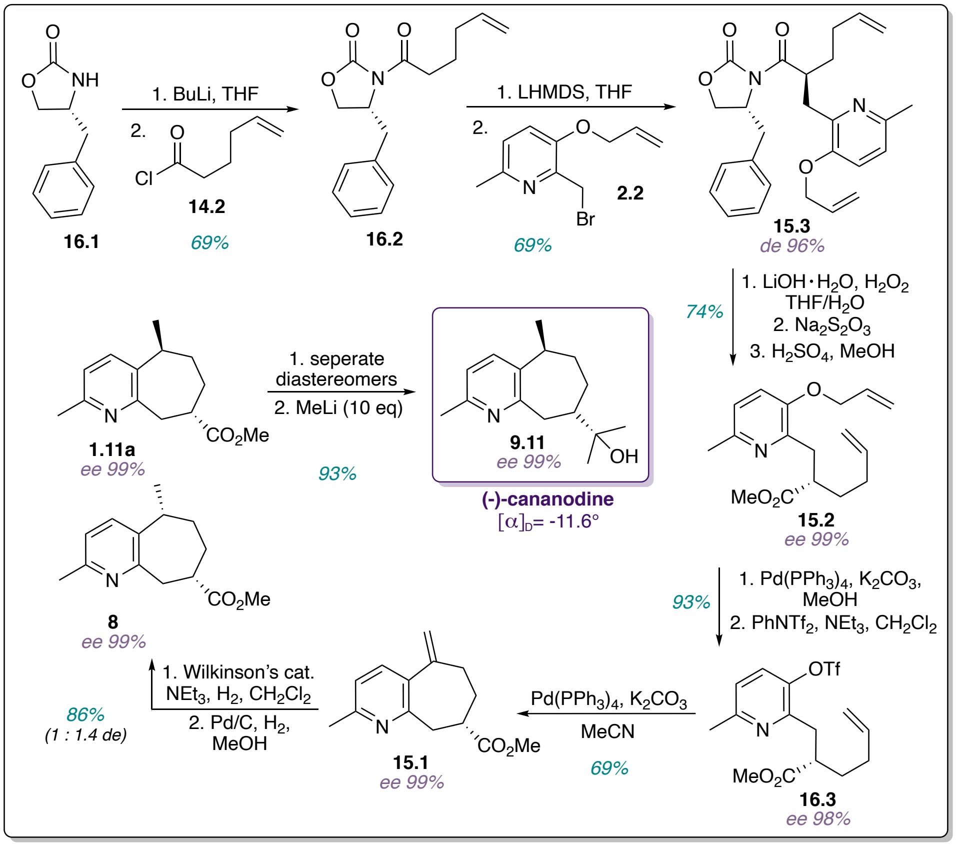
16.1
1. BuLi, THF
2.
Cl
14.2
69%
16.2
1. LHMDS, THF
2.
2.2
Br
69%
15.3
de 96%
1. LiOH·H2O, H2O2
THF/H2O
2. Na2S2O3
3. H2SO4, MeOH
74%
15.2
ee 99%
MeO2C
1. Pd(PPh3)4, K2CO3, MeOH
2. PhNTf2, NEt3, CH2Cl2
93%
OTf
16.3
ee 98%
Pd(PPh3)4, K2CO3
MeCN
69%
15.1
ee 99%
CO2Me
1. Wilkinson's cat.
NEt3, H2, CH2Cl2
2. Pd/C, H2,
MeOH
86%
(1 : 1.4 de)
8
ee 99%
1.11a
ee 99%
1. seperate diastereomers
2. MeLi (10 eq)
93%
9.11
ee 99%
OH
(-)-cananodine
[α]D= -11.6°

Table 4. Literature comparison of specific rotation $[\alpha]_D$

Compound	$[\alpha]_D$	Lit
16.2	-64.7°	-69.0°[82]
1.11a	+53.0°	-41.0°[16]
8	+53.2°	+17.0°[16]
9.11	-11.6°	-10.0°[11]

Optical and spectroscopic data of intermediates previously published in the literature were in excellent agreement with compounds produced in this study (Table 5) except for intermediate **8** (see Chapter 5.2). Spectroscopic data (MS, NMR, IR) of (-)-cananodine precursors with their opposite enantiomers gave identical results. Specific rotation values $[\alpha]_D$ observed were of equal magnitude and opposite sign of enantiomer pairs (Tables 2 and 4), proving the selectivity of the route. ^1H and ^{13}C NMR spectra of this target and (+)-cananodine intermediates synthesized in this study

(Scheme 14) were in excellent agreement. With several exceptions, spectra also matched those of the target compound by Zhang et al in 2021[12] in a recent study that also included apparent reporting errors (Table 5). Chiral GC analysis demonstrated the excellent selectivity of the route: ee% of all intermediates was greater than 97%. In conclusion, the selective synthesis of (-)-cananodine was achieved using identical methods of the synthesis of (+)-cananodine. All intermediates were thoroughly characterized and matched those of the opposite enantiomer. A final yield of 8% is reported after conquering yield optimization and characterization challenges which are discussed in Chapter 5.1. In Section 5.2, an effort will be made to elucidate reasons for discrepancies between specific rotation values in several past studies.

Table 5. Comparison of ^{1}H and ^{13}C NMR shifts observed between this study versus the first selective synthesis[12] of (-)-cananodine. Data is reported as [chemical shift, multiplicity, coupling constant (Hz)].

	Holliday et al		*Zhang et al*[12]	
	^{1}H	*^{13}C*	*^{1}H*	*^{13}C*
2	-	154.2	-	154.0
3	6.93, d (*7.8*)	120.7	6.92, d (*7.9*)	120.6
4	7.34, d (*7.7*)	132.4	7.33 (*7.9*)	132.4
5	2.97, m	35.3	2.95, m	35.1
6α	1.25, m	36.1	0.82, m	36.1
6β	1.89, ddq (*13.7, 6.4, 5.0*)	-	1.88, d (*12.9, 4.3*)	-
7β	1.60 dddd (*12.1, 12.1, 12.1, 3.6*)	32.6	1.58, m	32.7
7α	2.10, m	-	2.08, dt (*13.3, 2.5*)	-
8	1.42, m	48.0	1.40, t (*11.0*)	47.9
9β	2.88, dd (*13.2, 10.2*)	39.7	2.85, m	39.3
9α	3.22, app d	-	3.23, d (*13.3*)	-
4a	-	137.9	-	138.0
4b	-	160.9	-	160.9
8C	-	73.3	-	73.2
8-Me_2	1.26, s	27.6	*1.23, s (6H)*	27.7
	1.25, s	26.0	----------	25.6
Me-2	2.48, s	23.9	2.46	23.6
Me-5	1.32, d (7.0)	20.7	1.30, d	20.6

Chapter 5. Optimization and Characterization

5.1 Optimization

After successful synthesis of both target compounds, yield optimization was necessary to increase the efficiency of the route. The first several transformations posed the greatest threat to the overall yield of (+)- and (-)-cananodine. Important considerations critical to optimize each step include ensuring complete conversion of starting material, minimizing formation of side products, and maximizing extraction of crude products.

The most pressing issues that diminish the overall efficacy of the route surround the first three steps of the synthesis: alkylation of chiral auxiliary, alkylation of picolyl bromide, and the cleavage of the chiral auxiliary. Conversion to triflate **14.3** proceeded smoothly in high yield, but Heck cyclization remained difficult. Last, methods to reduce the exocyclic methylene group required significant attention to increase the ratio of desired diastereomer produced. In this section, discussion of each major issue and their solutions are detailed.

First and Second Alkylation

The first two steps of the synthesis were ultimately the lowest-yielding due to unavoidable formation of side product **28** (Figure 11). The maximum yield of both reactions after strategic procedural modification was 74%, modest improvement from an average of 58-63%. In step one, alkylation of **14.1** using *n*-BuLi and 5-hexenoyl chloride (**14.2**) produces hexenoyl-oxazolidinone **14.3** along with significant generation of side product **28**. Assuming that after reaction of the auxiliary with acid chloride, the resultant **14.3** is deprotonated at the α-C by unreacted base (Figure 11). This enolate proceeds to attack the nucleophilic carbonyl of other newly formed products, forming side product **28** after the chiral auxiliary functions as a leaving group upon collapse of the tetrahedral intermediate.

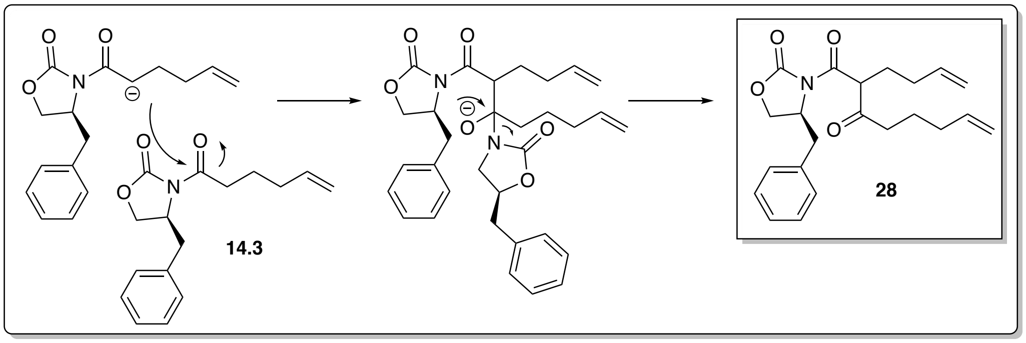

Figure 11. Proposed mechanism of side product formation during the first and second steps.

Before identification of side product **28**, several procedural modifications were tested to increase desired product formation. Various combinations of excess reagents, picolyl bromide and *n*-BuLi, were tested to access higher conversion of starting material to no avail. Optimization of this step was decidedly unsuccessful and progress toward the target compound continued.

The second alkylation proceeds by drop-wise addition of LHMDS to the alkylated Evans auxiliary to form an enolate that attacks the picolyl bromide to yield the alkylation product diastereoselectively. However, a sizeable fraction of the same side product **28** from the first alkylation is observed. The mechanism of this unfavorable side reaction is identical to alkylation 1, except **28** is formed from enolate attack on unreacted starting material **14.1**, rather than newly formed product **14.3**. This theory is supported by both ^{1}H and ^{13}C NMR analysis of isolated **28** plus observation via ^{1}H NMR of the crude product in which all hexenoyl-oxazolidinone is consumed, but a sizeable fraction of unreacted pyridyl bromide remained.

The initial procedure began with addition of base to starting material **14.3** very slowly at -78 °C followed by addition of pyridyl bromide after one hour. It was hypothesized that this slow addition of base and pausing before pyridine addition increases enolate attack on starting material. In an effort to mitigate the formation of **28**, several variations of the initial procedure were tested.

Hoping that immediate S_N2 substitution would occur following deprotonation, the alkylated auxiliary was deprotonated by LHMDS in the presence of the pyridyl bromide. First, base was added dropwise to a solution of both starting materials at -78 °C and allowed to slowly warm to room temperature overnight. Second, the order of addition was reversed in which the solution of starting material was added dropwise to the base at -78 °C. The final variation resembled the initial unoptimized method except that pyridyl bromide was immediately added after the base, pausing only 10 minutes rather than 60 minutes.

Unfortunately, all three trials were unsuccessful. Rampant side product formation was apparent and only trace product was formed. Purification of these trials yielded the minor fraction of product and two major fractions of side products: an inseparable mix of unknowns and a curious isolable compound whose spectroscopic profile resembled that of the picolyl bromide, but formed an uncharacteristic vibrant purple oil after purification. This side product was soon identified as dimerized pyridyl bromide starting material, whose formation further decreased the efficiency of the reaction.

The discouraging results of these trials for the first and second alkylation resulted in begrudging acceptance that further improvement of these troublesome alkylations was not feasible. Efforts were redirected to improve other problematic reactions.

Cleavage of chiral auxiliary

After diastereoselective alkylation promoted by the oxazolidinone auxiliary, its removal is necessary after stereochemistry at C8 is ensured. Rapid cleavage and esterification was assumed to readily produce ester **13.2** using NaOMe in MeOH.[8] A seemingly simple and predictable substitution reaction, this method failed spectacularly. Only an unexpected unknown side product was observed whose profile was eventually characterized as the hydroxyamide[81] **29** (Figure 12) after extensive analysis of IR, ^{1}H, ^{13}C, and COSY NMR data.

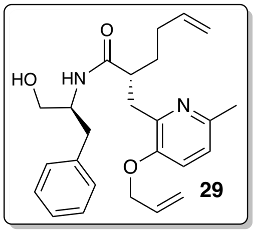

Figure 12. Hydroxyamide side product

After modifications testing temperature, alternative nucleophiles and their molar equivalents resulted only in hydroxyamide formation, this method was abandoned. In-depth literature investigation led to the featured method: a peroxide-mediated cleavage using LiOH and H_2O_2 in THF/H_2O (4:1) at 0 °C.[81] Formation of a peroxy-acid facilitates cleavage of the auxiliary which is quenched with $Na_2S_2O_3$ to isolate the intermediate carboxylic acid. When performed at room temperature, the hydroxyamide product persists as the major product. Careful maintenance of reaction conditions at 0 °C was imperative to eliminate hydroxyamide formation. After accessing the carboxylic acid, esterification is complete after refluxing the crude intermediate in MeOH with catalytic H_2SO_4 for 16-24 hours. Further optimization was achieved with diligent control of pH = 6 during the aqueous workup to avoid pyridine protonation at pH = 4 while maximizing extraction of the product.

Intramolecular Heck reaction

The second critical reaction, the intramolecular Mizoroki-Heck reaction, was demonstrated to efficiently produce the racemic carbocycle by the Vyvyan 2020 synthesis of (±)-cananodine.[10] Given their high yielding results, the cyclization using optically pure triflate was anticipated to proceed without incident. However, unsatisfactory conversion of starting material resulted in poor yields even after long reaction times (~48 hours). Incomplete triflate consumption was the primary issue, so to promote carbocycle formation, multiple 5 mol% additions of catalyst were added over 24 hours. Three additions every 8 hours were required to force reaction completion. Over time, this method of sequential additions began failing to efficiently yield pure product. A mixture of endocyclic isomers were observed by NMR that were inseparable by column chromatography, making characterization of the pure exocycle impossible. These reaction conditions were ineffective, lengthy, and wasteful, making optimization a high priority.

Analysis of the catalyst by ^1H NMR revealed a major impurity, triphenylphosphine oxide, that likely formed over time by degradation after repeated exposure to air. A simple and rapid remedy dramatically improved results by first washing the Pd catalyst with MeOH, removing the troublesome impurity that hindered reaction completion. This quick fix enabled optimization of this key reaction without further effort. Initially no more than 60-70% of triflate starting material was efficiently consumed, but after removing the impurity, complete conversion to the carbocycle product proceeded smoothly. Additionally, the increased efficiency reduced the lengthy reaction time, further minimizing isomerization of product to unwanted endocycle side products.

Reduction of exo-methylene group

The first envisioned synthetic route uses Pd/C with H_2 gas to hydrogenate the exocyclic methylene substituent. However, this system resulted in a 2:1 ratio of undesired rupestine G: *epi*-rupestine G. The overall conversion of starting material was in excellent yield, but the system was highly unfavorable as the major product was unwanted diastereomer **1.11c**.

Moving forward, Wilkinson's catalyst was assessed to test if greater diastereoselectivity could be achieved. Pure exocyclic starting material was subjected to the Rh-catalyst with triethylamine under H_2 atmosphere in methylene chloride. Analysis of crude material by ^1H NMR validated an increased diastereoselectivity of a 1:1 ratio (rupestine G: *epi*-rupestine G). However, an unexpected fraction of isomerized starting material **13.1** to an endocyclic alkene **30** which failed to undergo reduction. The two diastereomers were already difficult to separate by column chromatography, and the presence of the endocycle in the crude mixture made purification impossible. A secondary hydrogenation was necessary to complete the conversion to the two diastereomers, so the crude mix of products were purified to remove residual catalyst impurities without regard to separation of endocycle.

One strength of the Pd/C system is its ability to readily reduce trace endocyclic isomers. The purified mix of diastereomers and endocycle were resubjected to a second hydrogenation using this system resulting in successful endocycle hydrogenation, leaving only the two isomers to separate.

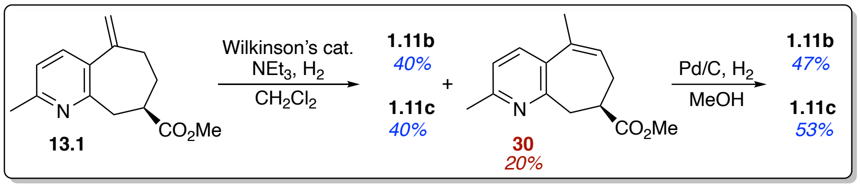

Scheme 17. Optimized hydrogenation of exocyclic alkene.

This optimization step increases the hydrogenation yield by 14%: from 33% production of desired diastereomer to 47%. The overall yield of (+)-cananodine increases by 4% and (-)-cananodine by 2%, making this optimization via catalyst selection a critical turning point in the final yield.

The last endeavor to increase the selectivity of the hydrogenation led to a collaboration with a research group in Spain that specializes in the synthesis of chiral phosphite-oxazoline ligands that have demonstrated compatibility with both pyridine substrates and exocyclic olefins.[83] Led by Dr. Monsterrat Diéguez, the exocycle **13.1** was shipped to Spain for screening with 18 chiral ligands to assess the diastereomeric ratio of **1.11b** versus **1.11c** produced using their unique catalyst system. Using 0.2 mol% Ir complexed to cyclooctadiene (cod) and the chiral ligand (L^x), and stabilized by tetrakis(3,5-bis(trifluoromethyl)phenyl)borate (Bar_F) under H_2 atmostphere in dichloromethane, the collaborating researchers sought to achieve an excess of the desired diastereomer that is the final intermediate before methyl ester reduction to the signature tertiary alcohol of cananodine (Figure 13).

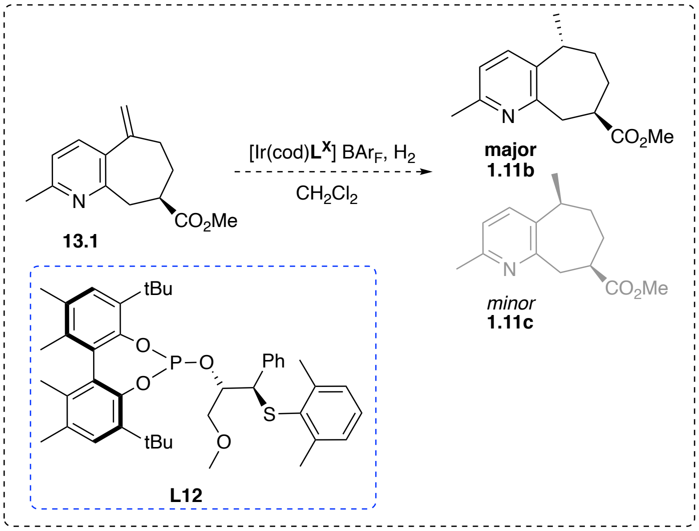

Figure 13. L12 was used to achieve a 2:1 dr (**1.11b**:**1.11c**) while a corresponding diastereomer produced a 1:2.8 dr of **1.11c**:**1.11b**.

The group's findings were promising: **L12** was able to produce an excess of desired *anti* material, while the *syn* diastereomer was the minor product, counter to results produced in this study. However, given the opportunity cost of the time required to synthesize the chiral ligand, ship starting material internationally, and the effort required to further increase dr of the desired product, the results produced were not as exceptional as expected. This first pass using the phosphite-oxazoline ligands to increase reduction selectivity was promising, but further work on this collaborative campaign is necessary to achieve the dr necessary to legitimize the costly, impractical aspects of international hydrogenation.

Protecting Group Manipulation

In an effort to cut steps and maximize yield, the triflate group was installed during synthesis of an alternate picolyl starting material substrate, **18.4**. This proposal (Scheme 18) sought to use the triflate group instead of the allyl ether as a phenol protecting group to refrain from the necessary deprotection and triflation steps intrinsic to the usage of the picolyl bromide **2.2**. In the same manner as Scheme 14 and 16, the chiral auxiliary **14.1** was alkylated using *n*-BuLi and 5-hexenoyl chloride (**14.2**) at -78 °C to afford **14.3**. Deprotonating **14.3** using LHMDS to alkylate using picolyl triflate **18.4** successfully yielded **18.5**, but within a mix of starting materials (**18.4** and **14.3**) plus various side products that all proved to be incredibly difficult to separate by TLC and flash column chromatography. The polarity of the mixture of materials were all surprisingly similar, and a wide array of solvents were screened to access desired product **18.5** to no avail.

Moving forward, a mixture of **18.5** and associated side products and starting materials were subjected to the peroxyacid cleavage treatment to assess if ester installation could improve separation of the inseparable complex. Methyl ester (**18.6**) was isolated in low yield and characterized to validate the outcome of this optimization attempt. However, due to the tricky nature of purifying the second alkylation product, this route was decidedly more detrimental to the overall yield compared to the lengthier original scheme due to the amount of product loss from overlap with side products during purification.

Scheme 18. Route optimization attempt using an alternative picolyl bromide starting material.

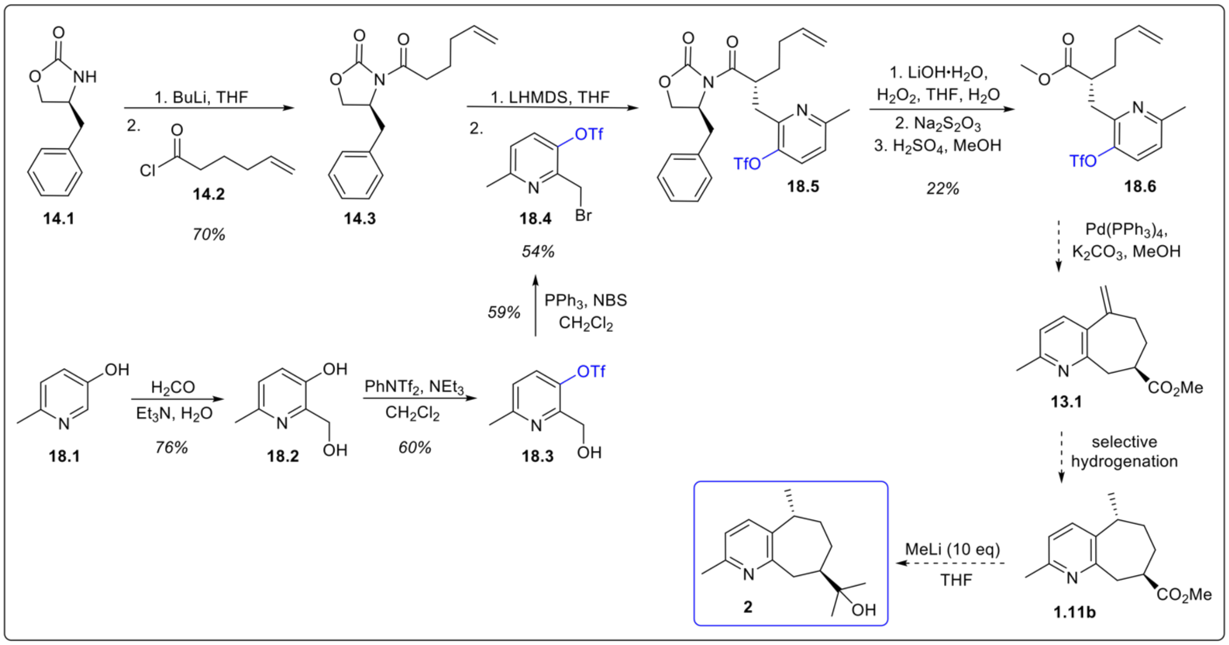
14.1
1. BuLi, THF
2.
14.2
70%
14.3
1. LHMDS, THF
2.
18.4
54%
18.5
1. LiOH•H₂O, H₂O₂, THF, H₂O
2. Na₂S₂O₃
3. H₂SO₄, MeOH
22%
18.6
Pd(PPh₃)₄, K₂CO₃, MeOH
13.1
selective hydrogenation
1.11b
MeLi (10 eq)
THF
2
59%
PPh₃, NBS
CH₂Cl₂
18.1
H₂CO
Et₃N, H₂O
76%
18.2
PhNTf₂, NEt₃
CH₂Cl₂
60%
18.3

If this route proved to be more practical, ester **18.6** would then be used to undergo the intramolecular Heck reaction to close the seven-membered ring, followed by selective hydrogenation to yield **1.11b** in the same fashion as the parent synthetic route. Finally, the target compound **2** would be afforded after six key steps by reduction with MeLi.

This attempt was worthwhile in that it validated the featured routes (Scheme 14 and 16) by demonstrating the necessity of completing the additional protection/deprotection steps. Although unknown at the time of conception, the longer route actually increases productivity by providing the necessary difference in substrate polarity required to tease apart the alkylation product from the mixture.

Another synthetic mission to access pyridyl triflate-oxazolidinone is proposed in Chapter 6 that provides inspiration for further optimization of both leaving group installation and hydrogenation selectivity (Scheme 19).

5.2 Characterization

During the first linear synthesis of the target intermediates, peculiar specific rotation values were measured that did not match values of previously reported documented compounds. Oftentimes, $[\alpha]_D$ observed was an order of magnitude larger or smaller from the expected value. Even more distressing, the opposite sign of the value was observed. Because all other means of spectroscopic verification were in agreement prior to $[\alpha]_D$ measurement, it was clear a transformation was occurring between purification/spectroscopic characterization and verification of $[\alpha]_D$. Necessitating analysis by ^{1}H NMR, it became clear immediately that the compound had changed since purification. Chemical shifts were quite different from those observed immediately following isolation. Using (-)-cananodine as an example, the first obvious indication as to what occurred was the dramatic shift of the pyridyl protons: the signals move downfield by ~0.75 ppm after measuring specific rotation (Figure 14). Second, following solvent removal after $[\alpha]_D$ measurement, the products that previously were clear, colorless oils, were observed to be white, crystalline solids that were insoluble in organic solvents. It was assumed that protonation of the pyridine had occurred during specific rotation acquisition so it was necessary to implement a basic aqueous workup using saturated sodium bicarbonate. With great relief, the original clear oil was recovered after solvent removal and resultant proton NMR signals observed shifted back to their characteristic chemical shifts.

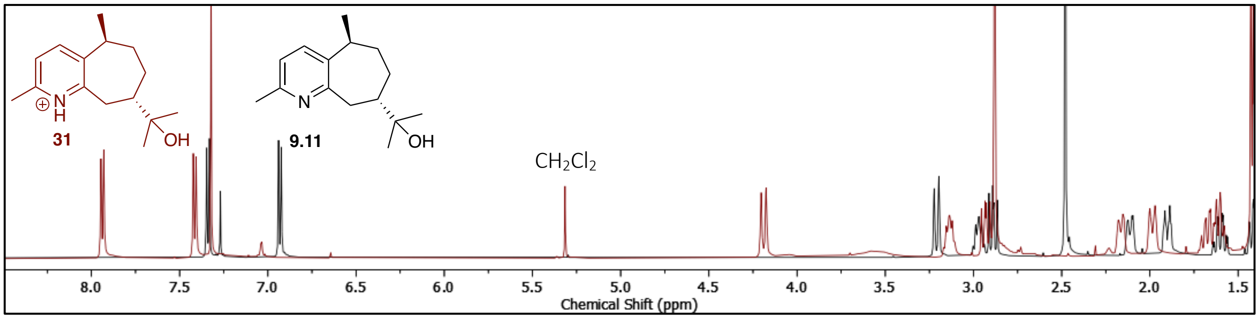

Figure 14. Overlay of ^{1}H NMR spectra: (-)-cananodine (**2**) versus protonated (-)-cananodine.

In some cases, the protonation of optically pure products led to epimerization. NMR analysis showed two or more products, assumedly diastereomers produced after exposure to highly acidic conditions. In this situation, it was necessary to discard the material, as the unwanted side products were not separable. A rapid litmus test of the chloroform used for specific rotation measurements confirmed the extreme acidity of the solvent (pH = 1). Moving forward, all chloroform was filtered over basic alumina prior to analysis of optically pure material to avoid the basic aqueous workup and potential epimerization.

Observation of this pyridine salt formation after protonation could help explain the discrepancies between optical rotation data reported by various research groups. Comparisons of values of previously synthesized intermediates align nicely except for *epi*-rupestine G of both enantiomers ((**1.11b, 8),** Table 2 and 4). However, since $[\alpha]_D$ of the enantiomer pair is of equal magnitude and opposite sign (Table 6), and both were synthesized and characterized using identical methods, the evidence points to the values reported in this study may be most reliable.

Table 6. Comparison of specific rotation $[\alpha]_D$ of both enantiomers. Concentration *c* is reported in g/100 mL $CHCl_3$.

(*S, R*)	$[\alpha]_D$	*c*
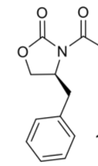 **14.3** 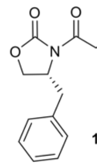 **16.2**	+57.0°, -64.1°	5.03, 5.01
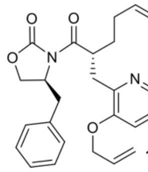 **13.3** 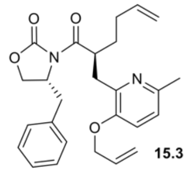 **15.3**	+36.2°, -35.5°	5.01, 5.08
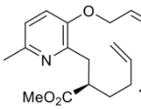 **13.2** 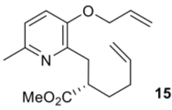 **15.2**	-9.7°, +9.3°	4.27, 5.02

(*S, R*)	$[\alpha]_D$	*c*
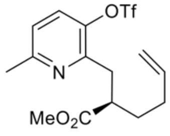 **14.4** 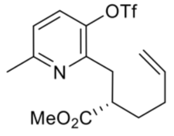 **16.3**	+1.7°, -1.4°	0.29, 4.12
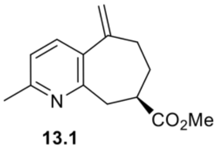 **13.1** 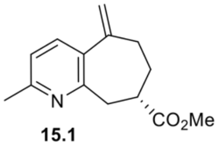 **15.1**	-71.2°, +70.4°	0.94, 0.76
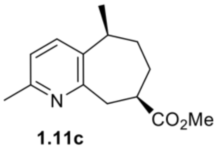 **1.11c** 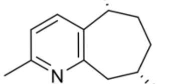 **8**	47.8°, -55.2°	0.09, 0.27
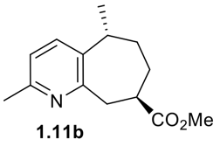 **1.11b** 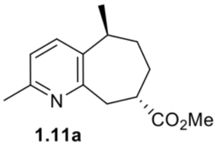 **1.11a**	+53.0°, +53.2°	0.10, 1.16
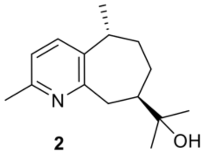 **2** 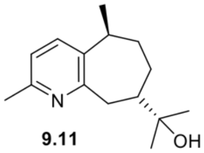 **9.11**	+12.0°, -11.6°	0.30, 0.44

Chapter 6. Conclusions

The successful synthesis and complete characterization of both target compounds was achieved in which all reactions yielded product over 68%, and many transformations were high yielding: up to 94%. Spectroscopic and optical rotation data were in excellent agreement- validating the viability of this amenable synthesis to access both enantiomers. The optical purity of each enantiomer was validated by both specific rotation in which $[\alpha]_D$ of the enantiomer pair is of equal magnitude and opposite sign (Table 6), and chiral gas chromatography where high enantiomeric excess (>96 ee%) was observed.

However, future work is necessary to further increase the diastereoselectivity of the hydrogenation to access the penultimate intermediates **1.11b** and **8** in greater excess. Scheme 19 details a new potential way this could be achieved through increased steric hindrance at C8 during the non-selective hydrogenation. By cleaving the chiral auxiliary last, the atom economy of the synthesis is increased by likely encouraging selectivity of the *syn* diastereomer via the increased steric hindrance as well as saving a step by removing the chiral auxiliary to yield the tertiary alcohol.

Scheme 19. Envisioned modification of hydrogenation.

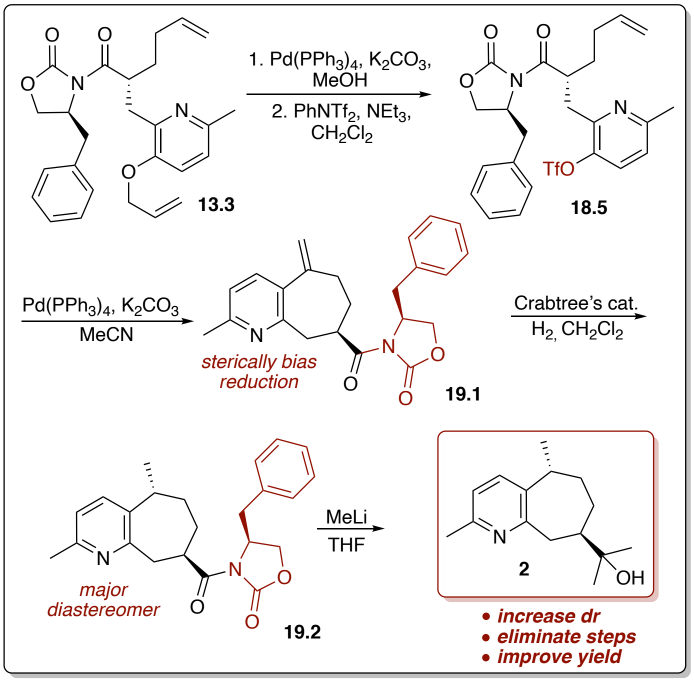
13.3
1. Pd(PPh$_3$)$_4$, K$_2$CO$_3$, MeOH
2. PhNTf$_2$, NEt$_3$, CH$_2$Cl$_2$
TfO
18.5
Pd(PPh$_3$)$_4$, K$_2$CO$_3$
MeCN
sterically bias reduction
19.1
Crabtree's cat.
H$_2$, CH$_2$Cl$_2$
major diastereomer
19.2
MeLi
THF
2
• increase dr
• eliminate steps
• improve yield

Progress made in this study provides the opportunity for further biological evaluation of both targets, and to elucidate the true potential of the enantiomers activity against HCC. Given the contradictory results between the IC_{50} measured in 2001[7] versus 2021,[11] strictly uniform assays are necessary to confirm if (+)-cananodine is a promising hit for further development as a lead towards treating HCC. In summary, both cananodine enantiomers were synthesized in an efficient and direct manner that allows for the ultimate determination of their biological activity. With final yields of 11% (**2**) and 8% (**9.11**) and enantiomeric excess (ee%) greater than 98%, the efficiency and selectivity of this synthetic route improves important aspects that prior attempts were lacking.

Chapter 7. Experimental

All glassware was oven-dried and all reactions using air sensitive materials was carried out under argon atmosphere. Also, when indicated, dry solvent from Inert PureSolv^{TM} Solvent Purification System (Et_2O, THF, CH_2Cl_2, CH_3CN) was used. All solvents that were not from the purification system was HPLC grade and used without further purification with the exception of MeOH which was dried over 3A molecular sieves (8-12 mesh, Acros Organics) and $CHCl_3$ which was flushed through basic alumina (Sorbtech, pH = 10). Celite (EMD Chemicals) containing diatomaceous earth, quartz, and cristobalite was not acid washed during manufacturing.

Starting materials that were commercially available were used without further purification: 5-hexenoic acid (>98%, Tokyo Chemical Industry Co., LTD), 6-methyl-pyridin-3-ol (98%, Combi-Blocks), N-Phenyl-bis(trifluoromethanesulfonamide ($PhNTf_2$) (99%, Oakwood Chemical), (*S*)- and (*R*)-4-benzyl-2-oxazolidinone (98%, Combi-Blocks). All catalysts utilized were commercially available ($Pd(PPh_3)_4$ (99%, Strem Chemicals, lot # L01412105 and # L03342206), Pd/C, (10% Pd, Aldrich Chemical Co., lot # 03803HP) and Wilkinsons catalyst (99%, Strem Chemicals, lot # B0170086)). All were used without further purification besides $Pd(PPh_3)_4$ which was washed with methanol and dried using vacuum filtration.

Each reaction involving extractive work-up with the organic solvents and aqueous solutions detailed was washed with saturated NaCl (brine), dried over Na_2SO_4, and concentrated using rotary evaporation. All flash column chromatography was conducted using silica gel (230-400 mesh, Silicycle) hand-packed with varying ratios of hexanes and ethyl acetate (hexanes:EtOAc) unless otherwise indicated. Silica G TLC plates (Sorbtech, polyester backed, thickness 200 μM, fluorescence UV_{254}) were used for monitoring reaction progress and flash chromatography.

Infrared spectra (IR) were collected on a ThermoiS10 FT-IR spectrometer equipped with a single bounce diamond ATR. All tabulated signals are reported in cm^{-1}. Spectra acquired as 'neat' were placed on the diamond ATR stage as a pure solid or liquid, or occasionally as films from pure compounds dissolved in $CDCl_3$ or CH_2Cl_2 then evaporated.

For NMR analysis, all samples were dissolved in deuterated chloroform (D-99.8%, +0.05% v/v TMS). ^1H and ^{13}C NMR spectra were acquired on a Varian MercuryPlus FT-NMR spectrometer (300 MHz) or Bruker Avance III FT-NMR spectrometer (500 MHz) and processed with MestreNova software. Chemical shifts are reported in ppm and coupling constants are reported in Hertz (Hz). ^1H NMR spectra in $CDCl_3$ are referenced to tetramethylsilane (TMS) at 0.00 ppm and reported using the format: chemical shift (ppm) [multiplicity (s = singlet, d = doublet, t = triplet, q = quartet, m = multiplet, app = apparent), coupling constant(s) (*J* in Hz), integral]. ^{13}C NMR spectra are referenced to $CDCl_3$ at 77.0 ppm.

Chiral gas chromatography (GC) was performed on a Varian CP3800 GC using an Agilent Cyclosil-B 30 m × 0.25 mm ID × 0.25 µm chiral column. All chiral samples were characterized using Method A.

Method A: Hold 5 minutes at 60 °C, ramp 5 °C/min to 240 °C, hold 5 minutes.

Specific rotation was measured using a Rudolph Digital Automatic polarimeter with a 10 cm quartz cell at room temperature (5 scans, wavelength = 589 nm).

Mass spectrometry was conducted using an Agilent 6545XT AdvanceBio LC-ESI-qTOF mass spectrometer to acquire HRMS spectra. An Agilent ZORBAX Eclipse Plus C18 column was used (2.1 x 50 mm, 1.8 µm). All samples were dissolved and diluted in CH_3CN (3-10 µg/mL) and eluted using a gradient of **A** (water, 0.1% formic acid) and **B** (CH_3CN, 0.1% formic acid). Sample injection volume was between 0.1-0.01 µL. Flow rate was 0.400 mL/min and maximum pressure was set to 1,100.00 bar. All samples were characterized using Method B.

Method B:

Time	A (%)	*B (%)*
0.00	95.00	5.00
1.00	95.00	5.00
6.00	5.00	95.00
6.50	5.00	95.00
6.60	95.00	5.00
8.00	90.00	10.00

2-(Hydroxymethyl)-6-methylpyridin-3-ol[84] (18.2)

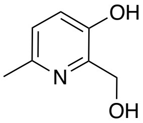

Notebook entry: 38HH, p 100

6-methylpyridin-3-ol (50.0 g, 0.458 mol), H_2O (200 mL), formaldehyde (37% in H_2O) (45 mL, 0.46 mol), and NEt_3 (64 mL, 0.46 mol) were added to a large flask for reflux overnight under air atmosphere. After the reaction was deemed complete by TLC (EtOAc) the reaction was cooled, then solvent was removed. Next, hot EtOH (200 mL) was added to dissolve the crude product to then slowly cool overnight. The resultant crystalline product was washed and dried using vacuum filtration to give pure diol. (49.5 g, 0.36 mol, 78%). mp = 153.5-155.0 °C (lit.[83] 153 °C)

(3-(Allyloxy)-6-methylpyridin-2-yl)methanol[85] (18.3)

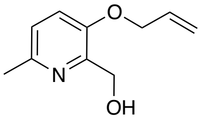

Notebook entry: 2HH, p 17

Acetone (375 mL), allyl bromide (18 mL, 25 g, 0.21 mol), 2-(hydroxymethyl)-6-methylpyridin-3-ol (24.3 g, 0.175 mol), and K_2CO_3 (49.8 g, 0.360 mol) were added sequentially and refluxed overnight under air atmosphere. The reaction was stopped ~24 hours later after analysis by TLC. The product was isolated after washing with acetone and drying using vacuum filtration. Solvent was removed and the resultant product **18.2** was used without further purification (33.8 g, 0.176 mol, 98%). mp = 53.0-55.7 °C (lit.[85] 51.9-52.8 °C)

3-(Allyloxy)-2-(bromomethyl)-6-methylpyridine[85] (2.2)

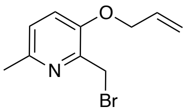

Notebook entry: 6HH, p 28

N-bromosuccinimide (16.97 g, 95.37 mmol), and pyridyl alcohol (**S2**) (16.56 g, 92.46 mmol) were put under argon atmosphere, followed by addition of dry DCM (275 mL). The solution was cooled to -78 °C then PPh_3 (25.45 g, 97.03 mmol) was added slowly in three additions over 45 minutes after which the reaction was left to stir for 3 hours. After all starting material was consumed, solvent was removed and filtered through silica (3:1 hexanes:EtOAc). Solvent was removed and **2.2** was isolated as a white solid (17.07 g, 70.48 mmol, 76%). mp = 39.4- 41.0 °C (lit.[85] 40.0-40.4 °C).

^{1}H NMR (500 MHz, $CDCl_3$): δ 7.11 (d, *J* = 8.6 Hz, 1H), 7.07 (d, *J* = 8.6 Hz, 1H), 6.07 (ddt, *J* = 15.6, 10.5, 5.0 Hz, 1H), 5.46 (ddt, *J* = 17.4, 1.7, 1.7 Hz, 1H), 5.34 (ddt, *J* = 10.7, 1.5, 1.5 Hz, 1H), 4.66 (s, 2H), 4.63 (ddd, *J* = 4.9, 1.5, 1.5 Hz, 2H), 2.50 (s, 3H) ppm.

Methyl 3-(3-(allyloxy)-6-methylpyridin-2-yl)propanoate (11.1)

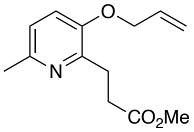

Notebook entry: 11HH, p 38.

A flask containing dry THF (50 mL) was cooled to -78 °C and LHMDS (12.0 mL, 12.0 mmol) was added. A solution of picolyl bromide (2.660 g, 10.99 mmol), methyl acetate (0.839 g, 11.33 mmol), and THF (40 mL) was added dropwise to the solution. After addition was complete (~2 hrs), the mixture was diluted in Et_2O and washed with NH_4Cl. The aqueous layer was extracted twice with Et_2O and combined organic layers were dried over Na_2SO_4 for one hour. Solvent was removed and the crude product was purified using flash chromatography (2:1 hexanes:EtOAc). Product **11.1** was isolated as a clear yellow oil (0.784 g, 3.33 mmol, 30%) as well as starting material **2.2** (1.071 g, 4.4 mmol, 40%).

IR: 3080, 3000, 2960, 1730, 1460, 1260, 1120, 990 cm^{-1}.
^{1}H NMR (500 MHz, $CDCl_3$): δ 7.04 (d, *J* = 8.5 Hz, 1H), 6.94 (d, *J* = 8.4 Hz, 1H), 6.03 (ddt, *J* = 15.7, 10.4, 5.1 Hz, 1H), 5.40 (dd, *J* = 15.6, 1.5 Hz, 1H), 5.30 (dd, *J* = 10.5, 1.5 Hz, 1H), 4.52 (d, *J* = 6.8 Hz, 2H), 3.68 (s, 3H) 3.17 (t, *J* = 7.9 Hz, 2H), 2.77 (t, *J* = 7.9 Hz, 2H), 2.47 (s, 3H) ppm.
^{13}C NMR (125 MHz, $CDCl_3$): δ 174.3, 150.9, 149.3, 149.1, 133.2, 121.7, 119.5, 118.0, 69.4, 52.1, 32.5, 27.8, 23.5 ppm.
HRMS: (ESI, q-TOF) *m/z* [M +H] calcd for $C_{26}H_{30}N_2O_4$ 236.1242; found 236.1283.

Methyl 3-(6-methyl-3-(((trifluoromethyl)sulfonyl)oxy)pyridin-2-yl)propanoate (11.2)

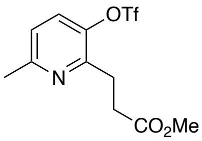

Notebook entry: 16-17HH, p 52-55

$Pd(PPh_3)_4$ (0.033 g, 0.029 mmol) and K_2CO_3 (0.959 g, 6.9 mmol) were added to a flask containing allyl ester (**11.1**) (0.548 g, 2.33 mmol) and put under argon. MeOH (14 mL) was added to the flask and the mixture was left to stir at room temperature overnight. The mixture was diluted in CH_2Cl_2 (50 mL) and washed with saturated NH_4Cl. The aqueous layer was extracted twice with CH_2Cl_2 before drying over Na_2SO_4. Solvent was removed and phenol was isolated as a white solid (0.448 g). Crude product was used without further purification.

$PhNTf_2$ (1.394 g, 3.9 mmol) was added to a flask with crude phenol and put under argon. This was dissolved in CH_2Cl_2 (18 mL) and NEt_3 was added (0.60 mL, 4.3 mmol). After stirring for 3 hours, the reaction was diluted in Et_2O (60 mL) and washed sequentially with sat. NH_4Cl, 10% NaOH and sat. NaCl. After drying over Na_2SO_4, solvent was removed and product was purified by flash chromatography (2:1 hexanes:EtOAc) giving **11.2** a clear yellow oil (0.606 g, 1.85 mmol, 82%).
IR: 2960, 1740, 1590, 1420, 1200, 1130, 1080, 867, 629 cm^{-1}.
^{1}H NMR (500 MHz, $CDCl_3$): δ 7.48 (d, *J* = 8.5 Hz, 1H), 7.08 (d, *J* = 8.4 Hz, 1H), 3.72 (s, 1H), 3.19 (t, *J* = 7.3 Hz, 2H), 2.87 (m, *J* = 7.1 Hz, 2H), 2.55 (s, 1H) ppm.
^{13}C NMR (125 MHz, $CDCl_3$): δ 173.0, 157.9, 151.5, 143.0, 129.0, 122.3, 118.5 (q, *J* = 320.2 Hz), 51.6, 31.3, 26.5, 23.8 ppm.
HRMS: (ESI, q-TOF) *m/z* [M +H] calcd for $C_{26}H_{30}N_2O_4$ 328.0422; found 328.0457.

(*Z*)-2-Buten-1-ol[86] (11.3)

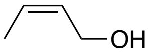

Notebook entry: 29HH, p 81

Ni(OAc)$_2$•4H$_2$O (4.436 g, 17.83 mmol) was added to a flask and put under argon. MeOH (95 mL) was added and cooled to 0 °C. Next NaBH$_4$ (0.674 g, 17.8 mmol) and (CH$_2$NH$_2$)$_2$ (3.0 mL, 44 mmol) was added to the black mixture, followed by addition of 2-butyn-1-ol (5.34 mL, 71.3 mmol) diluted in MeOH (36 mL). H$_2$ was then added using two 12 in. balloons filled with the gas. One was vented through the flask and the other was left to maintain the atmosphere overnight. The progress of the reaction was monitored using 1:1 pentane:Et$_2$O. After consumption of starting material, the suspension was taken up in Et$_2$O (70 mL) and filtered through Celite. The organic layer was washed with brine, then the aqueous layer was extracted three times using Et$_2$O. Combined organic layers were washed three times with sat. NaCl then dried over Na$_2$SO$_4$. Solvent removal and subsequent purification using flash column chromatography (pentane, 25% acetone) gave **11.3** a clear yellow oil (3.586 g, 49.74 mmol, 70%).

^{1}H NMR (500 MHz, CDCl$_3$): δ 5.54 (m, 2H), 4.15 (d, *J* = 6.4 Hz, 2H), 1.61 (d, *J* = 5.2 Hz, 3H), 1.42 (br s, 1H) ppm.

Pyridin-3-yl trifluoromethanesulfonate[87] (12.1)

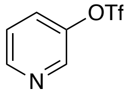

Notebook entry: 19HH, p 59.

PhNTf$_2$ (6.420 g, 17.97 mmol) was added to a flask with pyridin-3-ol (1.006 g, 10.58 mmol) and put under argon. This was dissolved in CH$_2$Cl$_2$ (60 mL) and cooled to 0 °C. To this mixture, Et$_3$N was added (2.50 mL, 18.0 mmol). Progress was evaluated by TLC (1:1 hexanes:EtOAc) and the reaction was complete after 2.5 hours. The mixture was diluted in Et$_2$O (50 mL) and washed sequentially with saturated NH$_4$Cl, 10% NaOH and saturated NaCl. The washed organic product was dried over Na$_2$SO$_4$ for one hour. Solvent was removed before purifying using flash chromatography (1:1 hexanes:EtOAc). The product **12.1** was isolated as a clear yellow oil (2.169 g, 9.560 mmol, 91%).

IR: 3070, 1420, 1200, 1130, 1020, 877, 811, 747, 700, 597 cm^{-1}.
^{1}H NMR (500 MHz, CDCl$_3$): δ 8.69 (dd, *J* = 4.7, 1.5 Hz, 1H), 8.64 (d, *J* = 2.9 Hz, 1H), 7.67 (ddd, *J* = 8.5, 2.9, 1.4 Hz, 1H), 7.47 (dd, *J* = 8.5, 4.7 Hz, 1H) ppm.
^{13}C NMR (125 MHz, CDCl$_3$): δ 149.6, 146.8, 142.9, 129.1, 124.7, 118.5 (q, *J* = 320.6 Hz) ppm.

2-Methylpyridin-3-yl trifluoromethanesulfonate[88] (12.2)

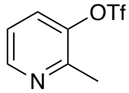

Notebook entry: 20HH, p 61.

PhNTf$_2$ (5.571 g, 15.60 mmol) was added to a flask with 2-methylpyridin-3-ol (1.005 g, 9.209 mmol) and put under argon. This was dissolved in CH$_2$Cl$_2$ (55 mL) and cooled to 0 °C. To this mixture, Et$_3$N was added (2.17 mL, 15.8 mmol). Progress was evaluated by TLC (1:1 hexanes:EtOAc) and the reaction was complete after 2.5 hours. The mixture was diluted in Et$_2$O (50 mL) and washed sequentially with saturated NH$_4$Cl, 10% NaOH and saturated NaCl. The washed organic product was dried over Na$_2$SO$_4$ for one hour. Solvent was removed before purifying using flash chromatography (1:1 hexanes:EtOAc). Product was isolated as a clear yellow oil (1.559 g, 6.445 mmol, 70%).

IR: 3080, 2970, 1600, 1420, 1210, 1130, 892, 818, 603 cm^{-1}.
^{1}H NMR (500 MHz, CDCl$_3$): δ 8.55 (dd, *J* = 4.7, 1.5 Hz, 1H), 7.60 (dd, *J* = 8.2, 1.5 Hz, 1H), 7.27 (dd, *J* = 8.4, 4.9 Hz, 1H), 2.64 (s, 3H) ppm.
^{13}C NMR (125 MHz, CDCl$_3$): δ 151.8, 148.7, 145.5, 129.0, 122.6, 118.4 (q, *J* = 320.6 Hz), 59.3 ppm.

5-Hexenoic acid[89] (S1)

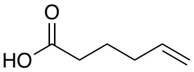

Notebook Entry: 84HH, pg. 213-215.

Cyclohexanone (6.21 mL, 60.1 mmol) was added to a 50 mL round bottom flask and dissolved in MeOH (10 mL). H$_2$O$_2$ (30%, 9.4 mL, 120 mmol) was added dropwise fast over 2-3 minutes. In a separate 250 mL round bottom flask, CuSO$_4$•5H$_2$O (15.01 g, 60.11 mmol) and FeSO$_4$•7H$_2$O (16.72 g, 60.14 mmol) were dissolved in H$_2$O (90 mL). After 50 minutes, the peroxide intermediate solution was added 2 mL at a time to the metal-hydrate solution, maintaining ~25 °C. After addition, the mixture stirred for 1.75 hours at which time Et$_2$O was added and the organic layer was extracted three times. The combined organic layers were washed three times with 10% NaOH and set aside, meanwhile collecting the aqueous layers. These basic aqueous portions were acidified to pH = 3 using 6M HCl, then product was extracted using Et$_2$O three additional times. Then combined organic layers were dried over Na$_2$SO$_4$. Crude acid was purified using flash column chromatography (3:1 hexanes: EtOAc) to give a light yellow oil (2.216 g, 19.41 mmol, 32%).

^{1}H NMR (500 MHz, CDCl$_3$): δ 5.78 (ddt, *J* = 16.9, 6.7, 10.2 Hz, 1H), 5.04 (dd, *J* = 17.1, 1.8 Hz, 1H), 5.00 (dd, *J* = 10.2, 2.0 Hz, 1H), 2.37 (t, *J* = 7.5 Hz, 2H), 2.12 (app q, 2H), 1.75 (app quintet, 2H) ppm.
^{13}C NMR (125 MHz, CDCl$_3$): δ 179.6, 137.5, 115.6, 33.2, 32.9, 23.7 ppm.

5-Hexenoyl chloride[90] (14.2)

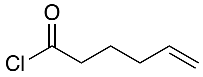

Notebook entry: 46HH pg. 119-120

5-hexenoic acid (3.95 mL, 33.7 mmol), CH_2Cl_2 and thionyl chloride (65 mL, 1.0 M in CH_2Cl_2, 65 mmol) were refluxed for 6 hours when the reaction was deemed complete by TLC (3:1 hexanes:EtOAc). Solvent was removed and the product (**14.2**) was used without further purification.

^{1}H NMR (500 MHz, $CDCl_3$): δ 5.75 (ddt, *J* = 17.0, 10.3, 6.7 Hz, 1H), 5.09-5.01 (m, 2H), 2.90 (t, *J* = 7.2 Hz, 2H), 2.11 (app q, 2H), 1.80 (app quintet, 2H) ppm.

(*S*)-4-Benzyl-3-(hex-5-enoyl)oxazolidin-2-one[82] (14.1)

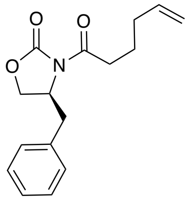

Notebook entry: 90HH, pg. 226.

(*S*)-4-Benzyl-2-oxazolidinone (3.943 g, 22.28 mmol) was put under argon and dissolved in THF (20 mL). The mixture was cooled to -78 °C. *n*-BuLi (13.9 mL, 22.4 mmol (1.6 M in hexanes)) was added dropwise and stirred for 30 minutes. 5-hexenoyl chloride (1.969 g, 14.85 mmol) was added in THF (15 mL). The reaction was allowed to warm to room temperature overnight. After reaction completion, sat. NH_4Cl was used to quench after dilution with EtOAc (25 mL). The aqueous layer was extracted twice with EtOAc. Combined organic layers were washed twice with sat. NaCl, then dried over Na_2SO_4. After solvent removal, the crude product was purified using flash column chromatography (3:1 hexanes:EtOAc) to give pure product **14.1** (2.835 g, 10.37 mmol, 70%) as a clear, yellow viscous oil.

$[\alpha]^{20}_D$ +57.0° (*c* 5.01, $CHCl_3$)
IR: 3070, 2930, 2360, 1771, 1700, 1390, 1210, 703, 669 cm^{-1}.
^{1}H NMR (500 MHz, $CDCl_3$): δ 7.34 (app t, 2H), 7.28 (app t, 1H), 7.21 (app d, 2H), 5.83 (dddd, *J* = 17.0, 10.1, 6.6, 6.6 Hz, 1H), 5.06 (dddd, *J* = 17.1, 1.9, 1.9, 1.9 Hz, 1H), 5.00 (dddd, *J* = 10.2, 1.2, 1.2, 1.2 Hz, 1H), 4.67 (dddd, *J* = 10.7, 7.5, 3.2, 3.2 Hz, 1H), 4.19 (app q, 1H), 4.16 (dd, *J* = 9.0, 3.0 Hz, 1H), 3.28 (dd, *J* = 13.4, 3.3 Hz, 1H), 2.95 (ddddd, *J* = 17.1, 17.1,17.1, 8.1, 6.6 Hz, 2H), 2.77 (dd, *J* = 13.4, 9.6 Hz, 1H), 2.15 (app q, 2H), 1.87-1.75 (m, 2H) ppm.
^{13}C NMR (125 MHz, $CDCl_3$): δ 173.2, 153.5, 137.8, 135.3, 129.4, 129.0, 127.4, 115.4, 66.2, 55.2, 37.9, 34.9, 33.0, 23.4 ppm.

(*R*)-4-Benzyl-3-(hex-5-enoyl)oxazolidin-2-one[82] (16.2)

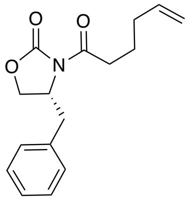

Notebook entry: 91HH, pg. 228.

(*R*)-4-Benzyl-2-oxazolidinone (3.943 g, 22.28 mmol) was put under argon and dissolved in THF (50 mL) and cooled to -78 °C. *n*-BuLi (13.9 mL, 22.2 mmol (1.6 M in hexanes)), was added dropwise and stirred for 1 hour. 5-hexenoyl chloride (1.969 g, 14.85 mmol) was added in THF (15 mL). The reaction was allowed to warm to room temperature overnight. After reaction completion, sat. NH_4Cl was used to quench after dilution with EtOAc (25 mL). The organic layer was removed and set aside. The aqueous layer was extracted two times with EtOAc. The combined organic layers were washed twice with sat. NaCl, then dried over Na_2SO_4. Solvent removal left a cloudy orange oil which was purified using flash column chromatography (3:1 hexanes:EtOAc) yielding pure product **16.2** as a clear, yellow oil (2.818 g, 10.31 mmol, 69%).

$[\alpha]^{20}_{D}$ -64.1° (*c* 5.08, $CHCl_3$)

IR: 3067, 2925, 1775, 1696, 1380, 1349, 1194, 702 cm^{-1}.

^{1}H NMR (500 MHz, $CDCl_3$): δ 7.34 (app t, 2H), 7.28 (app t, 1H), 7.21 (app d, 2H), 5.83 (dddd, *J* = 16.9, 10.2, 6.7, 6.7 Hz, 1H), 5.06 (dddd, *J* = 17.0, 1.6, 1.6, 1.6 Hz, 1H), 5.00 (dddd, *J* = 10.0, 1.2, 1.2, 1.2 Hz, 1H), 4.67 (dddd, *J* = 10.9, 7.7, 3.2, 3.2 Hz, 1H), 4.19 (app q, 1H), 4.16 (dd, *J* = 9.1, 3.0 Hz, 1H), 3.30 (dd, *J* = 13.4, 3.3 Hz, 1H), 2.96 (ddddd, *J* = 17.1, 17.1, 17.1, 8.1, 6.6 Hz, 2H), 2.77 (dd, *J* = 13.3, 9.5 Hz, 1H), 2.16 (app q, 2H), 1.88-1.75 (m, 2H) ppm.

^{13}C NMR (125 MHz, $CDCl_3$): δ 173.2, 153.5, 137.8, 135.3, 129.4, 129.0, 127.4, 115.4, 66.2, 55.2, 37.9, 34.9, 33.0, 23.4 ppm.

(*S*)-3-((*R*)-2-((3-(Allyloxy)-6-methylpyridin-2-yl)methyl)hex-5-enoyl)-4-benzyloxazolidin-2-one (13.3)

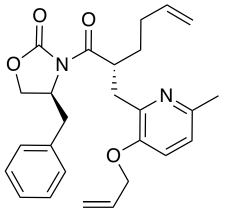

Notebook entry: 103HH, p 128-129

Starting material **14.1** (1.983 g, 7.256 mmol) was put under Ar and THF (10 mL) was added and stirred. This solution was cooled to 78 °C, then LHMDS (7.3 mL, 1.0 M in THF, 7.3 mmol) was added dropwise. After stirring for three hours, picolyl bromide (**2.2**) was dissolved in THF (15 mL) and added immediately. This was stirred over ice overnight, warming slowly to room temperature. The reaction was quenched with sat. NH_4Cl and diluted in EtOAc to extract two times. Organic layers were combined and washed twice with sat. NaCl and dried over Na_2SO_4. Crude product was purified using flash column chromatography (9:1 hexanes:acetone) and pure product **13.3** was isolated (0.926 g, 2.13 mmol, 71%).

[α]$^{20}_{D}$ +36.2° (*c* 5.03, $CHCl_3$)
Chiral GC: Method A: Retention times: 42.40 min. (major) and 43.95 min.(minor). 96% ee.
IR: 3063, 2927, 1782, 1695, 1454, 1387, 1257, 1189, 1102, 991, 911, 737, 700 cm^{-1}.
^{1}H NMR (500 MHz, $CDCl_3$): δ 7.30 (app t, 2H), 7.25 (app t, 1H), 7.20 (app d, 2H), 6.96 (d, *J* = 8.4 Hz, 1H), 6.87 (d, *J* = 8.3 Hz, 1H), 6.06 (ddt, *J* = 17.2, 10.4, 5.2 Hz, 1H), 5.82 (dddd, *J* = 16.9, 10.2, 6.6, 6.6 Hz, 1H), 5.42 (dddd, *J* = 17.2, 1.6, 1.6, 1.6 Hz, 1H), 5.30 (dddd, *J* = 10.7, 1.7, 1.7, 1.7 Hz, 1H), 5.02 (dddd, *J* = 17.1, 1.7, 1.7, 1.7 Hz, 1H), 4.95 (app dd, 1H), 4.63 (dddd, *J* = 10.2, 6.4, 3.2, 3.2 Hz, 2H), 4.53 (ddd, *J* = 5.2, 1.6, 1.6 Hz, 2H), 4.50 (dddd, *J* = 11.0, 6.8, 6.8, 4.3 Hz, 1H), 4.14-4.08 (m, 2H), 3.35 (dd, *J* = 13.3, 3.2 Hz, 1H), 3.31 (dd, *J* = 15.6, 10.1 Hz, 1H), 3.16 (dd, *J* = 15.6, 4.3 Hz, 1H), 2.53 (dd, *J* = 13.3, 10.6 Hz, 1H), 2.38 (s, 3H), 2.25-2.13 (m, 2H), 1.88 (dddd, *J* = 13.4, 9.9, 6.6, 6.6 Hz, 1H), 1.73 (dddd, *J* = 13.6, 9.3, 6.4, 6.4 Hz, 1H) ppm.
^{13}C NMR (125 MHz, $CDCl_3$): δ 176.7, 152.9, 150.7, 148.7, 148.4, 138.3, 136.1, 133.2, 129.4, 128.9, 127.1, 121.0, 118.4, 117.8, 114.8, 69.0, 65.8, 55.9, 40.2, 37.9, 34.3, 32.0, 31.4, 23.5 ppm.
HRMS: (ESI, q-TOF) *m/z* [M +H] calcd for $C_{26}H_{30}N_2O_4$ 435.2278; found 435.2280.

(*R*)-3-((*S*)-2-((3-(Allyloxy)-6-methylpyridin-2-yl)methyl)hex-5-enoyl)-4-benzyloxazolidin-2-one (15.3)

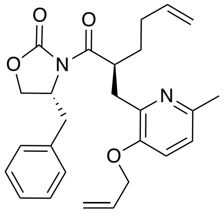

Notebook entry: 31HHB, pg 100.

Starting material (**16.2**) (0.743 g, 2.72 mmol) was put under Ar and THF (9 mL) was added and stirred. This solution was cooled to -78 °C, then LHMDS (2.75 mL, 1.0 M in THF, 2.73 mmol) was added dropwise then stirred for one hour. Next, picolyl bromide (**2.2**) (0.659 g, 2.72 mmol) was dissolved in THF (3 mL) and added immediately. This was stirred overnight, slowly warming to rt. The reaction was quenched with sat. NH_4Cl and the organic/aqueous layers were separated. The aqueous layer was extracted two times using CH_2Cl_2 and organic layers were combined and washed with sat. NaCl and dried over Na_2SO_4. Crude product was purified using flash column chromatography (9:1 hexanes:acetone) and pure product (**15.3**) was isolated as a clear yellow oil. (0.812 g, 1.86 mmol, 69%).

[α]$^{20}_{D}$ -35.4° (*c* 5.01, $CHCl_3$)
Chiral GC Analysis: Method A: Retention times: 40.675 min. (minor) and 42.162 min. (major) 96% ee.
IR: 3083, 2918, 2853, 1780, 1692, 1455, 1386, 1347, 1258, 1191, 914, 730, 700 cm^{-1}.
^{1}**H NMR** (500 MHz, $CDCl_3$): δ 7.31 (app t, 2H), 7.25 (app t, 1H), 7.20 (app d, 2H), 6.96 (d, *J* = 8.2 Hz, 1H), 6.87 (d, *J* = 8.2 Hz, 1H), 6.06 (ddt, *J* = 17.2, 10.3, 5.0 Hz, 1H), 5.82 (dddd, *J* = 17.0, 10.2, 6.6, 6.6 Hz, 1H), 5.42 (dddd, *J* = 17.2, 1.7, 1.7, 1.7 Hz, 1H), 5.30 (dddd, *J* = 10.7, 1.7, 1.7, 1.7 Hz, 1H), 5.02 (dddd, *J* = 17.1, 1.7, 1.7, 1.7 Hz, 1H), 4.95 (app dd, 1H), 4.63 (dddd, *J* = 10.2, 6.6, 3.1, 3.1 Hz, 1H), 4.53 (ddd, *J* = 5.0, 1.7, 1.7 Hz, 2H), 4.50 (dddd, *J* = 11.0, 6.8, 6.8, 4.3 Hz, 1H), 4.14-4.08 (m, 2H), 3.35 (dd, *J* = 13.3, 3.2 Hz, 1H), 3.31 (dd, *J* = 15.7, 10.1 Hz, 1H), 3.16 (dd, *J* = 15.6, 4.3 Hz, 1H), 2.53 (dd, *J* = 13.3, 10.5 Hz, 1H), 2.38 (s, 3H), 2.25-2.13 (m, 2H), 1.88 (dddd, *J* = 13.3, 10.0, 6.6, 6.6 Hz, 1H), 1.72 (dddd, *J* = 13.3, 9.4, 6.5, 6.5 Hz, 1H) ppm.
^{13}**C NMR** (125 MHz, $CDCl_3$): δ 176.7, 153.0, 150.6, 148.4, 148.2, 138.2, 136.1, 133.1, 129.4, 128.9, 127.1, 121.0, 118.4, 117.5, 114.8, 69.0, 65.8, 55.9, 40.2, 37.9, 34.3, 32.0, 31.4, 23.5 ppm.
HRMS (ESI, q-TOF) *m/z* [M +H] calcd for $C_{26}H_{30}N_2O_4$ 435.2278; found 435.2281.

Methyl (*R*)-2-((3-(allyloxy)-6-methylpyridin-2-yl)methyl)hex-5-enoate (13.2)

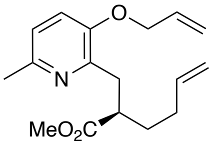

Notebook entry: 73HH, pg 116-117

LiOH•H_2O (0.340 g, 8.10 mmol) was placed in a flask and H_2O (2 mL) was added. This was cooled to 0 °C and H_2O_2 (1.84 mL (30%), 23 mmol) was added and stirred for 15 minutes. Starting material (**13.3**) (1.135 g, 2.607 mmol) was dissolved in THF (8 mL, final ratio 4:1, THF: H_2O) then added to the mixture. The reaction was stirred for 3 hours and deemed complete by TLC. $Na_2S_2O_3$ was used to quench the excess peroxides, stirring at 0 °C for 15 minutes. The solution was acidified to pH = 6 with NH_4Cl and product was extracted with EtOAc three times. The combined organic layers were washed with sat. NaCl and dried over Na_2SO_4. Solvent was removed using rotary evaporation, and the crude acid product was dissolved in MeOH (10 mL) and 8 drops H_2SO_4 was added. The reaction was stirred and refluxed overnight. After 24 hours, the reaction was complete by TLC. Solvent was removed and pH was neutralized using $NaHCO_3$ after dilution in EtOAc which was used to extract product three times from the aqueous layer. Combined organic layers were washed once with sat. NaCl and then dried over Na_2SO_4. After solvent was removed, the crude ester was purified using flash column chromatography using 2:1 hexanes:EtOAc. Pure product **13.2** was isolated as a clear, yellow oil (0.514 g, 1.78 mmol, 68%).

[α]$^{20}_{D}$ -9.7° (*c* 4.27, $CHCl_3$)
Chiral GC Analysis: Method A: Retention times: 37.60 min. (minor) and 37.62 min. (major) 99% ee.
IR: 3082, 2994, 2930, 2849, 1731, 1458, 1255, 1161, 991, 916, 813 cm^{-1}.
^{1}H NMR (500 MHz, $CDCl_3$): δ 7.01 (d, *J* = 8.3 Hz, 1H), 6.93 (d, *J* = 8.3 Hz, 1H), 6.05 (ddt, *J* = 17.3, 10.4, 5.5 Hz, 1H), 5.80 (dddd, *J* = 16.9, 10.2, 6.6, 6.6 Hz, 1H), 5.43 (dddd, *J* = 17.3, 1.7, 1.7, 1.7 Hz, 1H), 5.32 (dddd, *J* = 10.6, 1.5, 1.5, 1.5 Hz, 1H), 5.00 (dddd, *J* = 17.1, 1.6, 1.6, 1.6 Hz, 1H), 4.95 (dddd, *J* = 10.2, 1.3, 1.3, 1.3 Hz, 1H), 4.53 (ddd, *J* = 5.0, 1.6, 1.6 Hz, 2H), 3.66 (s, 3H), 3.15 (dd, *J* = 14.2, 8.2 Hz, 1H), 3.05 (dd, *J* = 14.2, 6.3 Hz, 1H), 3.00 (dddd, *J* = 8.6, 8.6, 6.4, 6.4 Hz, 1H), 2.45 (s, 3H), 2.17-2.03 (m, 2H), 1.83 (dddd, *J* = 14.9, 9.1, 9.1, 6.0 Hz, 1H), 1.64 (dddd, *J* = 11.5, 9.6, 6.3, 5.1 Hz, 1H) ppm.
^{13}C NMR (125 MHz, $CDCl_3$): δ 176.4, 150.5, 148.9, 148.4, 138.1, 132.9, 121.2, 118.8, 117.5, 114.8, 68.9, 51.3, 43.6, 34.5, 31.5, 31.2, 23.3 ppm.
HRMS (ESI, q-TOF) *m/z* [M +H] calcd for $C_{17}H_{23}NO_3$ 290.1751; found 290.1750.

Methyl (*S*)-2-((3-(allyloxy)-6-methylpyridin-2-yl)methyl)hex-5-enoate (15.2)

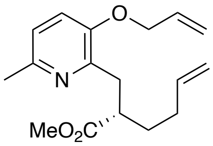

Notebook entry: 32HHB, pg 102

LiOH•H_2O (0.144 g, 3.42 mmol) was placed in a flask and H_2O (2 mL) was added. This was cooled to 0 °C and H_2O_2 (0.67 mL (30%), 8.6 mmol) was added and stirred for 30 minutes. Starting material (**15.3**) (0.741 g, 1.71 mmol) was dissolved in THF (8 mL, final ratio 4:1, THF: H_2O) then added to the mixture. The reaction was stirred overnight and deemed complete by TLC. $Na_2S_2O_3$ was used to quench the excess peroxides, stirring at 0 °C for 15 minutes. The solution was acidified to pH = 6 with NH_4Cl and acetic acid to extract product from aqueous layer with EtOAc four times. The combined organic layers were washed with sat. NaCl and dried over Na_2SO_4. Solvent was removed using rotary evaporation, and the crude acid product was dissolved in MeOH (15 mL) and 8 drops H_2SO_4 was added. The reaction was stirred and refluxed overnight. After 24 hours, the reaction was complete by TLC. Solvent was removed and pH was neutralized using $NaHCO_3$ after dilution in EtOAc which was used to extract product three times from the aqueous layer. Combined organic layers were washed once with sat. NaCl and then dried over Na_2SO_4. After solvent was removed, the crude ester was purified using flash column chromatography using 3:1 hexanes:EtOAc. Pure product (**15.2**) was isolated as a clear, yellow oil (0.364 g, 1.26 mmol, 74%).

$[\alpha]^{20}_D$ +9.3° (*c* 5.02, $CHCl_3$)
Chiral GC Analysis: Method A: Retention times: 37.60 min. (major) and 37.62 min. (minor) 99% ee.
IR: 3082, 2945, 2863, 1733, 1458, 1255, 1161, 995, 916, 814 cm^{-1}.
^{1}H NMR (500 MHz, $CDCl_3$): δ 6.97 (d, *J* = 8.3 Hz, 1H), 6.89 (d, *J* = 8.4 Hz, 1H), 6.03 (ddt, *J* = 17.2, 10.2, 5.0 Hz, 1H), 5.77 (dddd, *J* = 17.0, 10.3, 6.8, 6.8 Hz, 1H), 5.41 (dddd, *J* = 17.3, 1.7, 1.7, 1.7 Hz, 1H), 5.29 (dddd, *J* = 10.6, 1.6, 1.6, 1.6 Hz, 1H), 4.99 (dddd, *J* = 17.3, 1.9, 1.9, 1.9 Hz, 1H), 4.93 (dddd. *J* = 10.2, 1.2, 1.2, 1.2 Hz, 1H), 4.51 (ddd, *J* = 5.1, 1.7, 1.7 Hz, 2H), 3.64 (s, 3H), 3.13 (dd, *J* = 14.2, 8.3 Hz, 1H), 3.03 (dd, *J* = 14.2, 6.2 Hz, 1H), 2.98 (dddd, *J* = 8.6, 8.6, 6.3, 6.3 Hz, 1H), 2.42 (s, 3H), 2.15-2.01 (m, 2H), 1.80 (dddd, *J* = 14.6, 8.8, 8.8, 5.8 Hz, 1H), 1.62 (dddd, *J* = 11.4, 9.6, 6.4, 4.9 Hz, 1H) ppm.
^{13}C NMR (125 MHz, $CDCl_3$): δ 176.4, 150.5, 148.9, 148.4, 138.1, 133.0, 121.1, 118.8, 117.5, 114.8, 68.9, 51.3, 43.6, 34.6, 31.5, 31.2, 23.4 ppm.
HRMS (ESI, q-TOF) *m/z* [M +H] calcd for $C_{17}H_{23}NO_3$ 290.1751; found 290.1750.

Methyl (*R*)-2-((6-methyl-3-(((trifluoromethyl)sulfonyl)oxy)pyridin-2-yl)methyl)hex-5-enoate (14.4)

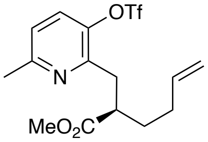

Notebook entry: 61HH, pg. 158

Pd(PPh_3)$_4$ (0.015 g, 0.013 mmol) was added to a flask containing pure ester starting material **13.2** (0.376 g, 1.30 mmol) and K_2CO_3 (0.538 g, 3.89 mmol). After establishing Ar atmosphere, MeOH (4 mL) was added and stirred overnight at room temperature. After this time, the mixture was filtered over Celite washing with EtOAc, followed by solvent removal. After diluting in CH_2Cl_2, NH_4Cl was added to neutralize pH. Product was extracted from the aqueous layer three times with CH_2Cl_2, then the combined organic layers were washed with sat. NaCl. Solvent was removed to give the crude phenol as a hazy orange oil (0.355 g) which was added to a flask containing $PhNTf_2$ (0.794 g, 2.22 mmol) and put under Ar. Dry CH_2Cl_2 (5 mL) was added and stirred before NEt_3 (0.31, 2.2 mmol) was added. This mixture was left to stir at room temperature overnight. Once deemed complete by TLC, the dark, cloudy blue solution was washed with 10% NaOH, sat. NH_4Cl, and sat. NaCl sequentially. This product was dried over Na_2SO_4, and solvent was removed to give a thick blue oil. The crude product was purified by flash column chromatography using 6:1 hexanes:EtOAc, leaving a clear, colorless oil (0.442 g, 1.16 mmol, 89%).

$[\alpha]^{20}_D$ +1.7° (*c* 0.29, $CHCl_3$)

Chiral GC: Method A: Retention times: 34.14 min. (major) and 34.28 min. (minor) 97% ee.

IR: 3076, 2961, 2848, 1739, 1427, 1259, 1216, 1012, 794 cm^{-1}.

^{1}H NMR (500 MHz, $CDCl_3$): δ 7.43 (d, *J* = 8.4 Hz, 1H), 7.05 (d, *J* = 8.4 Hz, 1H), 5.78 (dddd, *J* = 17.0, 10.3, 6.6, 6.6 Hz, 1H), 5.02 (app dd, 1H), 4.97 (app dd, 1H), 3.65 (s, 3H), 3.22 (dd, *J* = 14.8, 8.8 Hz, 1H), 3.09-3.04 (m, 1H), 3.00 (dd, *J* = 14.9, 5.1 Hz, 1H), 2.51 (s, 3H), 2.16-2.05 (m, 2H), 1.76 (app sextet, 1H), 1.67-1.60 (m, 1H) ppm.

^{13}C NMR (125 MHz, $CDCl_3$): δ 175.8, 158.1, 151.3, 143.3, 137.7, 129.0, 122.4, 118.5 (q, *J* = 320.2 Hz), 115.4, 51.7, 43.1, 33.9, 31.5, 31.4, 24.1 ppm.

HRMS (ESI, q-TOF) *m/z* [M +H] calcd for $C_{15}H_{18}F_3NO_5S$ 382.0931; found 382.0931.

Methyl (*S*)-2-((6-methyl-3-(((trifluoromethyl)sulfonyl)oxy)pyridin-2-yl)methyl)hex-5-enoate (16.3)

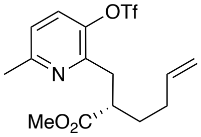

Notebook entry: 34HHB, pg. 111.

Pd(PPh$_3$)$_4$ (0.015 g, 0.013 mmol) was washed with MeOH and dried using vacuum filtration before addition to a flask containing pure ester starting material (**15.2**) (0.364 g, 1.26 mmol) and K$_2$CO$_3$ (0.522 g, 3.78 mmol). After establishing Ar atmosphere, MeOH (15 mL) was added and stirred overnight at room temperature. After this time, the mixture was filtered over Celite washing with EtOAc, followed by solvent removal. After diluting in CH$_2$Cl$_2$, NH$_4$Cl was added to neutralize pH. Product was extracted from the aqueous layer three times with CH$_2$Cl$_2$, then the combined organic layers were washed with sat. NaCl. Solvent was removed to give the crude phenol as a hazy orange oil (0.343) which was added to a flask containing PhNTf$_2$ (0.630 g, 1.76 mmol) and put under Ar. Dry CH$_2$Cl$_2$ (12 mL) was added and stirred before NEt$_3$ (0.28 mL, 2.02 mmol) was added. This mixture was left to stir at room temperature overnight. Once deemed complete by TLC, the dark, cloudy blue solution was washed with 10% NaOH, sat. NH$_4$Cl, and sat. NaCl sequentially. This product was dried over Na$_2$SO$_4$, and solvent was removed to give a thick blue oil. The crude product was purified by flash column chromatography using 6:1 hexanes:EtOAc, leaving a clear, colorless oil (0.428 g, 1.12 mmol, 93%).

[α]^{20}$_D$ -1.4° (*c* 4.12, CHCl$_3$)

Chiral GC Analysis: Method A: Retention times: 34.15 min. (minor) and 34.21 min. (major) 98% ee.

IR: 3081, 2952, 2854, 1735, 1458, 1425, 1210, 1136, 862 cm^{-1}

^{1}H NMR (500 MHz, CDCl$_3$): δ 7.43 (d, *J* = 8.4 Hz, 1H), 7.05 (d, *J* = 8.5 Hz, 1H), 5.78 (dddd, *J* = 17.0, 10.3, 6.6, 6.6 Hz, 1H), 5.03 (app dd, 1H), 4.97 (app d, 1H), 3.66 (s, 3H), 3.22 (dd, *J* = 15.0, 8.9 Hz, 1H), 3.09-3.04 (m, 1H), 3.00 (dd, *J* = 15.0, 5.2 Hz, 1H), 2.52 (s, 3H), 2.17-2.06 (m, 2H), 1.76 (app sextet, 1H), 1.69-1.62 (m, 1H) ppm.

^{13}C NMR (125 MHz, CDCl$_3$): δ 175.7, 157.9, 151.2, 143.1, 137.6, 128.9, 122.3, 118.5 (q, *J* = 320.2 Hz), 115.3, 51.6, 43.0, 33.7, 31.4, 31.3, 24.0 ppm.

HRMS (ESI, q-TOF) *m/z* [M +H] calcd for $C_{15}H_{18}F_3NO_5S$ 382.0931; found 382.0932.

Methyl (*R*)-2-methyl-5-methylene-6,7,8,9-tetrahydro-5*H*-cyclohepta[*b*] pyridine-8-carboxylate (13.1)

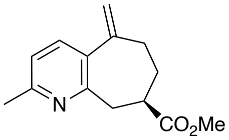

Notebook Entry: 81HH, pg. 206.

In a double-necked flask, K_2CO_3 (0.300 g, 2.17 mmol) and $Pd(PPh_3)_4$ (5 mol%, 0.026 g, 0.023 mmol) were added and put under Ar. CH_3CN (2 mL) was added and stirred. Starting material, triflate (**14.4**) (0.165 g, 0.433 mmol), was dissolved in CH_3CN (2.5 mL) and added to the solution. The reaction was refluxed for 6.5 hours when an additional 5 mol% catalyst was added (0.026 g $Pd(PPh_3)_4$, 0.023 mmol) and continued to reflux for additional 13 hours. The reaction was cooled and filtered over silica, washing with EtOAc (150 mL). The mixture was concentrated and crude product was purified using flash column chromatography (2:1 hexanes:EtOAc, R_f= 0.25). Pure clear, colorless product (**13.1**) was isolated (0.094 g, 0.41 mmol, 94%).

$[\alpha]^{20}_D$ -71.2° (*c* 0.94, $CHCl_3$)
Chiral GC: Method A: Retention times: 34.87 min. (major) and 35.04 min. (minor) 98% ee.
IR: 3073, 2943, 2855, 1730, 1590, 1435, 1165, 906, 828 cm^{-1}.
^{1}H NMR (500 MHz, $CDCl_3$): δ 7.40 (d, *J* = 7.8 Hz, 1H), 6.98 (d, *J* = 7.8 Hz, 1H), 5.18 (app s, 1H), 5.07 (app s, 1H), 3.69 (s, 3H), 3.26 (dd, *J* = 14.6, 1.4 Hz, 1H), 3.17 (dd, *J* = 14.7, 10.5 Hz, 1H), 2.76 (dddd, *J* = 9.8, 9.8, 4.3, 2.7 Hz, 1H), 2.65 (ddd, *J* = 14.0, 7.6, 3.8 Hz, 1H), 2.51 (s, 3H), 2.33 (ddd, *J* = 13.9, 9.8, 4.0 Hz, 1H), 2.15 (app dq, 1H), 2.00 (dddd, *J* = 13.6, 9.8, 9.8, 3.8 Hz, 1H) ppm.
^{13}C NMR (125 MHz, $CDCl_3$): δ 175.7, 156.4, 156.0, 148.4, 136.0, 135.3, 121.3, 115.5, 51.8, 41.8, 40.5, 33.8, 32.9, 24.1 ppm
HRMS: (ESI, q-TOF) *m/z* [M +H] calcd for $C_{14}H_{17}NO_2$ 232.1332; found 232.1336.

Methyl (*S*)-2-methyl-5-methylene-6,7,8,9-tetrahydro-5*H*-cyclohepta[*b*]pyridine-8-carboxylate (15.1)

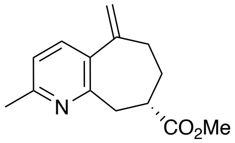

Notebook Entry: 13HHB, pg. 43.

$Pd(PPh_3)_4$ was washed with MeOH, then dried using vacuum filtration to give shiny yellow crystals (0.068 g, 0.060 mmol) which was added to a culture tube containing K_2CO_3 (0.822 g, 5.94 mmol) and put under Ar. CH_3CN (5 mL) was added and stirred. Starting material (**16.3**) (0.452 g, 1.19 mmol), was dissolved in CH_3CN (4 mL) and added to the solution. The reaction was refluxed for 5 hours when an additional 5 mol% catalyst was added (0.068 g $Pd(PPh_3)_4$, 0.060 mmol) and continued to reflux for additional 16 hours. At this time, the reaction mixture was cooled and filtered over silica, washing with EtOAc (100 mL). The mixture was concentrated and the crude product (brown oil) was purified using flash column chromatography (2:1 hexanes:EtOAc, R_f= 0.25). Pure clear, colorless product (**15.1**) was isolated (0.191 g, 0.819 mmol, 69%).

$[\alpha]^{20}_{D}$ +70.4° (*c* 0.76, $CHCl_3$)
Chiral GC Analysis: Method A: Retention times: 34.87 min. (minor) and 35.04 min. (major) 99% ee.
IR: 3082, 2950, 1863, 1733, 1590, 1169, 906, 733 cm^{-1}.
^{1}H NMR (500 MHz, $CDCl_3$): δ 7.40 (d, *J* = 7.8 Hz, 1H), 6.98 (d, *J* = 7.8 Hz, 1H), 5.18 (app s, 1H), 5.06 (d, *J* = 1.7 Hz, 1H), 3.69 (s, 3H), 3.26 (dd, *J* = 14.7, 1.4 Hz, 1H), 3.17 (dd, *J* = 14.5, 10.5 Hz, 1H), 2.76 (dddd, *J* = 10.1, 10.1, 4.3, 2.6 Hz, 1H), 2.66 (ddd, *J* = 14.0, 7.7, 3.9 Hz, 1H), 2.51 (s, 3H), 2.33 (ddd, *J* = 13.8, 9.6, 3.9 Hz, 1H), 2.15 (app dq, 1H), 2.00 (dddd, *J* = 13.6, 9.8, 9.8, 3.8 Hz, 1H) ppm.
^{13}C NMR (125 MHz, $CDCl_3$): δ 175.6, 156.4, 156.0, 148.4, 136.0, 135.2, 121.3, 115.5, 51.7, 41.8, 40.5, 33.8, 32.9, 24.1 ppm.
HRMS (ESI, q-TOF) *m/z* [M +H] calcd for $C_{14}H_{17}NO_2$ 232.1332; found 232.1333.

Methyl (5*R*,8*S*)-2,5-dimethyl-6,7,8,9-tetrahydro-5*H*-cyclohepta[*b*]pyridine-8-carboxylate (8)
Methyl (5*S*,8*S*)-2,5-dimethyl-6,7,8,9-tetrahydro-5*H*-cyclohepta[*b*]pyridine-8-carboxylate (1.11a)

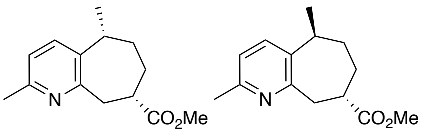

Notebook Entry: 14, 16-18HHB, pg. 54-60

To a flask containing starting material **15.1** (0.231 g, 1.00 mmol), Wilkinson's catalyst (0.046 g, 0.050 mmol) was added, then put under Ar atmosphere. Dry CH_2Cl_2 (10 mL) was added, followed by NEt_3 (0.21 mL, 1.50 mmol). H_2 gas (12" balloon) was run through the flask, and a second balloon was used to maintain H_2 atmosphere overnight. After purging the flask with Ar, the mixture was filtered over silica using EtOAc to wash. Solvent was removed leaving a brown, clear oil. The crude mixture of the two desired diastereomers and undesired endocycle were purified using flash column chromatography (1:1 hexanes:EtOAc) to give a mixture of both diastereomers and trace endocycle. Overlapping fractions were combined (0.207 g) and Pd/C (0.023 g, 10% w/w) was added and put under Ar atmosphere before addition of MeOH (12 mL). H_2 gas (12" balloon) was run through the flask, and a second balloon was used to maintain H_2 atmosphere overnight. The mixture was filtered over Celite and washed with EtOAc.The two products were purified using flash column chromatography (1:1 hexanes: EtOAc) and both the (*5S,8S*) diastereomer, **1.11a,** (0.085 g, 0.36 mmol) and the (*5R,8S*) diastereomer, **8**, was isolated (0.117 g, 0.50 mmol) as clear, colorless oils (87%, 1.4:1 dr)

Methyl (5*R*,8*S*)-2,5-dimethyl-6,7,8,9-tetrahydro-5*H*-cyclohepta[*b*]pyridine-8-carboxylate (8)

$[\alpha]^{20}_{D}$ +53.2° (*c* 1.16, $CHCl_3$)

Chiral GC Analysis: Method A: Retention times: 34.97 min. (minor) and 35.14 min. (major). 99% ee.

IR: 2921.9, 2847.3, 1733.8, 1460.4, 1436.5, 1157.8, 729.6 cm^{-1}.

^{1}H NMR (500 MHz, $CDCl_3$): δ 7.30 (d, *J* = 7.8 Hz, 1H), 6.92 (d, *J* = 7.8 Hz, 1H), 3.65 (s, 3H), 3.36 (dd, *J* = 14.7, 9.8 Hz, 1H), 3.29 (dd, *J* = 14.6, 3.0 Hz, 1H), 2.99 (dddd, *J* = 14.4, 7.2, 7.2, 3.4 Hz, 1H), 2.64 (dddd, *J* = 9.4, 9.4, 3.2, 3.2 Hz, 1H), 2.48 (s, 3H), 2.12 (dddd, *J* = 14.0, 10.7, 9.3, 3.2 Hz, 1H), 1.99 (ddq, *J* = 14.1, 10.6, 3.6 Hz, 1H), 1.84 (dddd, *J* = 14.0, 6.8, 6.8, 3.2 Hz, 1H), 1.76 (dddd, *J* = 14.1, 10.7, 3.4, 3.4 Hz, 1H), 1.32 (d, *J* = 7.4 Hz, 3H) ppm.

^{13}C NMR (125 MHz, $CDCl_3$): δ 175.7, 157.4, 154.8, 137.7, 136.1, 121.2, 51.7, 42.0, 40.6, 37.6, 32.2, 29.1, 23.9, 18.8 ppm.

HRMS (ESI, q-TOF) *m/z* [M +H] calcd for $C_{14}H_{19}NO_2$ 234.1489; found 234.1486.

Methyl (5*S*,8*S*)-2,5-dimethyl-6,7,8,9-tetrahydro-5*H*-cyclohepta[*b*]pyridine-8-carboxylate (1.11a)

$[\alpha]^{20}_{D}$ +53.0° (*c* 0.10, $CHCl_3$)

Chiral GC Analysis: Method A: Retention times: 35.76 min. (major) and 35.92 min. (minor) 99% ee.

IR: 3059.6, 2919.7, 2848.7, 1730.4, 1464.1, 1433.0, 1159.1, 729.5 cm^{-1}

^{1}H NMR (500 MHz, $CDCl_3$): δ 7.37 (d, *J* = 8.0 Hz, 1H), 6.98 (d, *J* = 7.8 Hz, 1H), 3.69 (s, 3H), 3.31 (dd, *J* = 14.0, 10.5 Hz, 1H), 3.25 (app d, 1H), 2.99 (app quin, 1H), 2.49 (s, 3H), 2.47 (dddd, *J* = 10.8, 10.8, 3.1, 3.1 Hz, 1H), 2.18-2.12 (m, 1H) 1.97 (dddd, *J* = 11.7, 11.7, 11.7, 4.2 Hz, 1H), 1.88 (dddd, *J* = 13.9, 5.3, 3.7, 1.7 Hz, 1H), 1.34 (d, *J* = 7.0 Hz, 3H), 1.31-1.23 (m, 1H) ppm.

^{13}C NMR (125 MHz, $CDCl_3$): δ 176.1, 158.8, 154.5, 137.7, 132.4, 121.2, 51.7, 42.1, 40.5, 35.0, 34.8, 33.9, 23.9, 20.4 ppm.

HRMS (ESI, q-TOF) *m/z* [M +H] calcd for $C_{14}H_{19}NO_2$ 234.1489; found 234.1488.

Methyl (5*S*,8*R*)-2,5-dimethyl-6,7,8,9-tetrahydro-5*H*-cyclohepta[*b*]pyridine-8-carboxylate (1.11c)
Methyl (5*R*,8*R*)-2,5-dimethyl-6,7,8,9-tetrahydro-5*H*-cyclohepta[*b*]pyridine-8-carboxylate (1.11b)

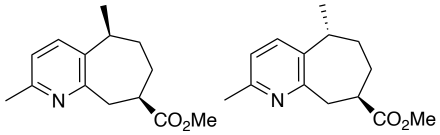

Notebook Entry: 20HHB, pg. 187-188.

To a flask containing starting material **13.1** (0.080 g, 0.35 mmol), Wilkinson's catalyst (0.019 g, 0.021 mmol) was added, then put under Ar atmosphere. Dry CH_2Cl_2 (3 mL) was added, followed by NEt_3 (0.07 mL, 0.5 mmol). H_2 gas (12" balloon) was ran through the flask, and a second balloon was used to maintain H_2 atmosphere overnight. After purging the flask with Ar, the mixture was filtered over silica using EtOAc to wash. Solvent was removed leaving a brown, clear oil. The crude mixture of the two desired diastereomers and undesired endocycle were purified using flash column chromatography (1:1 hexanes:EtOAc) to give a mixture of both diastereomers and trace endocycle.

Overlapping fractions were combined (0.048 g) and Pd/C (0.005 g, 10% w/w) was added and put under Ar atmosphere before addition of MeOH (6 mL). H_2 gas (12" balloon) was ran through the flask, and a second balloon was used to maintain H_2 atmosphere overnight. The mixture was filtered over Celite and washed with EtOAc. The two products were purified using flash column chromatography (1:1 hexanes: EtOAc) and both **1.11c** (0.040 g, 0.17 mmol) and **1.11b** were isolated (0.030 g, 0.13 mmol) as clear, colorless oils (86%, 1.3: 1 dr)

Methyl (5*S*,8*R*)-2,5-dimethyl-6,7,8,9-tetrahydro-5*H*-cyclohepta[*b*]pyridine-8-carboxylate

$[\alpha]^{20}_{D}$ -55.2° (*c* 0.27, $CHCl_3$)

Chiral GC Analysis: Method A: Retention times: 34.95 min. (major) and 35.12 min. (minor) 99% ee.

IR: 2933, 2353, 1732, 1590, 1462, 1161 cm^{-1}.

^{1}H NMR (500 MHz, $CDCl_3$): δ 7.30 (d, *J* = 7.8 Hz, 1H), 6.91 (d, *J* = 7.8 Hz, 1H), 3.61 (s, 3H), 3.36 (dd, *J* = 14.5, 9.7 Hz, 1H), 3.29 (dd, *J* = 14.7, 3.0 Hz, 1H), 2.99 (dddd, *J* = 14.3, 7.2, 7.2, 3.4 Hz, 1H), 2.65 (dddd, *J* = 9.6, 9.6, 3.2, 3.2 Hz, 1H), 2.48 (s, 3H) 2.12 (dddd, *J* = 14.0, 10.7, 9.4, 3.2 Hz, 1H) 1.98 (ddq, *J* = 14.0, 10.4, 3.5 Hz, 1H), 1.85 (dddd, *J* = 14.0, 6.9, 6.9, 3.2 Hz, 1H), 1.76 (dddd, *J* = 14.0, 10.7, 3.4, 3.4 Hz, 1H), 1.32 (d, *J* = 7.3 Hz, 3H) ppm.

^{13}C NMR (125 MHz, $CDCl_3$): δ 175.9, 157.6, 154.9, 137.9, 136.2, 121.4, 51.4, 42.2, 40.8, 37.8, 32.4, 29.2, 24.0, 18.9 ppm.

HRMS (ESI, q-TOF) *m/z* [M +H] calcd for $C_{14}H_{19}NO_2$ 234.1489; found 234.1489.

Methyl (5*R*,8*R*)-2,5-dimethyl-6,7,8,9-tetrahydro-5*H*-cyclohepta[*b*]pyridine-8-carboxylate

$[\alpha]^{20}_{D}$ -47.8° (*c* 0.09, $CHCl_3$)

Chiral GC: Method A: Retention times: 35.76 min. (minor) and 35.92 min. (major) 99% ee.

IR: 2930, 2851, 1734, 1464, 1433, 1159, 731 cm^{-1}.

^{1}H NMR (500 MHz, $CDCl_3$): δ 7.37 (d, *J* = 8.0 Hz, 1H), 6.98 (d, *J* = 7.8 Hz, 1H), 3.69 (s, 3H), 3.31 (dd, *J* = 14.0, 10.5 Hz, 1H), 3.25 (app d, 1H), 2.99 (app quin, 1H), 2.49 (s, 3H), 2.47 (dddd, *J* = 10.8, 10.8, 3.0, 3.0 1H), 2.18-2.12 (m, 1H), 1.97 (dddd, *J* = 11.8, 11.8, 11.8, 3.7 Hz, 1H), 1.88 (dddd, *J* = 14.0, 5.3, 3.8, 1.8 Hz, 1H), 1.34 (d, *J* = 7.0 Hz, 3H), 1.31-1.23 (m, 1H) ppm.

^{13}C NMR (125 MHz, $CDCl_3$): δ 176.2, 158.9, 154.5, 137.8, 132.4, 121.2, 51.8, 42.1, 40.6, 35.0, 34.8, 33.9, 23.9, 20.4 ppm.

HRMS (ESI, q-TOF) *m/z* [M +H] calcd for $C_{14}H_{19}NO_2$ 234.1489; found 234.1488.

2-((5*R*,8*R*)-2,5-Dimethyl-6,7,8,9-tetrahydro-5*H*-cyclohepta[*b*]pyridin-8-yl)propan-2-ol[7,8,12] (2)

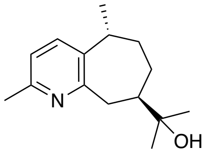

Notebook Entry: 120HH, pg. 291

Ester starting material **1.11b** (0.057 g, 0.24 mmol) was put under Ar, then THF (5 mL) was added and cooled to -78 °C. MeLi (0.80 mL, 2.60 mmol, 3.1 M in diethoxymethane) was added dropwise and stirred for 2 hours. The reaction was removed from the ice bath and deemed complete by TLC (EtOAc) after 15 minutes. Et_2O (20 mL) was added and the reaction quenched with sat. NH_4Cl. The organic layer was washed once with sat. NaCl, then dried over Na_2SO_4. Solvent was removed leaving product (**2**) as a clear, yellow gel. (0.056 g, 0.24 mmol, 99%).

$[\alpha]^{20}_D$ +12.0° (*c* 0.30, $CHCl_3$)
Chiral GC: Method A: Retention times: 36.54 min (minor) and 36.66 min (major). 99% ee.
IR: 3364, 2967, 2913, 2869, 1590, 1459, 1145, 920, 731 cm^{-1}.
^{1}H NMR (500 MHz, $CDCl_3$): δ 7.34 (d, *J* = 8.0 Hz, 1H), 6.93 (d, *J* = 8.0 Hz, 1H), 3.21 (app d, 1H), 2.97 (app quin 1H), 2.88 (dd, *J* = 13.4, 10.4 Hz, 1H), 2.48 (s, 3H), 2.14-2.08 (m, 1H), 1.89 (ddq, *J* = 13.7, 6.5, 4.9 Hz, 1H), 1.60 (dddd, *J* = 12.1, 12.1, 12.1, 3.6 Hz, 1H), 1.42 (dddd, *J* = 11.8, 10.3, 2.9, 1.5 Hz, 1H), 1.32 (d, *J* = 7.0 Hz, 3H), 1.26 (s, 3H), 1.25 (s, 3H), 1.30-1.21 (m, 1H) ppm.
^{13}C NMR (125 MHz, $CDCl_3$): δ 160.9, 154.3, 137.9, 132.4, 120.6, 73.3, 48.0, 39.8, 36.1, 35.3, 32.6, 27.6, 26.0, 23.9, 20.7 ppm.
HRMS (ESI, q-TOF) *m/z* [M +H] calcd for $C_{15}H_{23}NO$ 234.1852; found 234.1858.

2-((5*S*,8*S*)-2,5-Dimethyl-6,7,8,9-tetrahydro-5*H*-cyclohepta[*b*]pyridin-8-yl)propan-2-ol[12] (9.11)

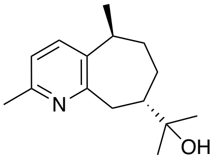

Notebook Entry: 19HHB, pg 61.

Ester starting material **1.11a** (0.075 g, 0.32 mmol) was put under Ar, then THF (12 mL) was added and cooled to -78 °C. MeLi (1.10 mL, 3.55 mmol, 3.1 M in diethoxymethane) was added dropwise and stirred for 1 hour. TLC (EtOAc) indicated all starting material was consumed. The reaction was diluted in Et_2O (20 mL), then quenched with sat. NH_4Cl. H_2O (5 mL) was added to dissolve resultant white precipitate. The layers were separated and the organic fraction was washed once with sat. NaCl, then dried over Na_2SO_4. Solvent removal by rotary evaporation gave pure product **9.11** as a clear, yellow gel. (0.070 g, 0.30 mmol, 93%).

$[\alpha]^{20}_{D}$ -11.6° (*c* 0.44, $CHCl_3$)
Chiral GC Analysis: Method A: Retention times: 36.54 min (major) and 36.64 min (minor). 99% ee.
IR: 3366, 2965, 2917, 2870, 1642, 1458, 1380, 1175, 922, 723 cm^{-1}.
^{1}H NMR (500 MHz, $CDCl_3$): δ 7.34 (d, *J* = 7.7 Hz, 1H), 6.93 (d, *J* = 7.8 Hz, 1H), 3.22 (app d, 1H), 2.97 (app quin 1H), 2.88 (dd, *J* = 13.2, 10.2 Hz, 1H), 2.48 (s, 3H), 2.12-2.08 (m, 1H), 1.89 (ddq, *J* = 13.7, 6.4, 5.0 Hz, 1H), 1.60 (dddd, *J* = 12.1, 12.1, 12.1, 3.6 Hz, 1H), 1.44-1.39 (m, 1H), 1.32 (d, *J* = 7.0 Hz, 3H), 1.26 (s, 3H), 1.25 (s, 3H), 1.29-1.21 (m, 1H) ppm.
^{13}C NMR (125 MHz, $CDCl_3$): δ 160.9, 154.2, 137.9, 132.4, 120.7, 73.3, 48.0, 39.7, 36.1, 35.3, 32.6, 27.6, 26.0, 23.9, 20.7 ppm.
HRMS (ESI, q-TOF) *m/z* [M +H] calcd for $C_{15}H_{23}NO$ 234.1852; found 234.1857.

(*R*)-2-((3-(Allyloxy)-6-methylpyridin-2-yl)methyl)-*N*-((*S*)-1-hydroxy-3-phenylpropan-2-yl)hex-5-enamide (29)

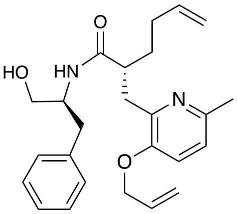

Notebook Entry: 45HH, pg 61.

This side product was isolated during the preliminary synthesis of intermediate **13.2**. NaOMe (0.131 g, 2.43 mmol) was put under Ar atmosphere then dissolved in MeOH (5 mL) and cooled to 0 °C. Starting material **13.1** (1.057 mmol, 2.428 mmol) was added and the mixture was stirred for 30 minutes. At this time, H_2O (20 mL) and sat. NH_4Cl (15 mL) was added and product was extracted three times using CH_2Cl_2. The combined organic layers were dried over Na_2SO_4 and solvent was removed. Crude product was purified using flash column chromatography (2:1 hexanes:EtOAc) and hydroxyamide **29** was isolated as an off-white solid (0.885 g, 2.16 mmol, 89%).

IR: 3267, 3022, 2924, 2859, 2100, 1649, 1458, 1259, 1054, 695 cm^{-1}.
^{1}H NMR (500 MHz, $CDCl_3$): δ 7.24 (app t, 2H), 7.18 (app t, 1H), 7.16 (app d, 2H), 7.01 (d, *J* = 8.4 Hz, 1H), 6.92 (d, *J* = 8.4 Hz, 1H), 6.53 (d, *J* = 7.8 Hz, 1H), 6.01 (ddt, *J* = 17.4, 15.7, 5.2 Hz, 1H), 5.75 (dddd, *J* = 16.9, 10.2, 6.7, 6.7 Hz, 1H), 5.39 (dddd, *J* = 17.2, 1.7, 1.7, 1.7 Hz, 1H), 5.29 (dddd, *J* = 10.5, 1.5, 1.5, 1.5 Hz, 1H), 4.98 (app dd, 1H), 4.93 (app d, 1H), 4.51 (app d, 2H), 4.09 (m, 1H), 3.66 (dd, *J* = 11.3, 3.4 Hz, 1H), 3.49 (dd, *J* = 11.3, 4.6 Hz, 1H), 3.08 (dd, *J* = 14.2, 3.7 Hz, 1H), 2.85 (m, 1H), 2.80 (app d, 2H), 2.43 (s, 3H), 2.03 (app q, 2H), 1.78 (m, 2H), 1.55 (m, 2H) ppm.
^{13}C NMR (125 MHz, $CDCl_3$): δ 175.6, 150.8, 148.6, 148.5, 138.2, 138.0, 132.7, 129.1, 128.5, 126.4, 121.8, 119.4, 117.8, 114.8, 69.0, 63.5, 52.7, 45.2, 37.1, 35.4, 32.0, 31.4, 22.9 ppm.

1-((*S*)-4-Benzyl-2-oxooxazolidin-3-yl)-2-(but-3-en-1-yl)oct-7-ene-1,3-dione (28)

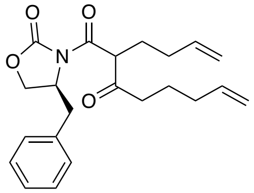

Notebook Entry: 44HH, pg 72.

This side product was isolated during synthesis and subsequent purification of intermediates **13.3**, **14.1**, **15.3**, and **16.2**. See experimental procedures for these compounds.

^{1}H NMR (500 MHz, $CDCl_3$): δ 7.33 (app t, 2H), 7.27 (app t, 2H), 7.20 (app d, 1H), 5.86-5.72 (m, 2H), 5.09-4.97 (m, 4H), 4.25-4.15 (m, 2H), 3.38 (m, 1H), 2.23-2.13 (m, 3H), 2.11-2.04 (m, 3H), 1.87-1.81 (m, 1H), 1.75-1.66 (m, 2H) ppm.

2-(Hydroxymethyl)-6-methylpyridin-3-yl trifluoromethanesulfonate (18.3)

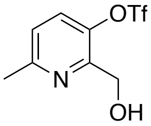

Notebook Entry: 99HH, pg 246.

Diol **18.2** (1.395 g, 10.03 mmol) and $PhNTf_2$ (5.359 g, 15.00 mmol) were added to a flask and put under Ar atmosphere. CH_2Cl_2 (30 mL) and acetone (5 mL) was added and stirred for 30 minutes before cooling to 0 °C. NEt_3 (2.4 mL, 17.23 mmol) was added and the reaction was left stirring for 3 hours. Solvent was removed before diluting in CH_2Cl_2 and the solution was washed with 10% NaOH, sat. NH_4Cl, and sat. NaCl sequentially, then dried over Na_2SO_4. Solvent removal by rotary evaporation gave a orange oil that crystallized after standing at room temperature which was purified using flash column chromatography (3:1 hexanes:EtOAc). Pure product **18.4** was isolated as a clear, yellow oil. (1.976 g, 7.286 mmol, 73%).

IR: 2924, 1460, 1421, 1215, 1138, 1072, 881, 850, 704, 627 cm^{-1}.
^{1}H NMR (500 MHz, $CDCl_3$): δ 7.55 (d, *J* = 8.5 Hz, 1H), 7.21 (d, *J* = 8.5 Hz, 1H), 4.57 (s, 2H), 2.60 (s, 3H) ppm.
^{13}C NMR (125 MHz, $CDCl_3$): δ 157.8, 150.5, 141.7, 129.5, 123.4, 118.5 (q, *J* = 318.8 Hz), 59.3, 23.7 ppm.

2-(Bromomethyl)-6-methylpyridin-3-yl-trifluoromethanesulfonate (18.4)

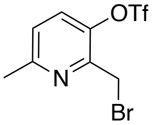

Notebook Entry: 19HHB, pg 61.

N-bromosuccinimide (1.434 g, 8.028 mmol) was added to a flask and put under Ar atmosphere. CH_2Cl_2 (6 mL) was added, then triflate **18.4** (1.976 g, 7.286 mmol), dissolved in CH_2Cl_2 (25 mL), was added. PPh_3 (2.106 g,8.029 mmol) was added in portions of 1/3 after stirring for 15 minutes after each addition. The reaction was deemed complete by TLC (3:1 hexanes: EtOAc) after 2.5 hours and the solution was filtered over silica using 3:1 hexanes:EtOAc. Solvent was removed, leaving pure product **18.5** as a clear oil (2.192 g, 6.561 mmol, 90%).

IR: 2960, 2922, 2860, 1460, 1429, 1217, 1132, 1072, 885, 849, 704, 621 cm^{-1}.
^{1}H NMR (500 MHz, $CDCl_3$): δ 7.55 (d, *J* = 8.5 Hz, 1H), 7.21 (d, *J* = 8.5 Hz, 1H), 4.57 (s, 2H), 2.60 (s, 3H) ppm.
^{13}C NMR (125 MHz, $CDCl_3$): δ 158.8, 148.7, 142.6, 129.7, 124.8, 118.5 (q, *J* = 318.8 Hz), 27.1, 24.0 ppm.

2-((*R*)-2-((*S*)-4-Benzyl-2-oxooxazolidine-3-carbonyl)hex-5-en-1-yl)-6-methylpyridin-3-yl trifluoromethanesulfonate (18.5)

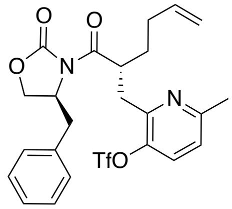

Notebook Entry: 104HH, pg. 256.

Starting material (0.274 g, 1.00 mmol) was put under Ar in a 15 mL flask, then dissolved in THF (5 mL). This solution was cooled to -78 °C, then LHMDS (1.20 mL, 1.20 mmol (1.0 M in THF)) was added drop-wise and stirred for 3 hours after removal from the ice bath. At this time, the reaction was cooled to -78 °C again and pyridyl bromide (0.314 g, 0.94 mmol) was added slowly. The flask remained in the ice bath to cool slowly overnight.

After this time, the reaction was quenched with saturated NH_4Cl (4 mL) then diluted in CH_2Cl_2 (20 mL). The organic layer was set aside, then the aqueous layer was extracted two additional times, then discarded. The combined organic layers were washed once with saturated NaCl, then dried over Na_2SO_4. Solvent was removed, leaving a hazy yellow oil. The crude product was then purified by flash column chromatography (6:1 hexanes:EtOAc, $R_f = 0.25$), giving a clear, colorless oil (0.274 g). This product contained trace amounts of starting material (**14.3**), making it necessary to accurately characterize this compound after completely pure product has been isolated in future syntheses.

Methyl (*R*)-2-((6-methyl-3-(((trifluoromethyl)sulfonyl)oxy)pyridin-2-yl)methyl)hex-5-enoate (18.6)

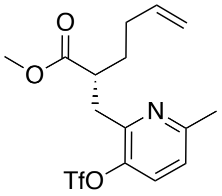

Notebook entry: 94HH, pg. 235.

LiOH•H_2O (0.042 g, 1.00 mmol) was placed in a flask and THF and H_2O (1.0 mL, 0.5 mL) was added. This was cooled to 0 °C and H_2O_2 (30% v/v, 0.20 mL, 2.56 mmol) was added and stirred for 15 minutes. Crude starting material (**18.5**) (0.262 g) was dissolved in THF (0.5 mL). The vial was rinsed twice with THF (0.25 mL) to achieve a final solvent ratio of 4:1, THF: H_2O. After 24 hours, the mixture was quenched with $Na_2S_2O_3$ and stirred for 15 minutes. The pH was neutralized with NH_4Cl and product was extracted using EtOAc three times. The combined organic layers were washed with sat. NaCl and dried over Na_2SO_4. Solvent was removed, leaving the crude material as a pale, yellow oil.

This crude material was dissolved in MeOH (10 mL) and 8 drops H_2SO_4 was added. The reaction was heated to 50 °C and refluxed for 36 hours, then cooled slowly overnight, due to ambiguous TLC results. MeOH was removed and excess acid was neutralized using $NaHCO_3$ after dilution in CH_2Cl_2. CH_2Cl_2 was used to extract product two times from the aqueous layer. Combined organic layers were washed one time with sat. NaCl and then dried over Na_2SO_4. After solvent was removed, the crude product was purified using flash column chromatography using 3:1 hexanes:EtOAc. Mostly pure product was isolated as a semi-crystalline, colorless solid. (0.014 g, 0.04 mmol).

IR: 3081, 2928, 2847, 1734, 1457, 1423, 1208, 1136, 869, 624 cm^{-1}.
^{1}H NMR (500 MHz, $CDCl_3$): δ 7.43 (d, *J* = 8.4 Hz, 1H), 7.05 (d, *J* = 8.4 Hz, 1H), 5.78 (ddt, *J* = 16.9, 10.2, 6.7 Hz, 1H), 5.03 (dd, *J* = 17.2, 1.8 Hz, 1H), 4.98 (dd, *J* = 10.2, 2.0 Hz, 1H), 3.65 (s, 3H), 3.22 (dd, *J* = 15.0, 8.9 Hz, 1H), 3.06 (dddd, *J* = 13.7, 8.4, 5.3 Hz, 1H), 3.00 (dd, *J* = 15.0, 5.2 Hz, 1H), 2.52 (s, 3H), 2.11 (m, 2H), 1.83 (dddd, *J* = 13.4, 8.4, 8.4, 6.4 Hz, 1H), 1.65 (dddd, *J* = 13.6, 9.2, 6.6, 5.5 Hz, 1H) ppm.
^{13}C NMR (125 MHz, $CDCl_3$): δ 175.6, 157.9, 151.2, 143.1, 137.7, 128.9, 122.2, 118.5 (q, *J* = 320.2 Hz), 115.3, 51.5, 43.0, 33.7, 31.1, 24.0 ppm.

Chapter 8. References

1. Hutchings, M. I.; Truman, A. W.; Wilkinson, B. Antibiotics: Past, Present and Future. *Curr. Opin. Microbiol.* **2019**, *51*, 72–80.
2. Newman, D. J.; Cragg, G. M. Natural Products as Sources of New Drugs over the Nearly Four Decades from 01/1981 to 09/2019. *J. Nat. Prod.* **2020**, *83*, 770–803.
3. Doak, B. C.; Over, B.; Giordanetto, F.; Kihlberg, J. Oral Druggable Space beyond the Rule of 5: Insights from Drugs and Clinical Candidates. *Chem. Biol.* **2014**, *21*, 1115–1142.
4. Kurek, J. Introductory Chapter: Alkaloids - Their Importance in Nature and for Human Life. In *Alkaloids - Their Importance in Nature and Human Life*; Kurek, J., Ed.; IntechOpen, 2019.
5. Büchi, G.; Goldman, I. M.; Mayo, D. W. The Structures of Two Alkaloids from Patchouli Oil. *J. Am. Chem. Soc.* **1966**, *88*, 3109–3113.
6. van Der Gen, A.; van Der Linde, L. M.; Witteveen, J. G. Synthesis of Guaipyridine and Some Related Sesquiterpene Alkaloids. *Recl. Trav. Chim. Pays-Bas* **1972**, *91*, 1433–1440.
7. Hsieh, T. J.; Chang, F. R.; Chia, Y. C.; Chen, C. Y.; Chiu, H. F.; Wu, Y. C. Cytotoxic Constituents of the Fruits of Cananga Odorata. *J. Nat. Prod.* **2001**, *64*, 616–619.
8. Craig, D.; Henry, G. D. Total Synthesis of the Cytotoxic Guaipyridine Sesquiterpene Alkaloid (+)-Cananodine. *European J. Org. Chem.* **2006**, *2006*, 3558–3561.
9. Shelton, P.; Ligon, T. J.; Dell Née Meyer, J. M.; Yarbrough, L.; Vyvyan, J. R. Synthesis of Cananodine by Intramolecular Epoxide Opening. *Tetrahedron Lett.* **2017**, *58*, 3478–3481.
10. Shelton, P. M. M.; Grosslight, S. M.; Mulligan, B. J.; Spargo, H. V.; Saad, S. S.; Vyvyan, J. R. Synthesis of Guaipyridine Alkaloids (±)-Cananodine and (±)-Rupestines D and G Using an Intramolecular Mizoroki-Heck Reaction. *Tetrahedron* **2020**, *76*, 131500.
11. Yusuf, A.; Zhao, J.-Y.; Aibibula, P.; Zhang, J.-B.; Huang, G.-Z.; Akber Aisa, H. Synthesis and in Vitro Biological Evaluation of Cananodine. *Heterocycles* **2021**, *102*, 506.
12. Zhang, C.; Wang, B.; Aibibula, P.; Zhao, J.; Aisa, H. A. Enantioselective Construction of Substituted Pyridine and a Seven-Membered Carbocyclic Skeleton: Biomimetic Synthesis of (-)-Rupestine D, (-)-Guaipyridine, (-)-Epiguaipyridine, and (-)-Cananodine and Their Stereoisomers. *Org. Biomol. Chem.* **2021**, *19*, 7081–7084.
13. Su, Z.; Wu, H.-K.; He, F.; Slukhan, U.; Aisa, H. A. New Guaipyridine Sesquiterpene Alkaloids from *Artemisia Rupestris* L. *Helv. Chim. Acta* **2010**, *93*, 33–38.
14. He, F.; Nugroho, A. E.; Wong, C. P.; Hirasawa, Y.; Shirota, O.; Morita, H.; Aisa, H. A. Rupestines F-M, New Guaipyridine Sesquiterpene Alkaloids from Artemisia Rupestris. *Chem. Pharm. Bull.* **2012**, *60*, 213–218.
15. Starchman, E. S.; Marshall, M. S.; Vyvyan, J. R. Synthesis of (±)-Rupestines B and C by Intramolecular Mizoroki-Heck Cyclization. *Tetrahedron Lett.* **2020**, *61*, 151837.
16. Yusuf, A.; Zhao, J.; Wang, B.; Aibibula, P.; Aisa, H. A.; Huang, G. Total Synthesis of Rupestine G and Its Epimers. *R. Soc. Open Sci.* **2018**, *5*, 172037.

[17] Aibibula, P.; Yusuf, A.; Zhao, J.; Wang, B.; Huang, G.; Aisa, H. A. Synthesis of (±)-Rupestine A and (±)-Rupestine J, Structural Reassignment of Rupestine A via ECD Analysis. *Chem. Pap.* **2021**, *75*, 5599–5603.

[18] Scheerer, J. R.; Leeth, E. B.; Sprow, J. A. Synthesis of Guaipyridine Alkaloids Rupestine M and L by Cycloaddition/Cycloreversion of an Intermediate 1,4-Oxazinone. *Synthesis,* **2023,** *5,* A-F.

[19] International Agency for Research on Cancer. Estimated Age-Standardized Incidence Rates (World) in 2020, Liver, Both Sexes, All Ages. **2020**.

[20] Llovet, J. M.; Kelley, R. K.; Villanueva, A.; Singal, A. G.; Pikarsky, E.; Roayaie, S.; Lencioni, R.; Koike, K.; Zucman-Rossi, J.; Finn, R. S. Hepatocellular Carcinoma. *Nat. Rev. Dis. Primers,* **2021**, *7*, 6.

[21] Schlessinger, J. Cell Signaling by Receptor Tyrosine Kinases. *Cell,* **2000**, *103*, 211–225.

[22] Zwick, E.; Bange, J.; Ullrich, A. Receptor Tyrosine Kinases as Targets for Anticancer Drugs. *Trends Mol. Med.* **2002**, *8*, 17–23.

[23] Györffy, B.; Schäfer, R. Biomarkers Downstream of RAS: A Search for Robust Transcriptional Targets. *Curr. Cancer Drug Targets,* **2010**, *10*, 858–868.

[24] Davies, H.; Bignell, G. R.; Cox, C.; Stephens, P.; Edkins, S.; Clegg, S.; Teague, J.; Woffendin, H.; Garnett, M. J.; Bottomley, W. Mutations of the BRAF Gene in Human Cancer. *Nature,* **2002**, *417*, 949–954.

[25] Hwang, Y. H.; Choi, J. Y.; Kim, S.; Chung, E. S.; Kim, T.; Koh, S. S.; Lee, B.; Bae, S. H.; Kim, J.; Park, Y. M. Over-Expression of c-Raf-1 Proto-Oncogene in Liver Cirrhosis and Hepatocellular Carcinoma. *Hepatol. Res.* **2004**, *29*, 113–121.

[26] Whittaker, S.; Marais, R.; Zhu, A. X. The Role of Signaling Pathways in the Development and Treatment of Hepatocellular Carcinoma. *Oncogene* **2010**, *29*, 4989–5005.

[27] Gedaly, R.; Angulo, P.; Hundley, J.; Daily, M. F.; Chen, C.; Koch, A.; Evers, B. M. PI-103 and Sorafenib Inhibit Hepatocellular Carcinoma Cell Proliferation by Blocking Ras/Raf/MAPK and PI3K/AKT/MTOR Pathways. *Anticancer Res.* **2010**, *30*, 4951–4958.

[28] McDonald, O. B.; Chen, W. J.; Ellis, B.; Hoffman, C.; Overton, L.; Rink, M.; Smith, A.; Marshall, C. J.; Wood, E. R. A Scintillation Proximity Assay for the Raf/MEK/ERK Kinase Cascade: High-Throughput Screening and Identification of Selective Enzyme Inhibitors. *Anal. Biochem.* **1999**, *268*, 318–329.

[29] Wilhelm, S.; Chien, D.-S. BAY 43-9006: Preclinical Data. *Curr. Pharm. Des.* **2002**, *8*, 2255–2257.

[30] Carlomagno, F.; Anaganti, S.; Guida, T.; Salvatore, G.; Troncone, G.; Wilhelm, S. M.; Santoro, M. BAY 43-9006 Inhibition of Oncogenic RET Mutants. *J Natl Cancer Inst* **2006**, *98*, 326–334.

[31] Wilhelm, S.; Carter, C.; Lynch, M.; Lowinger, T.; Dumas, J.; Smith, R. A.; Schwartz, B.; Simantov, R.; Kelley, S. Discovery and Development of Sorafenib: A Multikinase Inhibitor for Treating Cancer. *Nat. Rev. Drug Discov.* **2006**, *5*, 835–844.

[32] Wan, P. T. C.; Garnett, M. J.; Roe, S. M.; Lee, S.; Niculescu-Duvaz, D.; Good, V. M.; Jones, C. M.; Marshall, C. J.; Springer, C. J.; Barford, D. Mechanism of Activation of the RAF-ERK Signaling Pathway by Oncogenic Mutations of B-RAF. *Cell,* **2004**, *116*, 855–867.

33. Greten, T. F.; Korangy, F.; Manns, M. P.; Malek, N. P. Molecular Therapy for the Treatment of Hepatocellular Carcinoma. *Br. J. Cancer,* **2009**, *100*, 19–23.

34. Llovet, J. M.; Bruix, J. Molecular Targeted Therapies in Hepatocellular Carcinoma. *Hepatology* **2008**, *48*, 1312–1327.

35. Zhang, X.; Wang, Y.; Ji, J.; Si, D.; Bao, X.; Yu, Z.; Zhu, Y.; Zhao, L.; Li, W.; Liu, J. Discovery of 1,6-Naphthyridin-2(1H)-One Derivatives as Novel, Potent, and Selective FGFR4 Inhibitors for the Treatment of Hepatocellular Carcinoma. *J. Med. Chem.* **2022**, *65*, 7595–7618.

36. Kant, R.; Yang, M.-H.; Tseng, C.-H.; Yen, C.-H.; Li, W.-Y.; Tyan, Y.-C.; Chen, M.; Tzeng, C.-C.; Chen, W.-C.; You, K.; et al. Discovery of an Orally Efficacious MYC Inhibitor for Liver Cancer Using a GNMT-Based High-Throughput Screening System and Structure-Activity Relationship Analysis. *J. Med. Chem.* **2021**, *64*, 8992–9009.

37. Pouwer, R. H.; Richard, J.-A.; Tseng, C.-C.; Chen, D. Y.-K. Chemical Synthesis of the Englerins. *Chem. Asian J.* **2012**, *7*, 22–35.

38. Hardin Narayan, A. R.; Simmons, E. M.; Sarpong, R. Synthetic Strategies Directed towards the Cortistatin Family of Natural Products. *European J. Org. Chem.* **2010**, *19*, 3553–3567.

39. Ur Rashid, M.; Alamzeb, M.; Ali, S.; Ullah, Z.; Shah, Z. A.; Naz, I.; Khan, M. R. The Chemistry and Pharmacology of Alkaloids and Allied Nitrogen Compounds from Artemisia Species: A Review. *Phytother. Res.* **2019**, *33*, 2661–2684.

40. Obul, M.; Wang, X.; Zhao, J.; Li, G.; Aisa, H. A.; Huang, G. Structural Modification on Rupestonic Acid Leads to Highly Potent Inhibitors against Influenza Virus. *Mol. Divers.* **2019**, *23*, 1–9.

41. Miayaura, N. and Suzuki, A. Palladium-Catalyzed Cross-Coupling Reactions of Organoboron Compounds. *Chem. Rev.* **1995**, *95*, 2457–2483.

42. Krapcho, P.A.; Lovey, A.J. Decarbalkoxylations of Geminal Diesters, β-Keto Esters and α-Cyano Esters Effected by Sodium Chloride in Dimethyl Sulpoxide. *Tetrahedron Lett.* **1973**, *14*, 957–960.

43. Grubbs, R.H. Olefin-Metathesis Catalysts for the Preparation of Molecules and Materials. *Angew. Chem. Int. Ed.* **2006,** *45,* 3760-3765.

44. Blaise, E. E. C. R. Nouvelles Réactions de Dérivés Organométalliques. *Hebd. Seances Acad. Sci.* **1901**, *132*, 478–480.

45. Chichibabin, A. Dihydro Pyridine Synthesis. *J. Russ. Phys. Chem. Soc.* **1906**, *37*, 1229–1236.

46. Kolb, H. C.; VanNieuwenhze, M. S.; Sharpless, K. B. Catalytic Asymmetric Dihydroxylation. *Chem. Rev.* **1994**, *94*, 2483–2547.

47. Katsuki, T.; Sharpless, K. B. The First Practical Method for Asymmetric Epoxidation. *J. Am. Chem. Soc.* **1980**, *102*, 5974–5976.

48. Riley, H. L.; Morley, J. F.; Friend, N. A. C. 255. Selenium Dioxide, a New Oxidising Agent. Part I. Its Reaction with Aldehydes and Ketones. *J. Chem. Soc.* **1932**, 1875.

49. Mizoroki, T.; Mori, K.; Ozaki, A. Arylation of Olefin with Aryl Iodide Catalyzed by Palladium. *Bull. Chem. Soc. Jpn.* **1971**, *44*, 581–581.

[50] Heck, R. F.; Nolley, J. P. Palladium-Catalyzed Vinylic Hydrogen Substitution Reactions with Aryl, Benzyl, and Styryl Halides. *J. Org. Chem.* **1972**, *37*, 2320–2322.

[51] Wang, C.; Xiao, G.; Guo, T.; Ding, Y.; Wu, X.; Loh, T.-P. Palladium-Catalyzed Regiocontrollable Reductive Heck Reaction of Unactivated Aliphatic Alkenes. *J. Am. Chem. Soc.* **2018**, *140*, 9332–9336.

[52] Sabahi, M.; Theriot, K.J.; Becnel, B.F. United States Patent (19). 5,536,870, July 16, 1996.

[53] Eisenstadt, A.; Hasharon, R.; Keren, Y.; Motzkin, K. Process for the Preparation of Octyl Methoxy Cinnamate. 5,187,303, February 16, 1993.

[54] Holman, K. Palladium-catalyzed cascade reactions involving C–C and C– X bond formation: Strategic applications in natural product synthesis. *Chem. Soc. Rev.* **2021.** *50,* 7891-7908.

[55] Oxtoby, L. J.; Gurak, J. A.; Wisniewski, S. R.; Eastgate, M. D.; Engle, K. M. Palladium-Catalyzed Reductive Heck Coupling of Alkenes. *Trends Chem.* **2019**, *1*, 572–587.

[56] Lee, A.L. Enantioselective Oxidative Boron Heck Reactions. *Org. Biomol. Chem.* **2016**, *14*, 5357–5366.

[57] Lee, Y.S.; Alam, M. M.; Keri, R. S. Enantioselective Reactions of N-Acyliminium Ions Using Chiral Organocatalysts. *Chem. Asian J.* **2013**, *8*, 2906–2919.

[58] Ross, S. P.; Rahman, A. A.; Sigman, M. S. Development and Mechanistic Interrogation of Interrupted Chain-Walking in the Enantioselective Relay Heck Reaction. *J. Am. Chem. Soc.* **2020**, *142*, 10516–10525.

[59] Werner, E. W.; Mei, T.S.; Burckle, A. J.; Sigman, M. S. Enantioselective Heck Arylations of Acyclic Alkenyl Alcohols Using a Redox-Relay Strategy. *Science,* **2012**, *338*, 1455–1458.

[60] Sato, Y.; Sodeoka, M.; Shibasaki, M. Catalytic Asymmetric Carbon-Carbon Bond Formation: Asymmetric Synthesis of Cis-Decalin Derivatives by Palladium-Catalyzed Cyclization of Prochiral Alkenyl Iodides. *J. Org. Chem.* **1989**, *54*, 4738–4739.

[61] Carpenter, N.; Kucera, D.; Overman, L.E. Palladium-Catalyzed Polyene Cyclizations of Trienyl Triflates . *J. Org. Chem.* **1989**, *54*, 5846–5848.

[62] Yuan, Q.; Prater, M. B.; Sigman, M. S. Enantioselective Synthesis of γ-Functionalized Cyclopentenones and δ-Functionalized Cycloheptenones Utilizing a Redox-Relay Heck Strategy. *Adv. Synth. Catal.* **2020**, *362*, 326–330.

[63] Zhang, C.; Santiago, C. B.; Crawford, J. M.; Sigman, M. S. Enantioselective Dehydrogenative Heck Arylations of Trisubstituted Alkenes with Indoles to Construct Quaternary Stereocenters. *J. Am. Chem. Soc.* **2015**, *137*, 15668–15671.

[64] Mei, T.-S.; Patel, H. H.; Sigman, M. S. Enantioselective Construction of Remote Quaternary Stereocentres. *Nature,* **2014**, *508*, 340–344.

[65] Zhang, C.; Tutkowski, B.; DeLuca, R. J.; Joyce, L. A.; Wiest, O.; Sigman, M. S. Palladium-Catalyzed Enantioselective Heck Alkenylation of Trisubstituted Allylic Alkenols: A Redox-Relay Strategy to Construct Vicinal Stereocenters. *Chem. Sci.* **2017**, *8*, 2277–2282.

[66] Yuan, Q.; Sigman, M. S. Palladium-Catalyzed Enantioselective Relay Heck Arylation of Enelactams: Accessing α,β-Unsaturated δ-Lactams. *J. Am. Chem. Soc.* **2018**, *140*, 6527–6530.

[67] Patel, H. H.; Sigman, M. S. Palladium-Catalyzed Enantioselective Heck Alkenylation of Acyclic Alkenols Using a Redox-Relay Strategy. *J. Am. Chem. Soc.* **2015**, *137*, 3462–3465.

[68] Prater, M. B.; Sigman, M. S. Enantioselective Synthesis of Alkyl Allyl Ethers via Palladium-catalyzed Redox-relay Heck Alkenylation of *o* -alkyl Enol Ethers. *Isr. J. Chem.* **2019**. *60,* 452-460.

[69] Mei, T.-S.; Werner, E. W.; Burckle, A. J.; Sigman, M. S. Enantioselective Redox-Relay Oxidative Heck Arylations of Acyclic Alkenyl Alcohols Using Boronic Acids. *J. Am. Chem. Soc.* **2013**, *135*, 6830–6833.

[70] Hilton, M. J.; Cheng, B.; Buckley, B. R.; Xu, L.; Wiest, O.; Sigman, M. S. Relative Reactivity of Alkenyl Alcohols in the Palladium-Catalyzed Redox-Relay Heck Reaction. *Tetrahedron,* **2015**, *71*, 6513–6518.

[71] Zhu, M.; Du, H.; Li, J.; Zou, D.; Wu, Y.; Wu, Y. Synthesis of β-Heteroaryl Carbonyl Compounds via Direct Cross-Coupling of Allyl Alcohols with Heteroaryl Boronic Acids under Cooperative Bimetallic Catalysis. *Tetrahedron Lett.* **2018**, *59*, 1352–1355.

[72] Evans, D. A.; Ennis, M. D.; Mathre, D. J. Asymmetric Alkylation Reactions of Chiral Imide Enolates. A Practical Approach to the Enantioselective Synthesis of Alpha-Substituted Carboxylic Acid Derivatives. *J. Am. Chem. Soc.* **1982**, *104*, 1737–1739.

[73] Evans, D. A.; Chapman, K. T.; Bisaha, J. New Asymmetric Diels-Alder Cycloaddition Reactions. Chiral Alpha-Beta-Unsaturated Carboximides as Practical Chiral Acrylate and Crotonate Dienophile Synthons. *J. Am. Chem. Soc.* **1984**, *106*, 4261–4263.

[74] Evans, D. A.; Adams, D. J. Total Synthesis of (+)-Galbulimima Alkaloid 13 and (+)-Himgaline. *J. Am. Chem. Soc.* **2007**, *129*, 1048–1049.

[75] Evans, D. A.; Black, W. C. Total Synthesis of (+)-A83543A [(+)-Lepicidin A]. *J. Am. Chem. Soc.* **1993**, *115*, 4497–4513.

[76] Heravi, M. M.; Zadsirjan, V.; Farajpour, B. Applications of Oxazolidinones as Chiral Auxiliaries in the Asymmetric Alkylation Reaction Applied to Total Synthesis. *RSC Adv.* **2016**, *6*, 30498–30551.

[77] Mori, M.; Chiba, K.; Ban, Y. The Reactions and Syntheses with Organometallic Compounds. V. a New Synthesis of Indoles and Isoquinolines by Intramolecular Palladium-Catalyzed Reactions of Aryl Halides with Olefinic Bonds. *Tetrahedron Lett.* **1977**, *18*, 1037–1040.

[78] Ashimori, A.; Bachand, B.; Calter, M. A.; Govek, S. P.; Overman, L. E.; Poon, D. J. Catalytic Asymmetric Synthesis of Quaternary Carbon Centers. Exploratory Studies of Intramolecular Heck Reactions of (*Z*)-α,β-Unsaturated Anilides and Mechanistic Investigations of Asymmetric Heck Reactions Proceeding via Neutral Intermediates. *J. Am. Chem. Soc.* **1998**, *120*, 6488–6499.

[79] Oestreich, M.; Dennison, P. R.; Kodanko, J. J.; Overman, L. E. Thwarting β-Hydride Elimination: Capture of the Alkylpalladium Intermediate of an Asymmetric Intramolecular Heck Reaction. *Angew. Chem. Int. Ed.* **2001**, *40*, 1439–1442.

[80.] Dounay, A. B.; Hatanaka, K.; Kodanko, J. J.; Oestreich, M.; Overman, L. E.; Pfeifer, L. A.; Weiss, M. M. Catalytic Asymmetric Synthesis of Quaternary Carbons Bearing Two Aryl Substituents. Enantioselective Synthesis of 3-Alkyl-3-Aryl Oxindoles by Catalytic Asymmetric Intramolecular Heck Reactions. *J. Am. Chem. Soc.* **2003**, *125*, 6261–6271.

[81.] Beutner, G. L.; Cohen, B. M.; DelMonte, A. J.; Dixon, D. D.; Fraunhoffer, K. J.; Glace, A. W.; Lo, E.; Stevens, J.M.; Vanyo, D.; Wilbert, C. Revisiting the Cleavage of Evans Oxazolidinones with LiOH/H_2O_2. *Org. Process Res. Dev.* **2019,** *23,* 1378-1385.

[82.] Yamauchi, S.; Sugahara, T.; Akiyama, K.; Maruyama, M.; Kishida, T. Determination of the Stereochemistry of the Tetrahydropyran Sesquineolignans Morinols A and B. *J. Nat. Prod.* **2007**, *70*, 549–556.

[83.] Verendel, J. J.; Pamies, O.; Diéguez, M.; Andersson, P.G. Asymmetric Hydrogenation of Olefins Using Chiral Crabtree-type Catalysts: Scope and Limitations. *Chem. Rev.* **2014**, *114,* 2130-2169.

[84.] Govindachari, T. R.; Narasimhan, N. S.; Rajadurai, S. Synthesis of ethyl carpyrinate. *J. Chem. Soc.* **1957**, *51*, 560-563.

[85.] Vyvyan, J. R.; Dell, J. A.; Ligon, T. J.; Montanic, K. K.; Wall, S. H. Suzuki-Miyaura cross-coupling of 3-pyridyl triflates with 1-alkenyl-2-pinacol boronates. *Synthesis*, **2010**, *21*, 3637-3644.

[86.] Candito, D. A.; Dobrovolsky, D.; Lautens, M. Development of an Intramolecular Aryne Ene Reaction and Application to the Formal Synthesis of (±)-Crinine. *J. Am. Chem. Soc.* **2012**, *134*, 15572-15580.

[87.] Joseph, J. T.; Sajith, A.M.; Ningegowda, R. C.; Shashikanth, S. Room Temperature Carbonylation of (Hetero)-Aryl Pentafluorobenzenesulfonates and Triflates using Palladium-Cobalt Bimetallic Catalyst: Dual Role of Cobalt Carbonyl. *Adv. Synth. Catal*. **2017**, *359*, 419-425.

[88.] Guthrie, R. W.; Kaplan, G. L.; Mennona, F. A.; Tilley, J. W.; Kierstead, R. W.; Mullin, J. G.; LeMahieu, R. A.; Zawoiski, S.; O'Donnell, M. Pentadienyl carboxamide derivatives as antagonists of platelet activating factor. *J. Med. Chem.* **1989**, *32,* 1820-1835.

[89.] Deepak, V. D.; Mahmud, I.; Gauthier, M. Synthesis of carboxylated derivatives of poly(isobutylene-co-isoprene) by azide-alkyne "click" chemistry. *Polym. J.* **2019**, *51*, 327-335.

[90.] Kafka, S.; Kytner, J.; Silhankova, A.; Ferles, M. Hydroboration of 1-(5-Hexenyl)piperidine and trans-1-(3-hexenyl)piperidine. *Chem. Commun.* **1987**, *52,* 2035-2047.

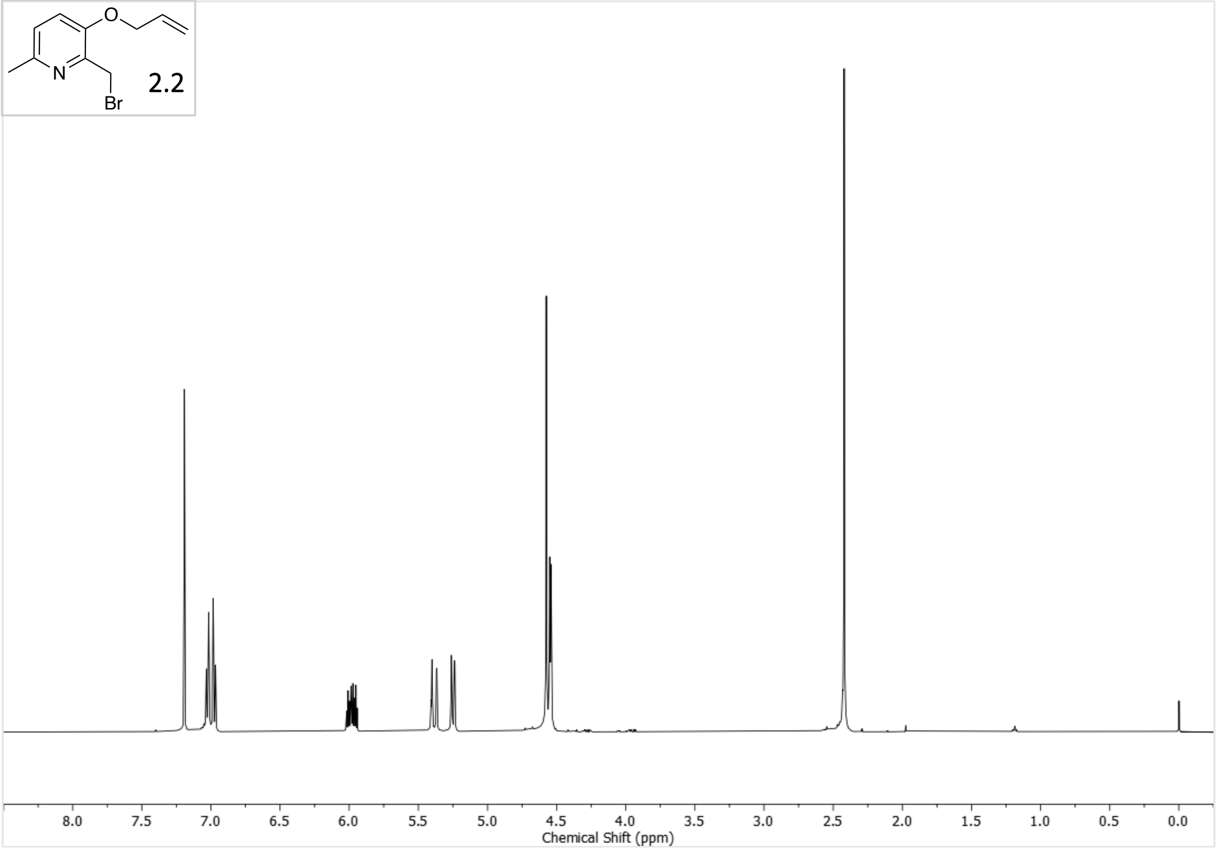
O
N
Br
8.0
7.5
7.0
6.5
6.0
5.5
5.0
4.5
4.0
3.5
3.0
2.5
2.0
1.5
1.0
0.5
0.0
Chemical Shift (ppm)

2.2

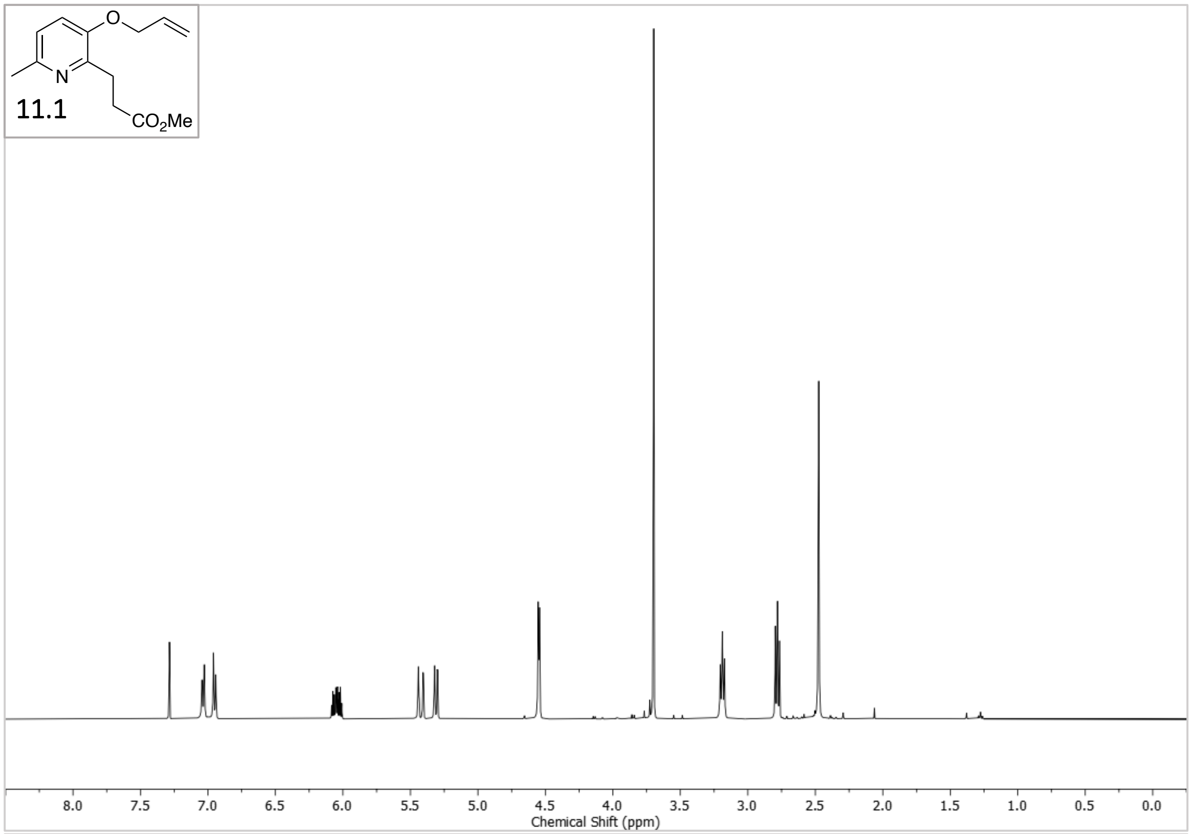
O
N
11.1
CO2Me
8.0
7.5
7.0
6.5
6.0
5.5
5.0
4.5
4.0
3.5
3.0
2.5
2.0
1.5
1.0
0.5
0.0
Chemical Shift (ppm)

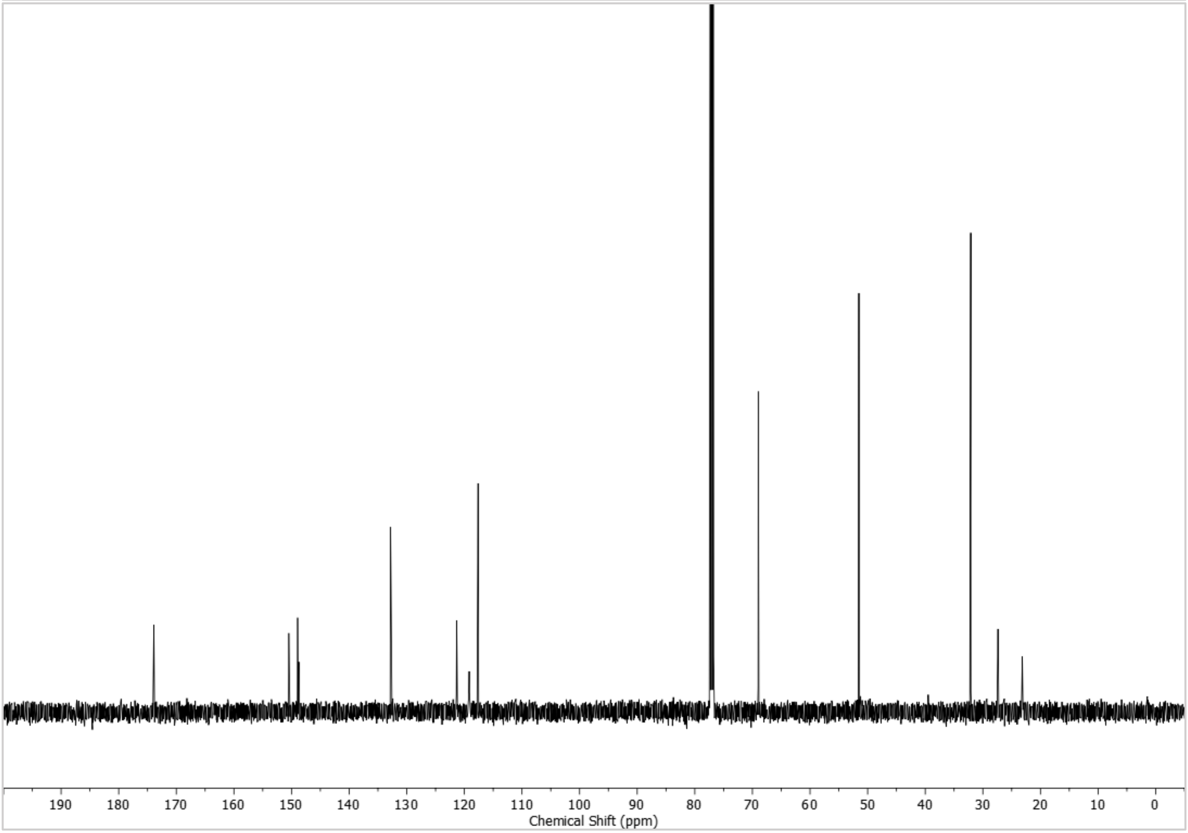
190
180
170
160
150
140
130
120
110
100
90
80
70
60
50
40
30
20
10
0
Chemical Shift (ppm)

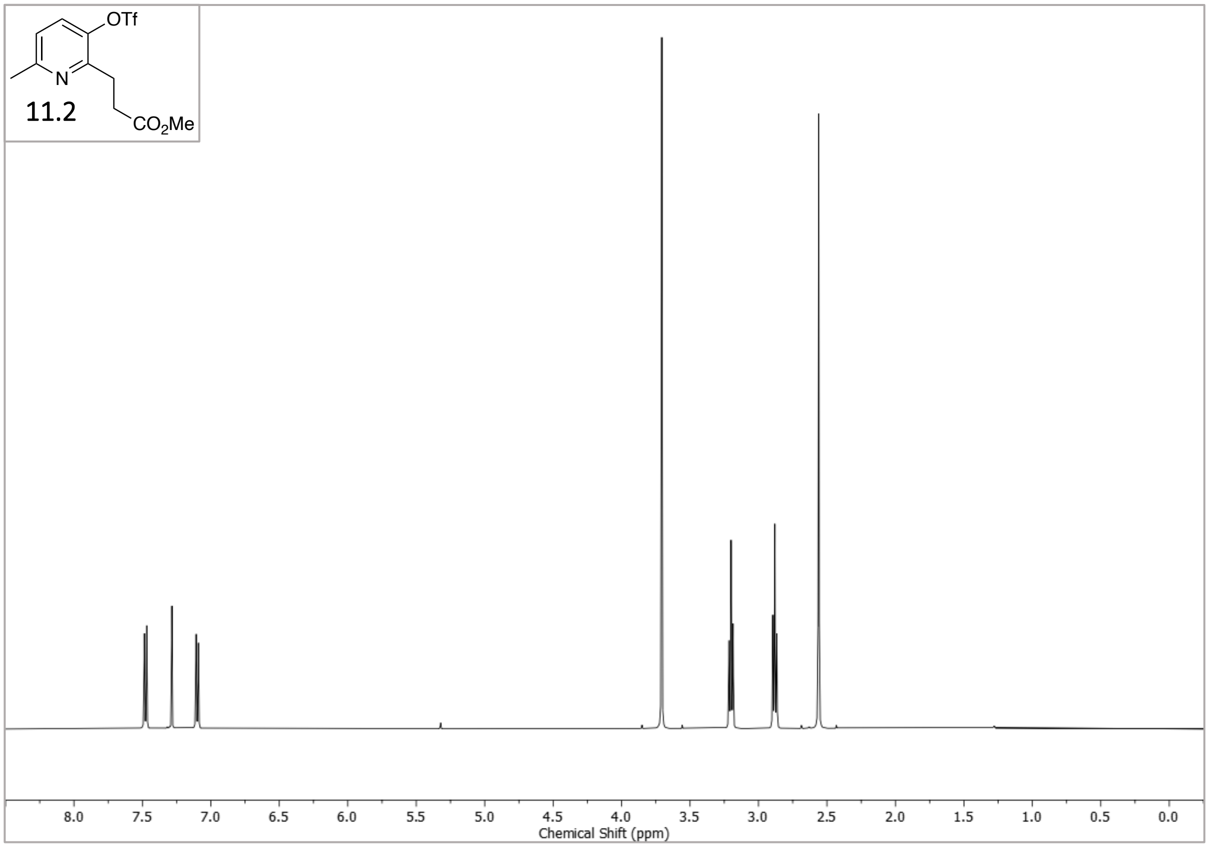
OTf
N
11.2
CO2Me
8.0
7.5
7.0
6.5
6.0
5.5
5.0
4.5
4.0
3.5
3.0
2.5
2.0
1.5
1.0
0.5
0.0
Chemical Shift (ppm)

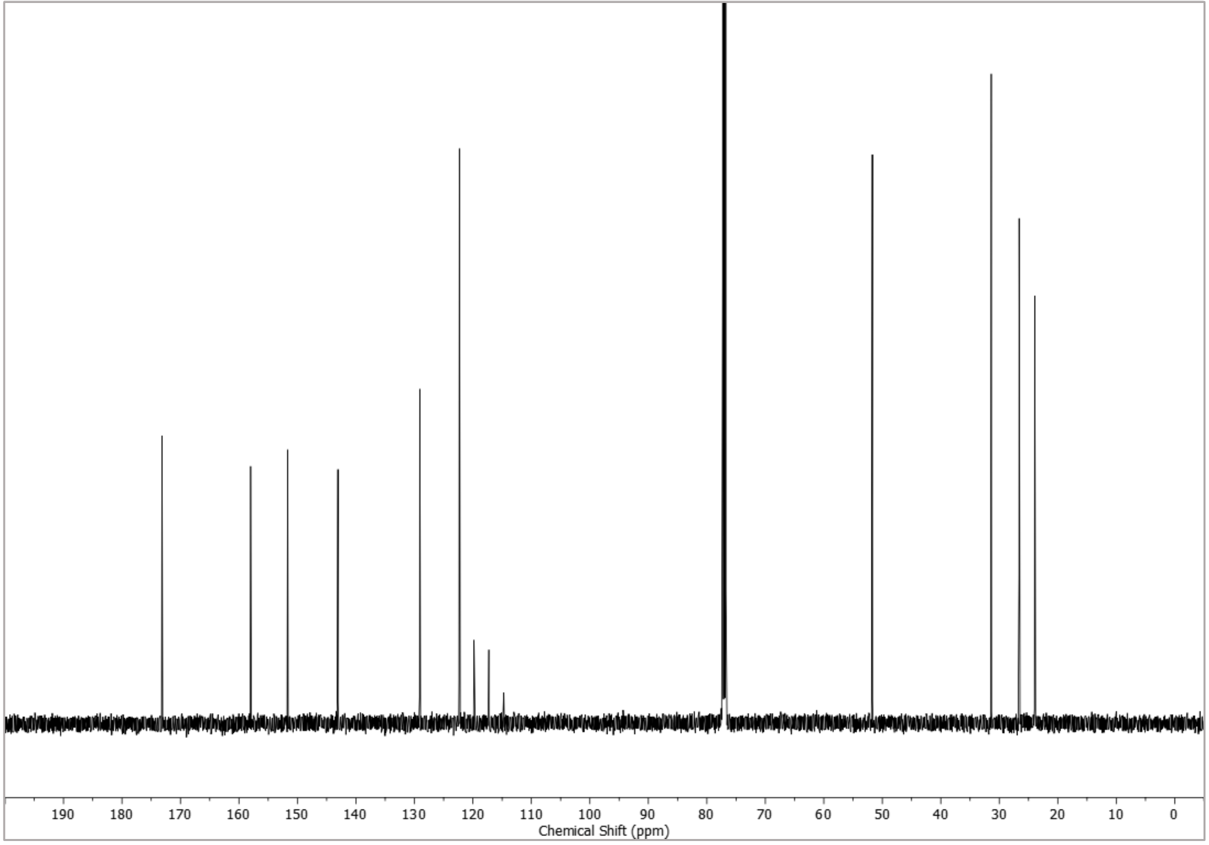
190
180
170
160
150
140
130
120
110
100
90
80
70
60
50
40
30
20
10
0
Chemical Shift (ppm)

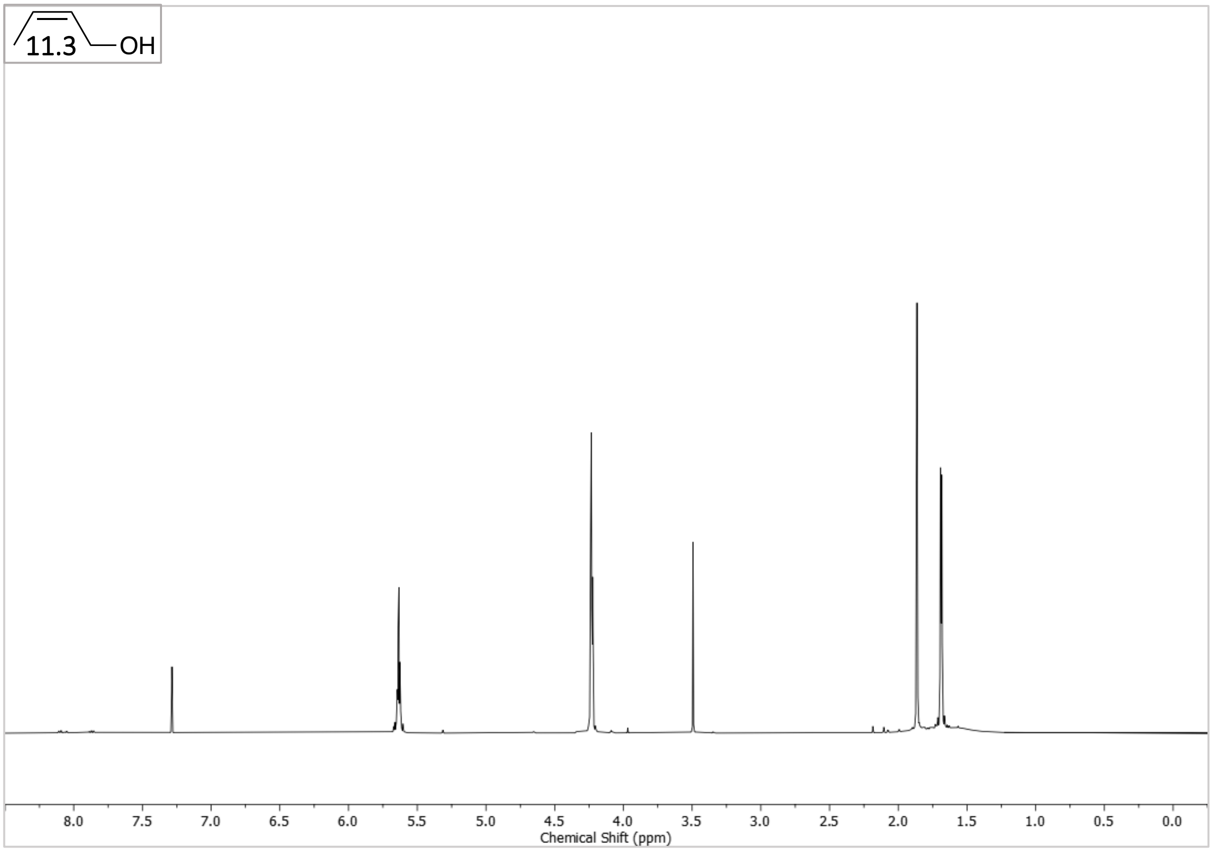
11.3
OH
8.0
7.5
7.0
6.5
6.0
5.5
5.0
4.5
4.0
3.5
3.0
2.5
2.0
1.5
1.0
0.5
0.0
Chemical Shift (ppm)

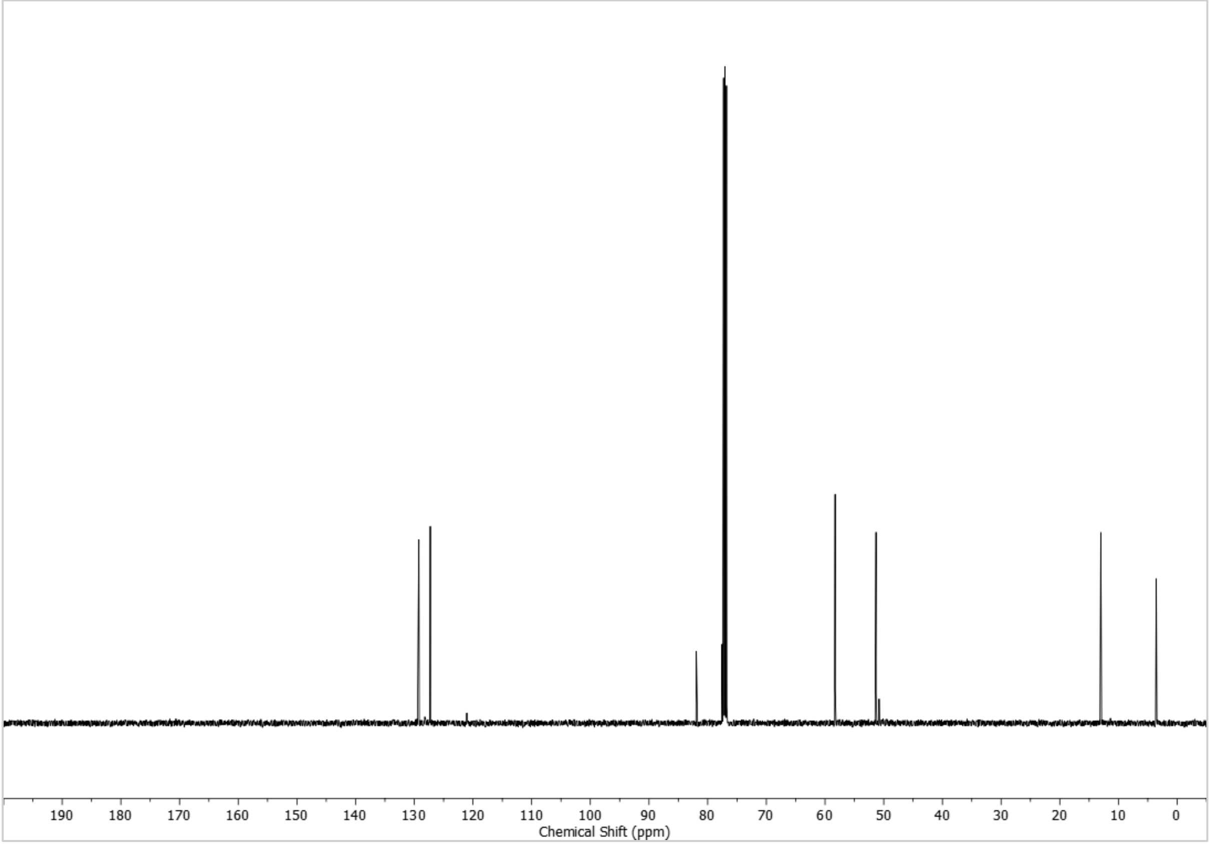
190
180
170
160
150
140
130
120
110
100
90
80
70
60
50
40
30
20
10
0
Chemical Shift (ppm)

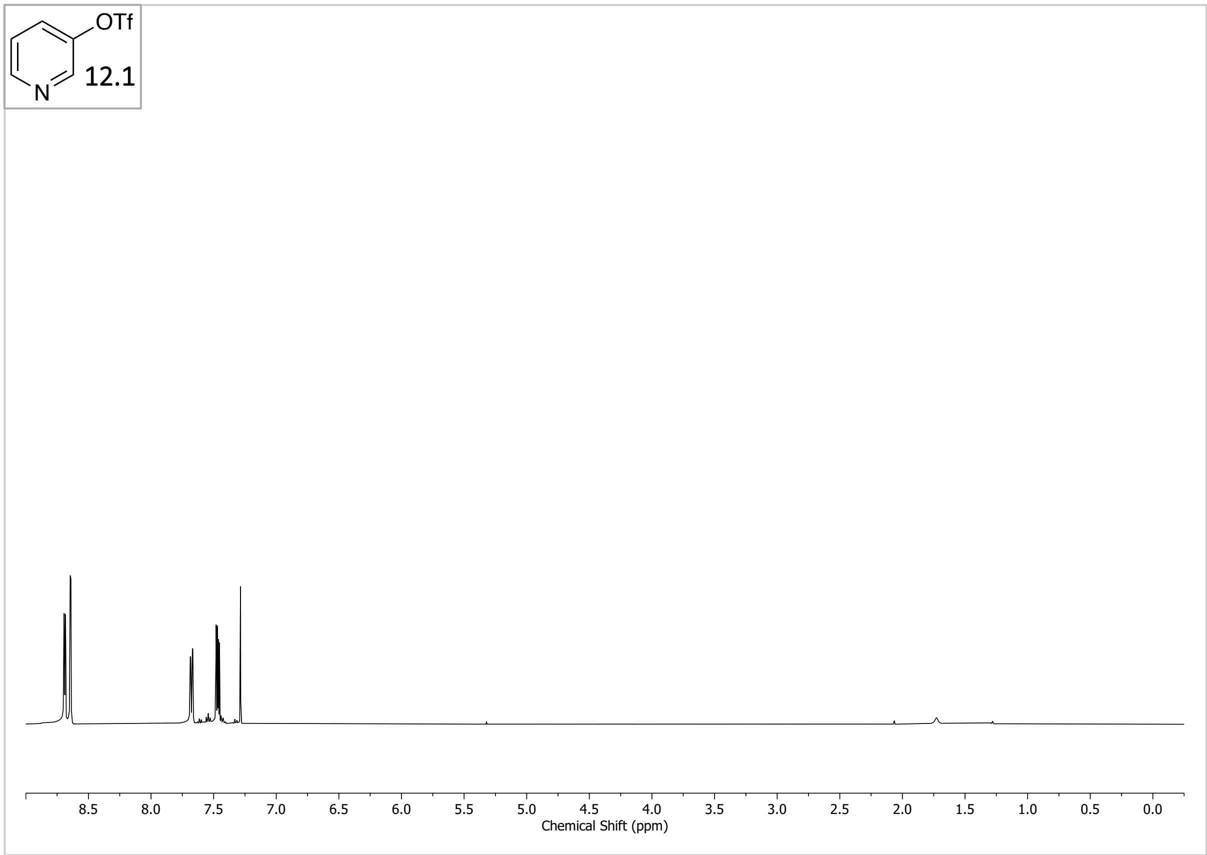
OTf
N
12.1
8.5
8.0
7.5
7.0
6.5
6.0
5.5
5.0
4.5
4.0
3.5
3.0
2.5
2.0
1.5
1.0
0.5
0.0
Chemical Shift (ppm)

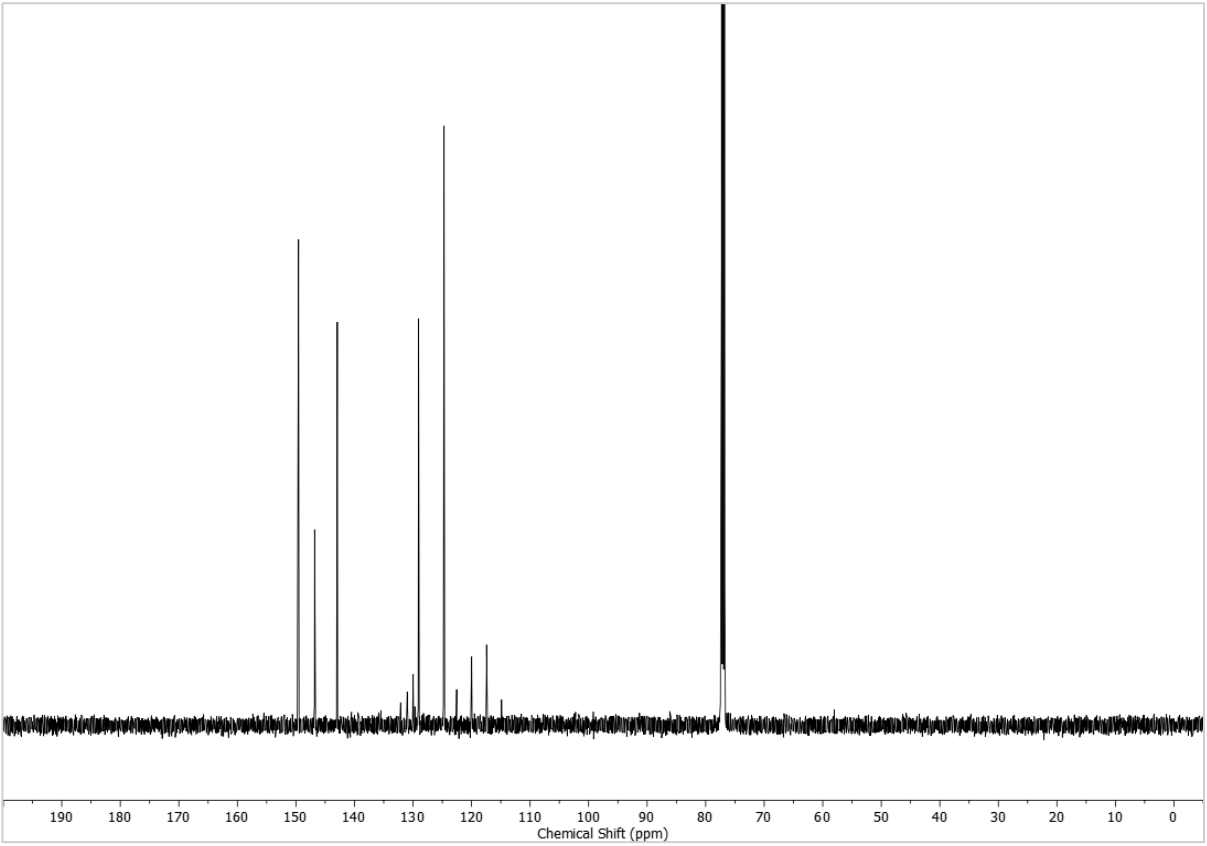
190
180
170
160
150
140
130
120
110
100
90
80
70
60
50
40
30
20
10
0
Chemical Shift (ppm)

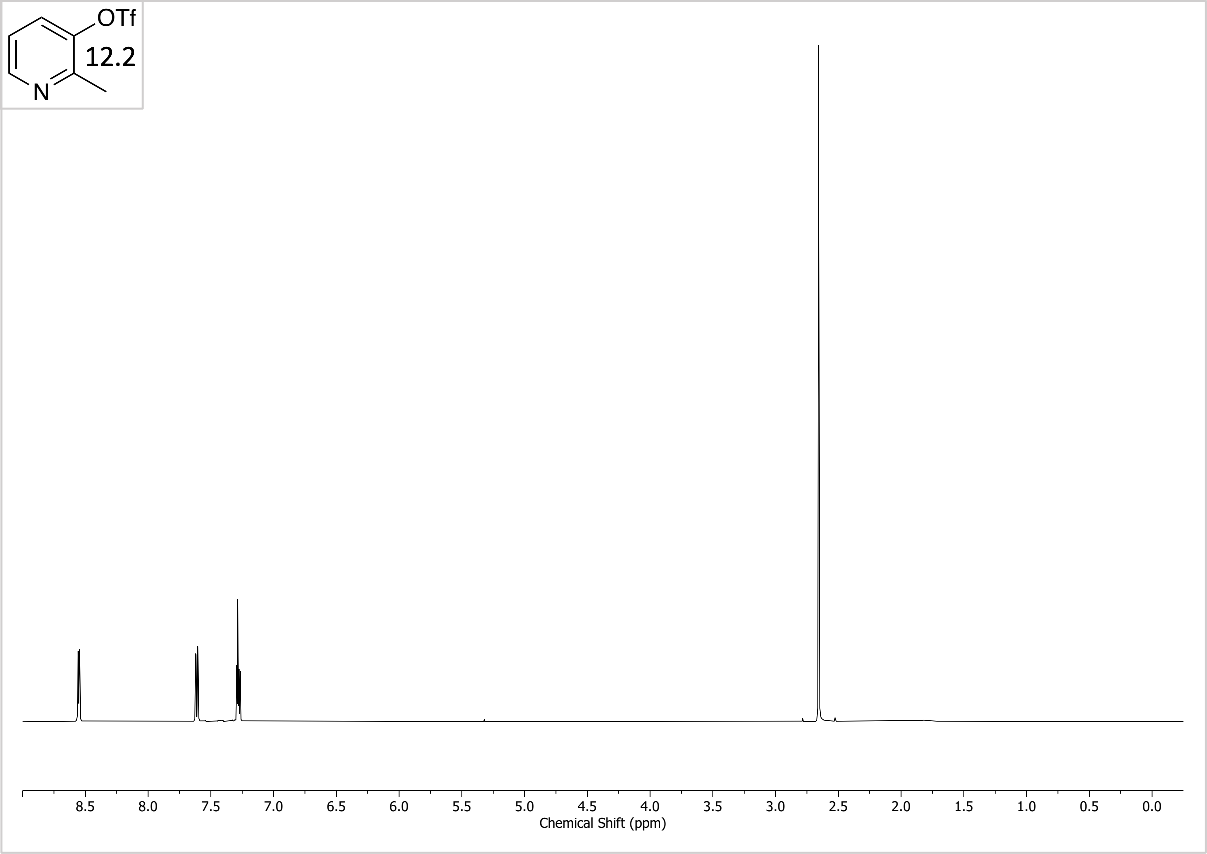

12.2

OTf
N
8.5
8.0
7.5
7.0
6.5
6.0
5.5
5.0
4.5
4.0
3.5
3.0
2.5
2.0
1.5
1.0
0.5
0.0
Chemical Shift (ppm)

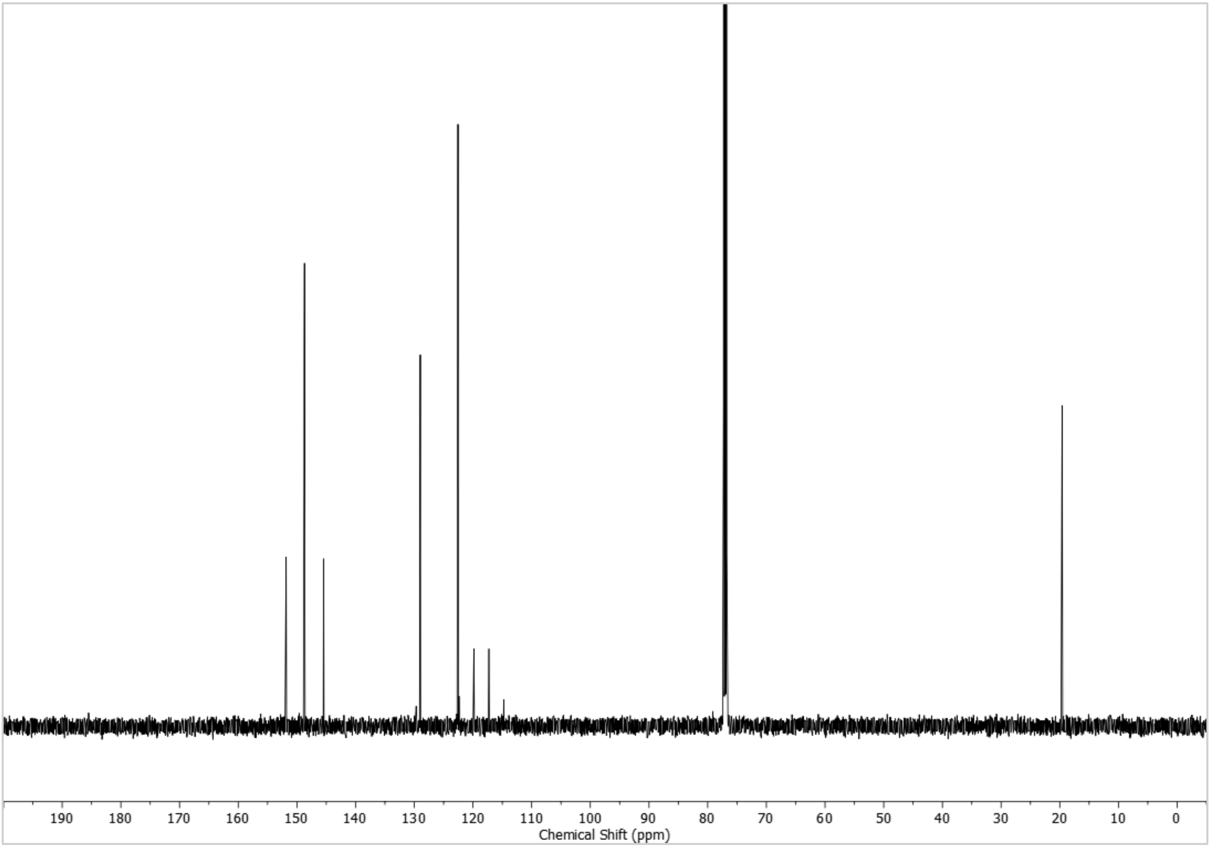

190
180
170
160
150
140
130
120
110
100
90
80
70
60
50
40
30
20
10
0
Chemical Shift (ppm)

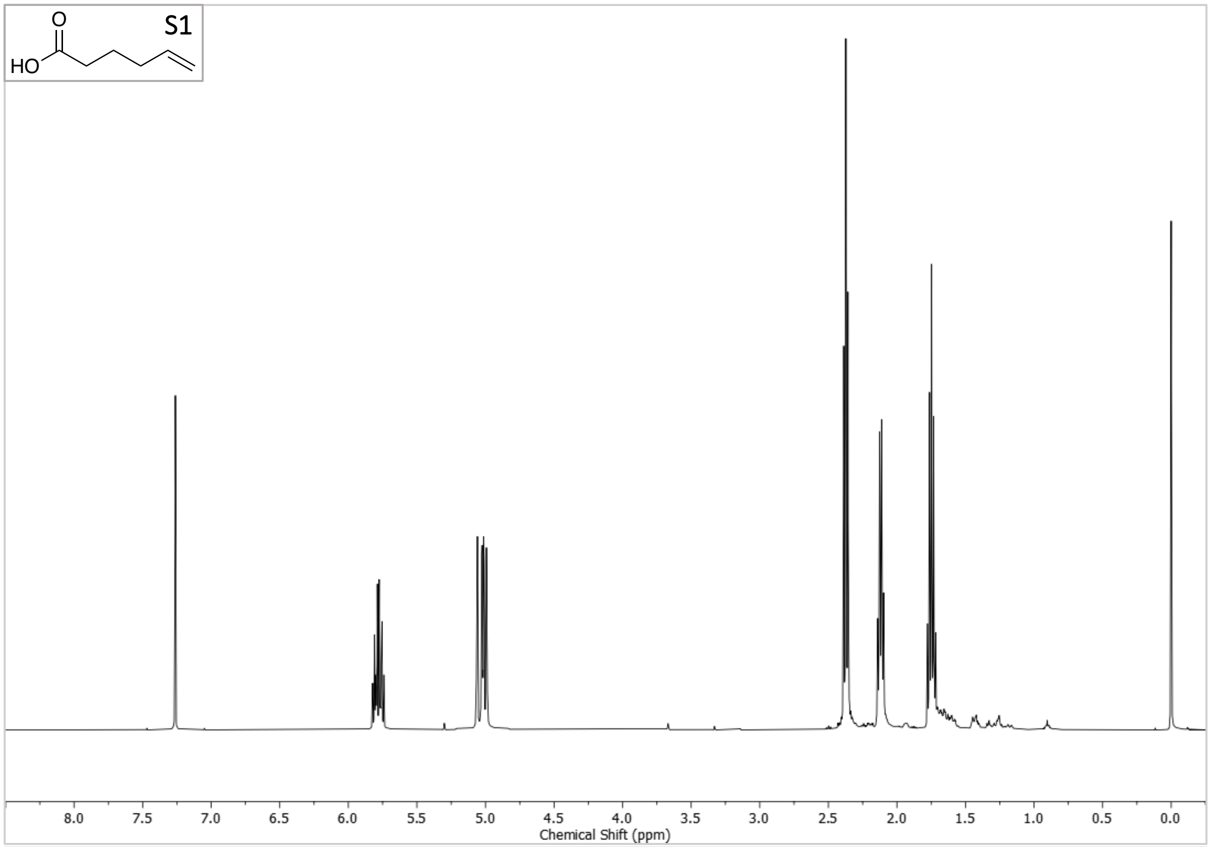
O
HO
S1
8.0
7.5
7.0
6.5
6.0
5.5
5.0
4.5
4.0
3.5
3.0
2.5
2.0
1.5
1.0
0.5
0.0
Chemical Shift (ppm)

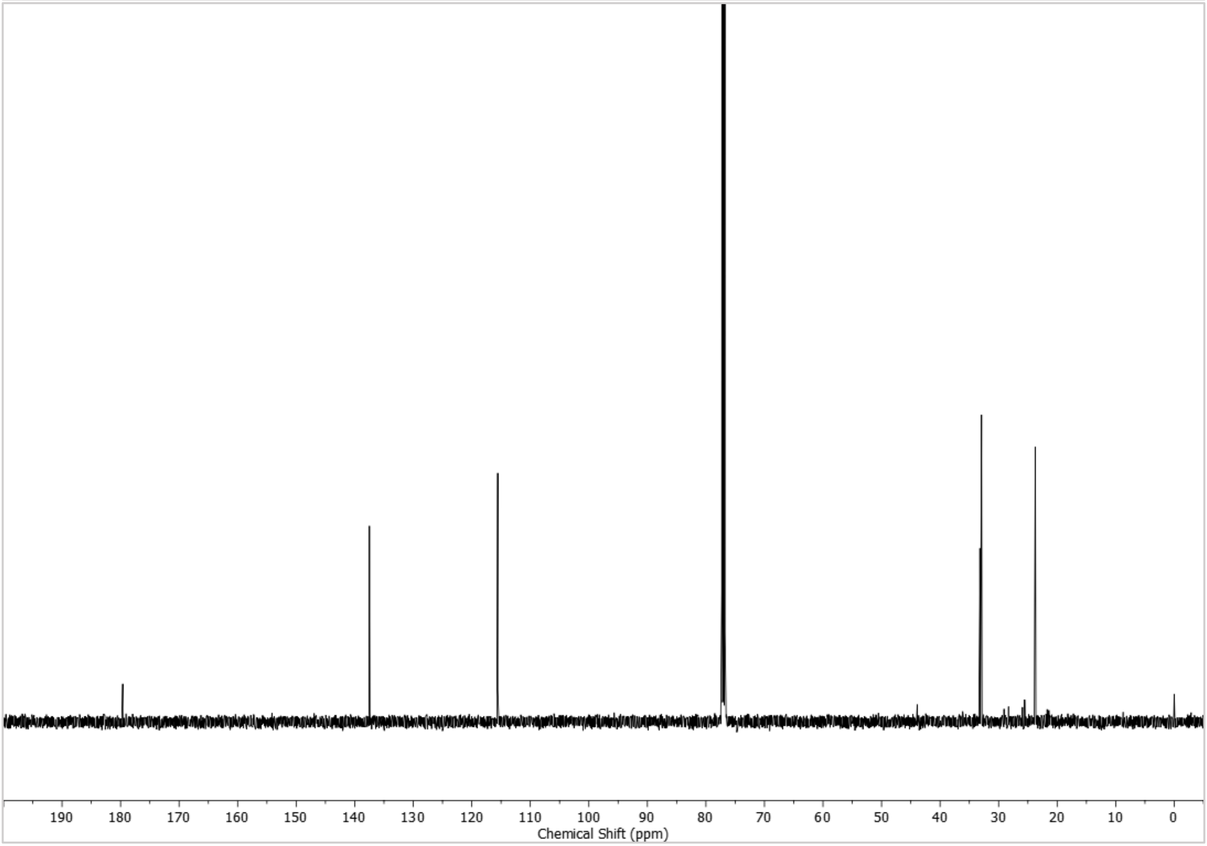
190
180
170
160
150
140
130
120
110
100
90
80
70
60
50
40
30
20
10
0
Chemical Shift (ppm)

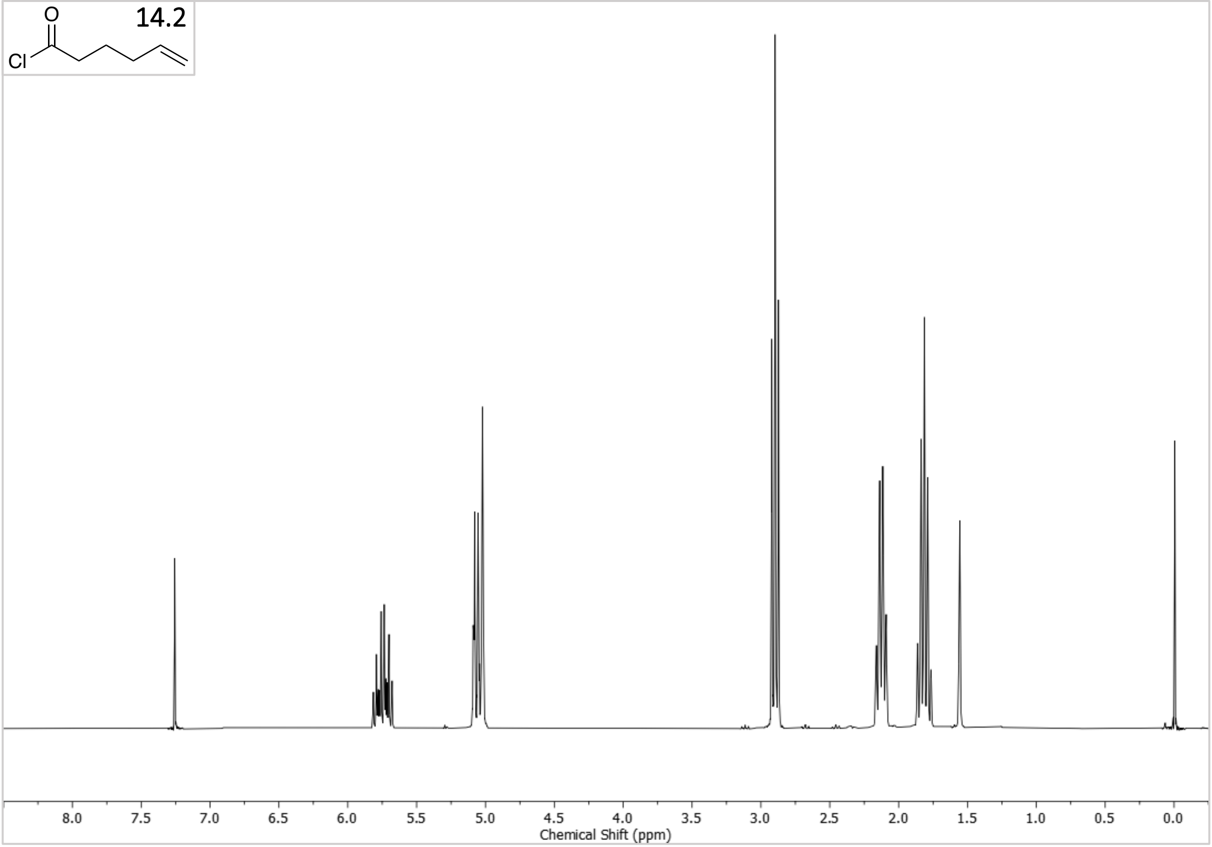
O
Cl
14.2
8.0
7.5
7.0
6.5
6.0
5.5
5.0
4.5
4.0
3.5
3.0
2.5
2.0
1.5
1.0
0.5
0.0
Chemical Shift (ppm)

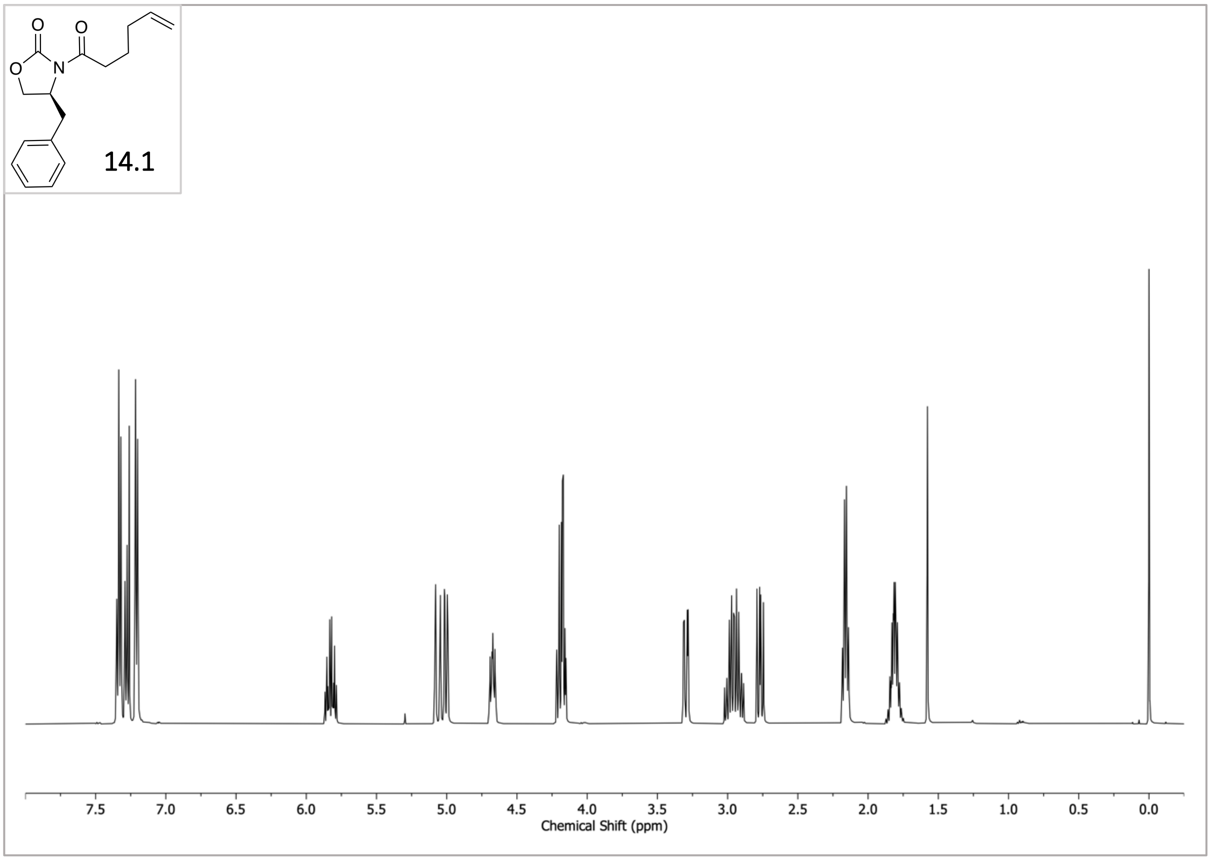

14.1

7.5
7.0
6.5
6.0
5.5
5.0
4.5
4.0
3.5
3.0
2.5
2.0
1.5
1.0
0.5
0.0
Chemical Shift (ppm)

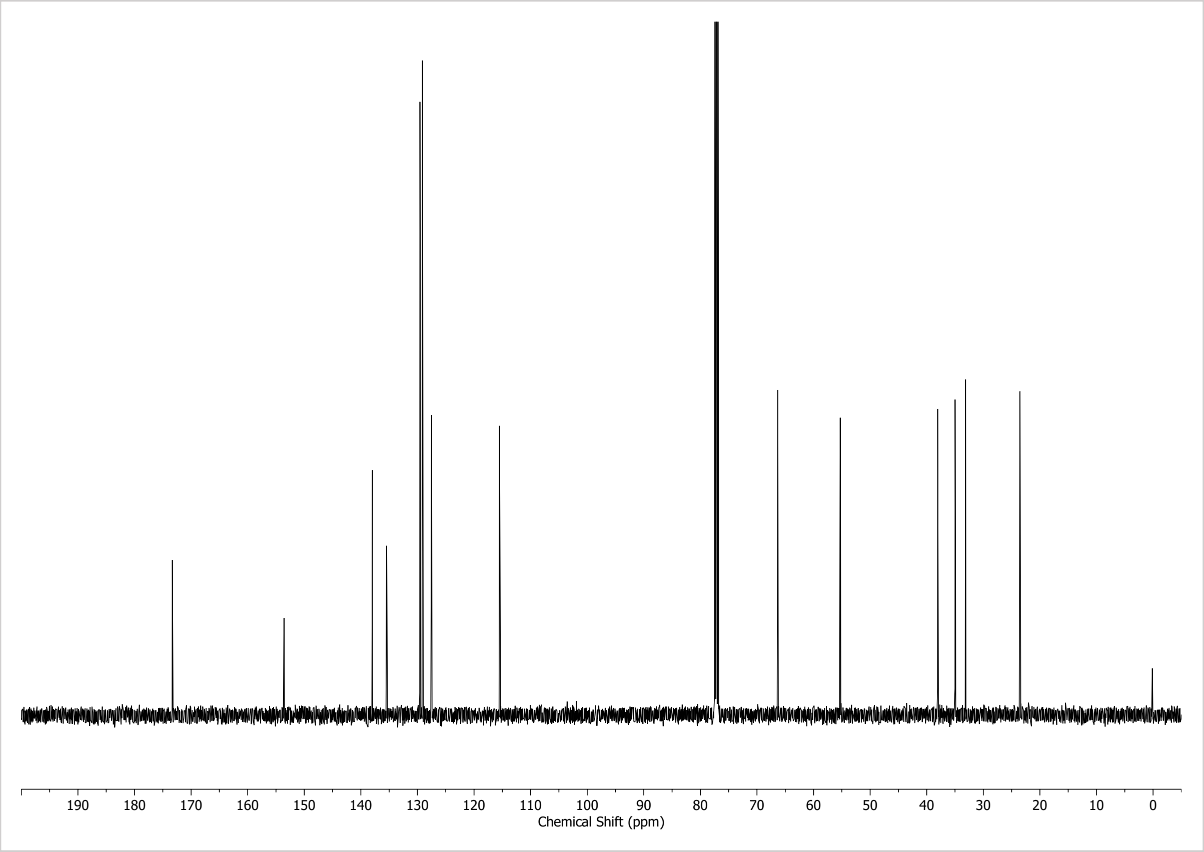

190
180
170
160
150
140
130
120
110
100
90
80
70
60
50
40
30
20
10
0
Chemical Shift (ppm)

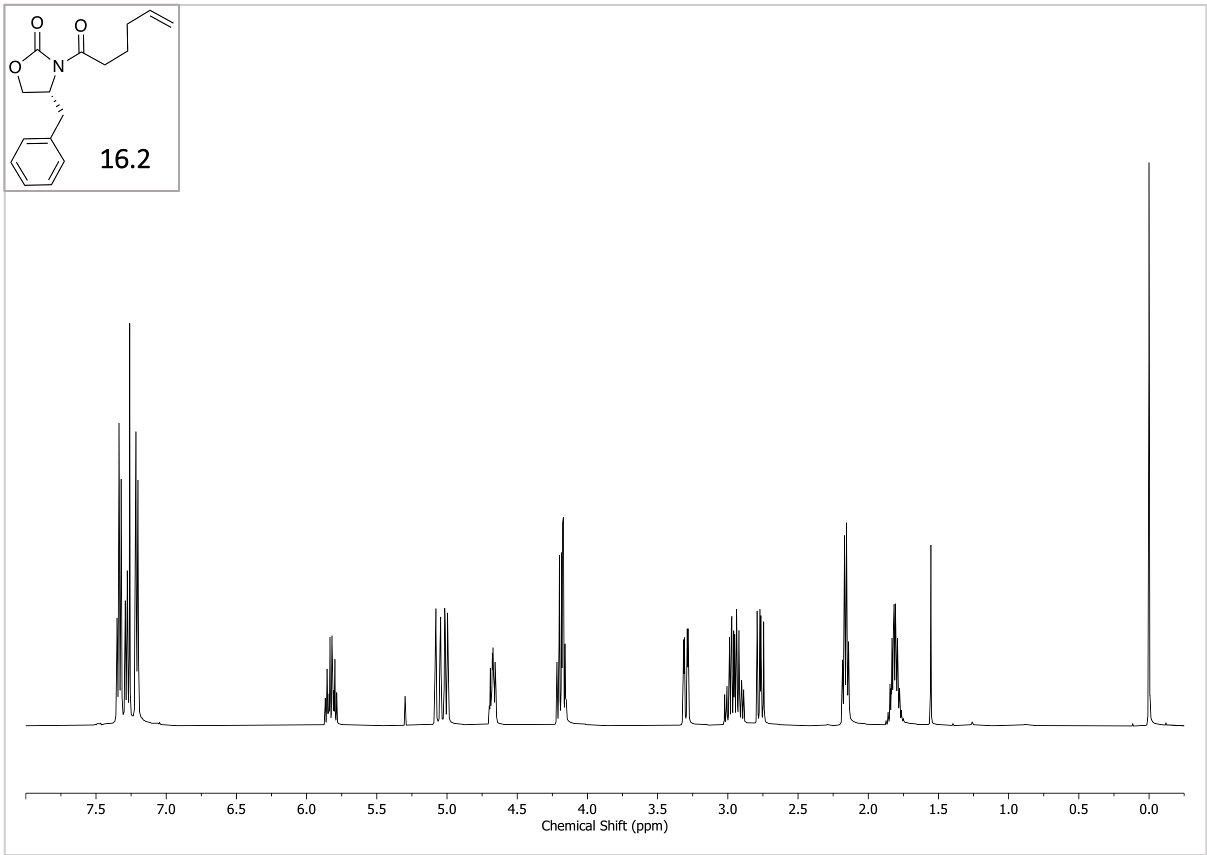

16.2

O
O
O
N
7.5
7.0
6.5
6.0
5.5
5.0
4.5
4.0
3.5
3.0
2.5
2.0
1.5
1.0
0.5
0.0
Chemical Shift (ppm)

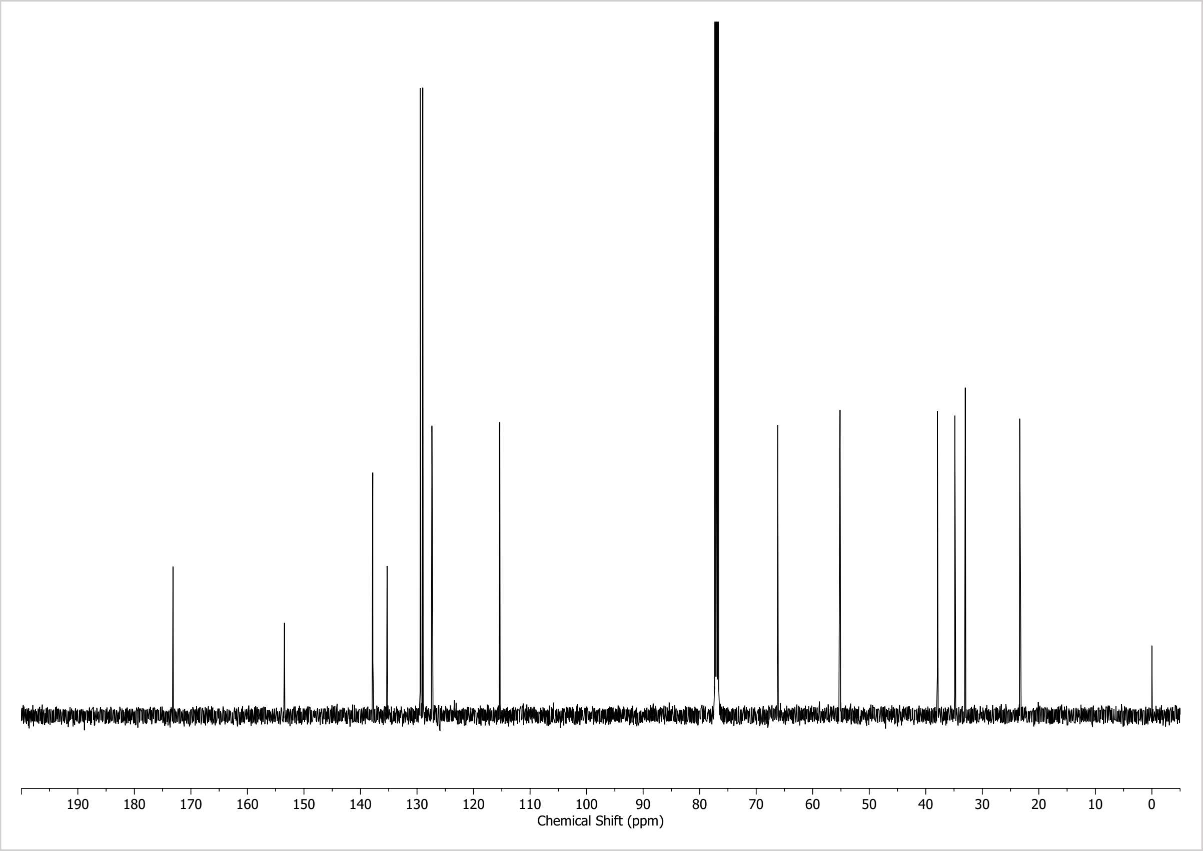

190
180
170
160
150
140
130
120
110
100
90
80
70
60
50
40
30
20
10
0
Chemical Shift (ppm)

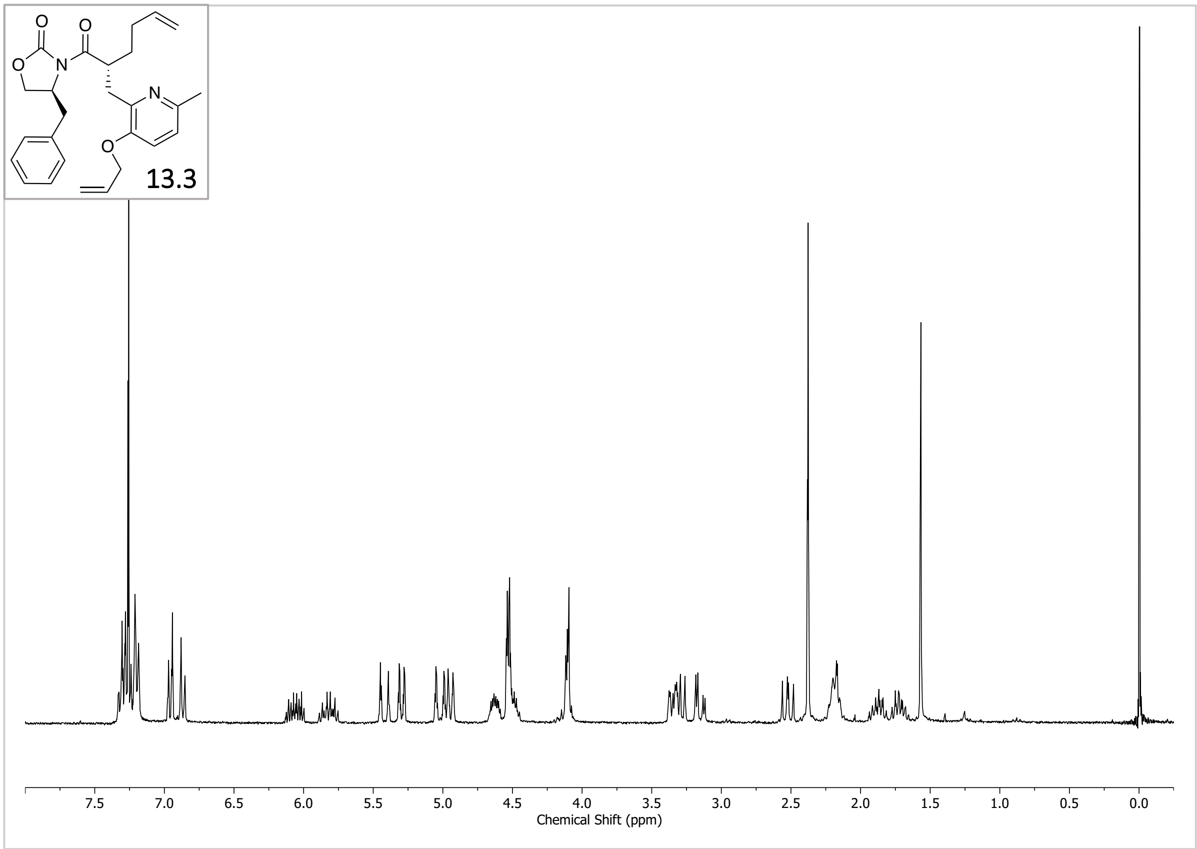
O
O
O
N
N
O
13.3
7.5
7.0
6.5
6.0
5.5
5.0
4.5
4.0
3.5
3.0
2.5
2.0
1.5
1.0
0.5
0.0
Chemical Shift (ppm)

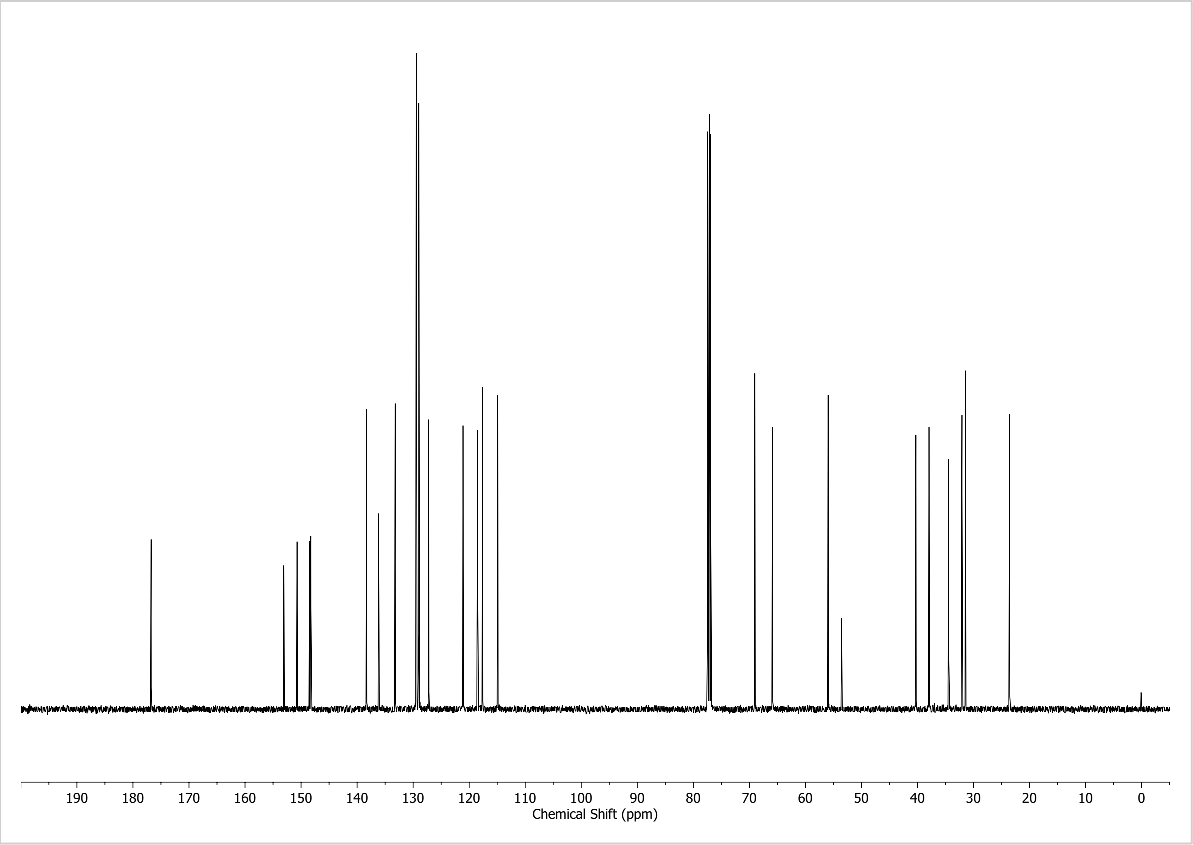
190
180
170
160
150
140
130
120
110
100
90
80
70
60
50
40
30
20
10
0
Chemical Shift (ppm)

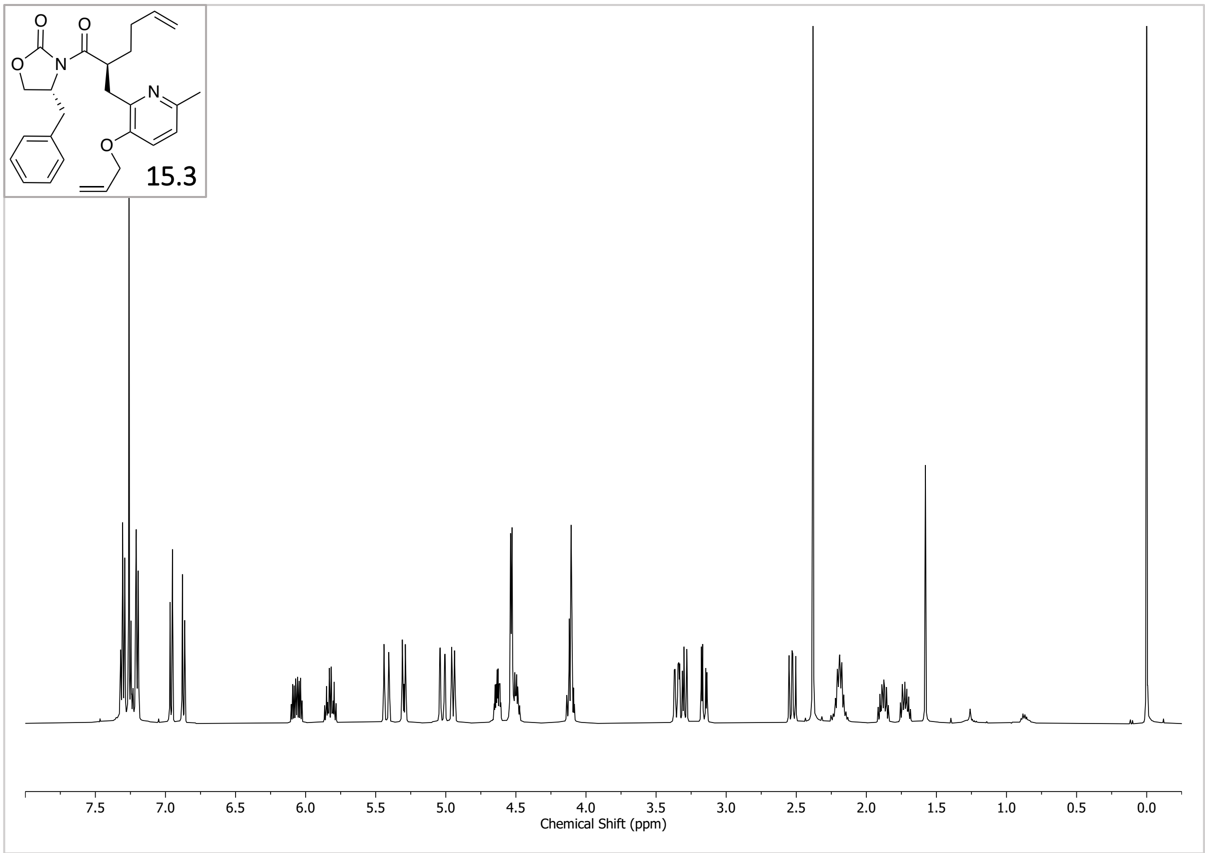
15.3

O
O
O
N
N
O
7.5
7.0
6.5
6.0
5.5
5.0
4.5
4.0
3.5
3.0
2.5
2.0
1.5
1.0
0.5
0.0
Chemical Shift (ppm)

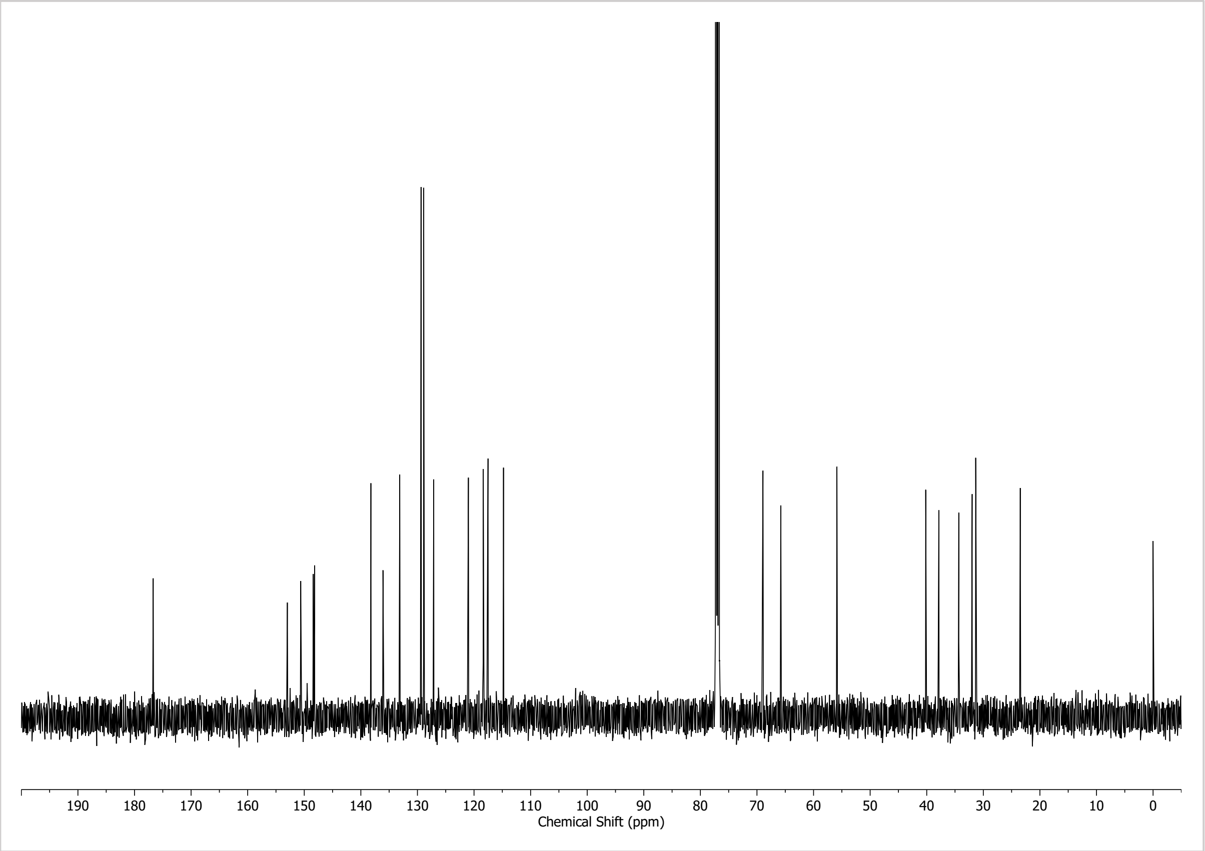
190
180
170
160
150
140
130
120
110
100
90
80
70
60
50
40
30
20
10
0
Chemical Shift (ppm)

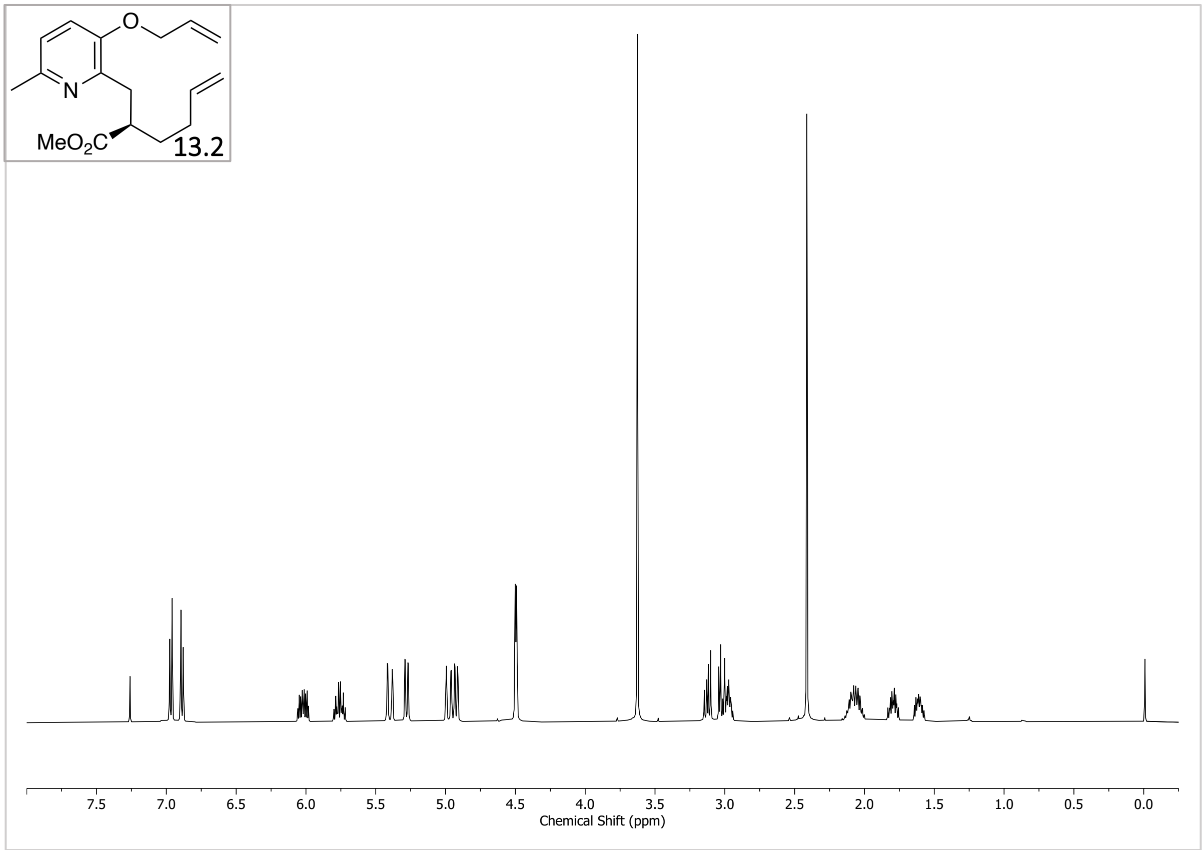
O
N
MeO2C
13.2
7.5
7.0
6.5
6.0
5.5
5.0
4.5
4.0
3.5
3.0
2.5
2.0
1.5
1.0
0.5
0.0
Chemical Shift (ppm)

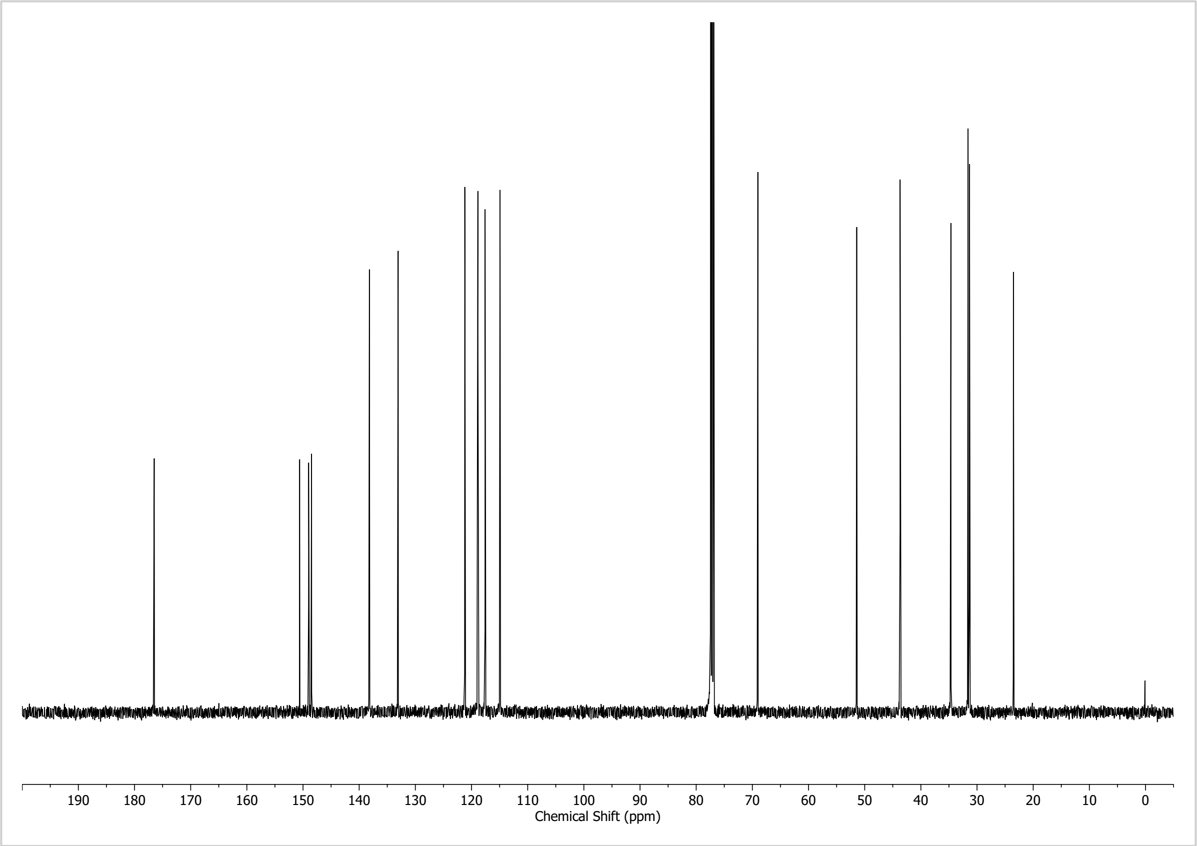
190
180
170
160
150
140
130
120
110
100
90
80
70
60
50
40
30
20
10
0
Chemical Shift (ppm)

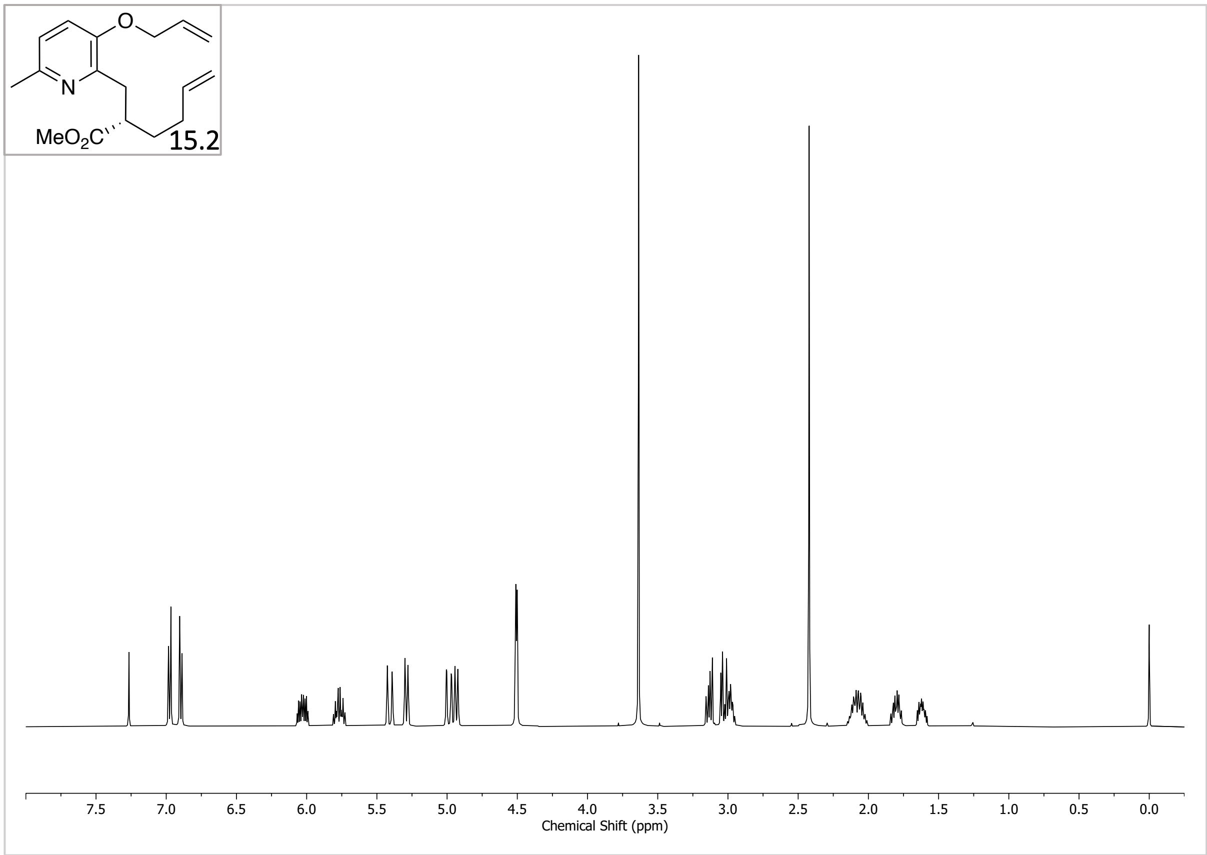
15.2
O
N
MeO2C
7.5
7.0
6.5
6.0
5.5
5.0
4.5
4.0
3.5
3.0
2.5
2.0
1.5
1.0
0.5
0.0
Chemical Shift (ppm)

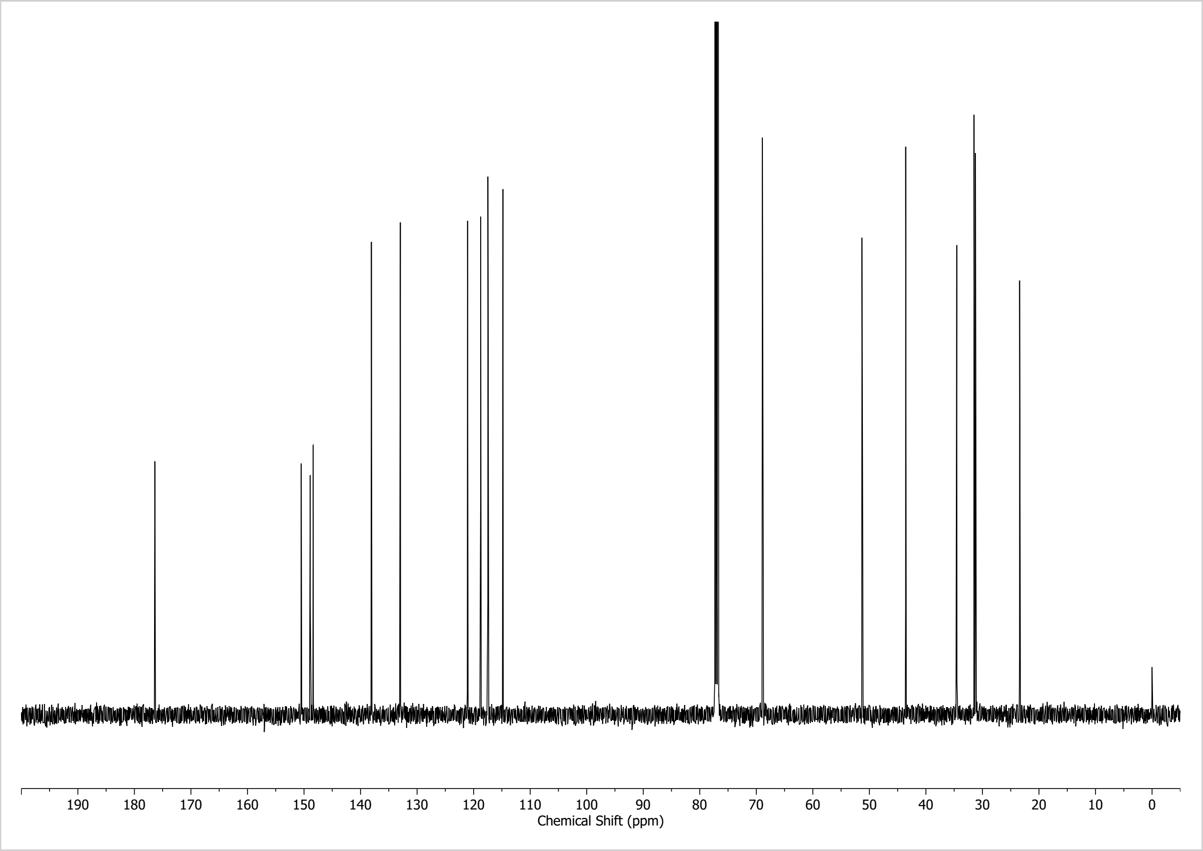
190
180
170
160
150
140
130
120
110
100
90
80
70
60
50
40
30
20
10
0
Chemical Shift (ppm)

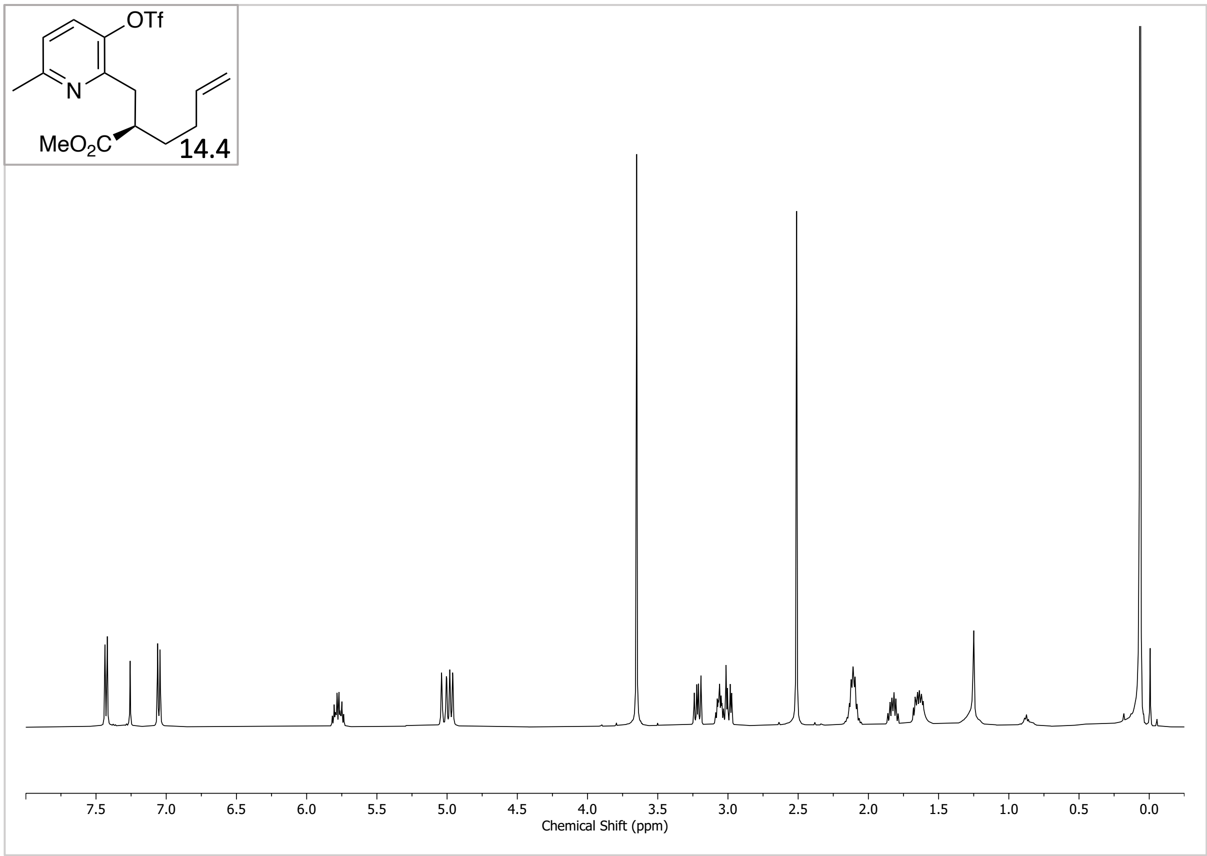
OTf
N
MeO2C
14.4
7.5
7.0
6.5
6.0
5.5
5.0
4.5
4.0
3.5
3.0
2.5
2.0
1.5
1.0
0.5
0.0
Chemical Shift (ppm)

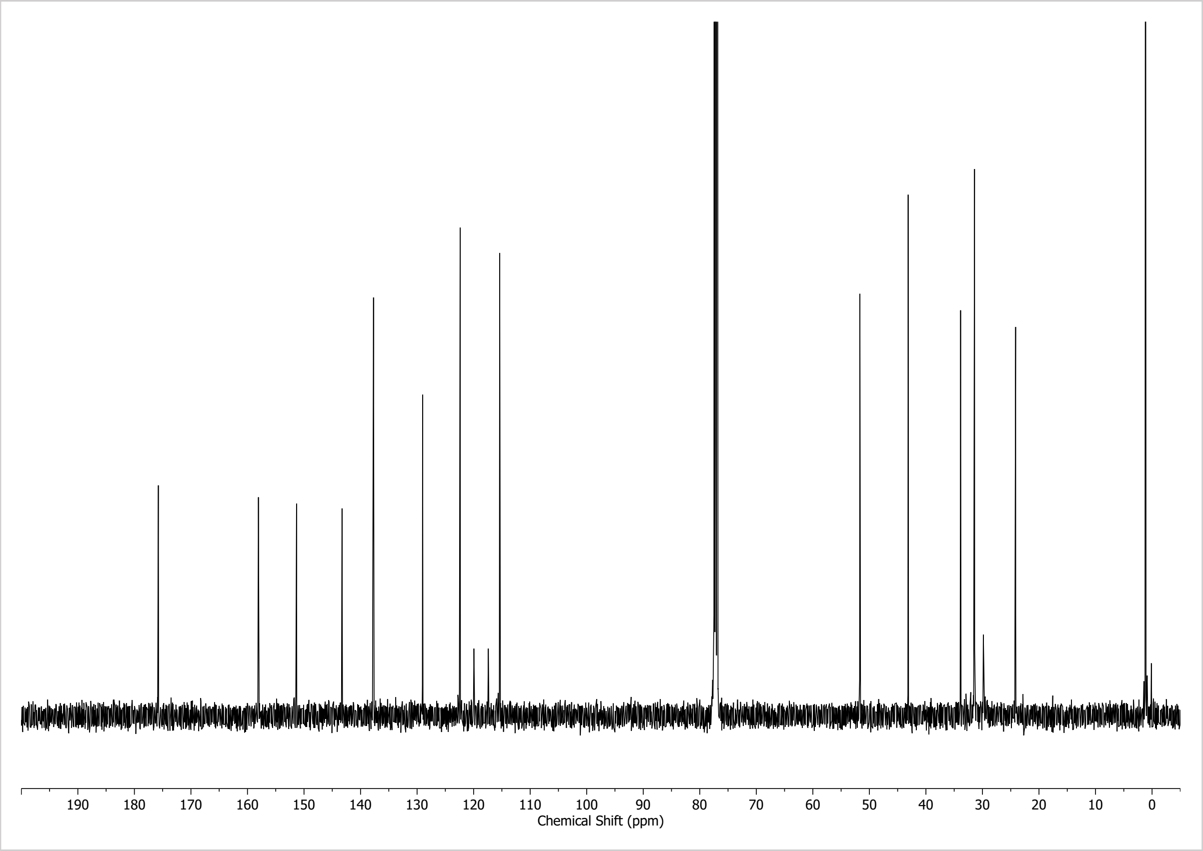
190
180
170
160
150
140
130
120
110
100
90
80
70
60
50
40
30
20
10
0
Chemical Shift (ppm)

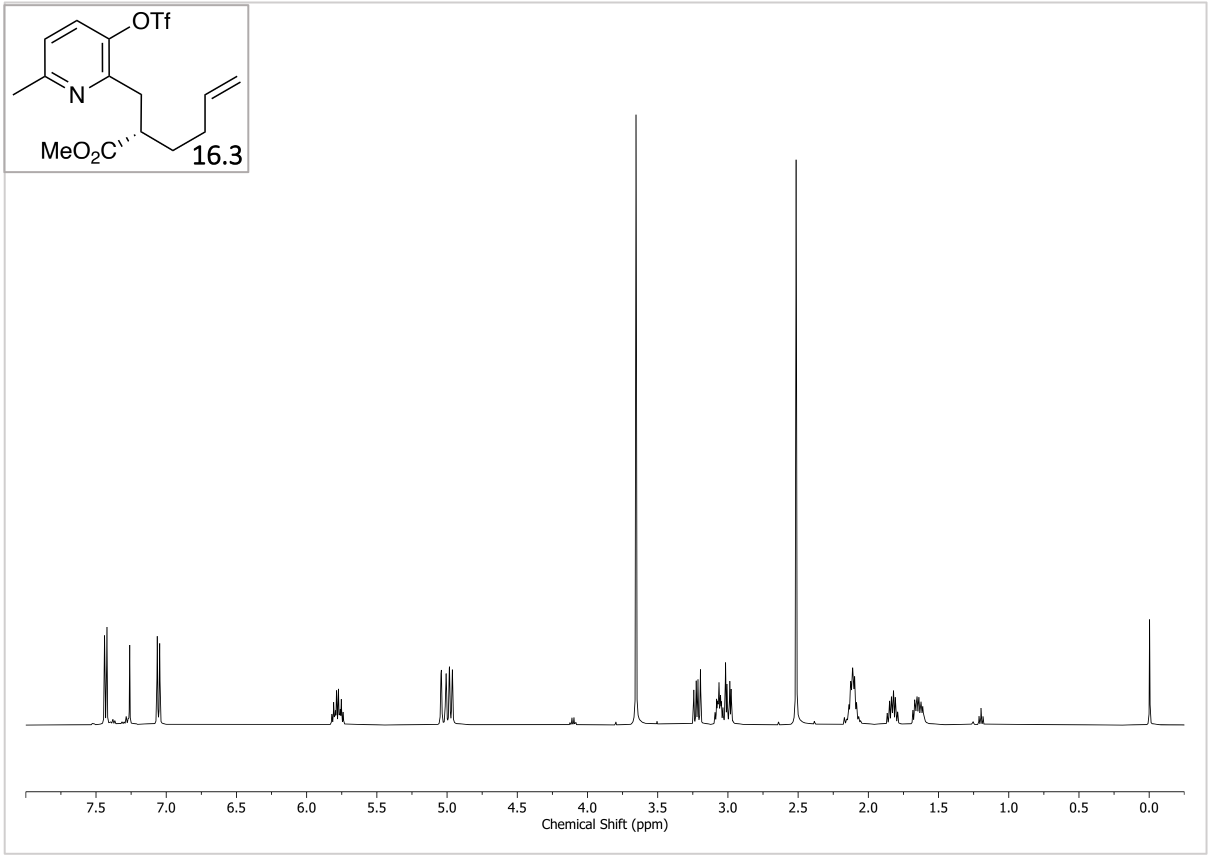
OTf
N
MeO2C
16.3
7.5 7.0 6.5 6.0 5.5 5.0 4.5 4.0 3.5 3.0 2.5 2.0 1.5 1.0 0.5 0.0
Chemical Shift (ppm)

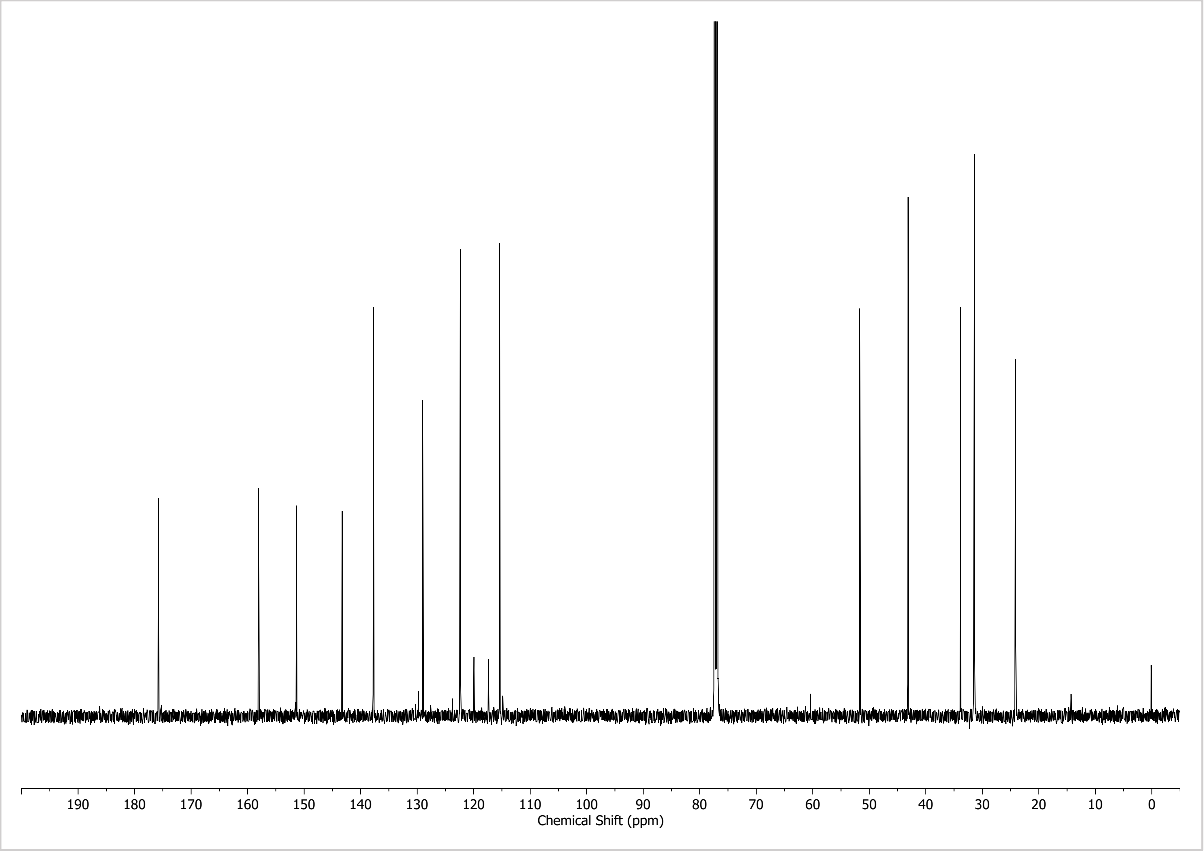
190 180 170 160 150 140 130 120 110 100 90 80 70 60 50 40 30 20 10 0
Chemical Shift (ppm)

13.1

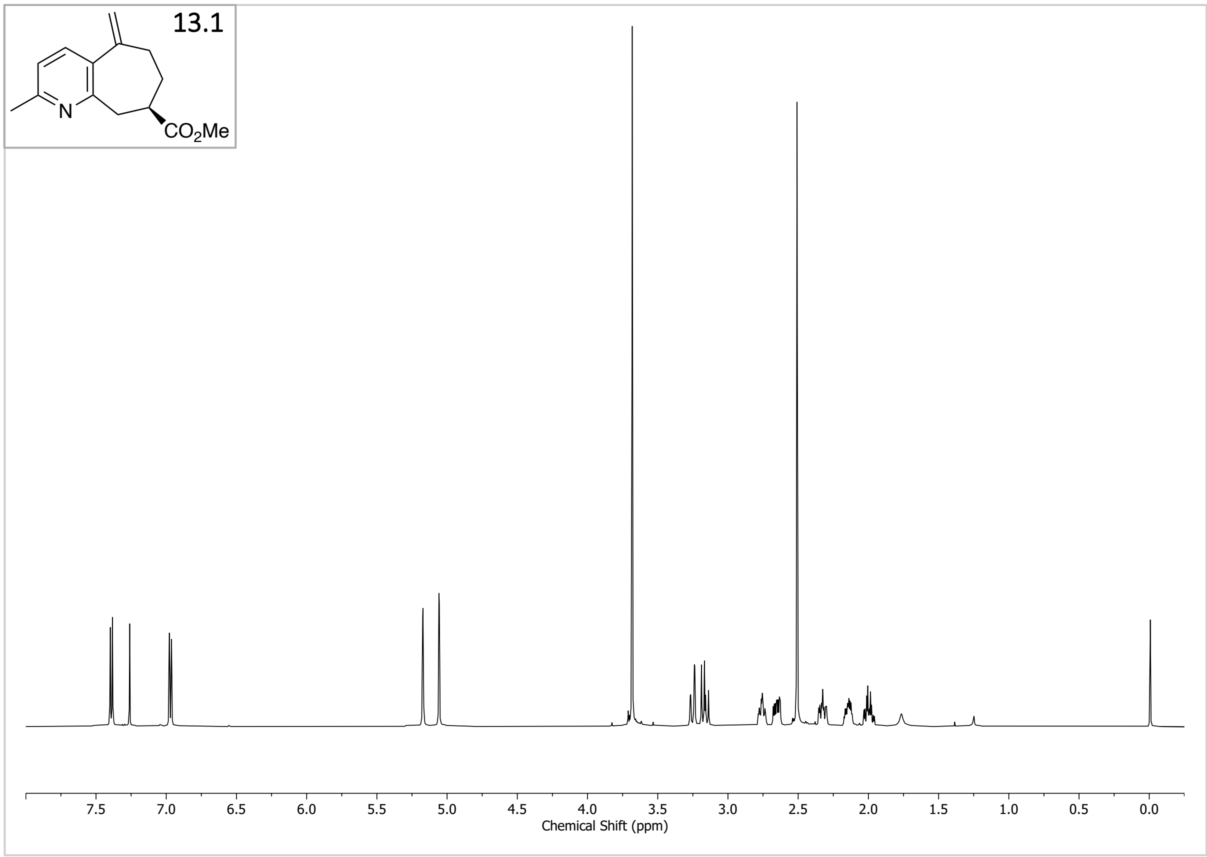
CO2Me
N
7.5
7.0
6.5
6.0
5.5
5.0
4.5
4.0
3.5
3.0
2.5
2.0
1.5
1.0
0.5
0.0
Chemical Shift (ppm)

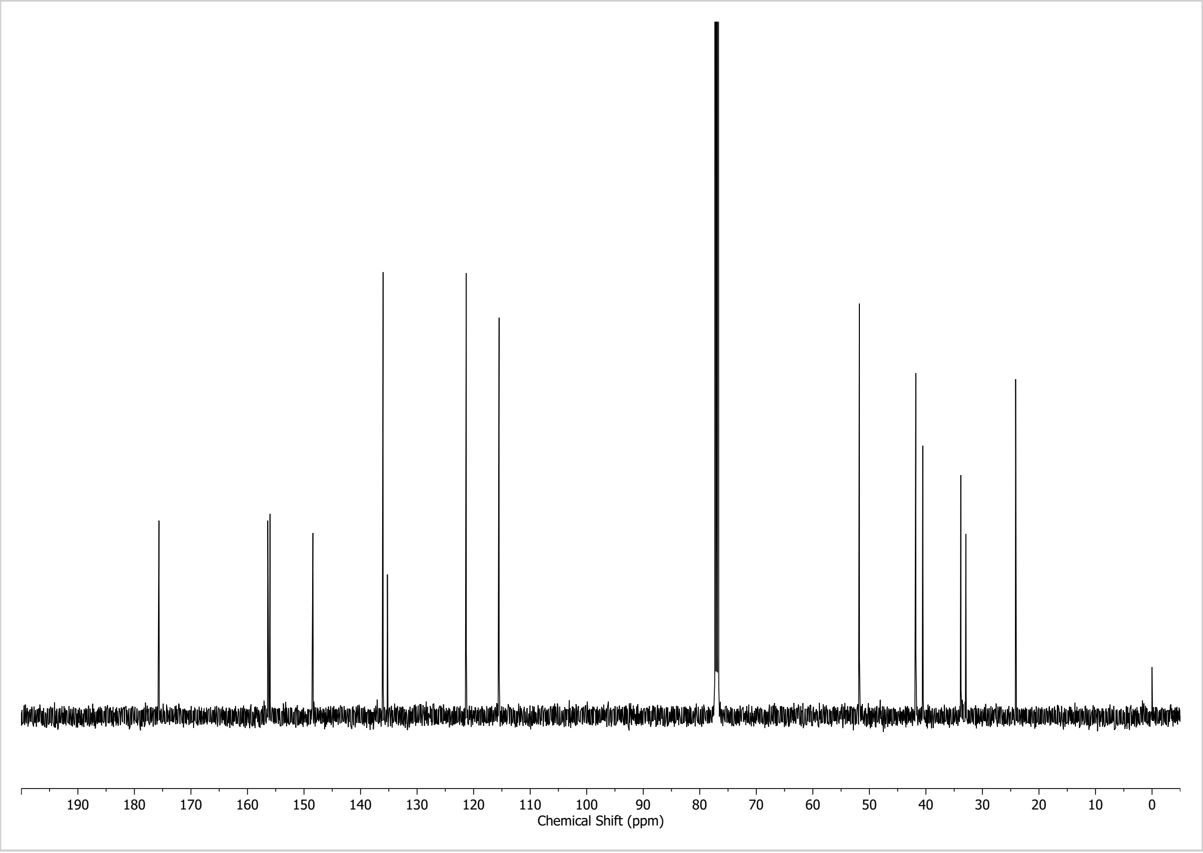
190
180
170
160
150
140
130
120
110
100
90
80
70
60
50
40
30
20
10
0
Chemical Shift (ppm)

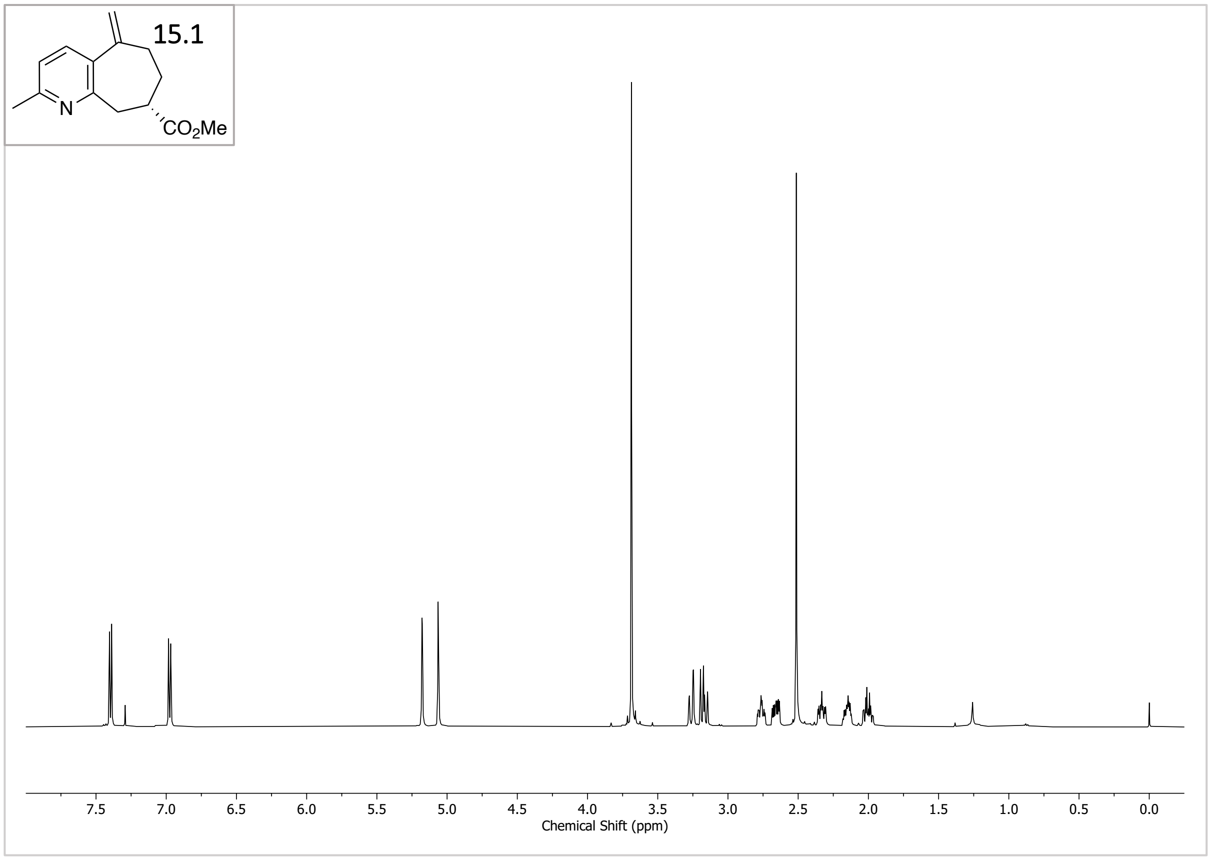
15.1

CO2Me
N
7.5
7.0
6.5
6.0
5.5
5.0
4.5
4.0
3.5
3.0
2.5
2.0
1.5
1.0
0.5
0.0
Chemical Shift (ppm)

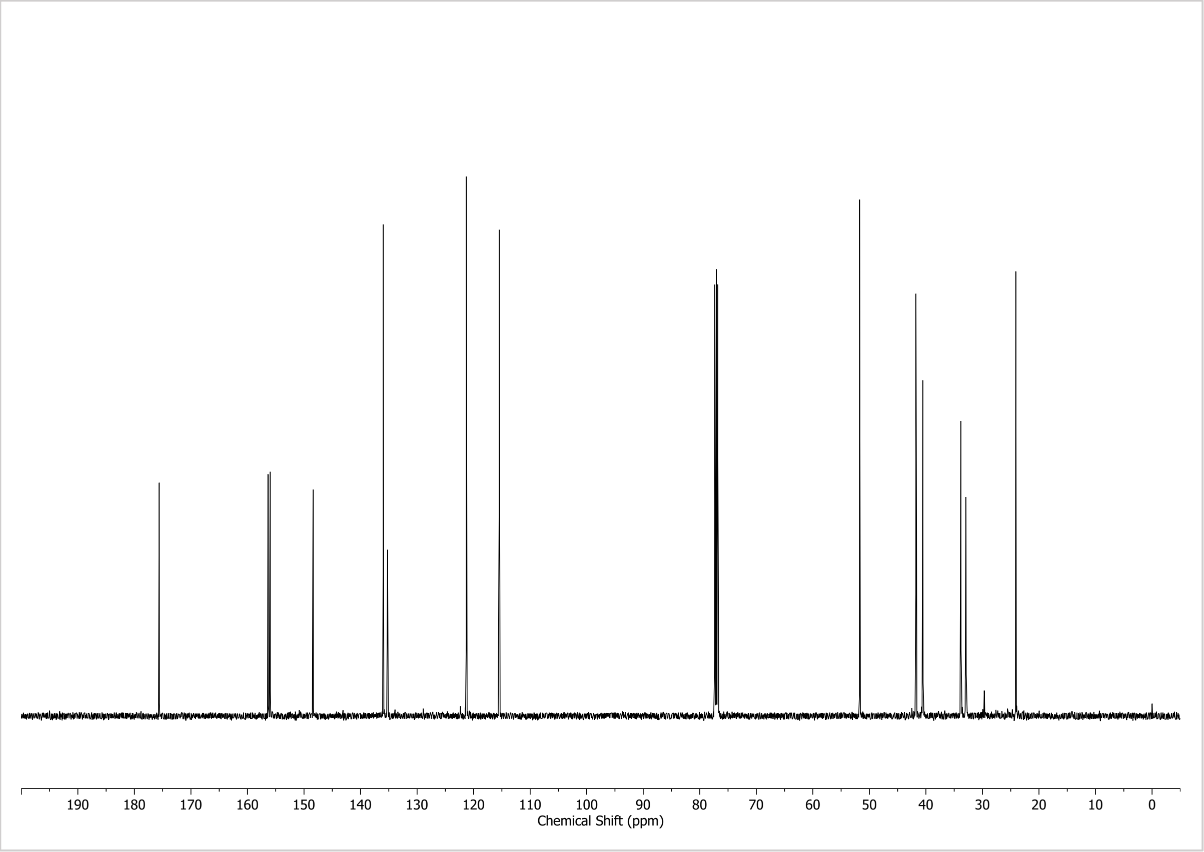
190
180
170
160
150
140
130
120
110
100
90
80
70
60
50
40
30
20
10
0
Chemical Shift (ppm)

1.11b

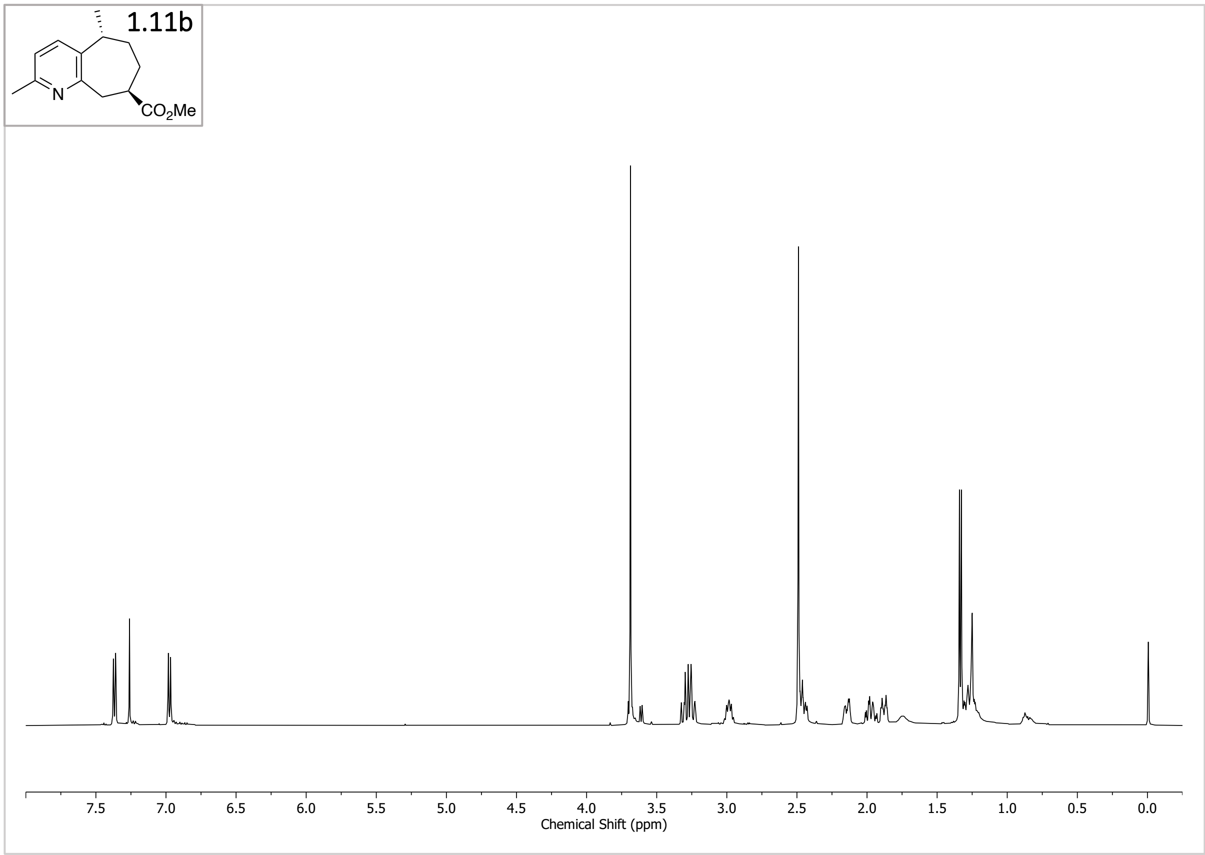
N
CO$_2$Me
7.5
7.0
6.5
6.0
5.5
5.0
4.5
4.0
3.5
3.0
2.5
2.0
1.5
1.0
0.5
0.0
Chemical Shift (ppm)

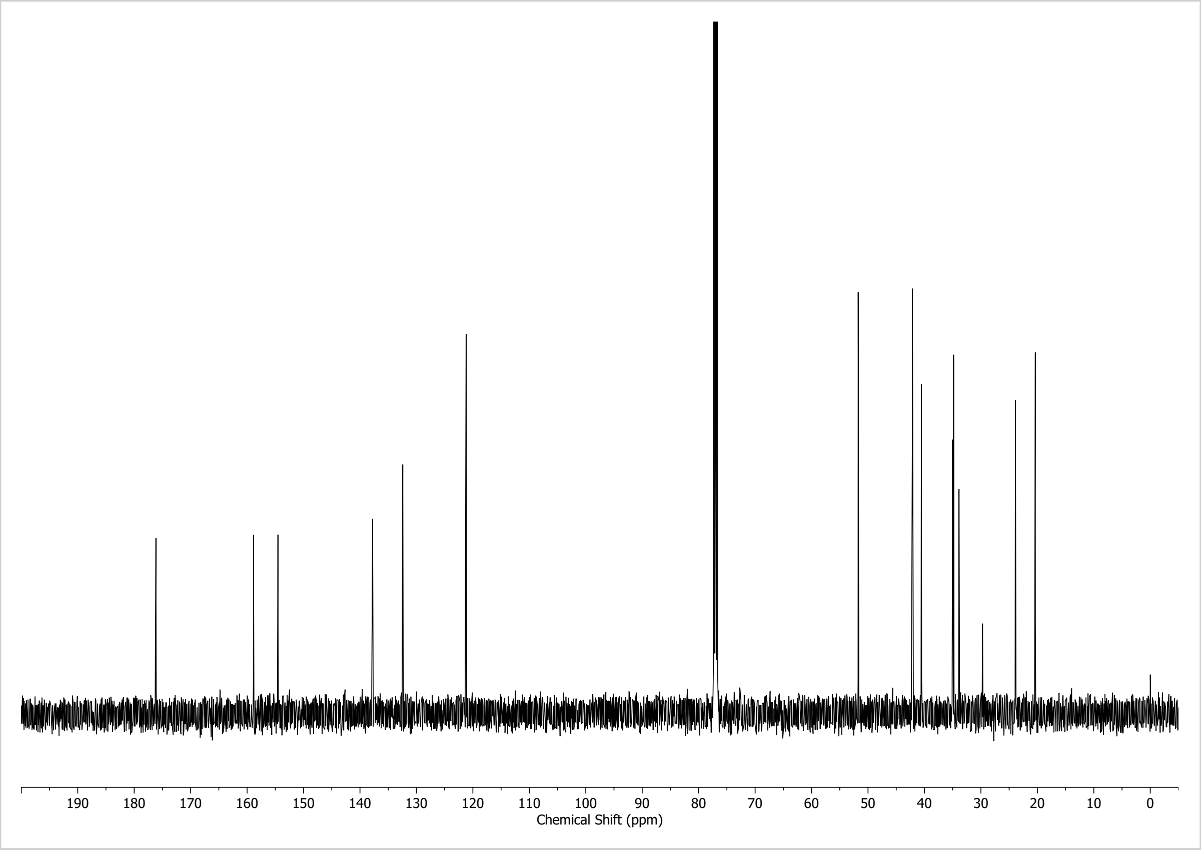
190
180
170
160
150
140
130
120
110
100
90
80
70
60
50
40
30
20
10
0
Chemical Shift (ppm)

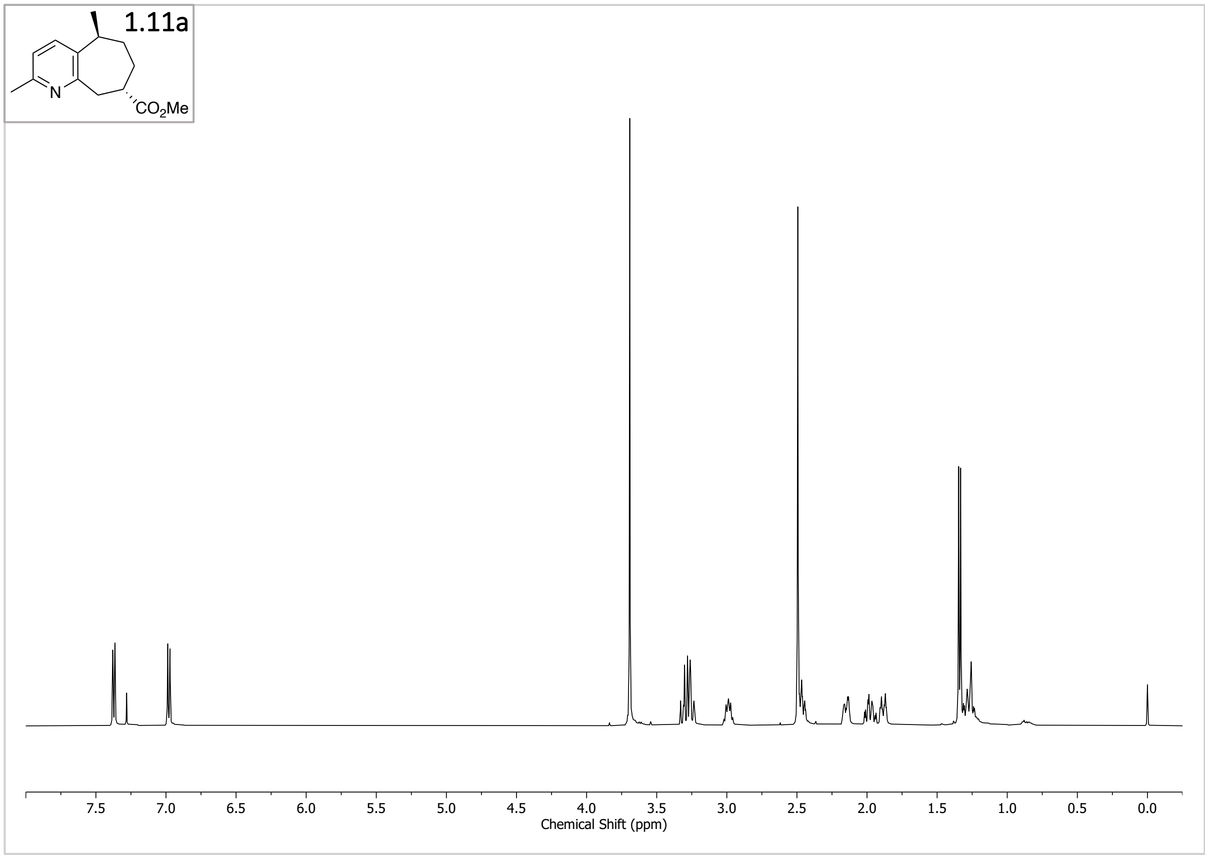
1.11a

N
CO2Me
7.5
7.0
6.5
6.0
5.5
5.0
4.5
4.0
3.5
3.0
2.5
2.0
1.5
1.0
0.5
0.0
Chemical Shift (ppm)

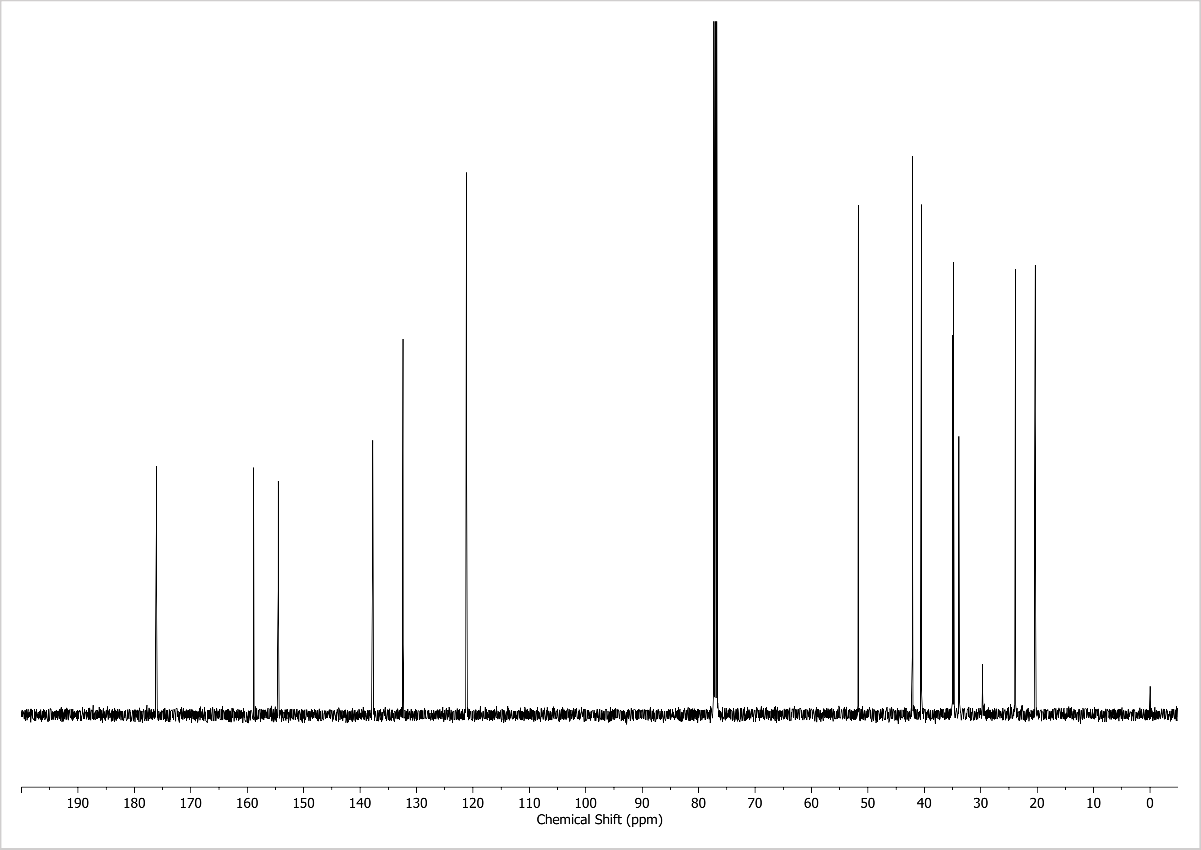
190
180
170
160
150
140
130
120
110
100
90
80
70
60
50
40
30
20
10
0
Chemical Shift (ppm)

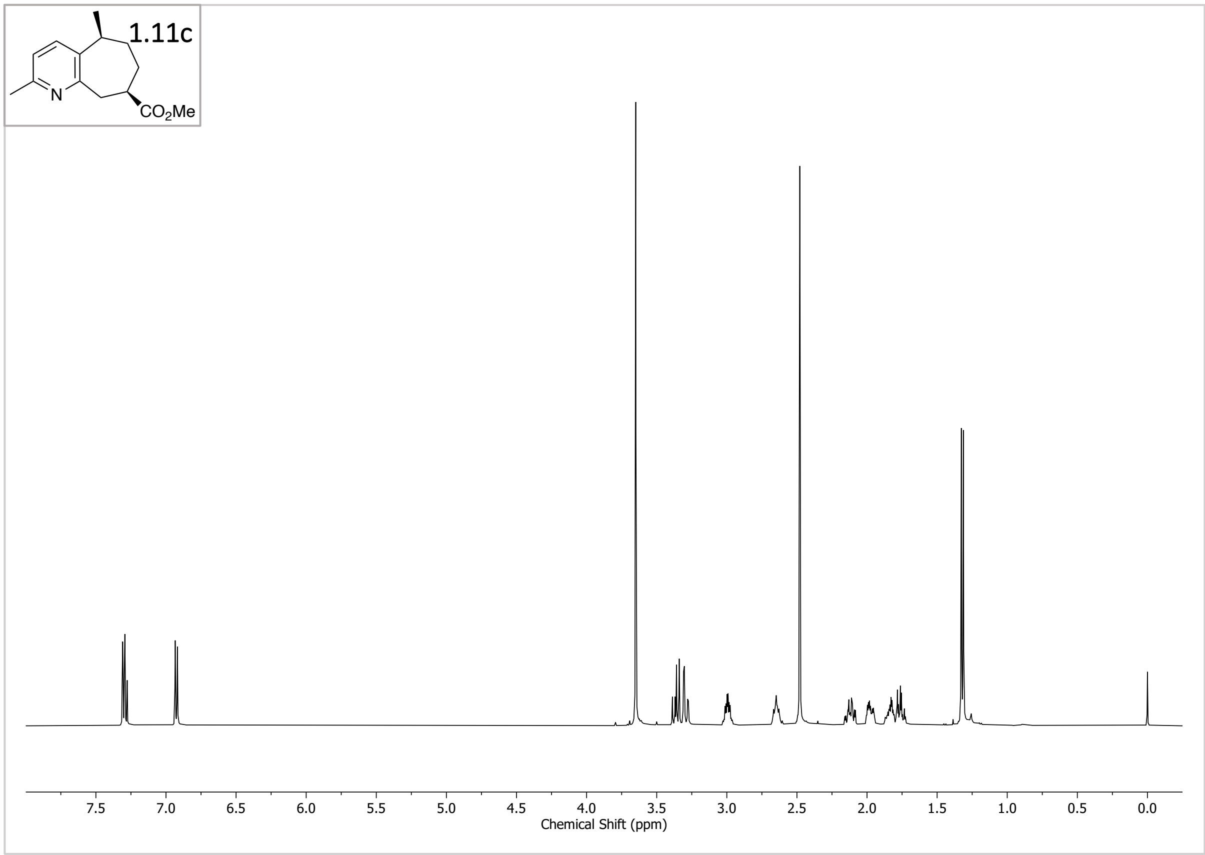

1.11c

N
CO$_2$Me
7.5
7.0
6.5
6.0
5.5
5.0
4.5
4.0
3.5
3.0
2.5
2.0
1.5
1.0
0.5
0.0
Chemical Shift (ppm)

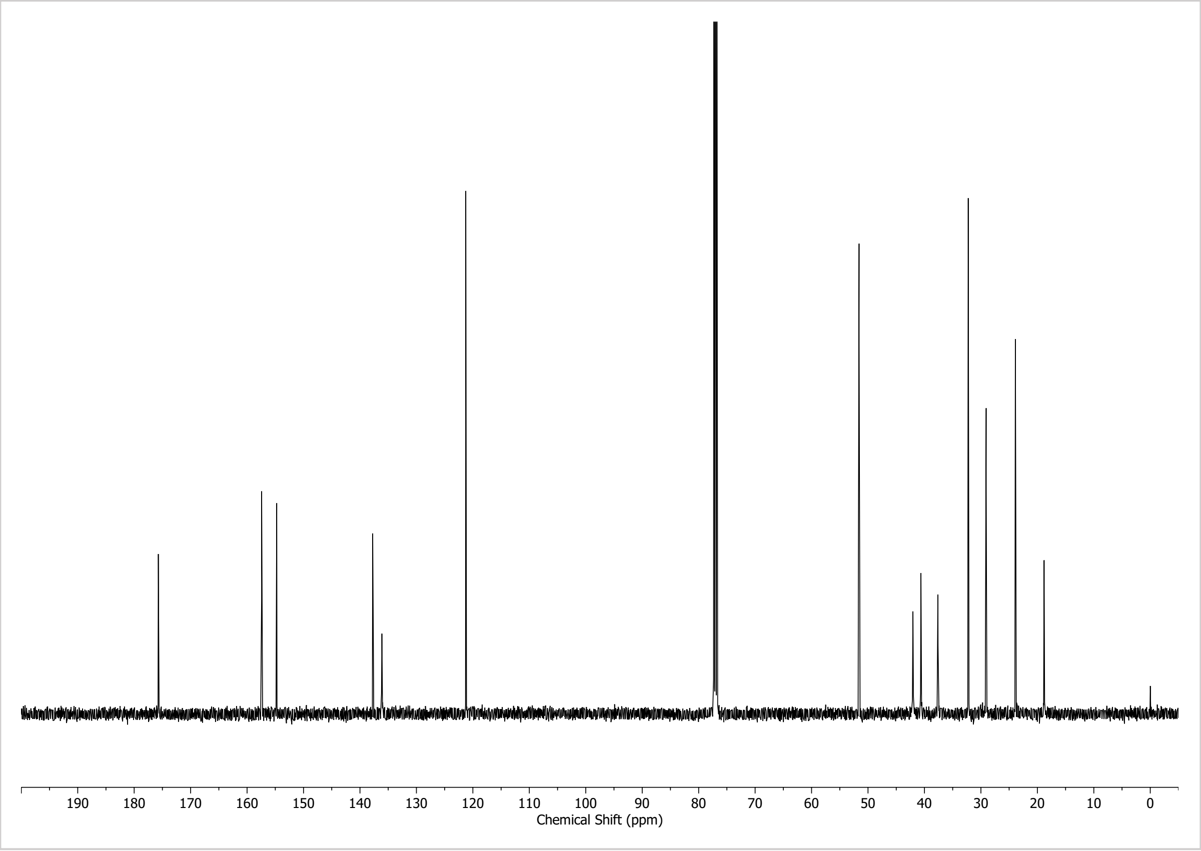

190
180
170
160
150
140
130
120
110
100
90
80
70
60
50
40
30
20
10
0
Chemical Shift (ppm)

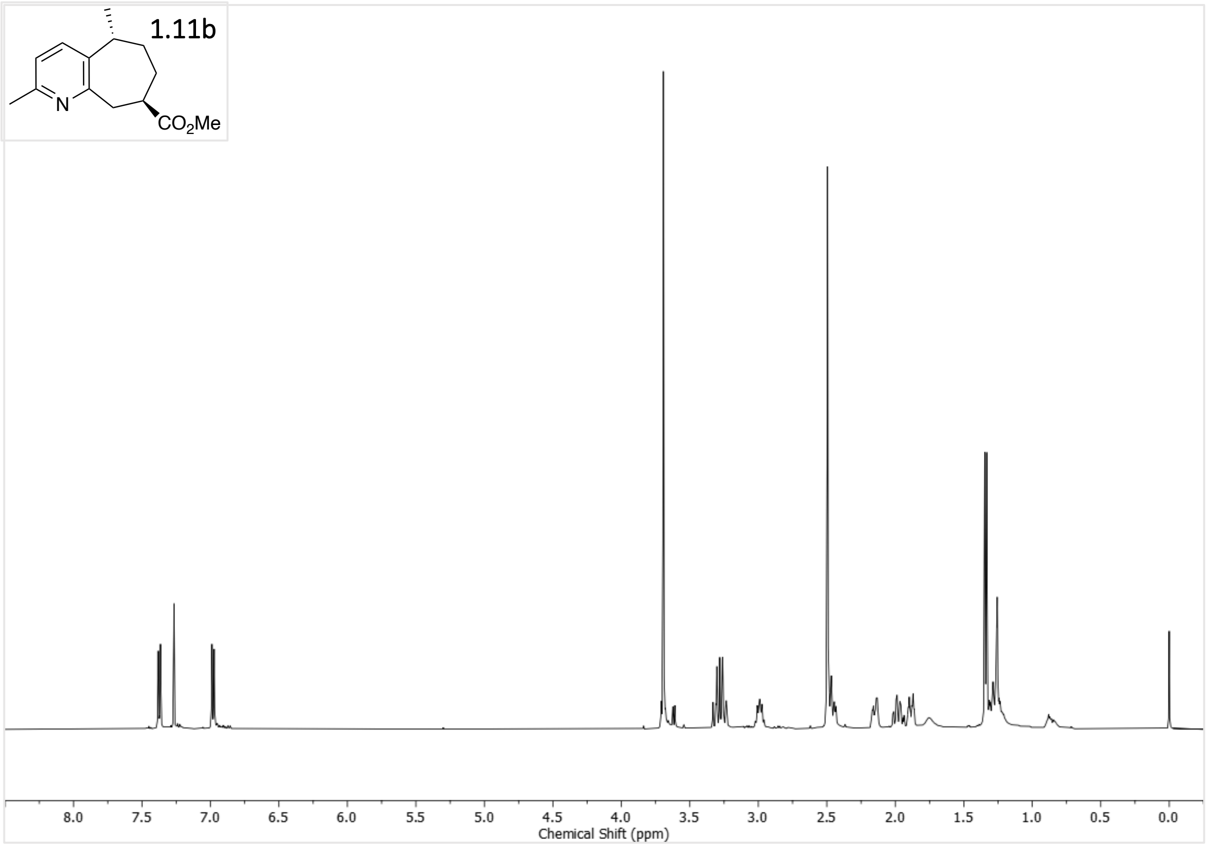
1.11b
N
CO2Me
8.0 7.5 7.0 6.5 6.0 5.5 5.0 4.5 4.0 3.5 3.0 2.5 2.0 1.5 1.0 0.5 0.0
Chemical Shift (ppm)

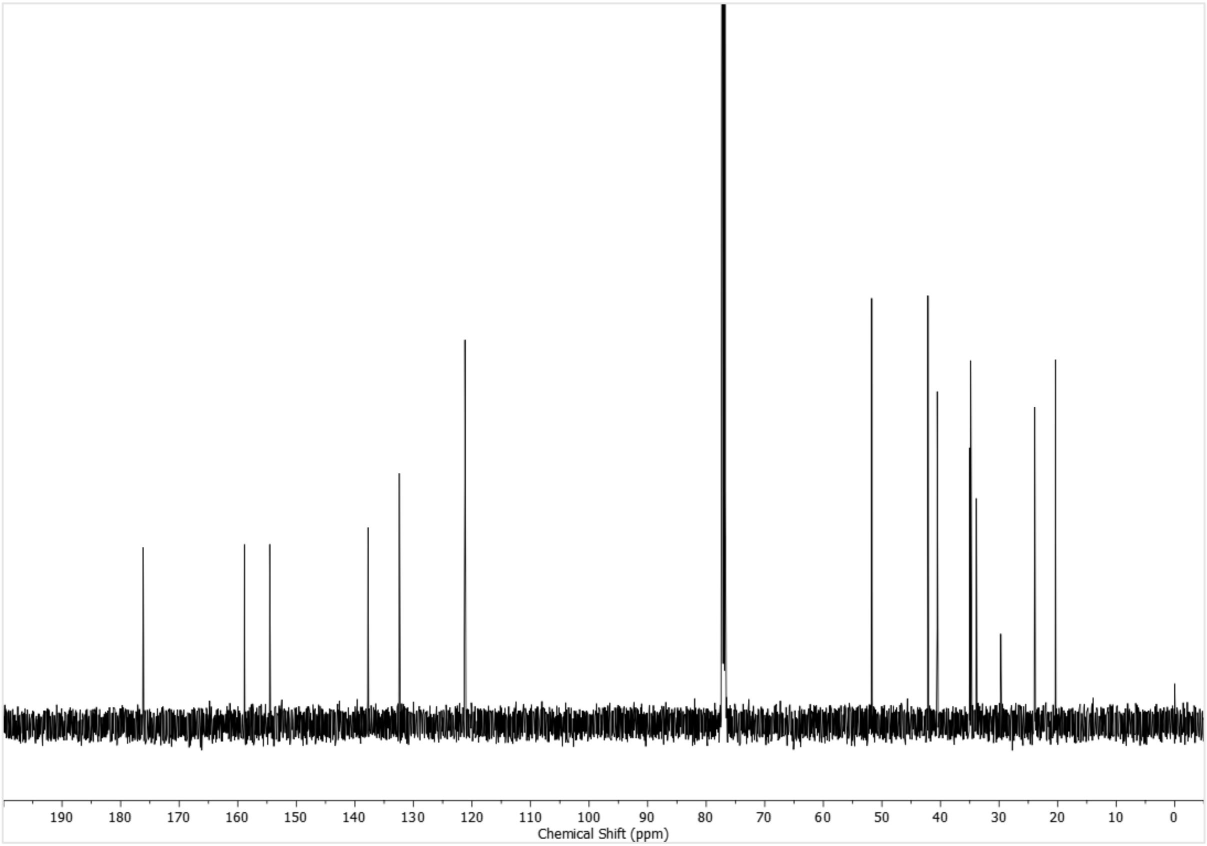
190 180 170 160 150 140 130 120 110 100 90 80 70 60 50 40 30 20 10 0
Chemical Shift (ppm)

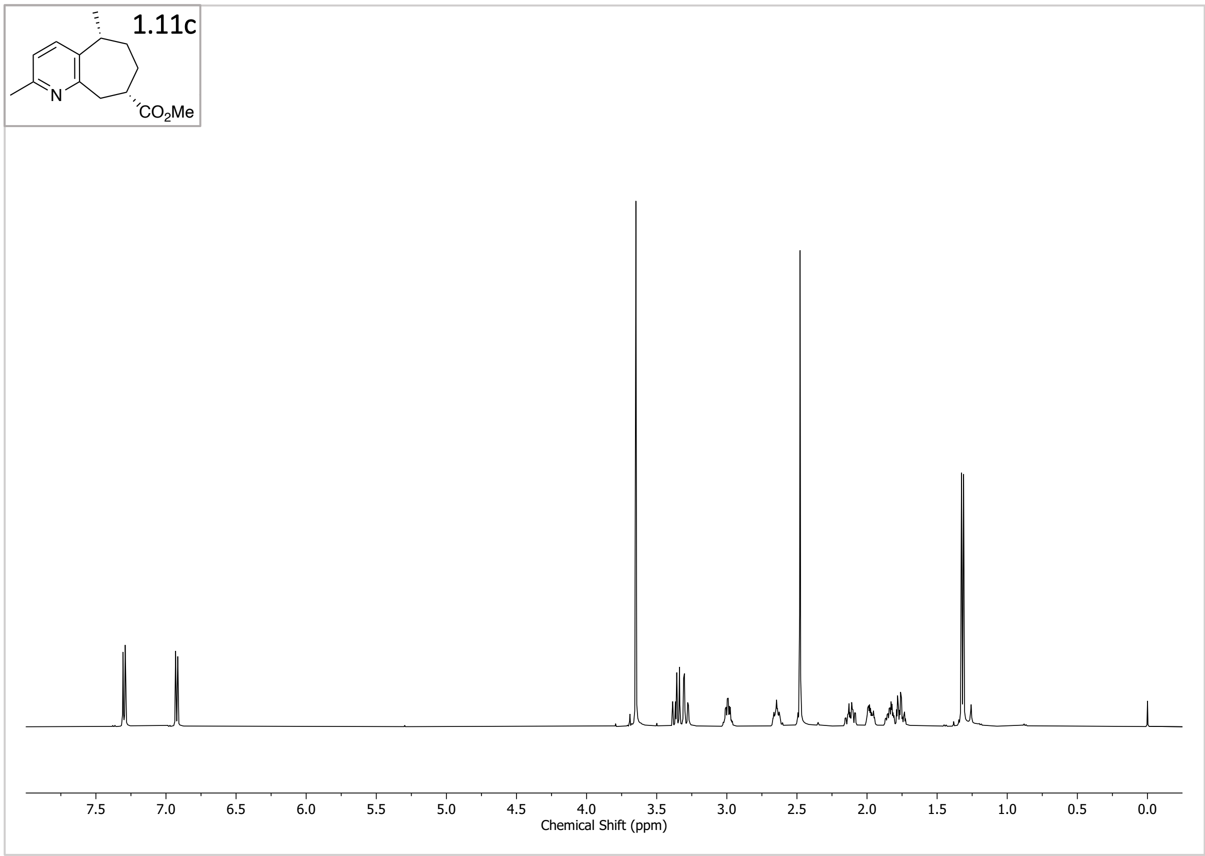
1.11c
N
CO$_2$Me
7.5
7.0
6.5
6.0
5.5
5.0
4.5
4.0
3.5
3.0
2.5
2.0
1.5
1.0
0.5
0.0
Chemical Shift (ppm)

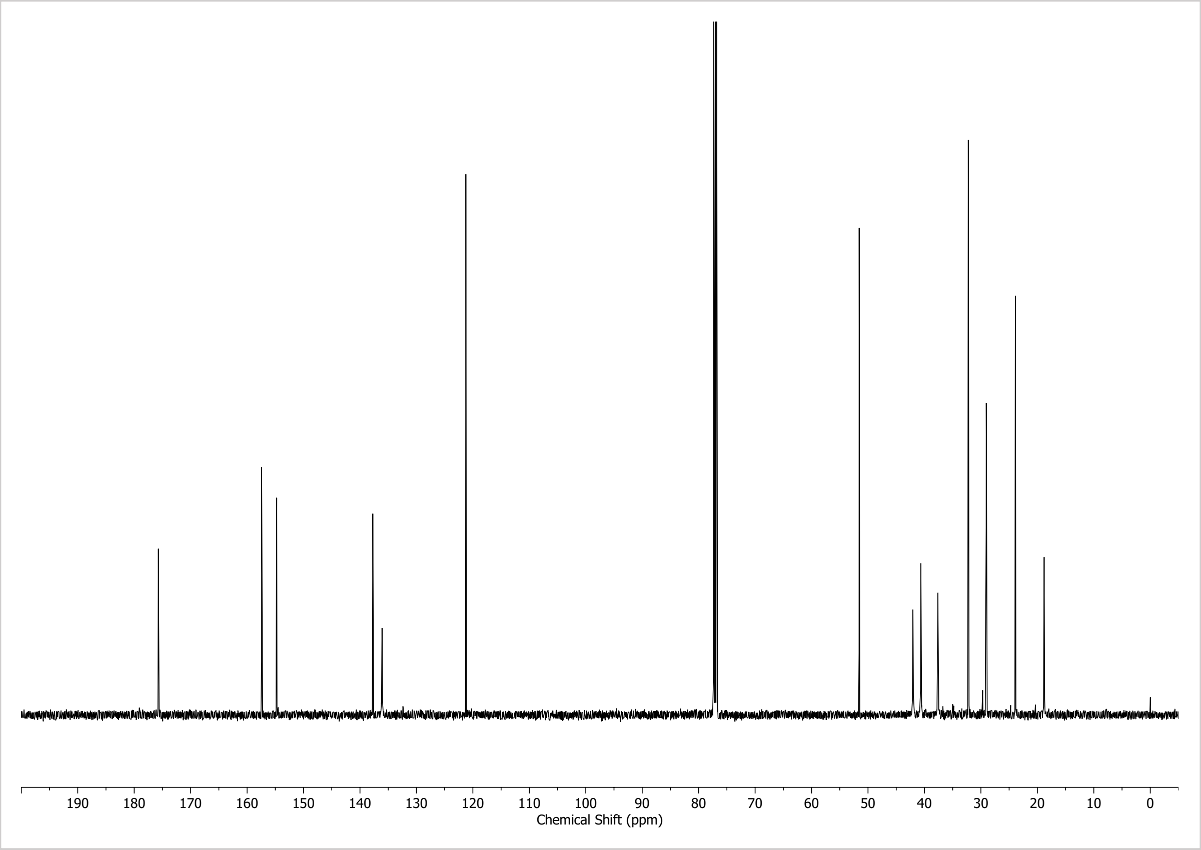
190
180
170
160
150
140
130
120
110
100
90
80
70
60
50
40
30
20
10
0
Chemical Shift (ppm)

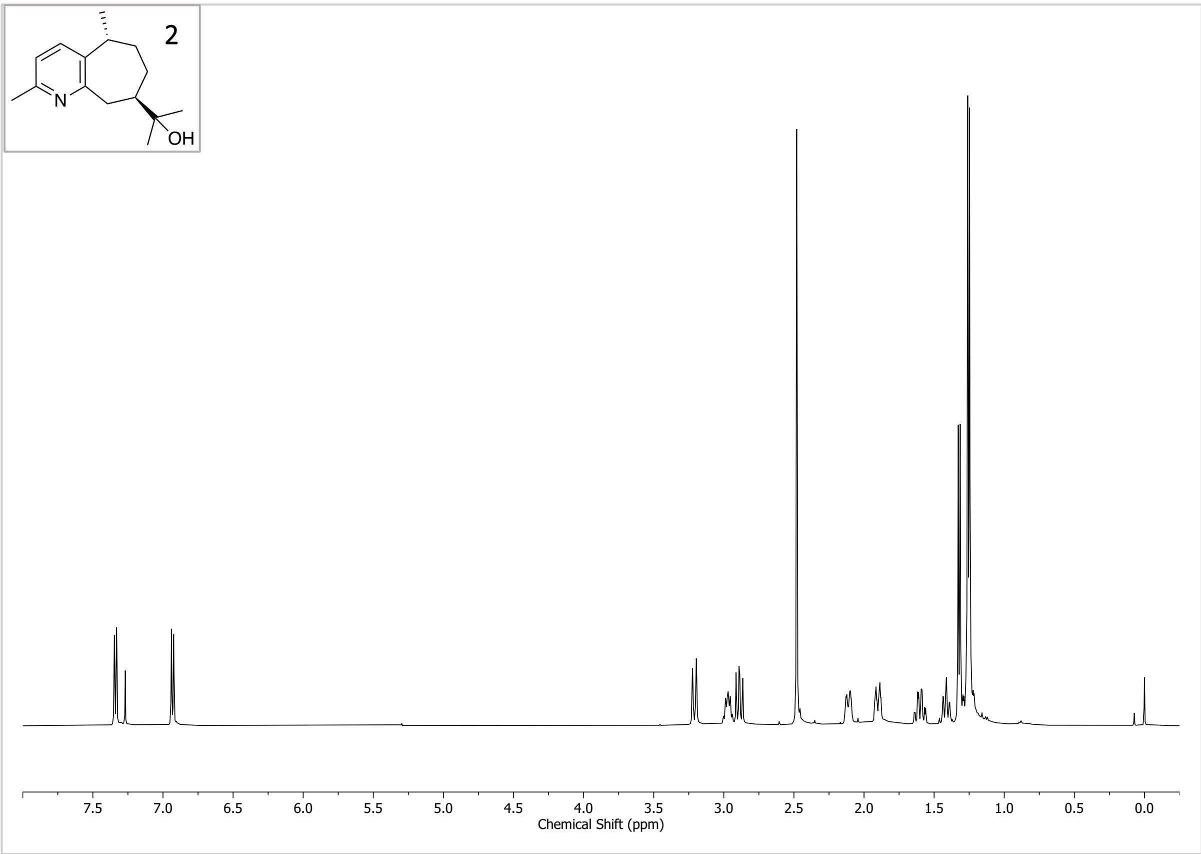
2
N
OH
7.5
7.0
6.5
6.0
5.5
5.0
4.5
4.0
3.5
3.0
2.5
2.0
1.5
1.0
0.5
0.0
Chemical Shift (ppm)

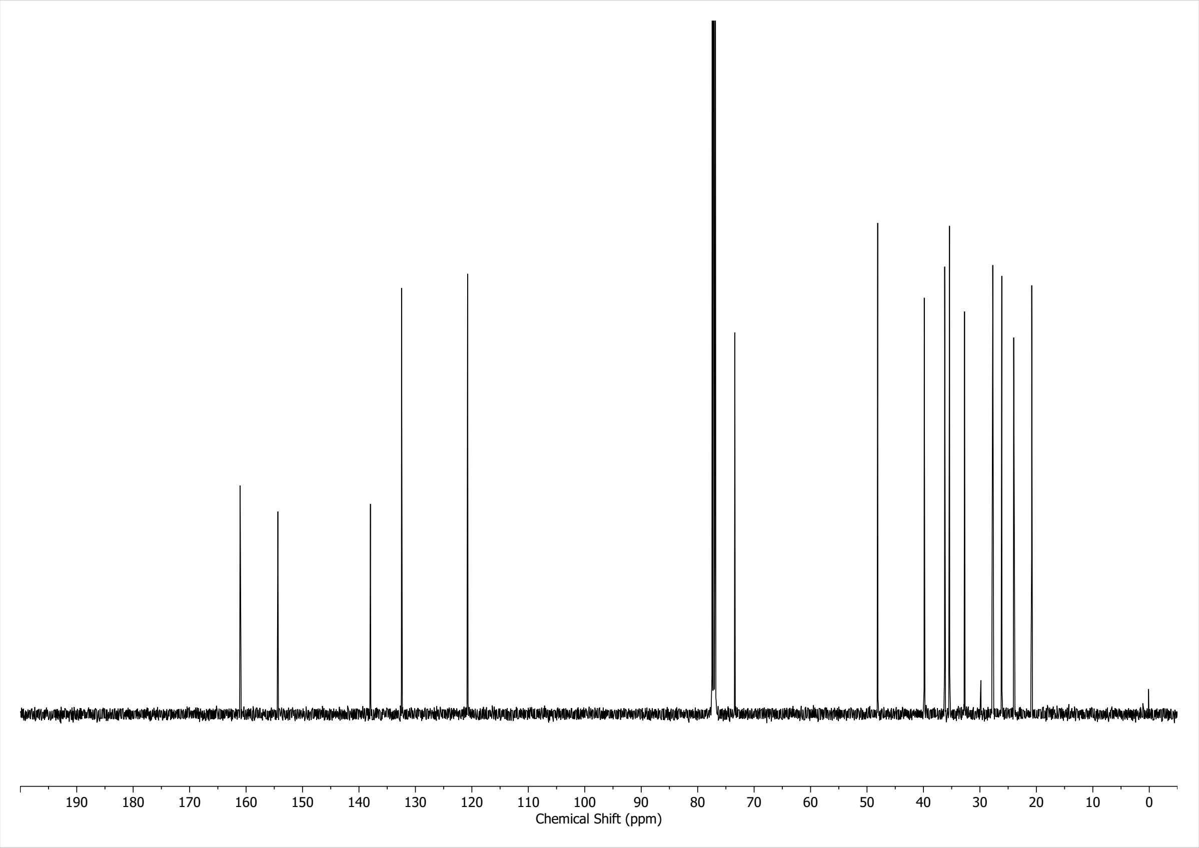
190
180
170
160
150
140
130
120
110
100
90
80
70
60
50
40
30
20
10
0
Chemical Shift (ppm)

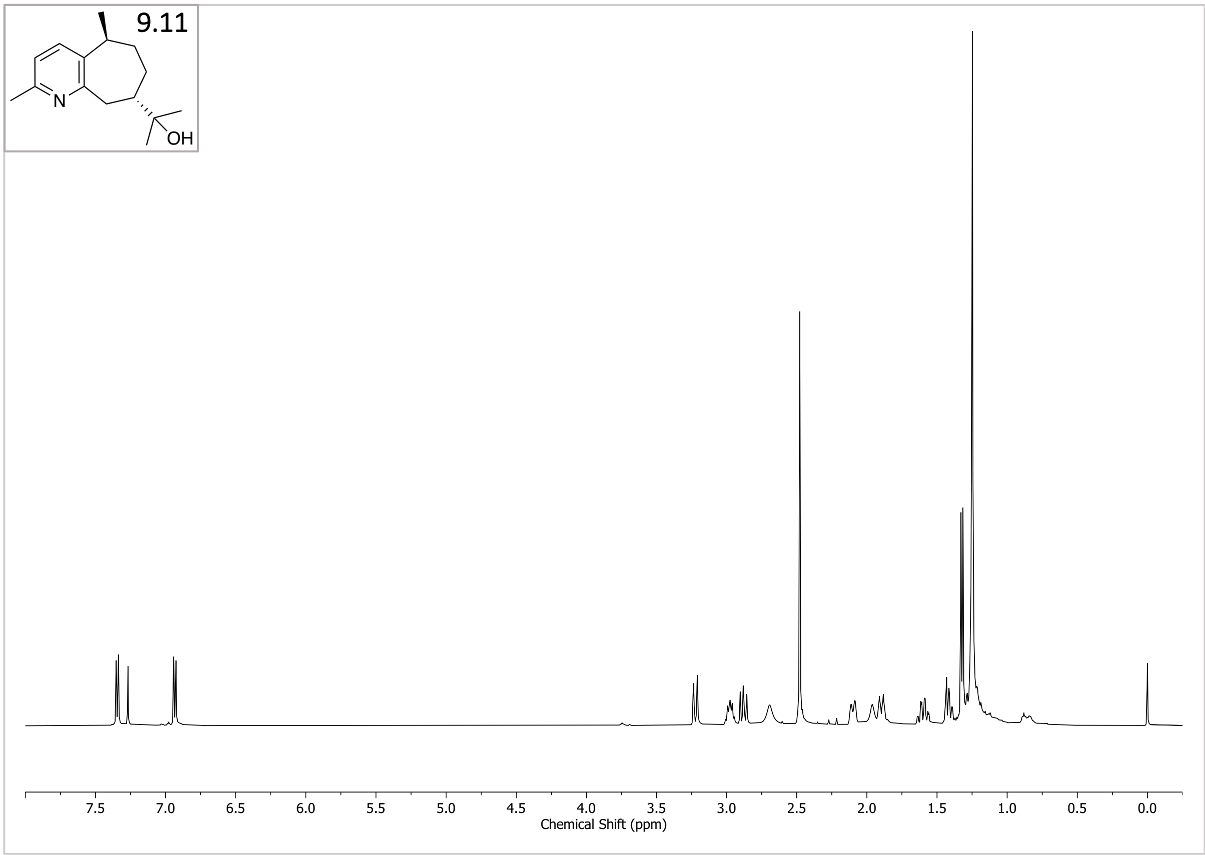
9.11
N
OH
7.5
7.0
6.5
6.0
5.5
5.0
4.5
4.0
3.5
3.0
2.5
2.0
1.5
1.0
0.5
0.0
Chemical Shift (ppm)

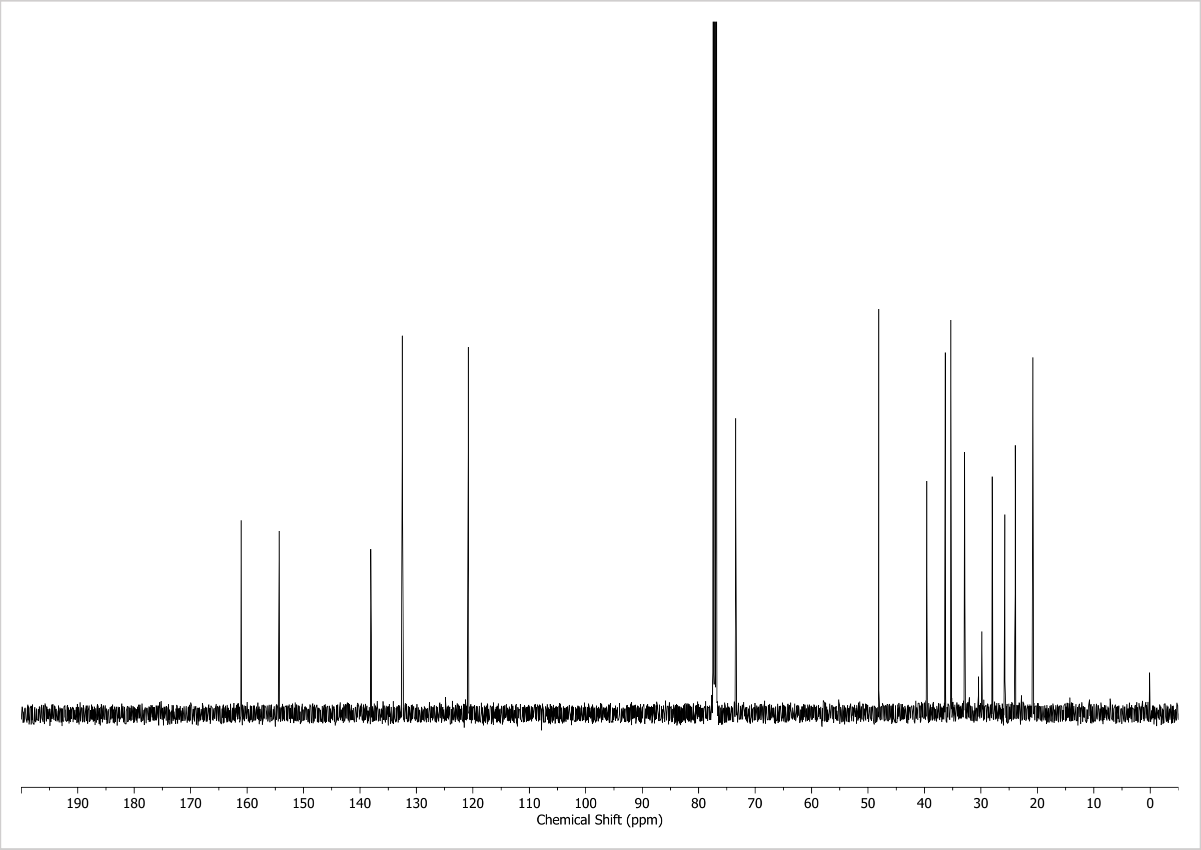
190
180
170
160
150
140
130
120
110
100
90
80
70
60
50
40
30
20
10
0
Chemical Shift (ppm)

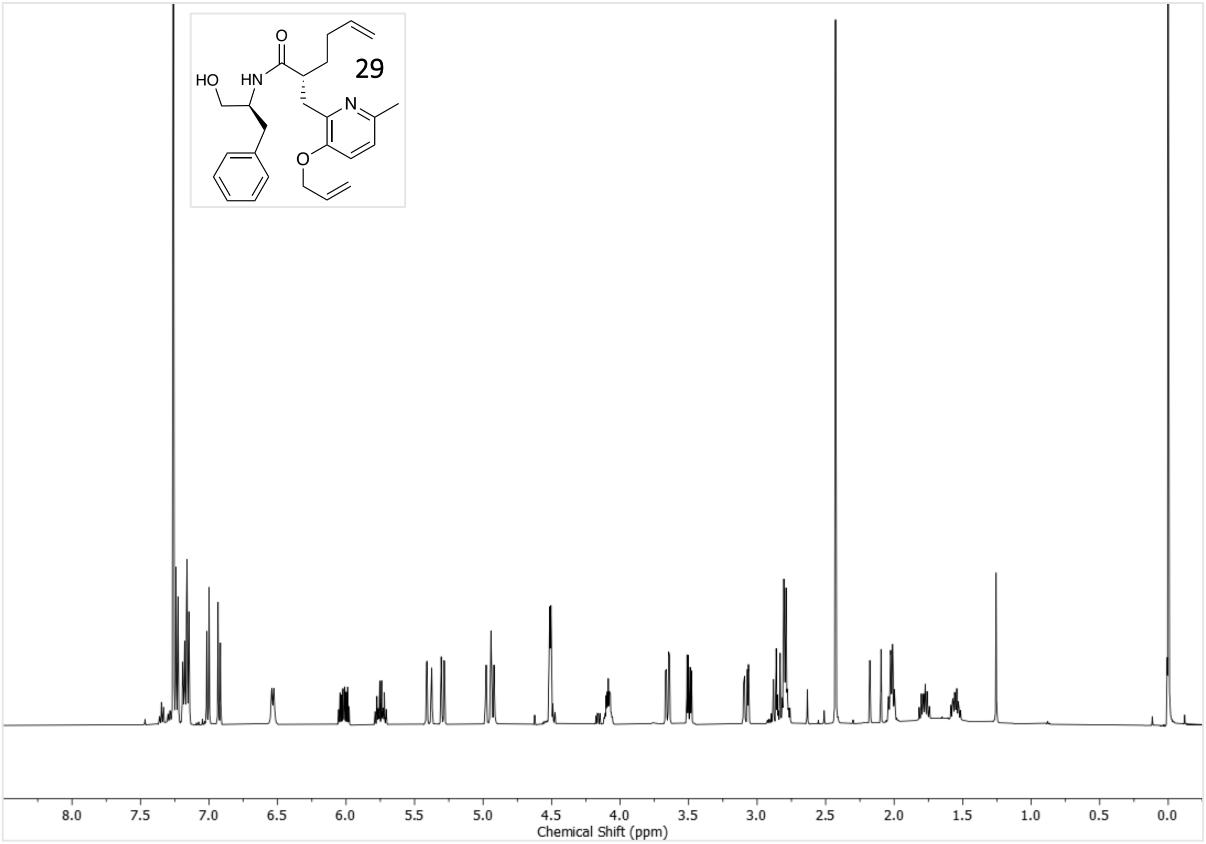
O
HN
HO
N
O
29
8.0
7.5
7.0
6.5
6.0
5.5
5.0
4.5
4.0
3.5
3.0
2.5
2.0
1.5
1.0
0.5
0.0
Chemical Shift (ppm)

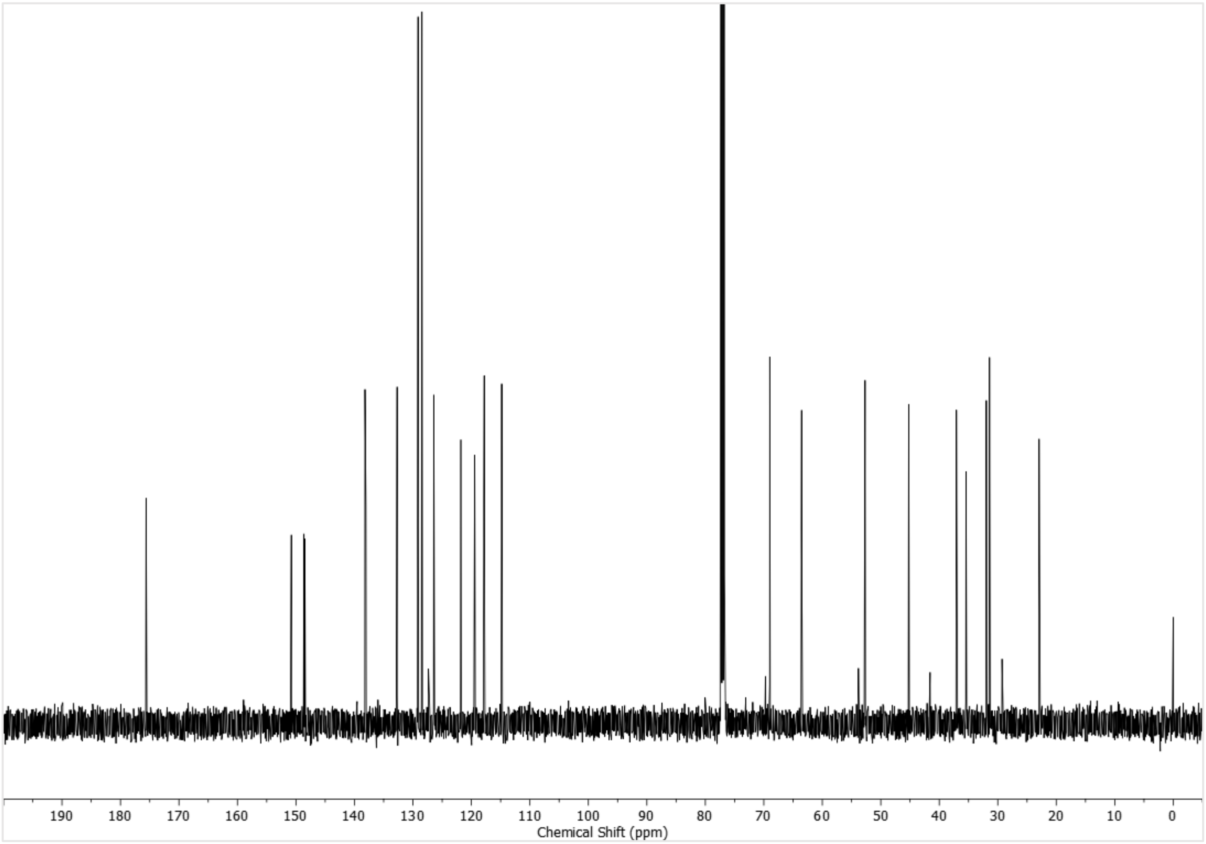
190
180
170
160
150
140
130
120
110
100
90
80
70
60
50
40
30
20
10
0
Chemical Shift (ppm)

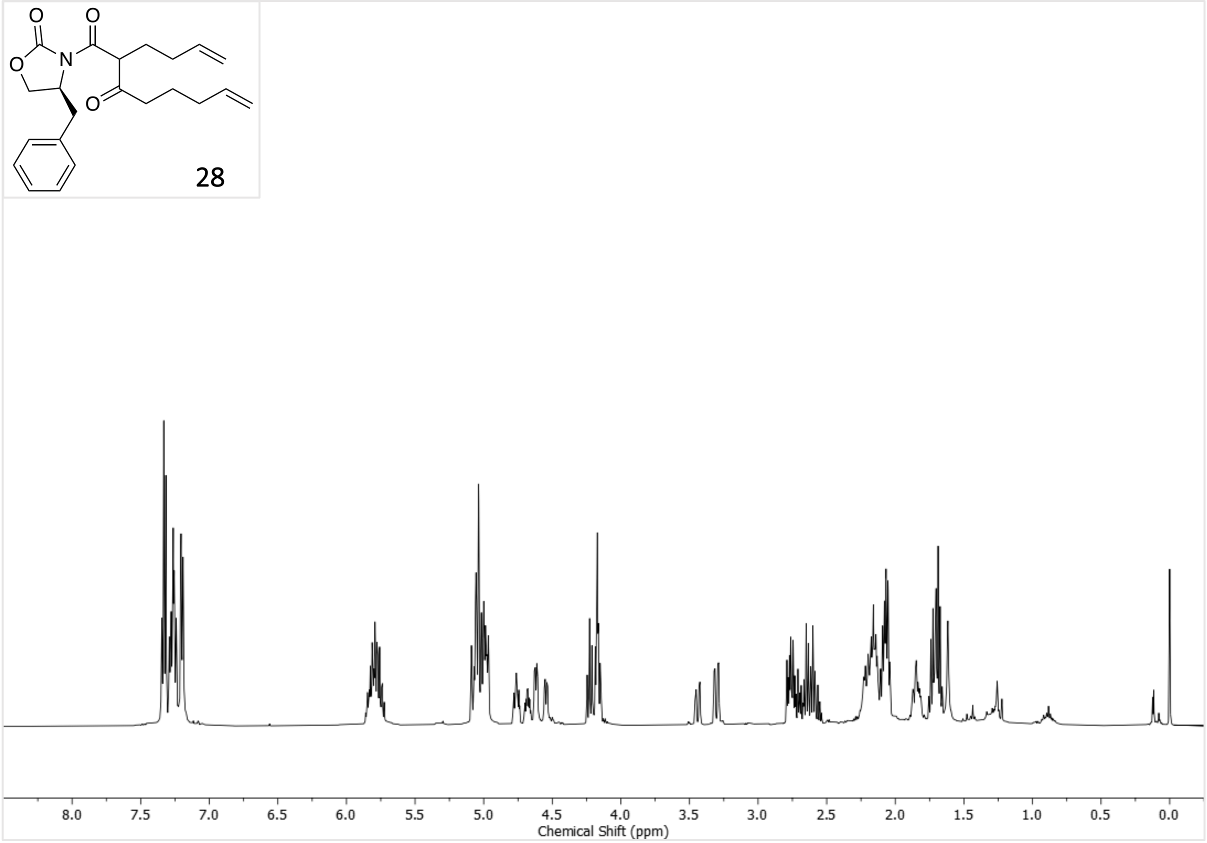

28

O
O
O
N
O
8.0
7.5
7.0
6.5
6.0
5.5
5.0
4.5
4.0
3.5
3.0
2.5
2.0
1.5
1.0
0.5
0.0
Chemical Shift (ppm)

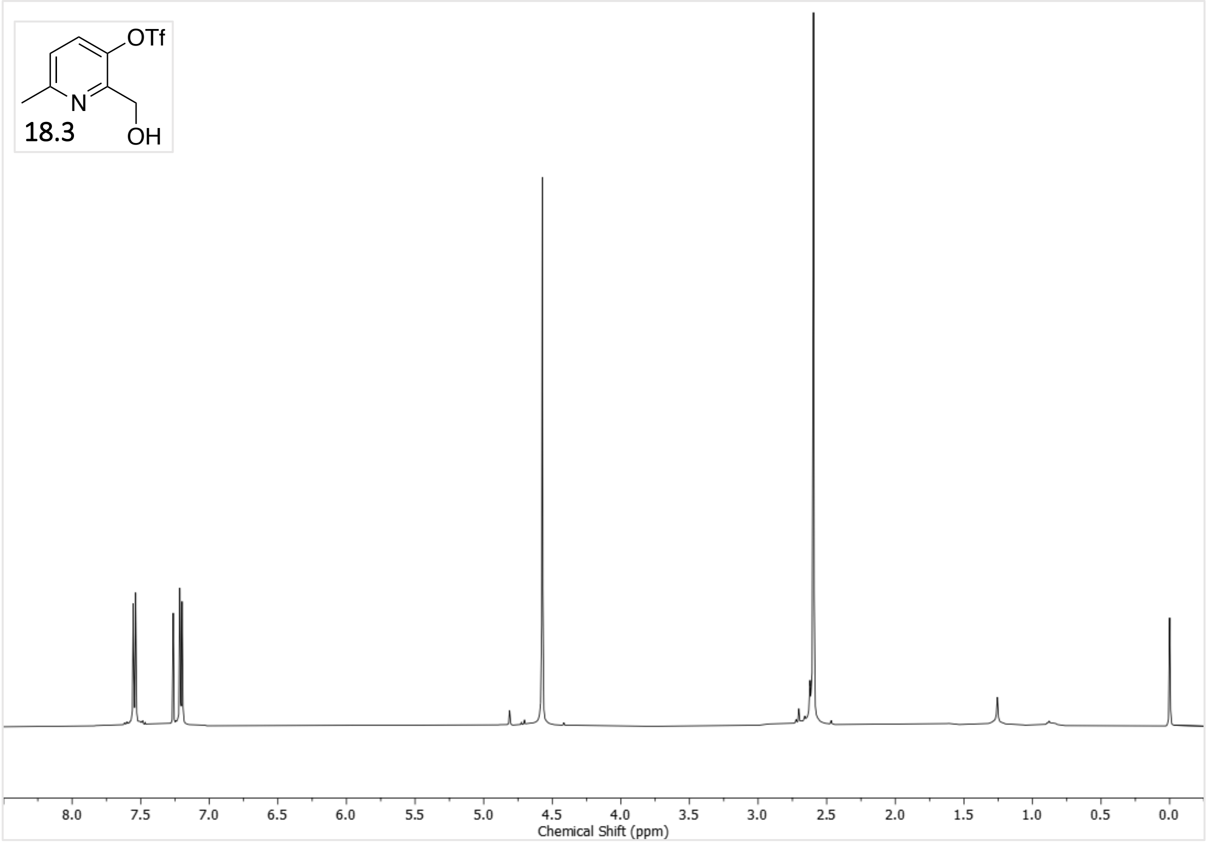
18.3
OTf
N
OH
8.0
7.5
7.0
6.5
6.0
5.5
5.0
4.5
4.0
3.5
3.0
2.5
2.0
1.5
1.0
0.5
0.0
Chemical Shift (ppm)

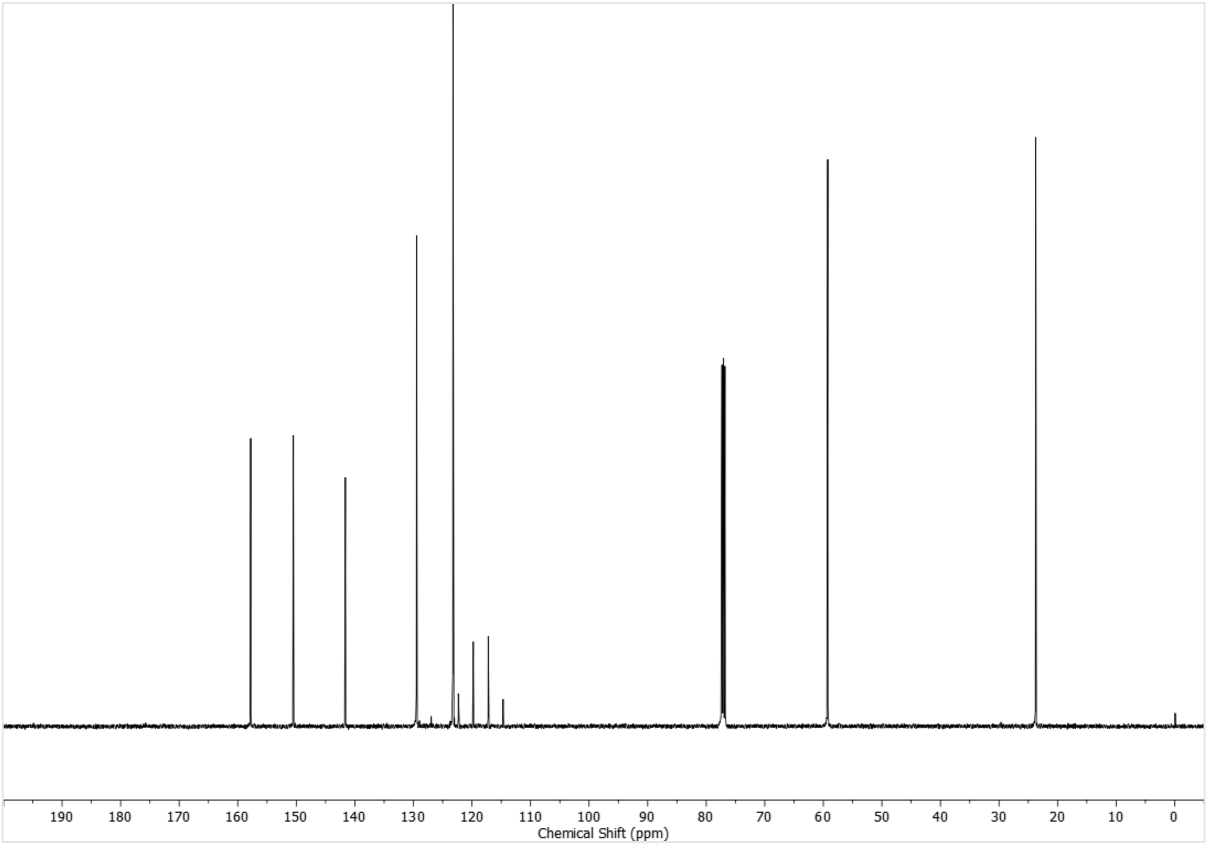
190
180
170
160
150
140
130
120
110
100
90
80
70
60
50
40
30
20
10
0
Chemical Shift (ppm)

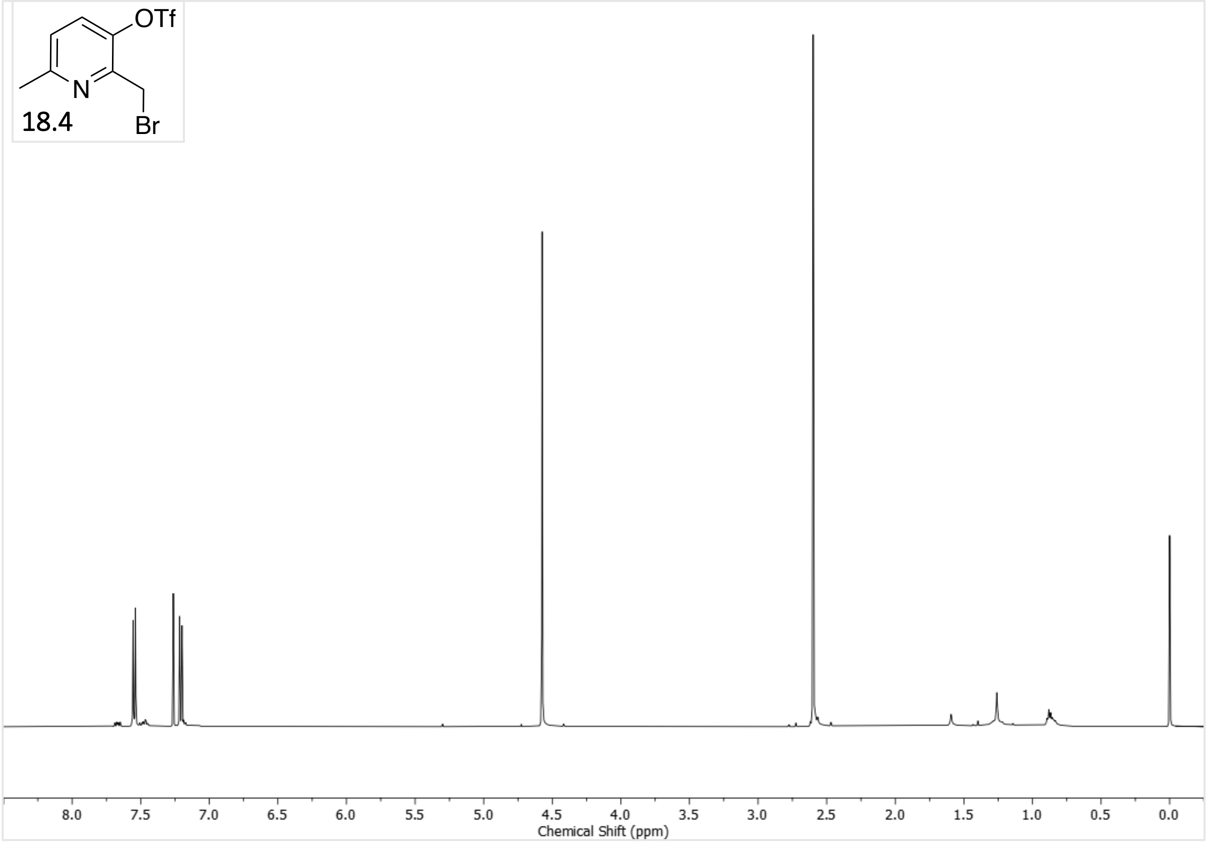

18.4

OTf
N
Br
8.0
7.5
7.0
6.5
6.0
5.5
5.0
4.5
4.0
3.5
3.0
2.5
2.0
1.5
1.0
0.5
0.0
Chemical Shift (ppm)

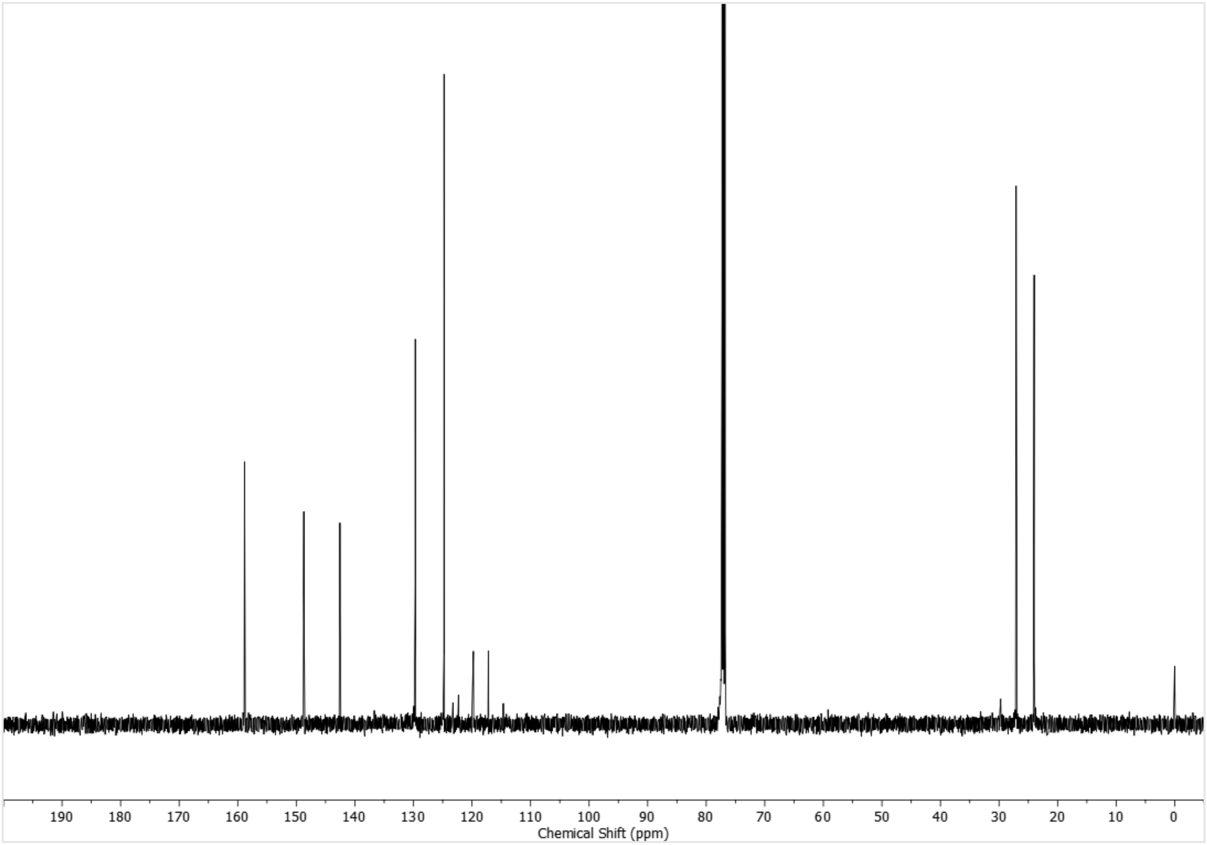

190
180
170
160
150
140
130
120
110
100
90
80
70
60
50
40
30
20
10
0
Chemical Shift (ppm)

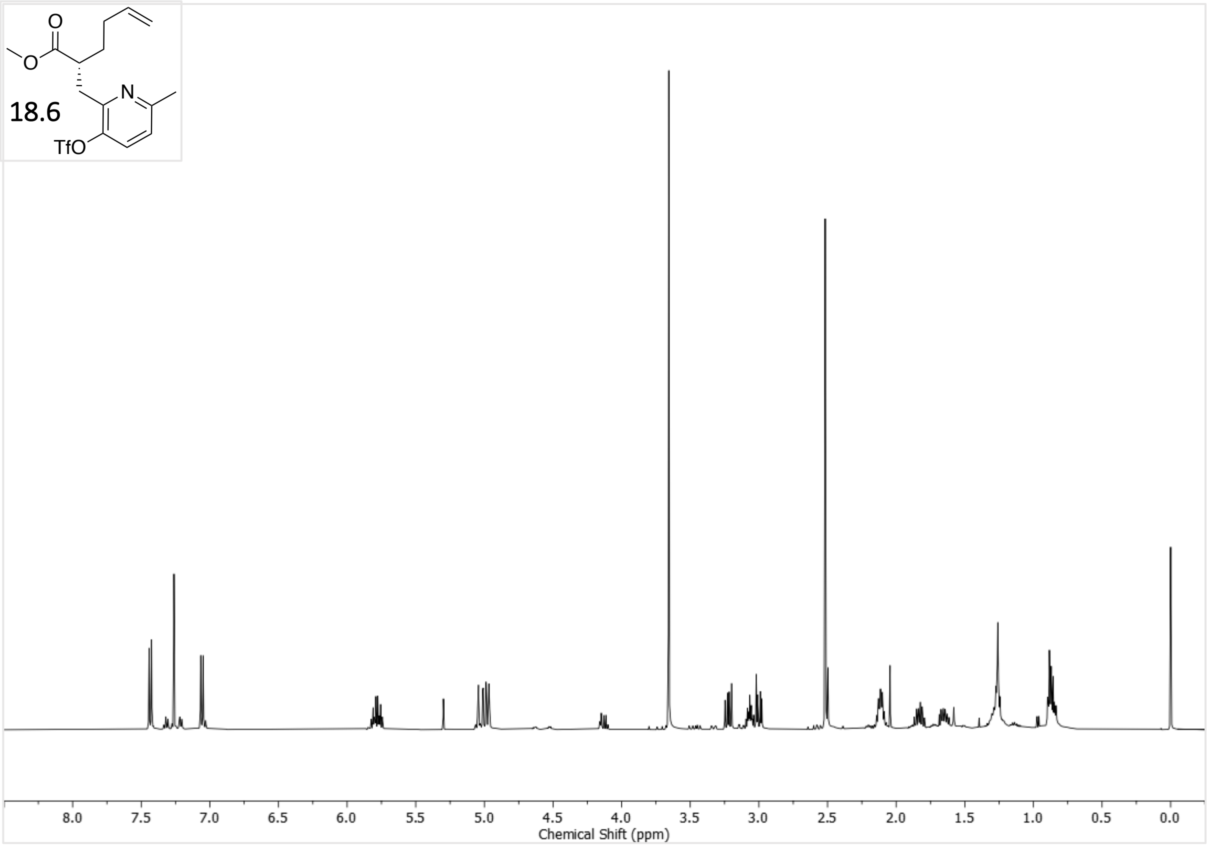
18.6
TfO
N
O
8.0
7.5
7.0
6.5
6.0
5.5
5.0
4.5
4.0
3.5
3.0
2.5
2.0
1.5
1.0
0.5
0.0
Chemical Shift (ppm)

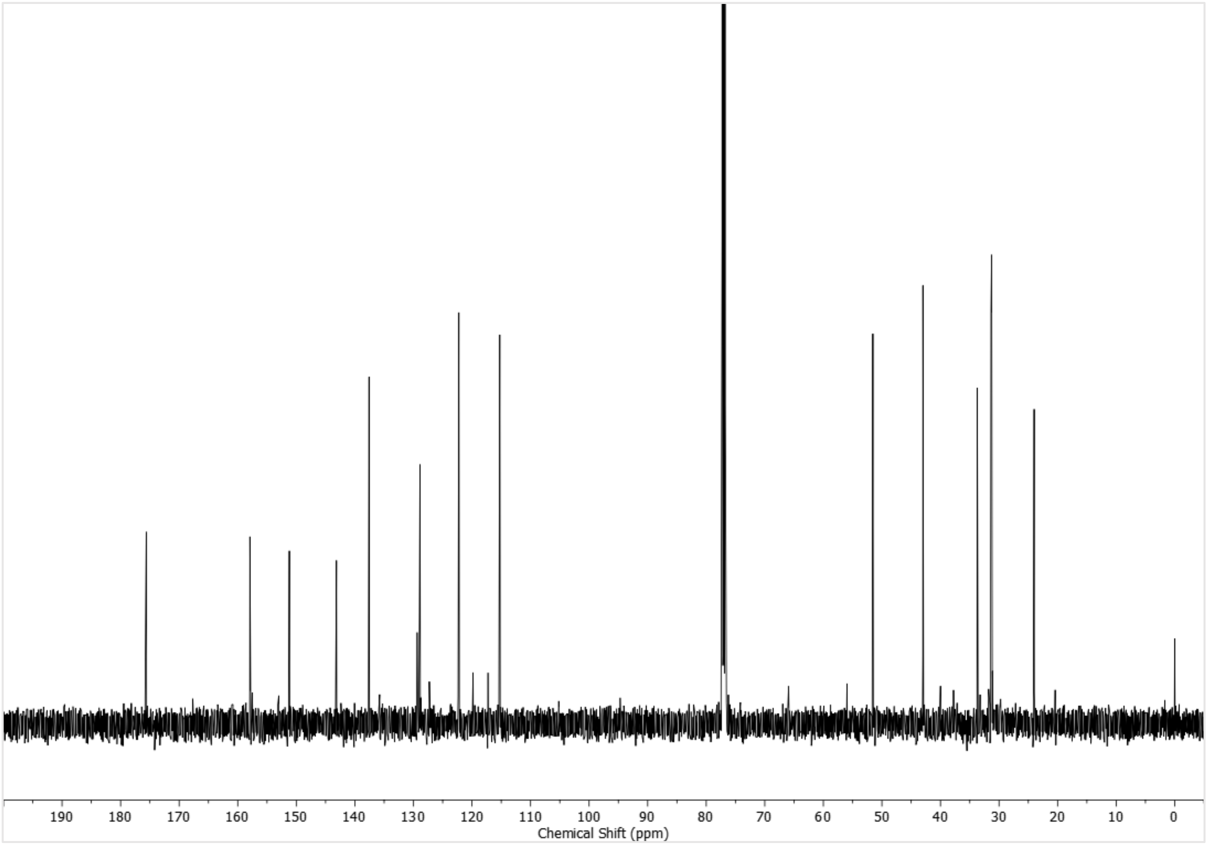
190
180
170
160
150
140
130
120
110
100
90
80
70
60
50
40
30
20
10
0
Chemical Shift (ppm)